ANALYSIS OF EXCAVATION IN SOFT CLAY STABILIZED BY CEMENT TREATMENT

A THESIS

submitted by

AZNEB ABDUL SALAM

for the award of the degree

of

DOCTOR OF PHILOSOPHY

DEPARTMENT OF CIVIL ENGINEERING
INDIAN INSTITUTE OF TECHNOLOGY MADRAS

MAY 2020

Dedicated to
my first teachers — my beloved parents,
my best friend - my wife
and
my lucky charm- my daughter

THESIS CERTIFICATE

This is to certify that the thesis entitled **ANALYSIS OF EXCAVATION IN CLAY STABILIZED BY CEMENT TREATMENT**, submitted by **AZNEB ABDUL SALAM**, to the **Indian Institute of Technology Madras**, for the award of the degree of **Doctor of Philosophy**, is a bonafide report of the research work done by him under our supervision. The contents of this thesis, in full or parts, have not been submitted to any other Institute or University for the award of any other degree or diploma. This research was carried out at Indian Institute of Technology, Madras.

Dr. Subhadeep Banerjee   **Dr. R.G. Robinson**

Research Advisor   Research Advisor

Associate Professor   Professor

Geotechnical Engineering Division   Geotechnical Engineering Division

Department of Civil Engineering   Department of Civil Engineering

IIT Madras, Chennai   IIT Madras, Chennai

Date: 04/05/2020

Place: Chennai - 600036

ACKNOWLEDGMENTS

ABSTRACT

KEYWORDS: Cement treated clay, excavation, failure envelope, Hoek Brown, plane strain, soft clay, triaxial.

Deep Excavations in thick deposits of soft clays require care, especially if soft ground exists well below the final formation level of excavation. In this case, the retaining wall suffers maximum deflection below the excavation level, by virtue of the retaining wall floating in soft ground and not reaching a hard stratum. The conventional bracings or struts can be provided only up to the final formation level of excavation. One of the viable solutions to tackle this problem is to improve the ground below the final excavation level using cement treatment, prior to the commencement of excavation. Deep cement mixing and jet grouting are the most common methods adopted for the same. The soil-cement slab so formed which covers the entire plan area of excavation, called *Embedded Improved Soil Raft or Embedded Improved Soil Strut,* is expected to control the wall deflections and the possible heaving of vertical supports. Since the dimension in out of plane direction is usually very large compared to the other dimensions, in most typical excavation problems, this raft can be approximated as a plane strain problem.

It is a usual practice to assess the strength properties of cement treated clay in the laboratory by performing conventional triaxial and unconfined compressive strength tests, which employ testing under axisymmetric condition. But plane strain testing would best represent the field condition in this case. A plane strain testing apparatus was developed, and plane strain testing was performed on cement treated clay. Clear differences in shear strength values were observed under plane strain condition compared to triaxial condition. A good comparison of the behaviour of cement treated clay under the two modes of testing has been brought out in this study.

A simple non-linear failure envelope was developed for cement treated clay based on the experimental results, for both triaxial and plane strain conditions. This failure envelope was then represented by a non-linear constitutive model, Hoek-Brown model, which follows generalised Hoek-Brown criterion. This allows direct implementation of failure envelope into a commercial software package. The developed failure envelope was then validated by simulating the

laboratory experiments, using a finite difference software, *FLAC*. The model was found to be capable of predicting the behaviour of cement treated clay, to reasonable accuracy. Hence, this model can serve as a simple non-linear constitutive framework for representing cement treated clay. Finally, two case studies of excavation problems were selected which have employed improvement of soil below the final formation level and were validated for lateral deflection of retaining wall. The improved layer properties were then replaced with triaxial and plane strain properties obtained in this study, using the developed failure envelope. Clear differences were observed in the lateral deflection of retaining wall while using triaxial and plane strain test results. Hence, this study establishes that for excavations stabilized by cement treatment, input properties should be selected based on the field stress conditions. This argument is expected to be valid across the other applications in geotechnical engineering.

TABLE OF CONTENTS

LIST OF TABLES

LIST OF FIGURES

ABBREVATIONS

ASTM	American Society of Testing Materials
CU	Consolidated Undrained
CD	Consolidated Drained
CTC	Conventional Triaxial Compression
CSSL	Cement-Stabilized Soil Layers
DW	Diaphragm Wall
E	Elastic Modulus
FE	Finite Element
FLAC	Fast Lagrangian Analysis of Continua
GL	Ground Level
IS	Indian Standards
kPa	Kilo-Pascal
kN	Kilo-Newton
LVDT	Linear Variable Displacement Transducer
MRRB	MR Residential Basement
NIOT	National Institute of Ocean Technology
PS	Plane Strain
SI	Inclinometer
SEM	Scanning Electron Microscopy
UCS	Unconfined Compressive Strength

NOTATIONS

English Symbols

a	Hoek-Brown parameter
c'	Effective cohesion
c_{eqv}	Equivalent cohesion of improved soil mass
c_{JGP}	Cohesion of jet grouted pile
c_{org}	Cohesion of untreated soil
G	Shear Modulus
I_r	Improvement ratio
K	Bulk Modulus
K_0	Coefficient of earth pressure at rest
M	Critical state parameter
m	Hoek-Brown parameter
N	Critical state parameter
p'	Mean normal effective stress
q	Deviator stress
s	Hoek-Brown parameter
Su	Shear Strength

Greek Symbols

σ_d	Deviator stress
$\sigma_1{}'$	Major effective principle stress
$\sigma_2{}'$	Intermediate effective principle stress
$\sigma_3{}'$	Minor effective principle stress
σ_t	Tensile strength
ϕ'	Angle of internal friction
γ	Unit weight
μ	Poisson's ratio
λ	Critical state parameter
κ	Critical state parameter
α_c	Empirical factor

CHAPTER 1

INTRODUCTION

1.1 BACKGROUND

Soft Clays possess low bearing capacity, low shear strength and high compressibility characteristics. Retaining structures in such soils undergo large deflection along with heaving of vertical supports, during excavation process. Provision of a strong retaining wall coupled with stiff bracings works out well above the final formation level. However, if a thick layer of soft clay is present below the final formation level, the retaining wall floats in soft clay and does not reach a hard stratum. Hence, maximum deflection of the wall is most likely to happen below the final formation level. In such cases, improving this soft soil below the final formation level by cement treatment, prior to excavation, would be viable option to ensure the safety of the excavation. Deep cement mixing method and jet grouting method have been proven to be successful techniques for the same (Sugawara et al., 1996; Tanaka, 1993; Liao and Tsai, 1993). The cement stabilization of soft soil below the final formation level of a deep excavation is focussed in the present study.

The ground improvement technique using deep mixing (DM) method involves mechanical mixing of soil with a cementitious binder, forming individual soil-cement columns or blocks. In deep mixing technique, cement imbibes water present in soil and reacts with clay particles to form pozzolanic products. This technique thereby alters the properties of the weak soil due to the complex reactions happening between soil and cement. Hence, this technique is widely used to improve the shear strength of weak soil and hence minimise ground settlements. This ground improvement technique is commonly employed to improve ground, for foundations in roads, railway and embankments, as hydraulic cut off walls, to mitigate liquefaction, as excavation support, for environmental remediation, etc. On the other hand, jet grouting involves injection of a stabilizing fluid or a slurry into the subsoil (or the soil under treatment) under high pressure and velocity. The soil stabilization is achieved by the hardening of the soil due to grouted fluid

within the soil. This method finds widespread applications like support for excavation, tunnelling, horizontal barriers, etc.

The practice of stabilizing an excavation in soft clay involves application of jet grouting or deep mixing method to improve the soft soil beneath the final formation level, prior to carrying out excavation works. This stabilization is generally performed from wall to wall, covering the entire plan area of excavation, resulting in the formation of a soil-cement slab beneath the final excavation level. Such an improved layer is called embedded improved soil strut or raft (Kongsomboon, 2002). In practice, most of the excavation problems are considered to be under plane strain condition. Hence, the improved layer which exists across the entire plane area of excavation shall also be studied using plane strain analysis.

It is common practice to obtain the properties of cement treated clay using conventional triaxial tests and unconfined compressive strength (UCS) tests. Both these tests, however, employ axisymmetric configuration for testing. For the problem considered in this study, testing under plane strain condition would best represent the field condition. Literature also suggests that significant differences exist in the behaviour of soil tested under plane strain and triaxial conditions. This aspect is often not considered in practice and triaxial test still seems to be resorted to even today assuming that same strength is obtained under the two conditions. It is worth mentioning that for natural soils, testing under plane strain condition results in higher strength than that under triaxial condition. Hence, this approximation happens to be on the conservative side for natural soils. However, there is no published study reported on the comparison of strength behaviour of cement treated clay under triaxial and plane strain testing conditions.

The most crucial parameter in the performance of any excavation problem is the lateral wall deflection of retaining wall (Hsieh et al., 2003). Hence, minimising the lateral wall deflection is very important. For the problem considered in this study, the cement treated clay layer is under plane strain condition. Hence, properties obtained from plane strain testing are essential to get reliable results.

There are numerous studies reported on numerical analyses of cement treated clay layers. The efficiency and reliability of any numerical analysis depend heavily on the constitutive models chosen for each geomaterial. A simple constitutive model which could represent the behaviour of cement treated clay is still unavailable in the literature. The popular Mohr-Coulomb model happens to be a misfit for this type of cement treated soil due to its inherent non-linear character. The non-linearity in cemented soils has been established by many researchers (Consoli et al., 2012; Sharma et al., 2011; Asghari et al., 2003; Panda and Rao, 1997; Sankar and Paul, 1997). Hence a simple non-linear constitutive model which can reasonably predict the behaviour of cement treated clay is also essential to be studied. This will play a pivotal role in simulation of excavation problems stabilized by cement treatment.

1.2 NEED FOR THE STUDY

Following are the research gaps identified for the current study.

1. Studies regarding the strength behaviour of cement treated soils are quite abundant. However, most of them are based on triaxial tests and UCS tests, where axisymmetric condition is used. Studies on plane strain testing of cement treated clay are scarce in the literature. Most of the geotechnical problems involving cement treated clay layers such as, cement treated soil strut, block or wall type improvement in embankments, etc. can be approximated as plane strain problems. Hence, plane strain testing would better represent the actual field condition of cement treated clay layer in these cases.

2. Comparison between plane strain testing results and triaxial results have been established in the literature for natural soils. The same has never been reported in case of cement treated soils.

3. The constitutive models developed for cement treated clays till date, are cumbersome to implement in a numerical platform. A simple constitutive model which can capture the non-linear behaviour of cement treated clay needs to be identified.

4. In excavation problems where a layer of clay beneath the final formation level is stabilized by cement treatment, the improved clay layer can be approximated as a plane strain problem. Studies on numerical analyses of such problems are viably available in the literature. However, the input properties for the cement treated clay layer are often

derived from strength parameters obtained by testing under axisymmetric conditions. In such problems where the main concern on the field is lateral deflection of retaining wall, inputs from the plane strain testing would better represent the field condition. However, no such studies have been reported in the literature.

1.3 OBJECTIVES

Based on the research gaps presented in the last section, the objectives of this research are formulated as follows:

1. To develop a plane strain apparatus and compare the strength behaviour of cement treated clay under plane strain and triaxial (axisymmetric) testing conditions.
2. To propose a failure envelope using a non-linear constitutive model, which can predict the behaviour of cement treated clay under different stress conditions.
3. To simulate the lateral deflection of retaining wall in excavation problems which are stabilized by cement treatment, and to compare the results with the input of triaxial and plane strain properties for the cement treated clay layer.

The scope of the present research is limited to cement contents of 10%, 15% and 20%, and effective confining pressures of 50 kPa, 100 kPa, 200 kPa and 400 kPa.

A finite difference software, *FLAC*, will be utilised in the numerical simulations.

1.4 ORGANISATION OF THE THESIS

The thesis is organized in to eight chapters. This chapter (**Chapter 1**) gives a brief introduction of the research topic adopted for this study and the objectives of this research. The crux of the remaining chapters is explained herein.

Current state of the art related to cement treatment of soft soil and the application of this technique to improve the base of excavation is reviewed in **Chapter 2**. The real field excavation problems stabilized by cement treatment are also discussed. A detailed discussion on plane strain apparatus used by various researchers, characteristics of plane strain testing and comparison with triaxial testing are also presented in this chapter.

The experimental programme carried out to understand the basic characteristics of the cement treated clay considered in this study, is explained in **Chapter 3**. The basic properties of clay used, cement-stabilization procedure and basic properties of cement treated clay are also discussed in this chapter.

Chapter 4 brings out the development of a plane strain apparatus and plane strain testing of cement treated clay specimens. The strength properties obtained under plane strain condition are compared with those obtained under triaxial (axisymmetric) conditions.

In **Chapter 5,** a failure envelope is developed for cement treated clay under triaxial and plane strain testing conditions. A non-linear constitutive model is selected to represent this failure envelope to readily implement in a numerical platform.

Chapter 6 discusses on the implementation of the failure envelopes discussed in **Chapter 5** in a finite difference simulation. The numerical simulations of laboratory plane strain and triaxial tests on cement treated clay, using the input properties obtained from the above failure envelopes, are also discussed. A comparison of simulated results with experimental results is also presented.

Chapter 7 presents validation of two selected case studies of excavation problems stabilized by cement treatment. The differences in the lateral deflection of retaining wall upon input of plane strain and triaxial properties are brought out through rigorous numerical simulations.

Finally, **Chapter 8** summarizes the major findings and conclusions drawn from this study.

CHAPTER 2

LITERATURE REVIEW

2.1 INTRODUCTION

Soft Clays are problematic soils as they possess low bearing capacity, low shear strength and high compressibility characteristics. They exist along several coastal belts in the world. Deep excavations in such soft soils often prove to be detrimental to the surrounding buildings and foundations, due to excessive deflection in the retaining wall and associated ground movements. When retaining structures are used to support the excavation in soft clays, they often float and undergo large deflection along with heaving of vertical supports (Tanaka, 1993). Provision of a strong retaining wall supported by stiff bracings above the final formation level, has been the common strategy adopted over the years. But if a thick layer of very soft clay is present below the final formation level, maximum deflection of the wall is most likely to happen below the formation level. In such cases, improving this soft soil below the formation level, prior to excavation, would be a good choice to ensure the safety of the excavation. This imparts strength to the soil below the final formation level of excavation and acts as a horizontal strut below the final excavation level. This technique is expected to reduce the deflection of retaining wall, below the final formation level of excavation. Deep mixing (DM) method and jet grouting method (JG) using cement treatment have been proven to be viable techniques for the same. However, deep mixing is preferred over jet grouting, due to excessive wastage and displacement in the latter (Lim, 2003). Hence, stabilization of excavation using deep mixing is focussed in this study.

2.2 DEEP MIXING

Deep mixing is an in situ ground improvement technique that improves the properties of weak soils by mechanically mixing them with a cementitious binder through hollow rotary shafts tipped with cutting tool. Binders like cement, fly ash, lime or bentonite are used, of which cement is the most common owing to better performance and is then called deep cement mixing. This technique was developed in Japan, where the first field test began in 1970 (Bruce, 2000). Soil-binder columns are thus formed with diameters ranging from 0.6 to

1.5m and can reach a depth of up to 30m for land operations and 70 m in marine works. Addition of cement alters the properties of the weak soil due to the complex reactions happening between the soil and cement. This enhances the properties of the soil to become more like soft rock. But this technique should be carefully monitored and executed in order to obtain satisfactory results. The mechanisms involved, when soil is treated with cement is discussed below.

Following the common notations used in cement chemistry, C herein denotes cement, S denotes silicate, A denotes aluminate and F denotes ferrite.

The main components of ordinary Portland cement are as follows:

a) Tri-calcium silicate, $3CaO.SiO_2$ (C$_3$S)

b) Di-calcium silicate, $2CaO.SiO_2$ (C$_2$S)

c) Tri-calcium Aluminate, $3CaO.Al_2O_3$ (C$_3$A)

d) Tetra-calcium Alumino-Ferrite, $4CaO.Al_2O_3.Fe_2O_3$ (C$_4$AF).

The improvement in engineering properties of soft soils upon introduction of cement is attributed to the reaction between soil and cement (Mitchell, 1981). Basically, two major reactions occur when soil is mixed with cement, viz. cement hydration reaction and pozzolanic reaction. The compounds of cement react with water already present in soil to form cement hydration products and is called hydration of cement. The predominant component in cement is $3CaO.SiO_2$, and hence reaction happens as shown in equation 2.1.

$$2(3CaO \cdot SiO_2) + 6H_2O = 3CaO \cdot 2SiO_2 \cdot 3H_2O + 3Ca\,(OH)_2 \qquad (2.1)$$
<div align="center">Cement Hydration Product</div>
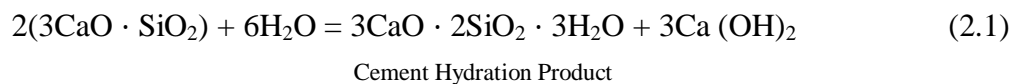
The formation of cement hydration product (expressed as $C_3S_2H_3$ or C-S-H) leads to reduction of water content in clay resulting in short term gain in strength. In addition, $Ca\,(OH)_2$ released during hydration reaction dissolves into water, producing more calcium ions, Ca^{2+} and hydroxyl ions, OH^-. The increase in hydroxyl ions results in creation of a high *pH* environment, under which silica and alumina in clay minerals dissolve in water and react with calcium ions to form calcium silicate and calcium aluminate gels. These gel like products formed (called tobermorite gel) are highly stable and provides cement like strength and stiffness to soil. This reaction is called pozzolanic reaction and the products formed are

called pozzolanic reaction products (Han, 2015). Figure 2.1 gives the chemical reactions involved when soil reacts with different types of binders.
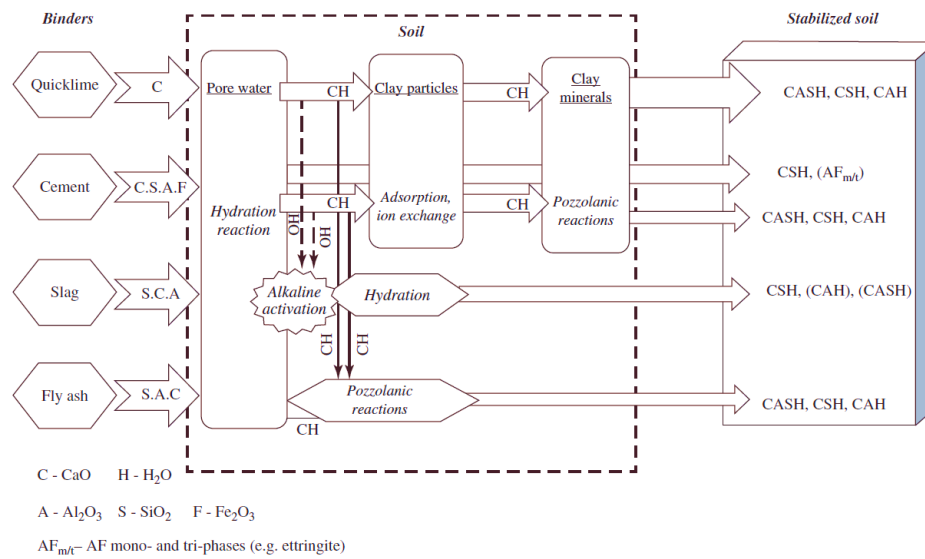
Figure 2.1 Chemical reactions involved when soil is mixed with different binders (Ahnberg and Johansson, 2005).

Hydration of the cement occurs immediately when it gets in contact with water, but the secondary reactions are slower and may continue for many months (Bruce 2000, Chew et al., 2004; Lorenzo and Bergado, 2004, 2006; Kamruzzaman et al., 2009; Han, 2015). The soil-binder composite material columns or blocks produced upon mixing with cement will result in enhanced engineering properties such as higher shear strength, lower permeability and lower compressibility. The degree of improvement in properties generally depends upon the properties of the native soil like type of clay minerals and water content, mixing efficiency, curing time and amount of binder (Tanaka, 1993).

This method has been successfully applied to excavation works for foundation and basement construction, foundations for construction of road and railway, embankment, airport and ports, and industrial projects. Deep mixing technique has been mostly used to improve soft cohesive soils with high moisture content and loose, saturated fine granular soils, but can also be used to reduce permeability and mitigate liquefaction in cohesionless soils (Han, 2015).

Generally, two types of mixing techniques are used: wet mixing and dry mixing. Wet method involves mixing of native soil with binders in slurry form using single auger, multi-auger or cutter-based techniques. In dry method, binders in powdered form are introduced into the soil using single auger technique, which reacts with water already present in the soil. Dry mixing

9

does not ensure homogeneity and adequate workability, which could jeopardize the degree of improvement in clays (Tan et al., 2002). Wet method results in a homogenous mix owing to better distribution of slurry across the area, pre-hydration of cement, longer mixing time, and hence higher strength. However, its application becomes difficult if the soil contains boulders and cobbles or if the ground is very stiff and dense. Table 2.1 shows the favourable soil properties for deep mixing method.

Table 2.1 Favourable Soil Properties for Deep Mixing (Elias, 2006)

Property	Favourable Soil Chemistry
pH	Should be greater than 5
Natural Water Content	Should be less than 200% (dry method) and less than 60% (wet method)
Organic Content	Should be less than 6% (wet method)
Loss on Ignition	Should be less than 10%
Humus Content	Should be less than 1%
Electrical Conductivity	Should be greater than 0.04mS/m

2.3 PROPERTIES OF CEMENT TREATED SOIL

2.3.1 Effect of Addition of Cement on Soil

Water content was found to decrease instantaneously upon addition of cement (Uddin et al., 1997; Chew et al., 2004; Lorenzo and Bergado, 2004; Ghee, 2006). This phenomenon was attributed to the hydration reaction and pozzolanic reaction. Calcium ions released by hydrated lime results in a flocculated clay structure, formed by clay clusters separated by large voids. Water gets trapped in these voids leading to an increase in effective size (Chew et al., 2004; Kamruzzaman et al., 2009). Atterberg limits of the base soil also get altered upon cementation. In many cases, liquid limit and plastic limit were found to increase with increase in cement content and curing time (Uddin et al., 1997; Chew et al., 2004; Lee et al., 2005; Ghee, 2006), whereas in some others, liquid limit decreased, and plastic limit increased (Petchgate et al., 2001). But in both cases, the bottom line was that plasticity index reduced considerably upon addition of cement.

The effect of cementation on the mechanical properties of soil depends on soil structure formed after cementation. Nagaraj et al. (1990) reported that clay microfabric consists of aggregated clay particles and the consequent enclosed capillary pore. Figure 2.2 (a) illustrates the microfabric of clay in its natural state, as reported by Horpibulsuk et al. (2005). It includes intra-aggregate pores between individual aggregates with a pore diameter less than 20 Å. Upon cementation, clay particles get welded by cementation bonds and become an engineering material, as shown in Figure 2.2 (b). The bond strength (σ_b) adds up to the effective stress to give an enhanced strength to the clay.
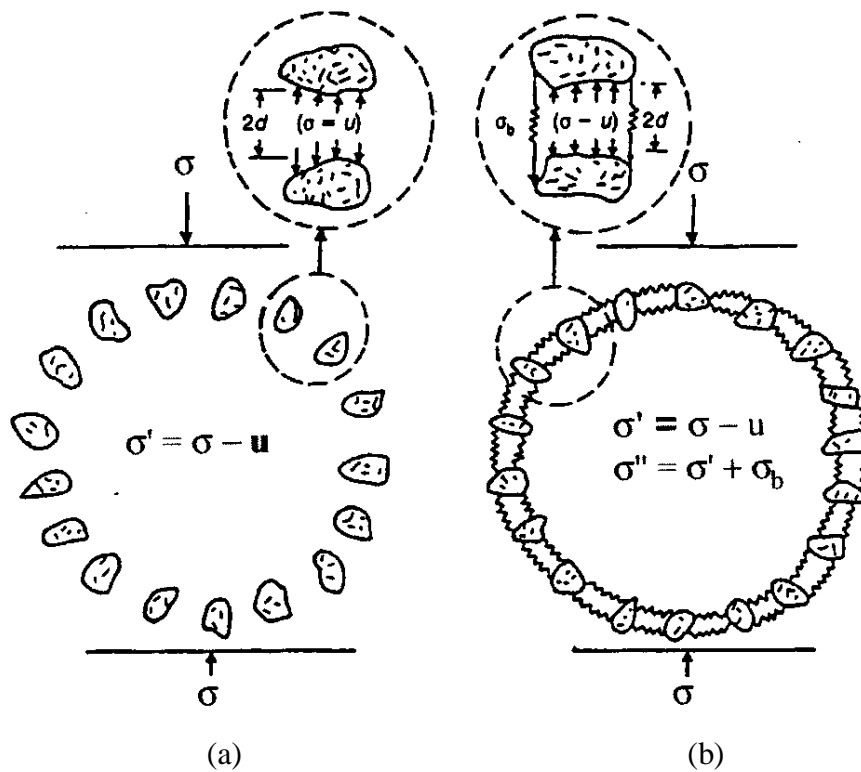
Figure 2.2 Microfabric of clay (a) Natural state and (b) Cemented state (Horpibulsuk et al., 2005)

2.3.2 Factors Affecting Strength of Cement Treated Soil

The shear strength of cement treated clay is a summation of the strength due to the cementation, q_b and the fabric, q_f (Horpibulsuk et al., 2003). Many studies have been carried

out, which explored the parameters governing strength gain upon cement treatment of soil and most of them were based on unconfined compressive strength.

Horpibulsuk et al. (2010) conducted extensive laboratory investigation based on micro-structural considerations and identified three important factors influencing the strength of cement treated clay, viz. cement content, curing time and water content. Some researchers established that cement content is a predominant parameter compared to curing time (Uddin et al., 1997; Ho and Chan, 2011). Cementation affects the structure of soil, makes it stiffer and hence greatly reduces the compressibility and compression index. Moreover, cementation increases the yield stress of soil and thus a higher yield stress is required in destructuration of the same (Tan et al., 2002).

The strength of cement treated clay was found to increase with increase in curing period. Kamruzzaman et al. (2009) reported that the pozzolanic reactions are significant for curing periods of up to 1 year. Curing period of one year allows notable amount of calcium ions to diffuse in the clay matrix to take part in pozzolanic reaction, resulting in the formation of more structured cement treated clay.

On the other hand, some others reported clay-water/cement ratio, w_c/C, as the most suitable micro structural parameter in the determination of strength of cement treated soft clays (Miura et al., 2001; Horpibulsuk et al., 2003; 2004; 2005; 2011). This parameter was found to represent both clay fabric as well as cement content. When the clay water content represents the micro-fabric of soft clay, the cement content controls the level of bonding of that fabric. If this ratio remains the same, strength and deformation characteristics have been reported to be identical. For deep mixing applications, the engineering behaviour of cement treated clays is primarily governed by this parameter, whereas the effect of fabric is negligible (Miura et al., 2001). Lee et al. (2005) proved that both soil/cement ratio and water/cement ratio, or the relative proportion of soil-cement-water ratio could govern the strength of cement treated clay.

Lorenzo and Bergado (2004) established that the ratio of after-curing void ratio and cement content, e_{ot} /A_w, is an effective parameter which determines the unconfined compression strength of cement treated soil. This ratio is expected to include the effects of cement content, curing time and most importantly, the clay water content. An increase in this ratio would imply a decrease in strength and vice-versa.

In short, factors like cement content, clay-water/cement ratio, ratio of after-curing void ratio/cement content and curing time were found to have predominant effects on the strength of cement treated soil.

2.3.3 Optimum Cement Content

The notion that the strength of cement treated soil keeps on increasing with increase in cement content is not entirely true. Horpibulsuk et al. (2010) reported that strength development upon increase in cement content can be classified into three zones – active zone, inert zone and deterioration zone. The maximum strength development happens during active zone wherein strength keeps on increasing with increase in cement content. In this zone, cement per grain contact increases with increase in cement content, leading to an increased bonding strength. Further increase in cement content leads to negligible increase in strength, up to certain limit. This zone is called inert zone. Addition of cement beyond this zone leads to decrease in strength, which falls in the deterioration zone. Figure 2.3 would give a better idea regarding this. Hence, there exists a cement content beyond which the addition of cement does not result in a commensurate amount of strength gain and is hence, uneconomical. This cement content is referred to as 'optimum cement content' in this thesis.

The explanations for this trend from micro-structural considerations were also provided using SEM analysis. At very low cement content, the micro-structure was similar to uncemented soil, due to insufficient amount of cement. With increase in cement content, more hydration products were found to occupy the pores. The amount of cementitious products also increased, which enhanced the bonding strength and also filled the pores. Hence, in the active zone, the pore volume was significantly reduced, which directly resulted in strength development. In the inert zone, no substantial increase in hydration products and cementitious products were visible. This is because, cement content in excess of active zone does not react much with the clay particles. Hence, pore volume was also relatively unchanged. In the deterioration zone, hydration and cementitious products were significantly reduced. The cement added in this zone was too high that it immediately imbibes the water from the clay and hence, results in reduced hydration and pozzolanic reactions. Therefore, the strength reduces drastically in this zone.
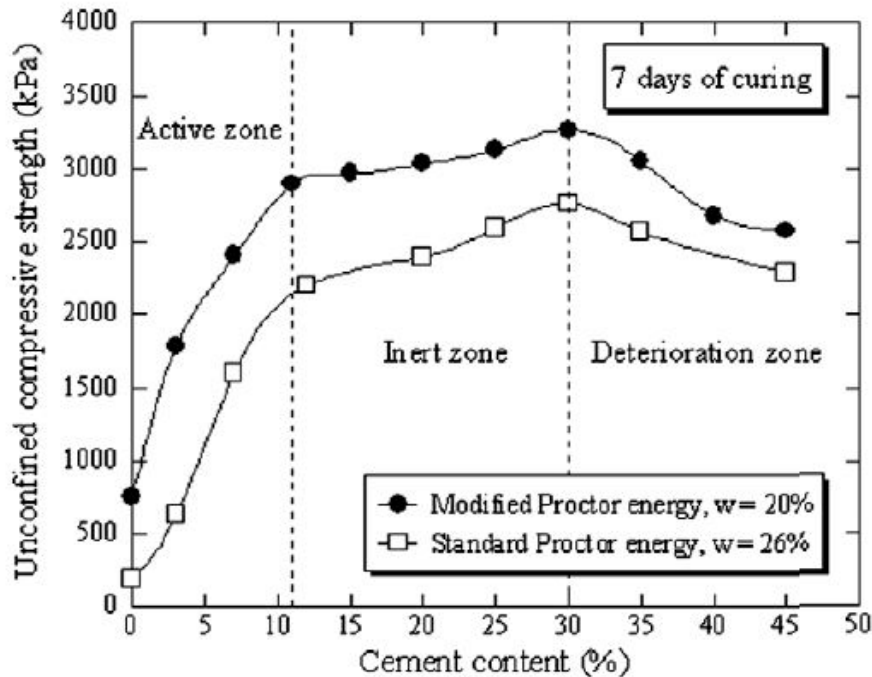
Figure 2.3 Effect of increase in cement content on strength of cement treated clay
(Horpibulsuk et al., (2010)

2.4 DEEP EXCAVATIONS IN SOFT GROUND

2.4.1 Stabilization of Excavation

Severe scarcity of quality land for infrastructure development demands the utilization of underground space for subways, tunnels, deep basements, underground roads and deep sewerage systems. These developments would require deep excavations, mostly near to existing critical structures. Local experience in Taiwan had shown that deep excavations caused excessive ground movements and their effects spread out to a distance of at least three to four times the excavation depth and hence, should be executed with utmost care (Woo and Moh, 1990). The ground settlement associated with any deep excavation is closely related to the type of support system in place, groundwater table, excavation geometry, soil profile and construction procedures (Yoo and Lee, 2008). In some cases, soft ground may be very thick and may exist well below the final excavation level. Consequently, a thick stratum of soft clay would exist up to great depths, even exceeding 50m. In such conditions, carrying out deep excavations would cause uncontrolled ground movements which could have deleterious effects on the adjacent structures. The most conventional solution for the problem would be

14

provision of a strong retaining wall with good support systems. But if soft soil exists well below the final excavation level, the retaining wall would float in the soft soil and consequently suffer maximum deflection below the final formation level (Chew et al., 1997; Kusakabe, 1996; Tanaka, 1993; Wong and Patron, 1993). Provision of struts below this level is impossible and hence cannot solve the problem. Moreover, since struts are installed only after a certain depth of excavation, wall deflection would have already taken place to some degree.

To control the wall deflection below the final formation level of excavation, a more feasible solution is to improve a layer of soft soil to sufficient thickness below this level, prior to carrying out excavation, using ground improvement techniques like deep mixing (DM) and jet grouting (Shirlaw et al., 2006; Tanaka, 1993, 1994; Gaba, 1990; Wong et al., 1998). However, deep mixing is nowadays preferred compared to jet grouting, as it produces less waste and does not cause excessive displacement by virtue of high pressure used in the jet (Lim, 2003).

2.4.2 Embedded Improved Soil Strut or Raft

The efficacy of improving a layer of soil below the excavation depends on the amount of lateral restraint provided by the improved layer against wall deflection and vertical restraint provided against basal heave in the passive side (Kongsomboon, 2002; Lim, 2003; Tan et al., 2003). Usually, the entire soil layer within the excavation zone between the two retaining walls is improved, before excavation commences. The improved layer so formed is called *Embedded Improved Soil Strut (*Kongsomboon, 2002*) or Embedded Improved Soil Raft* (Haibo, 2009). Hence, an embedded improved soil raft refers to a continuously improved composite ground of soil cement columns that overlap with each other and acts like a strut below the excavated ground level (Tanaka, 1993; Lim, 2003). Analysis of such a strut is usually performed by assuming composite values for the entire soil layer. Basically, such a layer will consist of overlapping short columns produced by deep mixing or jet grouting. Successful application of such a raft has been reported by many researchers (O'Rourke and McGinn, 2006; His and Yu, 2005; Kongsomboon, 2002; Wong and Poh, 2000; O'Rourke and O'Donnell, 1997; Nakagawa et al., 1996; Tanaka, 1993). In practice, the properties of this improved layer are verified in the field by taking out vertically cored cylindrical samples and then testing in the laboratory. A weighted average method which summates these elemental properties of soil-cement columns and untreated in-situ soils is then employed to determine

the properties of embedded improved soil raft (Haibo, 2009; Hsiung et al., 2006; Hsieh et al., 2003; Ou et al., 1996). A uniform mobilised stress and strain energy are assumed throughout the improved layer (Wang et al., 2002; Omine et al., 1998). However, some researchers have also made efforts to determine the strength properties mobilised in the lateral direction (Yang et al., 2011; Haibo, 2009).

If the width of excavation is very large, the provision of raft becomes too expensive. In such cases, only a part of the entire width of soil is improved such that it is good enough to provide the necessary restraint. This is called an *Embedded Improved Soil Berm* and is expected to function like a horizontal floating pile (Yaodong et al., 2008; Yaodong, 2004; Lim, 2003; Tan et al., 2003; Kongsomboon, 2002). Since such a berm has only one end in contact with the wall and the other in the soil matrix, analysis is complicated and would require correctly scaled tests like centrifuge studies to understand the mechanisms involved. Figure 2.4 illustrates the concepts of embedded improved soil raft and embedded improved soil berm.

(a)   (b)
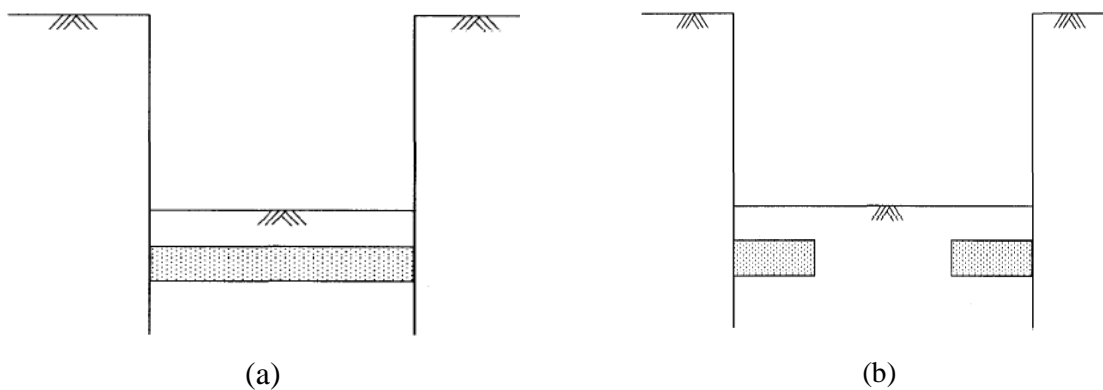
Figure 2.4 (a) Embedded improved soil raft and (b) Embedded improved soil berm
(Yaodong, 2004)

Kongsomboon (2002) carried out extensive centrifuge studies to find out the behaviour of an excavation, stabilised by embedded improved soil. Three models of excavations; TW/O, TST and TB-L100, were considered in centrifuge containers of internal width of 150 mm, length of 400 mm and a depth of 480 mm, and the tests were carried out at a scale of 1:100.

TW/O   =   a normal excavation where no soil was improved

TST   =   an embedded improved soil strut

TB-L100   =   an embedded improved soil berm of length 100 mm with the same thickness as TST and 50 mm of soil left untreated

Figure 2.5 gives the details of different configurations used. The model retaining wall considered in the analysis was made of aluminium alloy with a thickness of 4 mm and embedded 160 mm into the ground. This would represent a concrete diaphragm wall of 0.6 m thickness, embedded to a depth of 16 m into the ground and having an equivalent bending stiffness (*EI*) of approximately 384×10^3 kNm^2/m in prototype scale.
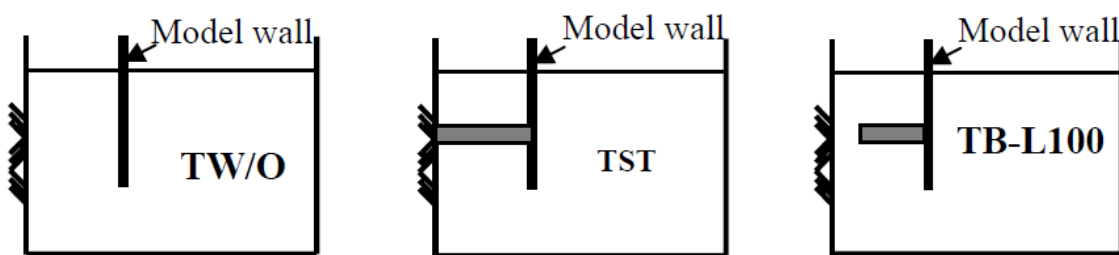
Figure 2.5 Models of excavation (Kongsomboon, 2002)

The performance of each of the configurations were assessed in terms of lateral displacement of the wall measured at a point 30mm above the ground level and the surface settlement of the ground at a distance 50mm behind the wall. Figure 2.6 reveals that TST was extremely effective in controlling lateral wall deflection and ground movements. TB-L100 was also effective in the early stages of excavation, after which it becomes similar to TW/O. This shows that use of a berm should be carefully used as the failure could be sudden and catastrophic. Meticulous design is hence required if an embedded improved berm is to be used.

2.4.3 Plane Strain Analysis of Excavation

A number of excavations with ground improvement mostly require 3D finite element analysis for accurate results. This demands large computer storage and computation time because of the use of a finer mesh. Moreover, the input material properties strongly influence the accuracy of the analysis. Owing to the above problems, many researchers (Finno et al., 1991; Ng and Lings, 1995; Hashash and Whittle, 1996; Ou et al., 1996; Hsi and Yu, 2005; Yoo and

Lee, 2008; Hashash et al., 2010) assumed symmetric *plane strain excavation geometry* for simplified analysis of deep excavations and their results were seen to be in good agreement with the field observations. Certain other researchers (Ou et al., 1996; Finno et al., 2007; Ignat et al., 2015) have compared the results of 3D and plane strain analysis (2D) of deep excavations to understand the validity of such an assumption.
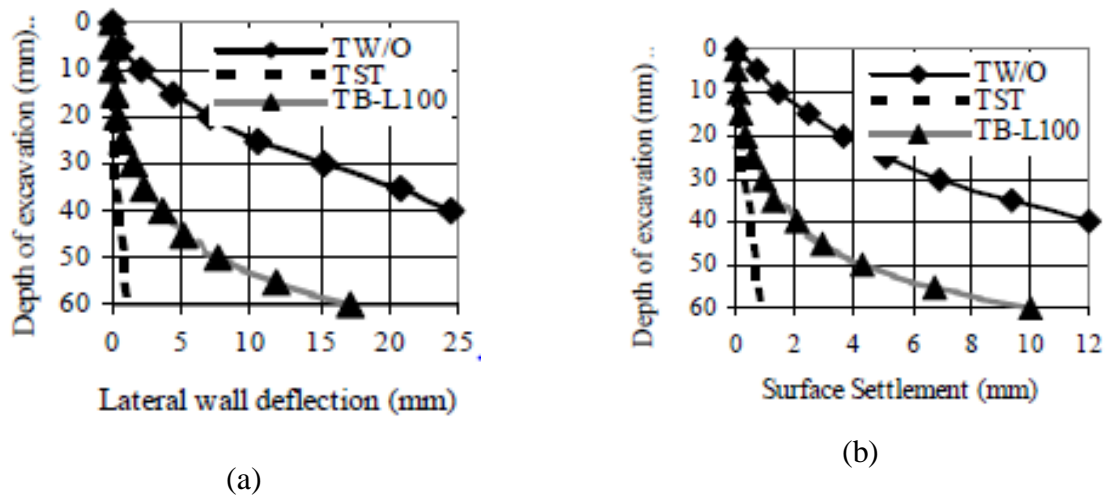
Figure 2.6 Centrifuge test results for different models of excavation (a) Lateral wall deflection and (b) surface settlement (Kongsomboon, 2002)

Finno et al. (2007) did extensive research to find out when an excavation could be suitably modelled as a plane strain problem, considering the fact that deep excavation problems are inherently three dimensional. For this purpose, 3D and plane strain (2D) analyses of the same excavation problems were performed and the results were compared. Two excavation geometries were selected for the parametric studies, viz. 20 x 20 m and 80 x 80 m. Excavation depths of 9.8, 13.4, and 16.3 m were considered. The lateral movement of soil behind the wall was analysed using 3D and 2D plane strain analysis. The results are given in Figure 2.7, where ordinate and abscissa refer to lateral soil movement and excavation depth, respectively. As can be seen in the figure, 3D analysis recorded lesser movements than plane strain simulations for the smaller excavations. However, the results seem to be comparable for larger excavations. The comparison of results was quantified in terms of Plane strain ratio (PSR), which was defined as the maximum movement in the centre of an excavation wall

evaluated by 3D simulation divided by that evaluated by a plane strain analysis. PSR value of nearly one was obtained for L/H_e greater than 6, L and H_e being the length of the side where movements were measured and depth of excavation, respectively. This implies that plane strain and 3D analysis gave similar results for L/H_e greater than 6. However, large variation was observed for L/H_e less than 2, showing that a higher restraint would be provided when excavation is deeper compared to its length.
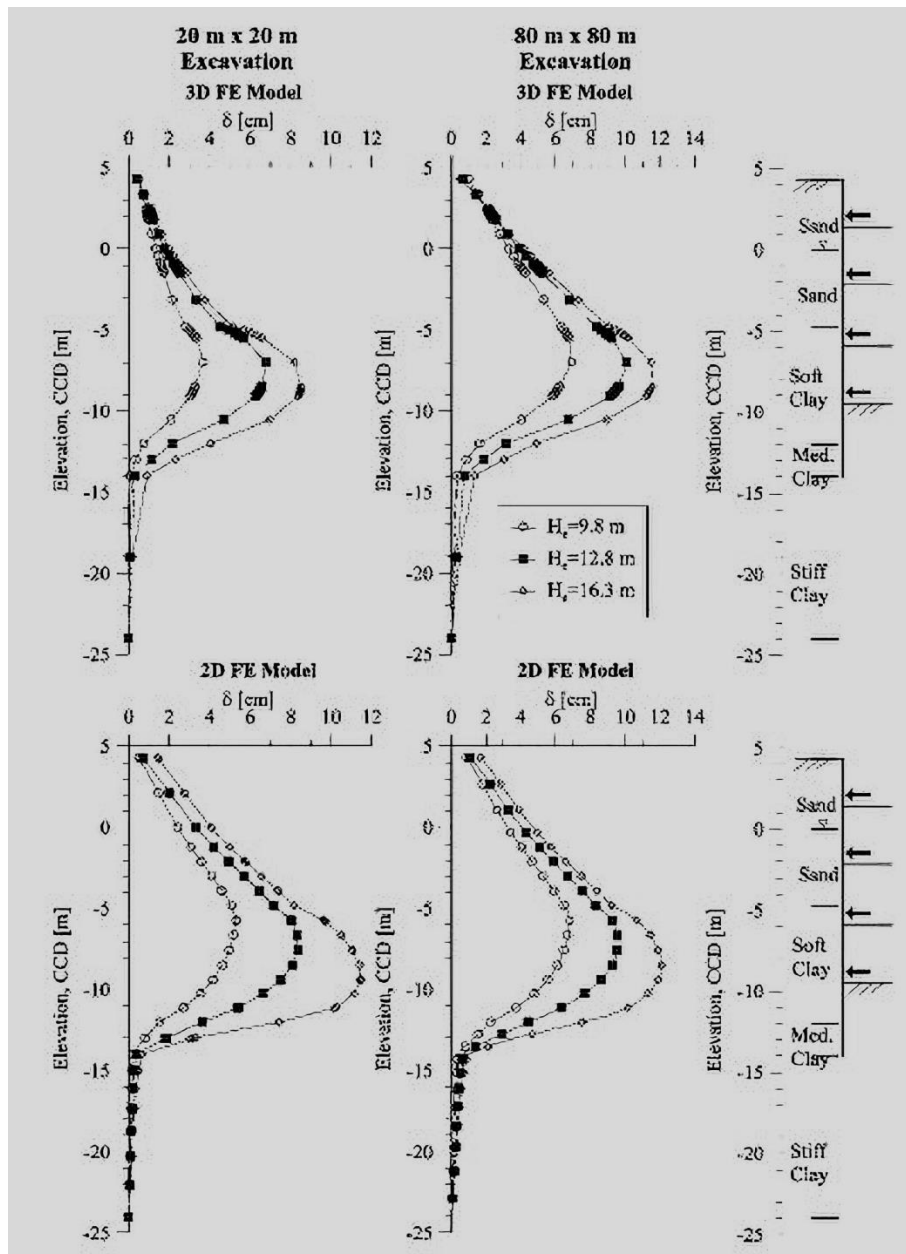
Figure 2.7 Lateral movement of soil behind the wall under 3D and 2D (plane strain) FE analysis (Finno et al., 2007)

Ou et al. (1996) used a 3D Finite Element program for the analysis of a deep excavation with column type of ground improvement in soft clay. Two methods of analyses such as Real Allocation Simulation (RAS) and Equivalent Material Stiffness (EMS) were adopted to study the performance of excavation stabilized by deep cement mixing. RAS method involved assigning actual properties to treated zones and untreated zones separately and then simulating the interaction between soil zones and the excavation support system. EMS method involved employing composite material properties to the entire layer and was used for plane strain analysis. Equation 2.3 was proposed to assess the properties of the composite ground.

$$P_{eq} = P_g I_r^m + P_c(1 - I_r^m) \qquad (2.3)$$

where, P_{eq} = equivalent soil parameters for composite ground; P_g = treated soil parameters; Pc = untreated soil parameters; m = equivalent parameter index; I_r = improvement ratio, defined as the ratio of treated soil area to the total area.

A value of m equal to 1 was used for the case in which external forces act directly on both the untreated soil and treated soil. If the external forces acted on the untreated soil, which in turn transmitted the forces to the treated soil, m equal to 1 cannot be used.

RAS method was quite difficult to perform and required large computer storage and computational time. But 3D EMS method performed using appropriate 'm' value in the above equation yielded wall deflections close to RAS method in a relatively short time and less effort. In addition, a slight modification in equation (2.3) facilitated plane strain analysis possible on column type improvement. In this case, when m value was multiplied by 0.88 in equation (2.3), close agreements were obtained between 3D RAS method and 2D plane strain analysis, which proves that deep mixing application in a deep excavation could be approximated as a plane strain problem.

In the light of the above review, it is evident that deep excavation stabilized by embedded improved soil strut can be approximated as a plane strain problem. It is a common practice to obtain the required properties of soil using laboratory testing and using them to evaluate the field response. If the field problem could be approximated as a plane strain problem, laboratory testing of soil under plane strain conditions would best represent the field

behaviour. It is a common practice among researchers to use properties obtained from triaxial tests and unconfined compressive strength tests as input parameters for the improved layer, while simulating field problems. However, these tests employ axisymmetric configuration and using such results for plane strain excavation problems may result in inaccurate simulation of field behaviour. Some researchers (Hashash et al., 2010) have tried converting the shear strength parameters obtained from triaxial test to plane strain parameters. These conversions are empirical in nature and cannot be used for all types of soils. Hence, conducting plane strain tests in the laboratory and using those results for simulation would be the best practice for better evaluation of performance of excavation and form a major part of this research.

2.5 PLANE STRAIN TESTING OF SOIL

In the Conventional Triaxial Compression (CTC) test, a cylindrical soil specimen of standard dimensions, generally maintaining length to diameter ratio of 2, is stressed under axisymmetric conditions. But most of the geotechnical engineering problems in the field, like earthen dams, retaining wall, deep excavations, embankments, strip footing, etc. can be approximated as plane strain problems, since the shape of construction impedes movement in one direction. Hence, plane strain testing would better represent soils under such conditions. Even though triaxial tests are capable of representing most of the important features of constitutive behaviour of soil, soil behaves differently under plane strain condition (Mita et al., 2004). Furthermore, the transition from homogeneous strains to strain localization cannot be captured by triaxial test as it does not permit unimpeded development of shear bands (Desrues et al., 1985).

In plane-strain (PS) state, the soil is allowed to deform only in two directions and the deformation in the third dimension is zero. The principal stress values would be different in three directions with the intermediate principal stress acting in the restrained direction. Most of the studies in the past to understand the plane strain behaviour of soils are for sand. Plane strain testing of clay has also been performed by some researchers (Vaid, 1968; Hambly, 1972; Mitachi, 1980; Campanella and Vaid, 1974; Topolnicki, 1990; Viggiani et al., 1994; Lo et al., 2000; Mita, 2002; Prashant and Penumadu, 2004; Alshibli and Akbas, 2007; Fauziah and Nikraz, 2008; Wang et al., 2014), but the available data is insufficient to give a comprehensive strength behaviour of clay under plane strain conditions. However, there are limited, or no studies reported on plane strain behaviour of cemented clays. As mentioned

earlier, the embedded improved soil strut or raft provided at the base of excavation could be approximated as a plane strain problem and hence plane strain testing would give a better insight into its behaviour.

2.5.1 Plane Strain Apparatus

The first plane strain testing was conducted by Kjellman in 1936 using a principal stress controlled testing device combining three pairs of rigid plates (Mita, 2002). This apparatus was later used by various other researchers but reported problems of 'corner junction' at the intersection of plates. Thereafter, plane strain testing on a number of highly sophisticated apparatus has been reported. Most of them had arrangements to directly measure the value of intermediate principal stress (out of plane stress), for example, Conforth (1964), Hambly (1972), Drescher et al. (1990), Yasin et al. (1999), Mita (2002) and Wanatowski and Chu (2005).

In order to impose plane strain condition, different researchers used different arrangements. Hambly (1972) used rigid glass plates to achieve plane strain condition. Later some other researchers (Drescher et al., 1990; Viggiani et al., 1994) used rigid walls and tie rods to restrict movement in one direction. Wanatowski and Chu (2005) used steel platens, while many others used acrylic plates (Yasin, 1999; Alshibli et al., 2000, 2004; Alshibli and Akbas, 2007) in order to achieve plane strain condition. Perspex® plates were also often used (Lo et al. 2000, Fauziah and Nikraz, 2008). Table 2.2 gives comprehensive details about the various plane strain devices used by researchers and the corresponding specimen sizes adopted.

The apparatus developed by Wanatowski and Chu (2005) is of interest to this thesis and is shown in Figure 2.8. It was designed for a specimen of size 60 x 60 mm and 120 mm height. The lateral movement in one direction was arrested using platens, fixed in position by a pair of horizontal tie rods. The intermediate principal stress was directly measured using 4 submersible total stress transducers. Drainage was provided by a pair of 38 mm porous stones kept at top and bottom of the specimen. Tests were conducted on Changi sand, which was a marine dredged silica sand. The study intended to capture the strain softening and instability behaviour under plane strain condition.

Table 2.2 Summary of Plane Strain Devices Used

Sl No.	Author	Soil Type	Specimen Size (W x L x H) mm	Measurement of σ_2	Confining Plates
1	Conforth (1964)	Sand	51 x 406 x 102	Null Technique	End Clamp
2	Lee (1970)	Sand	28 x 71 x 61 28 x 71 x 71	No	Stainless Steel
3	Hambly (1972)	Clay	50 x 135 x 135	No	Glass
4	Mitachi and Kitago (1980)	Clay	50 x 50 x 120	Pressure Cells	Rigid
5	Marachi et al. (1981)	Sand	25 x 216 x 101	No	
6	Desrues et al. (1985)	Sand	70 x100 x 130 100 x 100 x 100	No	
7	Tatsuoka et al. (1986)	Sand	40 x 80 x 105	Horizontal Load Cell	Acrylic
8	Peters et al. (1988)	Sand	45 x 114 x 127	4 Instrumented Bars	Lucite
9	Drescher et al. (1990)	Sand	40 x 80 x 140	No	Rigid walls & tie rods
10	Mokni and Desrues (1998)	Sand	100 x 35 x 340	No	Glass
11	Yasin et al. (1999)	Sand	80 x 160 x 200	Horizontal Load Cell	Acrylic & Steel
12	Alshibli et al. (2000)	Sand	83.3 x 80.8 x 152.4	No	Lexan wall
13	Lo et al. (2000)	Clay	40 x 120 x 120	No	Perspex
14	Mita (2002)	Clay	36 x 72 x 85	Using Stress Cells	Rigid walls & tie rods
15	Alshibli et al. (2004)	Sand	60 x 120 x 180	No	Acrylic Plates
16	Wanatowski and Chu (2005)	Sand	60 x 60 x 120	4 Submersible pressure transducers	Stainless Steel Plates
17	Koseki et al. (2005)	Cemented Sand	60 x 80 x 160	Horizontal Load Cell	Plexiglass
18	Alshibli and Akbas (2007)	Clay	48 x 60 x 135 48 x 60 x 129	No	Acrylic
19	Thakur et al. (2017)	Clay	60 x 34 x 120	No	Glass
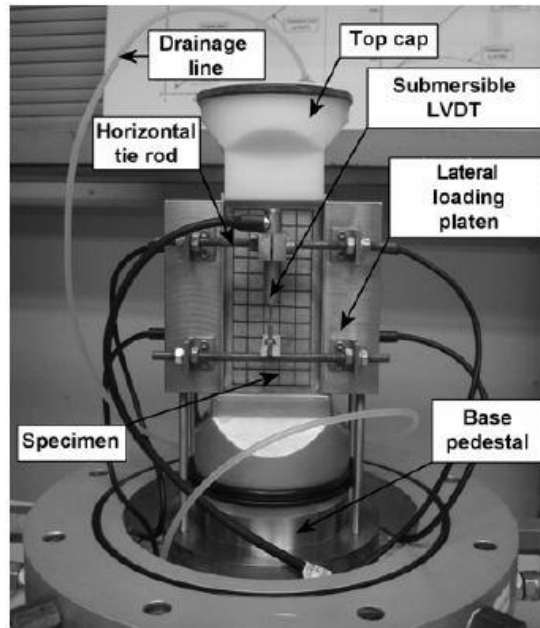
Figure 2.8 Apparatus developed by Wanatowski and Chu (2005)

2.5.2 Comparison of Plane Strain and Triaxial Test Results

The failure modes of specimens tested under PS loading and CTC are different. Peters et al. (1988) proved that the formation of shear bands is highly dependent on the mode of shearing, in case of dense to medium dense sand. It was observed that the initiation of shear bands happened even before reaching peak stress, in case of soil tested under plane strain condition. On the other hand, triaxial test showed a lot of resistance in the development of shear band and resulted in more complex deformation patterns. This was later verified by other researchers (Peric et al., 1992; Mokni and Desrues, 1999; Alshibli et al., 2000, 2003; Alshibli and Akbas, 2007). It is also to be pointed out that shear banding in the hardening regime showed a strong influence on the peak strength value of soil tested under plane strain conditions (Lade and Wang, 2001). Hence, extensive experimental investigation is essential to clearly understand the differences in behaviour of soil tested under plane strain and axisymmetric conditions.

For tests on sand, higher shear strength parameters were obtained under plane strain condition compared to axisymmetric condition. This difference was also found to increase with increase in confining pressure and specimen density (Conforth, 1964; Lee 1970; Hambly, 1972; Marachi et al., 1981; Peters et al., 1988; Alshibli et al., 2000, 2003, 2004; Wanatowski and Chu, 2007). Furthermore, PS specimens failed at higher peak stress and showed severe

softening post peak behaviour compared to CTC specimens at lower confining pressures (Alshibli et al., 2000, 2003; Wanatowski and Chu, 2007). For higher confining pressures, PS specimens and CTC specimens gave relatively same peak stress values and the amount of softening was also found to be minimal. Lee (1970) carried out drained and undrained tests on saturated fine-grained sand under triaxial and plane strain loading conditions and observed that plane strain specimens attained higher principal stress ratio compared to triaxial specimens. Typical stress-strain plots obtained for plane strain and triaxial tests obtained by Marachi et al. (1981) and Lee (1970) are given in Figures 2.9 and 2.10, respectively.

Alshibli and Akbas (2007) performed plane strain and triaxial tests on NC clays and reported the same trend as in sands. The undrained shear strength was found to be higher in case of plane strain specimens compared to triaxial testing. Typical plots are given in Figure 2.11. In both cases, specimens were consolidated and then sheared under undrained conditions. They observed that plane strain specimens developed distinct shear bands whereas triaxial specimens underwent diffuse bulging failure. This pattern was earlier observed by various other researchers in case of sands (Peric et al., 1992; Desrues, 1998; Alshibli et al., 2003). Most importantly, shear bands were initiated in plane strain specimens in the hardening regime, i.e. before reaching peak stress. This is as per the experimental findings of previous research done on sand (Desrues et al., 1985; Peters et al., 1988). But it was also pointed out that plane strain specimens consolidated under K_0 condition gave normalized undrained shear strength values close to triaxial conditions.

Chang et al. (1999) reported the same trend as Alshibli and Akbas (2007), in case of NC soils. But in case of heavily OC soils, the normalized shear strength ($s_u/\sigma_{v\,max}'$) in triaxial test (TXCK0UC) was found to be higher than that in plane strain test (PSCK0UC). In fact, $s_u/\sigma_{v\,max}'$ was found to decrease with OCR. This reverse trend was found to be in line with the findings of Koutsoftas and Ladd (1985) as shown in Figure 2.12.

Furthermore, plane strain specimens failed at lower strains compared to triaxial specimens in case of sands as well as NC clays (Peters et al., 1988; Alshibli et al., 2003; Alshibli and Akbas, 2007). This could prove to be dangerous on the field. In addition, in triaxial compression test the axisymmetry is lost upon initiation of shear band and hence the reliability of post peak results becomes arguable (Peters et al., 1988). Thus, plane strain test gives a better representation of post peak behaviour, since plane strain condition is maintained even after shear band formation.
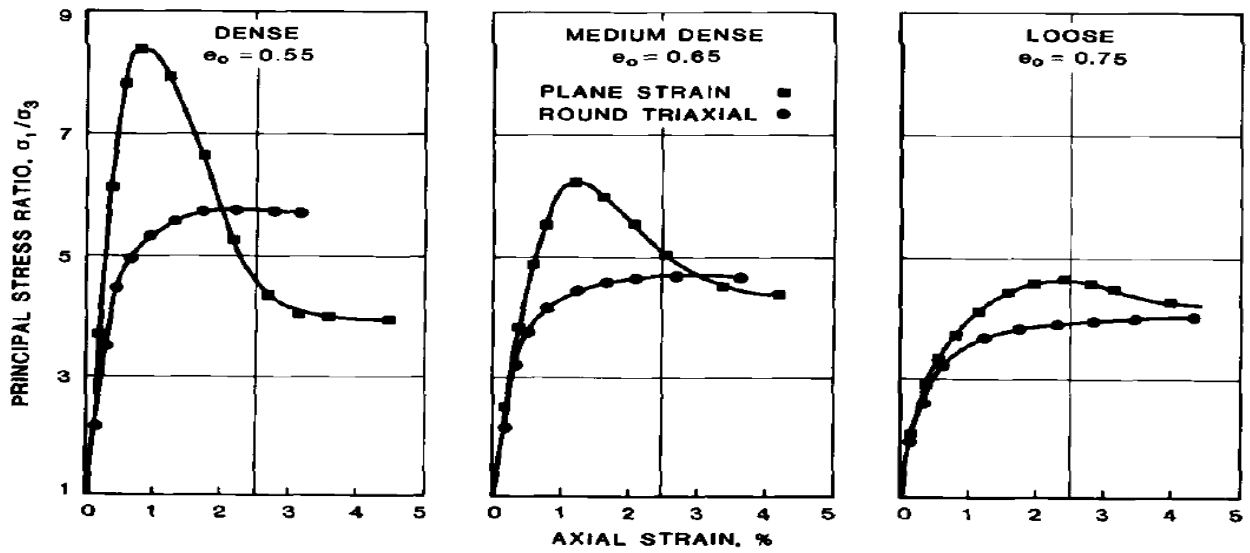
Figure 2.9 Stress-strain relationship for plane strain and triaxial specimen at $\sigma_3 = 70$ kPa

(Marachi et al., 1981)
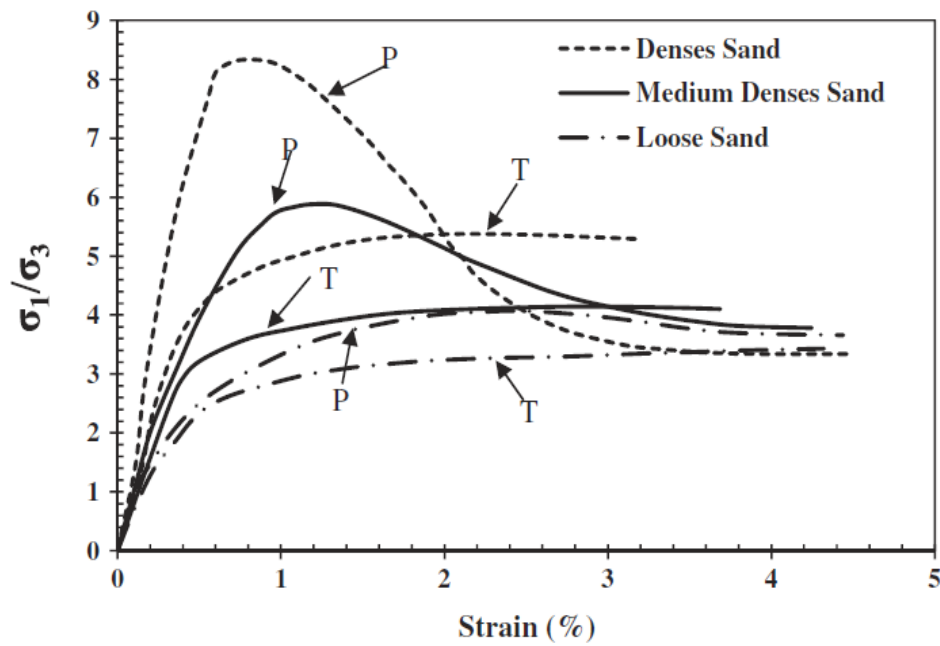
Figure 2.10 Comparison between plane strain and triaxial tests in sands (Lee, 1970)
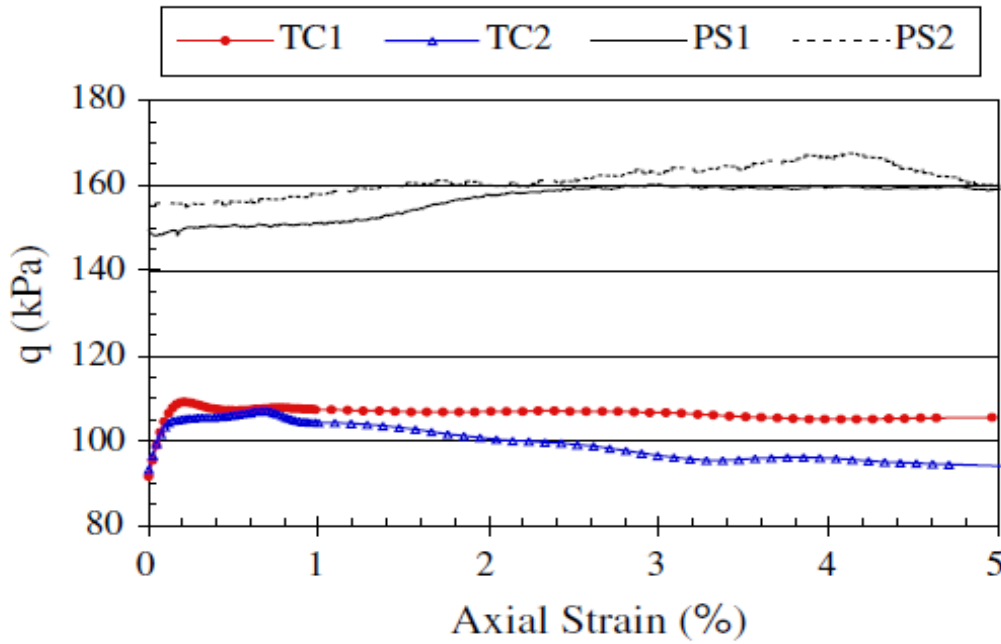
Figure 2.11 Comparison between plane strain and triaxial tests in normally consolidated clays

(Alshibli and Akbas, 2007)
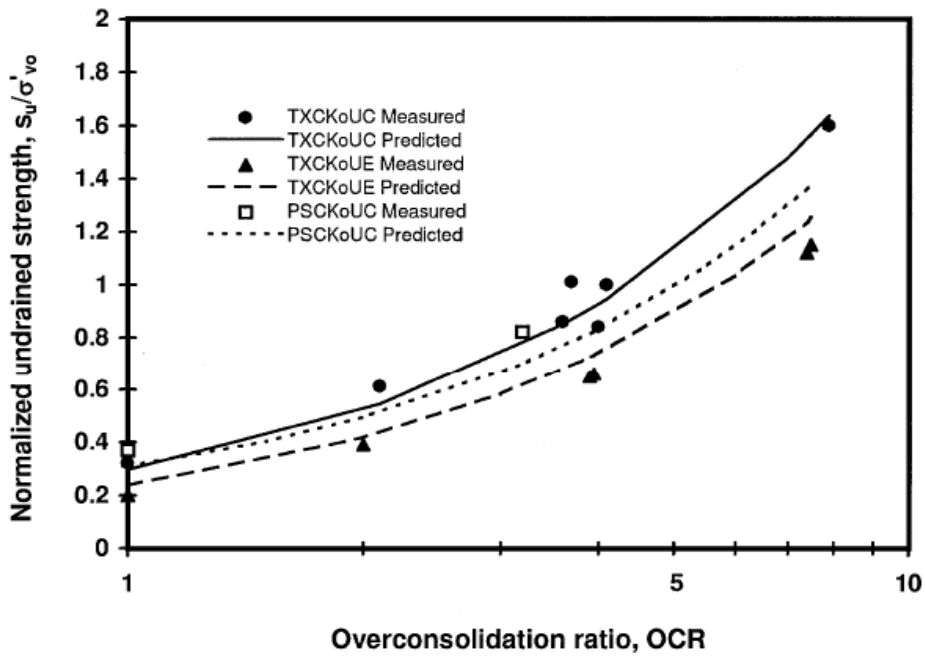
Figure 2.12 Predicted undrained strength ratio for various shear modes for an offshore plastic

clay (data from Koutsoftas and Ladd, 1985 and Chang et al., 1999).

From the above review, it is clear that soil behaves differently under plane strain and triaxial testing conditions. However, this aspect needs to be investigated for cement treated clays.

2.5.3 Issues in Plane Strain Testing

Peric et al. (1992) carried out extensive work to investigate the susceptibility for bifurcation of sample loaded under different configurations, by studying the discontinuous bifurcation solutions for elasto-plastic solids. It could be analytically proved that plane strain test is more susceptible to bifurcation compared to triaxial test. This aspect had already been proven experimentally by Marachi et al. (1981) and Peters et al. (1988). Peric et al. (1992) also added that the intermediate principal stress value (stress in the restrained direction) in plane strain test keeps on continuously changing and is the reason for bifurcation. On the other hand, restriction on this out of plane stress in case of triaxial test provides resistance to bifurcation.

Another important aspect is measurement of intermediate principal stress (σ_2). As pointed out in Table 2.2, many researchers have resorted to direct measurement of σ_2. This, however, requires special arrangements and hence some others have evaluated σ_2 by calculation. The latter, however, requires accurate determination of Poisson's ratio. Usually, for clays subjected to undrained loading, a Poisson's ratio of 0.5 is used. But since cement treated soils exhibit limited lateral deformation compared to natural soils, value of 0.5 needs not to be correct. Literature does not give a clear indication about the value of Poisson's ratio to be adopted for cement treated clay under undrained condition.

For most of the geotechnical applications involving cement treated fine grained soil under drained loading, Poisson's ratio of 0.15 to 0.35 is usually adopted (Newcomb and Birgisson, 1999). Variation of predicated peak strength using the above range was found to be 14% (Mita, 2002). Hence, an average value of 0.25 has been adopted by some researchers under drained condition (Mita et al., 2004; Liu et al., 2006). Ou et al., (1996) assumed a drained Poisson's ratio of 0.3 before failure and 0.49 near or at failure. Some other literatures (CDIT, 2002; Bruce et al., 2013) state that Poisson's ratio of in-situ cement treated soil can be taken as 0.25 to 0.45, irrespective of unconfined compressive strength.

2.6 NUMERICAL ANALYSIS OF EXCAVATIONS STABILIZED BY CEMENT TREATMENT

Two-dimensional and three-dimensional numerical analyses of cement-admixed soil slab in deep excavations have been carried out by many researchers (Pan et al., 2019; Wang et al., 2019; Pan et al., 2018; Dong et al., 2016; Modoni et al., 2016; Liu et al., 2015; Li et al., 2011; Yang et al., 2011; Lee et al., 2010; Lim, 2003; Kongsomboon, 2002; Chew et al., 1997). Some other researchers (Hsieh et al., 2003; Ou et al., 1996) analysed excavations stabilized by deep cement mixed columns beneath the final formation level, by assigning equivalent soil properties for the entire composite layer. In other words, the analysis is similar to that of cement-admixed soil slab and hence, can be considered to be the same type of stabilization considered in this study.

Lee et al. (2010) highlighted that two-dimensional analysis should not be carried out in case of complex excavation problems, which are inherently three-dimensional. The authors opined that the large scale collapse of Nicoll highway in Singapore could have been averted, had a three-dimensional analysis noticed the criticality of the eastern end of excavation. However, three-dimensional analysis should be carried out with utmost care and are extremely complex to model. Hence, for most of field excavation problems stabilized by a cement treated soil slab at the base, researchers have settled for a two-dimensional plane strain analysis. Careful plane strain analysis has helped in obtaining reasonably accurate results (Hsi and Yu, 2005; Rutherford, 2004; Hsieh et al., 2003).

In design, the cement treated soil layer is analysed as a uniform Tresca material under undrained condition, wherein the strength is assumed to be one-half of the unconfined compressive strength (Liu et al., 2015; Li et al., 2011; Yang et al., 2011; Kongsomboon, 2002). However, some researchers pointed out that this approach has many deficiencies, explained as follows. Cement treated clay has a relatively high coefficient of consolidation owing to its high stiffness (Tyagi et al., 2017). Hence, cemented soil layer is essentially not under undrained condition. Xiao et al. (2014) noted that loading and drainage conditions influence the behaviour of cement treated clay, ranging from strain softening to strain hardening. At very high effective confining pressures, cement treated clay undergoes structural collapse resulting in reduced deviator stress at yielding. Hence, assuming the strength as half of unconfined compressive strength may be unconservative. Furthermore, a Tresca material is assumed to have infinite tensile strength. However, the tensile strength of

cement treated clay has been reported as 12 to 16% of unconfined compressive strength (Pan et al., 2016). Hence, use of Tresca model for cement treated clay may not be conservative. Furthermore, imperfect mixing and positioning error which are unavoidable in deep cement mixing leads to spatial variability in cement treated clay (Pan et al., 2018; Liu et al., 2015; Chen et al., 2016; Namikawa and Koseki, 2013). Hence, use of a single strength value becomes questionable.

In short, the conventional approach followed for analysis of cement treated clay slab in excavation problems suffer from the above setbacks. Pan et al. (2019) suggested the following improvements in design.

1. Cement treated soil slab is not necessarily under undrained conditions. It ranges from nearly undrained to drained conditions. While, undrained loading leads to quick rise in stress levels and subsequent collapse, drained loading leads to very large displacements. Hence, the design should consider the drainage conditions existing on the field.

2. The global strength and stiffness values are highly affected by random spatial variation in cement treated clay. Hence, the global behaviour of cement treated clay should be assessed considering the spatial variation in strength and modulus. Such a design approach was proposed by Liu et al. (2015), and then further developed by Pan et al. (2019).

3. The design framework should consider the effect of confining pressure.

2.7 CONSTITUTIVE MODEL FOR CEMENT TREATED CLAY

The mechanical behaviour of engineering materials is generally explained using constitutive models. Simple elasto-plastic models like Mohr-Coulomb model have gained wide acceptance due to their clarity and simplicity. The inability of these models to capture the key features of certain geomaterials has forced researchers to develop complex models involving multi yield surfaces. However, these complex models with too many parameters should be carefully used, as it may lead to hidden inaccuracies and numerical instability (Wroth and Houlsby 1985). It is rather desirable to develop simple constitutive models involving minimum number of input parameters and capable of capturing the core features of the soil under consideration. The numerical simulation of excavations stabilized by cement treated

soil slab becomes effective and reliable, only when the right constitutive model is selected for the cement treated soil layer.

It is well understood that, for cement treated clays, the natural structure of clay is altered by the formation of a soil-cement structure in between the soil particles. Hence, the behaviour of such stabilized clays is entirely different from the actual clay in its natural or reconstituted state. Selection of a good constitutive model for cement treated clays has been a topic of research for quite a long time. One characteristic feature observed in cement treated clays is strain softening behaviour post peak deviator stress. This happens due to crushing of soil-cement structure (Lee et al., 2004). Researchers have developed various constitutive models to capture this behaviour. In general, two broad categories of constitutive models have been in use for cement treated clays, viz. (i) critical state framework models and (ii) a combination of bounding surface plasticity and multi surface kinematic bubble models (Yapage and Liyanapathirana, 2017). Important models based on critical state framework were proposed by Gens and Nova (1993), Kasama et al. (2000), Vatsala et al. (2001), Liu and Carter (2002), Liu et al. (2006), Horpibulsuk et al. (2010), Suebsuk et al. (2010) and Taiebat et al. (2010). These models could capture softening plasticity by employing the concepts of yield, plastic potential surfaces and softening rules. These models are quite efficient and remain the popular choice among researchers. However, most of these models involved several input parameters of which some of them have no clear physical meaning. The use of these models for simulating field problems is difficult.

To account for the shortcomings of conventional elasto-plastic models, constitutive models combining the bounding surfaces and multi-surface kinematic bubble models were proposed by many researchers (Kavvadas and Amorosi, 2000; Rouainia and Wood, 2000; Wheeler et al., 2003; Lee et al., 2004 and Baudet and Stallebrass, 2004). These models were developed to capture stiffness non-linearity in the elastic domain, stress history dependency of the material and also introduced damage type mechanism to capture bond degradation. These models can simulate the most complex behaviour of cemented soils, including cyclic loading and unloading. However, these models do not consider the cohesion value in cemented soils and crushing of soil-cement structure, which are the most important features observed in laboratory tests. Moreover, the incorporation of these models into numerical platforms is often cumbersome as it involves too many parameters and hence, their application is generally limited.

A simple constitutive model would be ideal, involving minimum number of parameters which could be conveniently obtained from laboratory triaxial tests and which could be readily incorporated into a numerical software package. One such model was proposed by Yapage and Liyanapathirana (2017), by extending the Mohr-Coulomb model to incorporate the strain softening behaviour of cement treated clay. Softening was introduced by varying the mobilised friction angle, dilation angle and cohesion, as linearly decreasing functions of plastic deviatoric strains. The input parameters used were the peak and residual values of friction angle, dilation angle, cohesion and plastic deviatoric strain. These parameters were derived from the laboratory triaxial tests. This model could simulate the behaviour of cement treated clay with reasonable accuracy. However, the model assumes linear failure envelope for cement treated clay, to obtain the shear strength parameters. The non-linearity in failure envelope of cement treated clay has already been established in the literature (Consoli et al., 2012; Sharma et al., 2011; Asghari et al., 2003). Use of a non-linear constitutive model is hence, desirable to realistically capture the behaviour of cement treated clay. Often, a lot of emphasis is given to capture the strain softening behaviour after peak deviator stress. However, owing to the brittle nature of cement treated clay, the specimen undergoes breakage soon after peak deviator stress is achieved. Moreover, in field problems, peak strength of cement treated clay is mainly focussed (Pan et al., 2018). Hence, reasonable simulation of the behaviour of cement treated clay up to the peak deviator stress would be sufficient.

For analysis of cement treated soil slab in excavation problems, researchers have used different constitutive models. Kongsomboon (2002) utilised the conventional Mohr-Coulomb model to analyse the improved layer, in an effort to simulate the centrifuge tests undertaken by the author (as explained in section 2.4.2). Reasonably accurate results were obtained with the use of this simple constitutive model. The same model was successfully used for improved layer for the simulation of MRRB project in Taiwan (Hsieh et al., 2003), KPE project in Singapore (Hsi and Yu, 2005) and Common services tunnel in Singapore (Lee et al., 2010; Wang et al., 2019). The cement treated soil slab was assumed to follow the Tresca criterion under undrained condition in all the above cases. Hence, the cement treated layer was provided with zero friction and cohesion equal to half the unconfined compressive strength, with Poisson's ratio equal to 0.5. However, some researchers (Pan et al., 2019, 2018; Liu et al., 2015; Chen et al., 2016; Xiao et al., 2014; Namikawa and Koseki, 2013) pointed out serious deficiencies for the use of this approach in excavation problems. This was

discussed in detail in the previous section and will not be repeated herein. More advanced effective stress models (like C3 model) have been proposed by many other researchers (Pan et al., 2019, 2018) to take care of random spatial variation in cement treated slab, lateral compression forces on the slab, actual drainage conditions in the field, the effect of confining pressure, etc. The bottom line is, as Tyagi et al. (2017) pointed out, Mohr-Coulomb model is still the most popular model used for cement treated clay. The absence of a simple alternative has made the researchers overlook the other complexities associated with the field problems.

2.8 SUMMARY OF LITERATURE REVIEW

Based on the review above the important findings relevant to this research are summarised as follows:

The provision of a cement treated soil slab below the final formation level of an excavation, called embedded improved soil strut or raft, is greatly effective in controlling the lateral deflection of retaining wall, especially when the wall floats in soft clay. Most of the excavation problems can be analysed as plane strain problems, provided there are no major complexities involved. Hence, this cement treated soil slab can be also analysed as a plane strain problem, as it covers the entire plan area of excavation. However, the properties of this improved layer are often determined in the laboratory, under axisymmetric condition. Unconfined compressive strength tests and triaxial tests are commonly used to determine the properties of cement treated clay. Ideally, the properties of cement treated clay should be determined under plane strain condition, to best represent this field condition. Unfortunately, no study till date, has addressed this issue. In the least, no study has been reported, exploring the characteristics of cement treated clay under plane strain condition. Hence, the behaviour of cement treated clay under plane strain condition should be first established. These properties should be then used to represent the properties of cement treated slab in an excavation problem.

Though Mohr-Coulomb model is the most popular model used for cement treated soil, it follows a linear failure envelope. Cemented soils exhibit non-linear nature and hence, a non-linear constitutive model is ideal. However, most of the advanced models available in the literature are too complicated and their use is limited. Hence, a simple non-linear model which can represent most of the features of cement treated clay still needs to be developed.

From the above literature review, the research gaps have been identified and are listed below:

- The behaviour of cement treated clay under plane strain condition needs to be established. A Comparison of these results with the results under triaxial condition would give a better idea about the behaviour of this geomaterial under different field conditions.

- For an excavation stabilized by deep mixing, the input properties for cement treated layer should be ideally from plane strain testing.

- Most of the advanced constitutive models which are available for cement treated soils are quite complicated. Hence, a simple model which can represent most of the features of cement treated soils including the non-linear characteristics would be ideal.

CHAPTER 3

EXPERIMENTAL PROGRAMME AND METHDOLOGY

3.1 INTRODUCTION

Cement treatment is a popular ground improvement technique adopted for soft and problematic clays like soft marine clays. In India, marine clays exist in abundance along the coastal belt and are characterized by low shear strength and high compressibility characteristics. These soils pose problems for geotechnical structures and are often improved by cement treatment. Hence, marine clay was selected for this study.

For excavations carried out in thick deposits of soft clays, the clay below the final excavation level is often improved by deep cement mixing or jet grouting, to control the lateral deflection of retaining wall below the final excavation level. This soil-cement slab so formed, called embedded improved soil strut, exists under plane strain condition. Therefore, ideally the properties of cement treated clay should be determined under plane strain testing conditions, for accurate analysis of the above excavation problem.

As brought out in Chapter 1, one of the main objectives of this study is to compare the shear strength behaviour of cement treated clay under plane strain and triaxial testing conditions. The following experimental programme was planned to achieve the above objective.

1. Procurement of sufficient quantity of marine clay
2. Determination of basic properties of clay
3. Preparation of specimens for testing
4. Determination of optimum remoulding water content for mixing with cement
5. Unconfined compressive strength of cement treated clay specimens
6. Tensile strength of cement treated clay
7. Triaxial testing of cement treated clay

8. Development of plane strain testing apparatus and testing.

Triaxial and plane strain tests will be discussed in detail in Chapter 4. Rest of the experimental programme will be discussed in this chapter. The scope of this experimental programme is limited to cement contents of 10%, 15% and 20%, which are typically used in Deep Soil Mixing applications.

3.2 MATERIALS AND METHODS

About 2.5 cubic metres of marine clay was procured from National Institute of Ocean Technology (NIOT) campus, Chennai, India. The soil had large amounts of shells and other coarse substances. Hence, it was necessary to process the soil to remove the shells and other foreign materials before testing. The soil was first thoroughly air dried by placing them on tarpaulin sheets under the Sun for few weeks. The entire quantity of soil was then pulverised. Only the fraction passing through standard 1 mm IS sieve size was used for the experimental programme. The processed soil was stored in airtight bins to avoid contamination and ingress of moisture.

OPC 53 grade Portland cement was used for cement treatment. 100 kg of cement was procured. Since properties of cement get altered if exposed to atmosphere or moisture, small quantities of cement were packed in zip lock covers and were then stored in airtight bins. Quantity of cement in each zip lock cover was selected such that one portion would be sufficient for one batch of sample preparation. This ensures that the rest of the cement is not contaminated.

3.2.1 Basic Properties of Soil

The basic properties of the soil were determined as per Indian Standard testing procedures, mentioned in various parts of IS 2720. Atterberg limits such as liquid limit and plastic limit were determined as per IS 2720 (Part 5) – 1985. Liquid limit was determined using Casagrande apparatus and plastic limit was determined using thread rolling method. Shrinkage limit was found out using shrinkage dish method mentioned in IS 2720 (Part 6) – 1972. The values of Atterberg limits are listed in Table 3.1.

Grain size analysis was carried out in accordance with IS 2720 (Part 4) – 1985. The soil was initially wet sieved through 75µ IS sieve. The portion retained on the sieve was oven dried and subjected to dry sieve analysis. The fraction passing through 75µ was analysed by hydrometer analysis. The combined grain size distribution curve was established by combining the dry and wet sieve analysis results and is shown in Figure 3.1. The percentage sizes of sand, silt and clay were then determined. Based on the Atterberg limits and grain size details, the soil is classified as CH, as per IS 1498 (1970). Specific gravity of the soil was determined using density bottle method, as per IS 2720-Part 3 (1985). pH of the soil was determined using electrometric method described in IS 2720 (Part 26) – 1987. Organic content was found out using loss of ignition method, in accordance with ASTM D2584 (Part 18). All the basic properties of the soil are given in table 3.1.

Table 3.1 Basic properties of soil

Soil Properties	Values
Liquid Limit (%)	59
Plastic Limit (%)	24
Plasticity Index (%)	35
Shrinkage Limit (%)	11
Sand (%)	43
Silt size (%)	20
Clay size (%)	37
Specific Gravity	2.71
pH	7.65
Electrical Conductivity (milli Siemens)	3.11
Organic content (%)	
(Loss of ignition method)	2.83
Activity	0.95
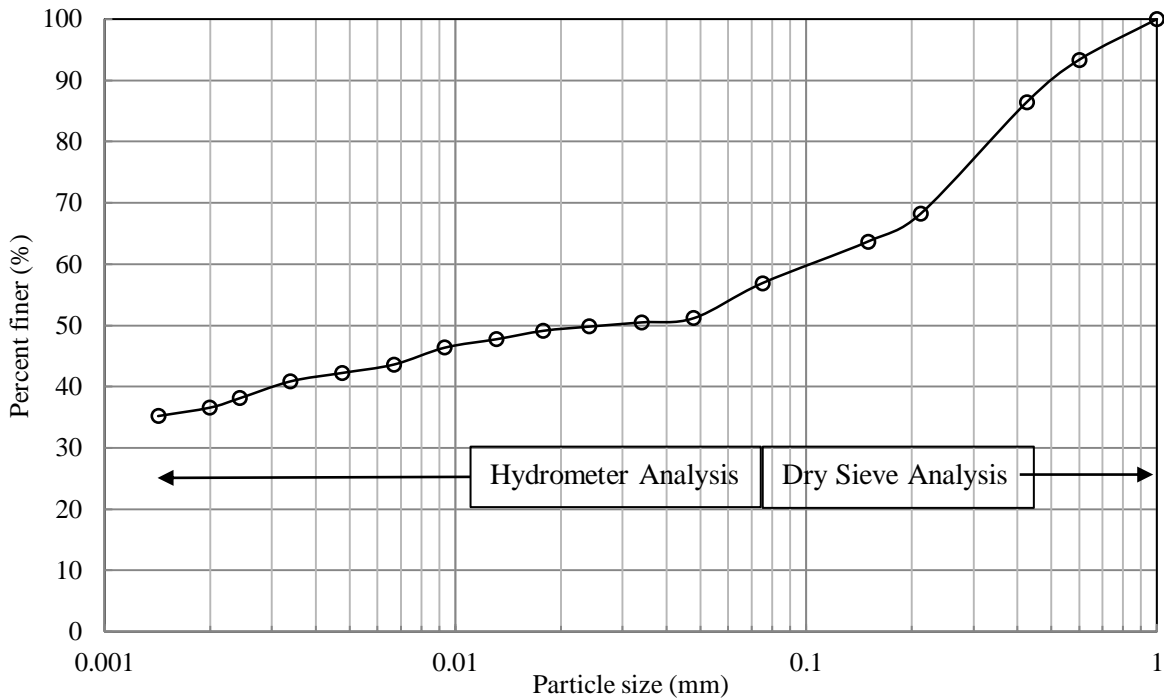
Figure 3.1 Grain size distribution curve

3.2.2 Mixing of Cement in Clay

Two types of mixing techniques are generally used for mixing soil with cement; wet mixing and dry mixing. Cement is added in slurry form in case of wet mixing and in powder form in dry mixing. Dry mixing does not ensure homogeneity and adequate workability. This method is only adopted when clay has excess moisture. On the other hand, wet mixing results in a homogenous mix, owing to better distribution of slurry across the area, pre-hydration of cement, longer mixing time, and hence results in higher strength (Tan et al., 2002). Hence, this method was used in this study.

The amount of water available in clay before mixing plays a crucial role in strength development. Water added to clay before the addition of cement, called as remoulding water content, w^* (Lorenzo and Bergado, 2004), plays a very important role in strength of cement

treated soils. The remoulding water content at which the cement treated sample gives highest strength will be called optimum remoulding water content in this study and must be carefully determined. For this purpose, cement treated specimens were prepared at various remoulding water contents, ranging from 1 to 2 times the liquid limit of base soil. Three specimens were prepared for each water content. Remoulding water content was calculated based on weight of soil solids. The moisture content already present in the air dried soil sample was also accounted for, in the calculation. The water-cement ratio required to ensure complete hydration of a cement mix is 0.42 (Neville, 1995). A water-cement ratio of about 0.6 has been adopted by some researchers (Lorenzo and Bergado, 2004; Bushra and Robinson, 2012). Cement was introduced in slurry form, at the same water-cement ratio of 0.6. Cement content was calculated in terms of dry weight of soil and samples were prepared at 10% cement content. All the specimens were cured in a desiccator for 28 days before testing. The temperature and relative humidity in the desiccator were 25 ± 3 degree Celsius and close to 95%, respectively. Unconfined Compressive Strength (UCS) tests were then performed on these specimens. Testing was performed at a deformation rate of 0.625 mm/min, as per guidelines in IS 2720 (Part 10) - 1991. The average UCS (of three specimens) values recorded for each remoulding water content were plotted against the corresponding remoulding water contents (normalised by liquid limit of base clay), as shown in Figure 3.2. As can be seen in the figure, the highest UCS value was recorded by specimens prepared at 1.20 times the liquid limit of base clay. Hence, this remoulding water content was considered as the optimum remoulding water content and all the specimens henceforth, will be prepared at this water content. Similar optimum water content was reported in the previous studies and this value is not expected to get altered at different cement contents (Lorenzo and Bergado, 2004; Bushra and Robinson, 2009 and 2012).

Having established the optimum remoulding water content, the following procedure was followed for preparing cement-admixed clay.
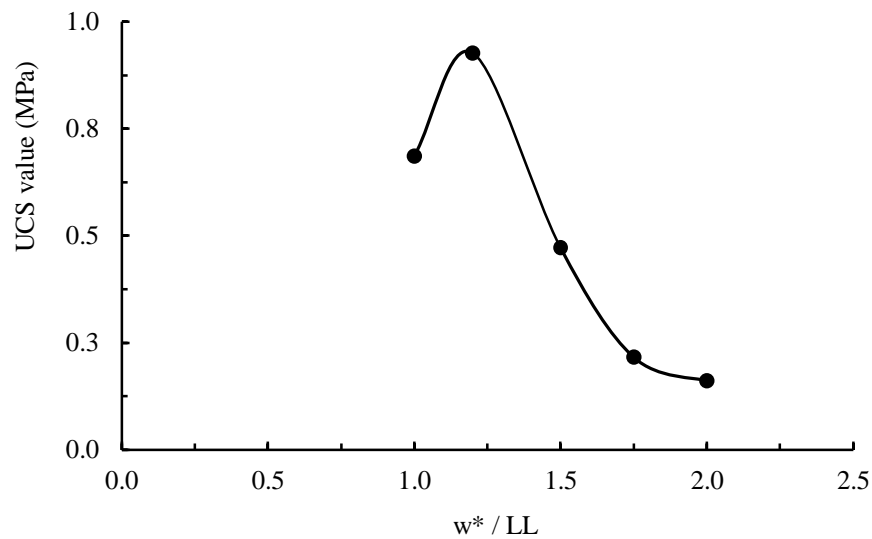
Figure 3.2 Determination of remoulding water content

- The required quantity of clay was taken.

- The moisture content of soil sample was noted.

- Amount of water equal to optimum remoulding water content was added to the clay sample.

- The mixture was mixed well in a Hobart mixer for at least 20 minutes.

- The required quantity of cement was taken in a bowl.

- Water was added to this cement, for a water-cement ratio of 0.6.

- The cement slurry was added to the clay-water mix and the entire mixture was thoroughly mixed in a Hobart mixer for 10 minutes.

- The sample was poured into the prescribed moulds layer by layer, providing good tamping at each layer. Silicon grease was applied inside the moulds to help in easy ejection of specimen.

- After 1 day of casting, the specimen was taken out of the mould and trimmed for the required height. The specimens were wrapped in cling films and cured in desiccator for 28 days.

3.3 STRENGTH TESTS ON CEMENT TREATED CLAY

The strength of cement treated clay was first determined with the help of two most popular and simple tests, viz. unconfined compression strength tests and tensile strength tests.

3.3.1 Unconfined Compressive Strength Tests

The unconfined compression test is by far the most popular method of soil strength testing because it is one of the fastest and cheapest methods of measuring shear strength. The method is used primarily for saturated, cohesive soils recovered from thin-walled sampling tubes. The unconfined compression test is inappropriate for dry sands or crumbly clays because the materials would fall apart without lateral confinement. Since, cement treated clays have inherent cohesion and can withstand their self-weight, this test can be easily used. Hence, many researchers have relied upon this testing method to verify the effectiveness of cement stabilization (Uddin et al., 1997; Consoli et al., 2007).

In the present study, UCS tests were conducted on cylindrical specimens of 50 mm diameter and 100 mm height. Guidelines given in IS 2720 (Part 10) – 1991 was followed for testing. A deformation rate of 0.625 mm/min was selected for shearing. Specimens were prepared in the method mentioned in the previous section. Two to three specimens were prepared for each cement content and the average of UCS values was designated as the UCS value for each cement content. Average UCS values of specimens prepared at cement contents ranging from 5% to 30% are given in Table 3.2. The stress-strain curves of UCS tests for different cement contents are shown in Figure 3.3.
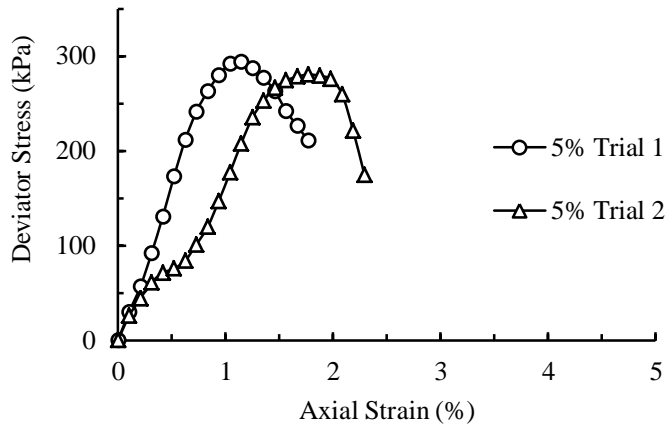
(a)
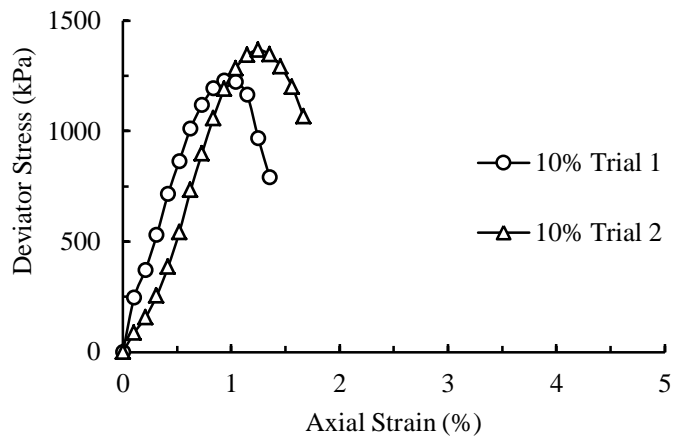
(b)
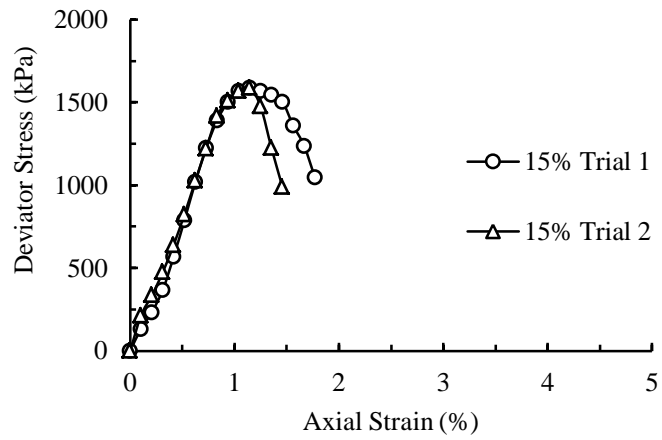
(c)
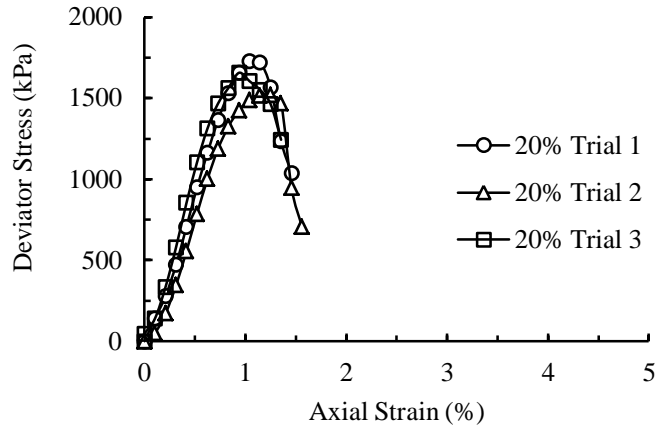
(d)
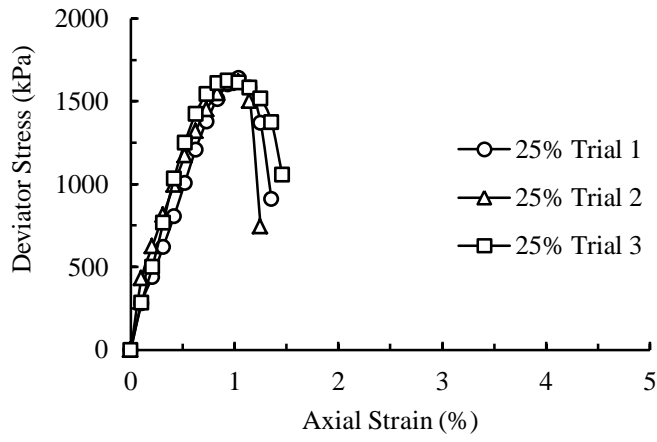
(e)
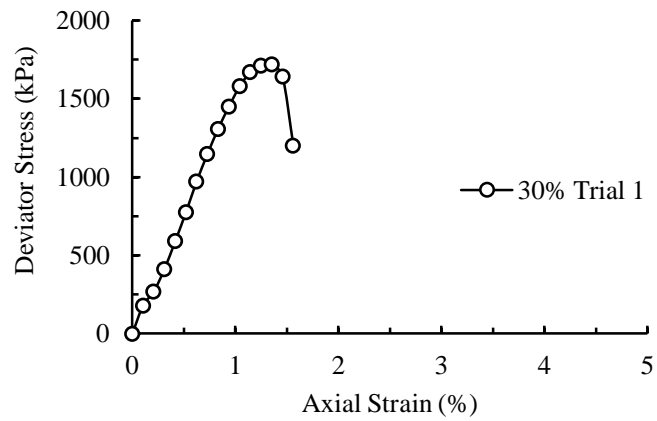
(f)

Figure 3.3 UCS results for cement contents of (a) 5% (b) 10% (c) 15% (d) 20% (e) 25% and (f) 30%

As can be seen in Table 3.2, an abrupt increase in UCS value by around 351% was visible with increase in cement content from 5% to 10%. About 23% increase was found when cement content was increased from 10% to 15%. However, with further increase in cement content from 15% to 20%, the increase in UCS was found to be less than 3%. Another 10% increase in cement content from 20% to 30% led to increase in UCS value of merely 2%. In other words, strength of this cement treated clay does not increase significantly upon addition of more cement, beyond 15%. Hence, 15% cement content can be considered as optimum cement content. At this cement content, maximum strength is achieved and addition of cement beyond this value does not contribute to strength development. Hence, the scope of this study will be limited to cement contents of 10%, 15% and 20%.

Table 3.2 Average UCS values for cement treated clays

Cement Content (%)	Average UCS Values (kPa)
5	287
10	1298
15	1588
20	1635
25	1640
30	1670

3.3.2 Tensile Strength of Cement Treated Clay

Tensile properties of geomaterials play an important role in many geotechnical engineering problems. Compacted soil layers in dams, clay liners in landfills, cement stabilized crushed rocks in pavements, etc. are generally checked for tensile cracking. This type of cracking happens when the developed tensile stress exceeds the tensile strength of the material. Soil-cement columns or walls formed by deep cement mixing have been widely used for foundations, to mitigate liquefaction, as supports for excavations, etc. Research has shown that these improved columns or walls are often susceptible to tensile cracking due to bending moments caused by

external forces (Nguyen et al., 2016). The embedded improved soil strut is also susceptible to tensile cracks due to the underlying uplift pressure imposed by soil and groundwater (Wang et al., 2019). Hence, exploring the tensile strength of cement treated clay is important in this study.

Tensile strength of cement treated soil is usually determined by two methods, tensile splitting strength test (also called Brazilian test) and direct tension test. Split tensile strength is the more popular of the two, owing to the ease with which it can be performed. This method has been included in most standards as a method to evaluate the tensile strength (ASTM C496). Owing to the difference in stress conditions, the tensile strength obtained vary with the type of test used. Some researchers (Kawasaki et al., 1981) have reported a lower tensile strength value under Brazilian test compared to direct tension test. Namikawa and Koseki (2007) performed extensive numerical simulations to explain the differences in behaviour of cement treated soils subjected to different types of tensile strength tests. The Brazilian test was found to underestimate the tensile strength due to the shear failure that happens below the loading strip. Moreover, the stress condition is not well-defined at the boundaries in this type of testing and is hence not considered as an element test (Namikawa and Koseki, 2007). Direct tension test was found to be more appropriate and reliable for cement treated soils (Namikawa et al., 2017) and this method will be used in this study as well. Furthermore, Hoek and Brown (2018) has stated that it is unacceptable to include Brazilian test in the Hoek Brown analysis, because of its complex stress distribution and the influence of the stress concentrations at the loading points. Not many direct tension test data have been reported in case of cement treated clays. A new apparatus was hence, developed in this study to estimate the tensile strength of cement treated clay.

Apparatus Description

The tension testing apparatus was designed and fabricated at the workshop facilities of Department of Civil Engineering, Indian Institute of Technology Madras, Chennai. Figure 3.4 shows the components of the apparatus. The apparatus was made of stainless steel and was designed to accommodate a cylindrical specimen of 50 mm diameter and 100 mm height. Since direct tension test involves pulling the specimen from top and bottom simultaneously in the vertical direction, the apparatus was designed as two coaxial cylindrical parts of 50 mm diameter

and 50 mm length each, as shown in Figure 3.4 (a). This was to force the specimen to fail at half the length. This is justified because the cement treated clay specimen was prepared such that it is homogenous. The two individual parts of the apparatus were given an interlocking step cut at one end so that they could be easily connected to accommodate a full length specimen, as shown in Figure 3.4 (b). Grooves were provided inside the cylinders to firmly grip the specimen. This technique was used by Indraratna et al. (2009). Moreover, cement treated soils may undergo minor shrinking in diameter after 28 days curing period. This may loosen the specimen against the walls of the cylinder and the specimen might just come out while testing without taking any tensile load. Grooves were expected to take care of this too. The apparatus also consisted of two discs, to be used for top and bottom cylinders. The top disc facilitated mounting of the top cylinder to the load cell. The bottom disc was used to screw the bottom cylinder to the loading frame.

At the time of sample preparation, top and bottom cylinders were kept together, and the joint was wrapped with an adhesive tape to avoid leakage of the sample. The bottom disc was screwed to the bottom cylinder to seal the bottom. The cement mixed clay sample was prepared in the same way as mentioned in section 3.4. The mix was poured into the mould in layers, providing tamping at each layer to get rid of entrapped air. After the sample was poured to the full length of the cylinders, top disc was screwed to the cylinders and was allowed to cure for 28 days. The entire mould was wrapped with cling film to avoid loss or ingress of moisture.

Testing Methodology

Once the specimens were ready for testing, the adhesive tape was removed, and the entire apparatus was carefully mounted to the loading frame, as shown in Figure 3.5. The screw beneath the bottom disc allows screwing the apparatus to the frame. The screw over the top disc was then used to mount the apparatus to the load cell. Minor adjustments were made to the frame to facilitate confining the apparatus between the load cell and base of frame.

Bottom Disc

Top Disc

Bottom cylinder

Top cylinder

(a)

Grooves inside cylinder

Interlocking step cut
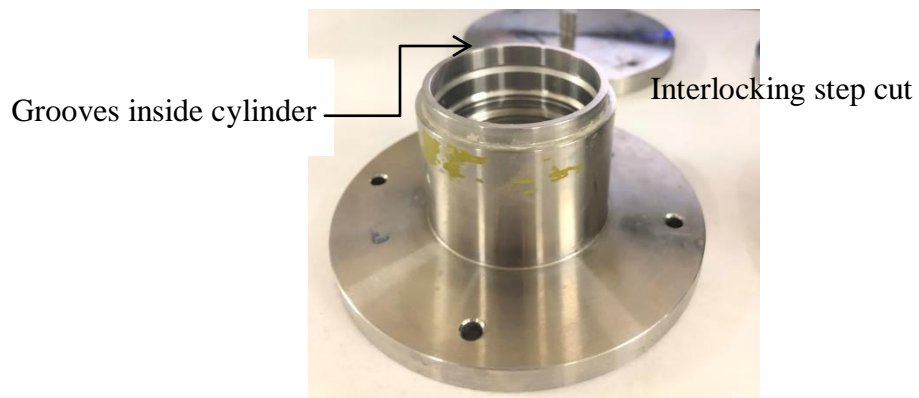
(b)

Figure 3.4 Tensile testing apparatus (a) Components and (b) Closer view of cylindrical part
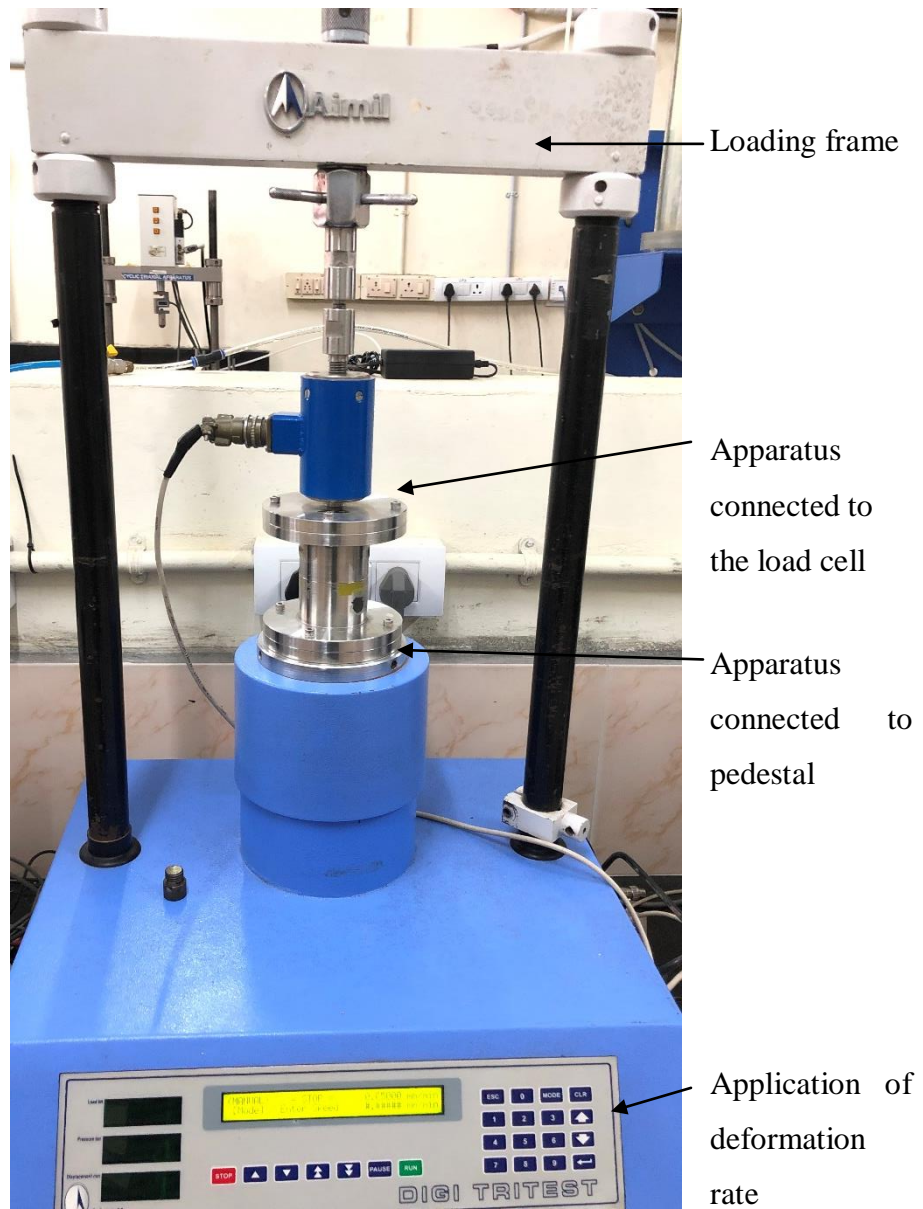
Figure 3.5 Tensile testing apparatus assembled in the loading frame

The top part of the apparatus being stationary, the frame was now moved downwards at a specified deformation rate to induce tensile stresses inside the specimen. A closer view of the apparatus under testing is shown in Figure 3.6 (a). Strain controlled tensile tests were conducted at a deformation rate of 0.05 mm/min for all the specimens. As shown in Figure 3.6 (b), the completion of test was marked by breakage of the sample at half the length of sample. At this stage, load cell recorded a residual value which includes the weights of top disc, top cylinder and half the specimen under suspension. This residual value was deducted from all the tensile load readings to obtain the true tensile load taken by the specimen. The peak tensile load divided by the cross-sectional area was evaluated as the final tensile strength of the specimen.

Results and Discussion

Tensile testing was conducted for cement contents of 10%, 15% and 20%. The variation of tensile stresses with the axial strain for various cement contents are shown in Figure 3.7. Compared to 10% cement content, 15% and 20% showed abrupt breakage after reaching the peak tensile stress. The drop in strength was higher for 20% cement content, after failure. This points towards the increase in brittle nature of cement treated clay with increase in cement content. The tensile strengths corresponding to different cement contents are shown in Table 3.3. Tensile strength for 10% cement content is much less compared to other cement contents. However, 15% cement content showed an increase in tensile strength by about 397% compared to 10% cement content. Further increase in cement content by 5% (i.e. 20% cement content) resulted in a strength gain of merely 10%. Hence, 15% cement content can be considered to be optimum cement content, very similar to the case of UCS.

Load cell

Tensile testing apparatus

Pedestal of the loading frame

(a)

Failure of specimen along the joint
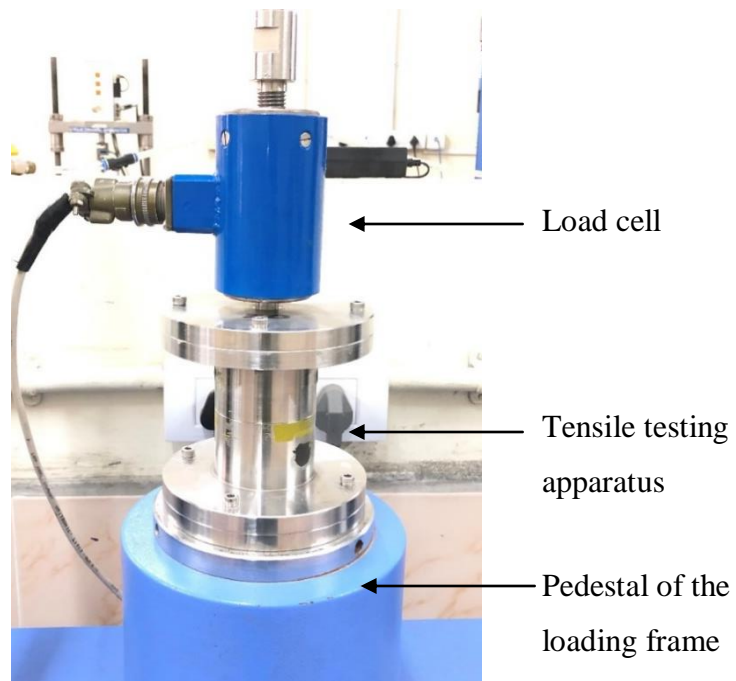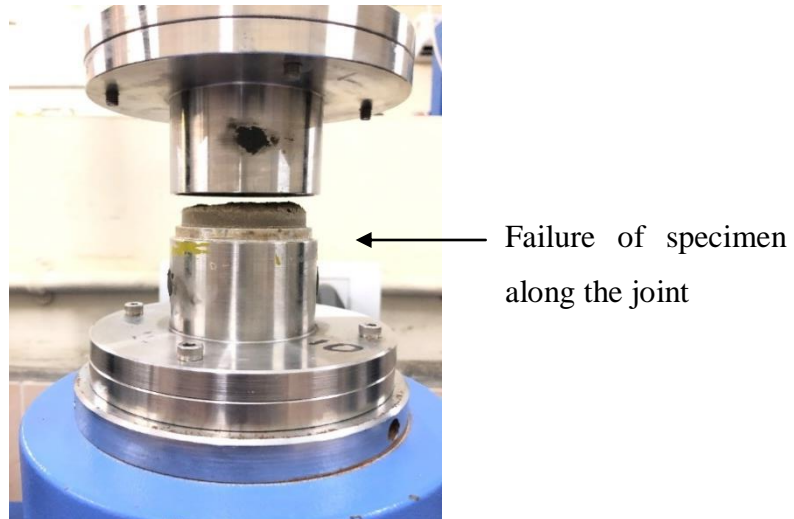
(b)

Figure 3.6 Tensile testing apparatus (a) Testing in progress and (b) After testing is complete
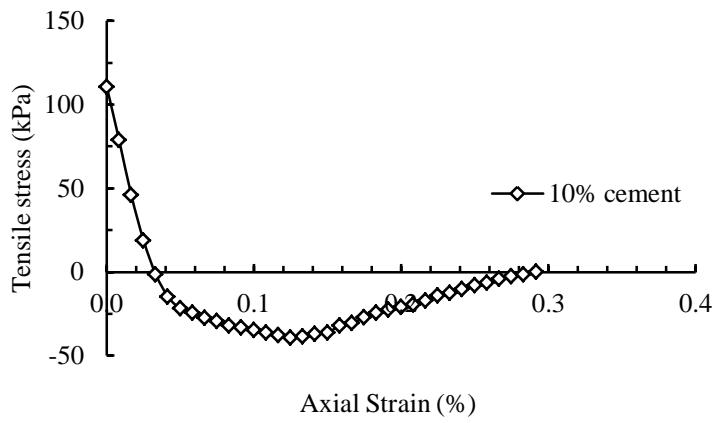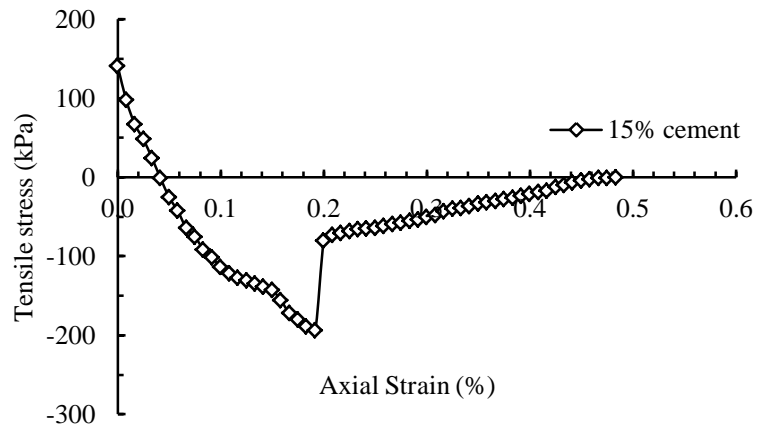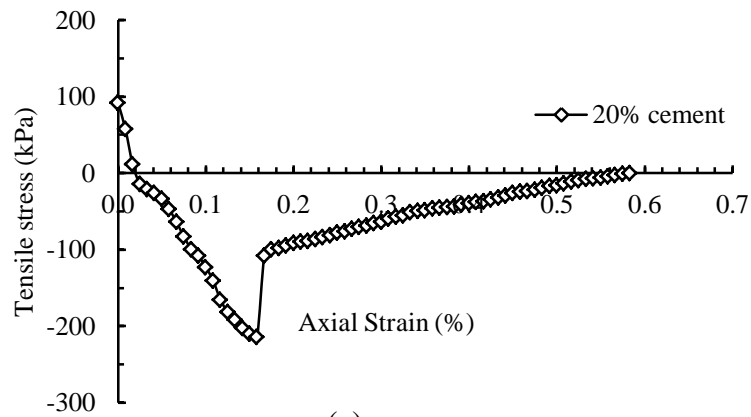
Figure 3.7 Variation of tensile stresses versus axial strain for (a) 10% cement content (b) 15% cement content and (c) 20% cement content

Table 3.3 Tensile strength values for different cement contents

Cement content (%)	Tensile strength, σ_t (kPa)	UCS values (kPa)	Ratio of direct tensile strength to UCS (%)
10	39	1298	3
15	194	1588	12
20	214	1635	13

The ratios of direct tensile strength to UCS are also provided in Table 3.3. Researchers have reported that the Brazilian tensile strength of cemented soils falls in the range of 9% to 12% of unconfined compressive strength (Clough et al., 1981). Some others have reported this ratio to be 10% (Das et al., 1995). It is to be noted this assumption does not work for all cement contents. While 15% and 20% cement contents managed to stay in the above range, 10% cement content recorded a value nowhere close to it.

In other words, the bonding strength generated for 10% cement content was not found to be sufficient to develop a tensile strength of at least 10% of its UCS value. However, further increase of 5% cement content yielded much higher tensile strength by 397%. Cement content beyond 15% cement content did not result in significant increase in tensile strength. Hence, 15% cement content was found to be the optimum cement content in terms of tensile strength and unconfined compressive strength.

3.4 SUMMARY

The experimental programme and methodology were explained in this chapter. Basic properties of clay were determined using standard testing methods. Both UCS testing and tensile strength testing on cement treated clay pointed towards the existence of an optimum cement content (15%). The triaxial and plane strain tests on cement treated clay will be discussed in the next chapter.

CHAPTER 4

SHEAR BEHAVIOUR OF CEMENT TREATED CLAYS UNDER PLANE STRAIN AND TRIAXIAL CONDITIONS

4.1 INTRODUCTION

One of the main objectives of the present study is to compare the strength behaviour of cement treated clays tested under conventional triaxial and plane strain testing conditions. As discussed in Chapter 2, it is established in the literature that the behaviour of natural soil is different under the two modes of shearing.

Due to very low shear strength, soft clays are often improved by cement treatment. The shear strength of cement treated clays is usually determined using Conventional triaxial compression (CTC) testing or unconfined compression strength (UCS) testing. Both the tests are performed under axisymmetric conditions. However, there are situations in the field where the cement treated soil layer can be approximated to be under plane strain condition. Cement stabilization of soil beneath the final formation level of excavations, block or wall type improvement in embankments, etc. are examples for such situations. Performing plane strain (PS) tests would better represent the field condition under such circumstances. Studies on the behaviour of cement stabilized soil under plane strain condition are limited.

This chapter discusses the development of a plane strain apparatus for testing of cement treated clays. The differences in shear behaviour of cement treated clay compared to triaxial testing are also discussed.

4.2 SPECIMEN PREPARATION

The importance of optimum remoulding water content at which the strength is the maximum has already been discussed in Chapter 3. A remoulding water content of 1.2 times the liquid limit of

clay will be adopted for the preparation of all the specimens and will be calculated based on the dry weight of soil solids. The moisture naturally present in clay is also accounted for, while calculating the optimum remoulding water content. Before adding cement, clay was thoroughly mixed with the amount of water equal to the optimum remoulding water content. To ensure uniform mixing, the sample was thoroughly mixed in a Hobart mixer for 20 minutes. Cement was then added in slurry form at a water-cement ratio of 0.6, to the prepared clay-water mix. The sample is again mixed in Hobart mixer for another 10 minutes. The sample was found to harden quickly and hence, care was taken to meticulously note the time and prevent drying. This procedure was followed for all the specimens. Three cement contents of 10%, 15% and 20% were used in the study and were calculated in terms of dry weight of soil.

Triaxial specimens of 50 mm diameter and 120 mm long were prepared in stainless steel cylindrical moulds. It is a common practice to prepare multiple specimens using a single mix. However, owing to the time delay caused between filling the first and last moulds, homogeneity issues were observed in the prepared specimens. This is caused due to the setting of cement treated sample with time. To prepare homogenous specimens, a box of 210 x 146 x 70 mm was fabricated. The box and cylindrical moulds are shown in Figure 4.1 (a). These dimensions were decided based on the size of the three moulds and the volume of mix likely to be displaced while inserting the moulds into the box. Soil-cement mix, after thorough mixing, was transferred to the box in three layers. Sufficient tamping was provided after pouring each layer to get rid of entrapped air. Once the box has been filled up to about three quarters, the moulds were pushed into the box containing soil-cement mix, as illustrated in Figure 4.1 (b). By this method, it is expected to achieve uniform properties for all the three specimens. The box is then kept covered, to avoid loss of moisture. After one day of casting, the specimens were removed from the mould and trimmed to 100 mm long and cured in desiccator for 28 days.
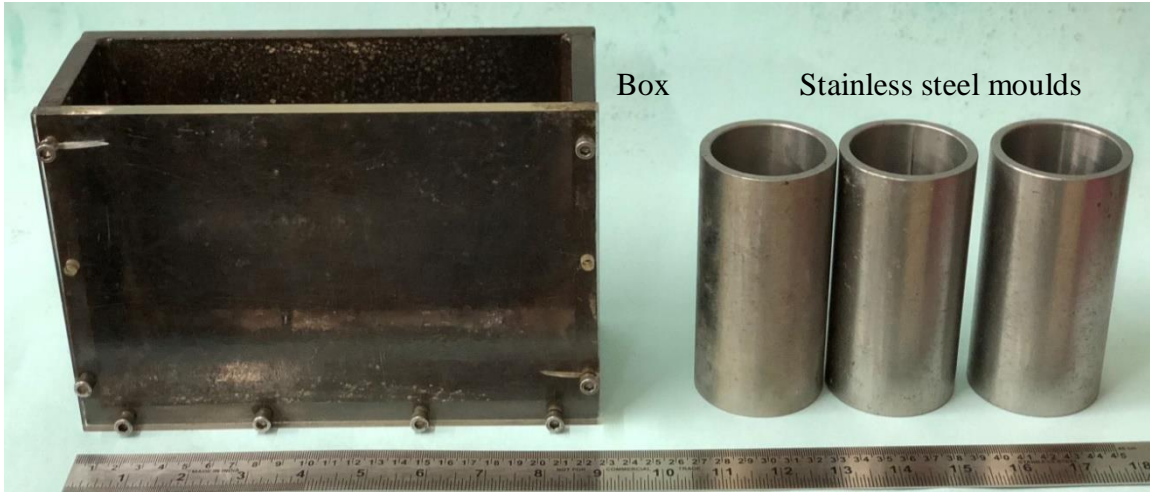
(a)
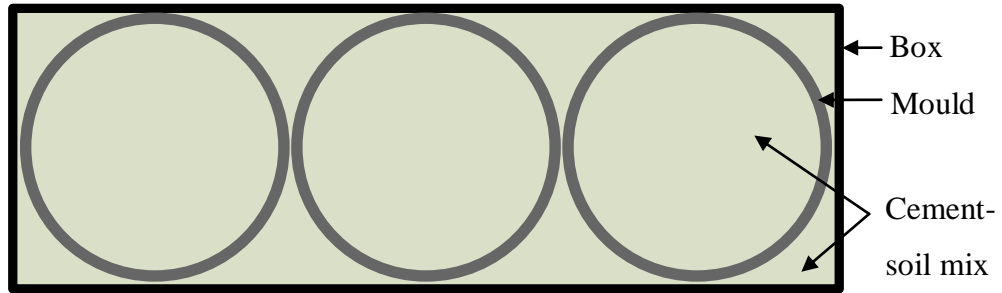
(b)

(c)

Figure 4.1 (a) Triaxial sample preparation box and moulds (b) Sample preparation and (c) Triaxial specimen cured for 28 days.

As far as plane strain specimens are concerned, the size of prismatic specimens to be used for testing, needs to be first decided. After analysing the apparatus used by various researchers, it was understood that no standard procedure exists in determination of specimen size for plane strain testing. Different sizes were used by various researchers and were discussed in Chapter 2. Hence, a tried and tested specimen size of 60 mm by 60 mm cross section and 120 mm long, used by Wanatowski and Chu (2005), was selected for this study.

The plane strain specimens were prepared in a mould consisting of five pieces of acrylic plates of 25 mm thickness each, joined together by means of appropriate screws. The plane strain specimen preparation mould is shown in Figure 4.2. Top and bottom of the mould are shown in Figures 4.2 (a) and 4.2 (b). Three such moulds were fabricated to facilitate preparation of three specimens at a time. The soil-cement mix was prepared in the same way as discussed before. After assembling the mould, the mix was poured into the mould in three layers. Since, prismatic specimens are likely to get chipped off at edges, a sample preparation box as mentioned in triaxial specimens, would be difficult. Hence, to ensure homogeneity, the first layers in the three moulds were poured simultaneously. Proper tamping was provided in the moulds to get rid of entrapped air. Due to see-through nature of the acrylic plates, good care could be taken to remove air voids. The subsequent layers were filled in the same way. This method is expected to prepare homogenous specimens. The extra length of the sample was trimmed off after one day of casting with the help of a spacer plate, as shown in Figure 4.2 (a). Spacer plate had a projection on one side with dimensions of 59.5 x 59.5 x 10 mm such that it could go easily into the mould. The screws connected to the bottom of mould were removed and the other screws were loosened, so that the projection of spacer plate was free to move inside the mould. The bottom of the mould is shown in Figure 4.2 (b). The bottom plate was then pushed upwards using spacer plate such that the extra length of the sample was pushed outside the mould, which could be trimmed off. Prismatic specimens of exact dimensions were then wrapped in cling film and cured in desiccator for 28 days. A prismatic plane strain specimen hence prepared and cured for 28 days, is shown in Figure 4.2 (c).
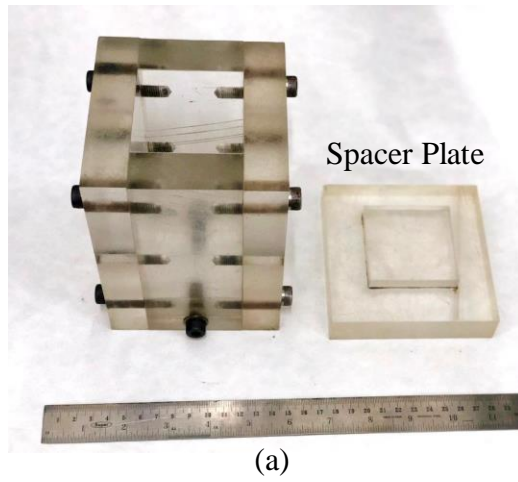
(a)

(b)

(c)

Figure 4.2 (a) Plane strain specimen preparation mould (b) Bottom of mould and (c) Plane strain specimen cured for 28 days.

4.3 TRIAXIAL TESTING PROGRAM

Consolidated undrained triaxial tests were carried out on cylindrical specimens of 50 mm diameter and 100 mm height, using a fully automated VJ Tech triaxial apparatus. The apparatus could apply deformation to a precision of 0.0001 mm/min. An external load cell of 10 kN capacity and an external pore pressure transducer of 1000 kPa capacity were used for measurements of load and excess pore water pressure respectively. Back pressure and cell pressure lines were de-aired before placing the specimen. VJ Tech hydraulic pressure-volume controllers of 3000 kPa capacity were used for the application of cell and back pressures. These controllers can measure the volume changes during the consolidation and shearing stages. Two-way drainage was facilitated by providing 50 mm diameter porous stones on top and bottom of the specimen.

Specimens were prepared at cement contents of 10%, 15% and 20%. Specimens of all the cement contents were tested at confining pressures of 50, 100, 200 and 400 kPa. Testing was carried out in three stages, viz. saturation, consolidation and shearing. Saturation of the specimen was performed at an effective pressure of 10 kPa and pressure increments of 50 kPa were applied till a B-value greater than 0.95 was achieved. Normally, saturation of cement treated specimens would take weeks to complete. To accelerate the saturation process, a loading cap with top drain arrangement was used, as shown in Figure 4.3 (a). The saturation stage was initiated by applying a back pressure of 40 kPa and a cell pressure of 50 kPa. During this increment, the valve connected to top drain was opened and water was circulated from the bottom. The pressure difference thus created, forces the air bubbles inside the specimen to move out. The procedure was continued till clear water starts to come out and the valve was closed. This method greatly helped in accelerating the saturation process. A back pressure of 290 kPa was found to be sufficient to attain a B-value of 0.95. Top drain method used here helped in completing the saturation within one day. Consolidation was then performed at the desired effective confining pressure and volume change was measured by noting the change in volume in the back pressure controller. This stage was stopped when no more volume change was visible.
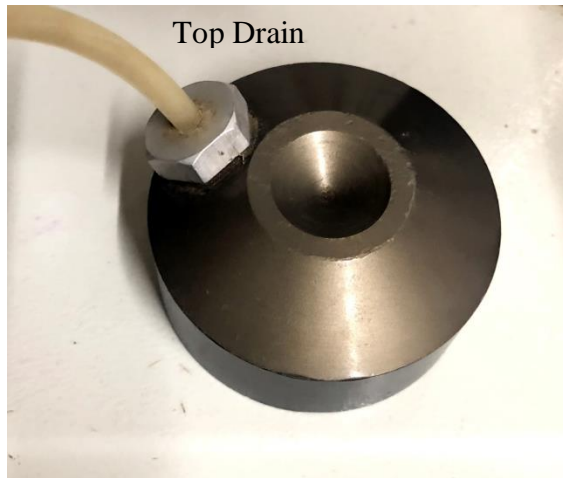
Top Drain

(a)

(b)

Figure 4.3 Triaxial testing (a) Loading cap with top drain and (b) Set-up used

The dimensions of the specimen at the start of shearing were also calculated using the measured volume change. Consolidation stage was found to be complete within 15 to 20 minutes.

Shearing could be carried out at a fast rate in this case, as per Head (1986). However, a slow deformation rate of 0.025 mm/min was adopted, owing to the brittle nature of cement treated clays. Shearing was performed under undrained conditions, by keeping the back pressure valve closed during the entire stage. Figure 4.3 (b) shows the triaxial test set-up used in this study. Load and excess pore water pressures were measured throughout this stage. Post peak regime was also captured by continuing the shearing till a residual value was obtained. Plots of deviator stress versus axial strain, excess pore water pressure versus axial strain and q-p' (where q is the deviator stress and p' is the mean effective stress) stress path were made.

4.4 PLANE STRAIN APPARATUS

A plane strain apparatus was developed as a part of this study. Schematic of the test setup is shown in Figure 4.4. This apparatus is similar to the one developed by Wanatowski and Chu (2005). The base pedestal of an existing triaxial cell of 220 mm diameter and 350 mm high was removed and was replaced with a new pedestal to suit plane strain requirements. The specimen dimensions being 60 x 60 x 120 mm, the plane strain condition was imposed on two opposite faces (60 x 120 mm), using a rigid pair of platens. A 70 mm diameter membrane was found to be suitable for the specimen size used.

The pedestal had a 60 mm square projection at one end (as shown in Figure 4.5 (a)) so that the platens could be placed rigidly along one side and also had provision for 38 mm diameter porous stone (as shown in Figure 4.5 (b)). This projection, 10 mm thick, was followed by a circular portion circumscribing the square portion which enables smooth installation of the rubber membrane. The platens were kept at the space between square and circular portion. In order to ensure robustness of the pedestal, bottom of the pedestal had an increased diameter of 100 mm and it was screwed to the base of the cell. Proper O-rings were also provided below the pedestal, to ensure water tightness, as shown in Figure 4.6 (a).
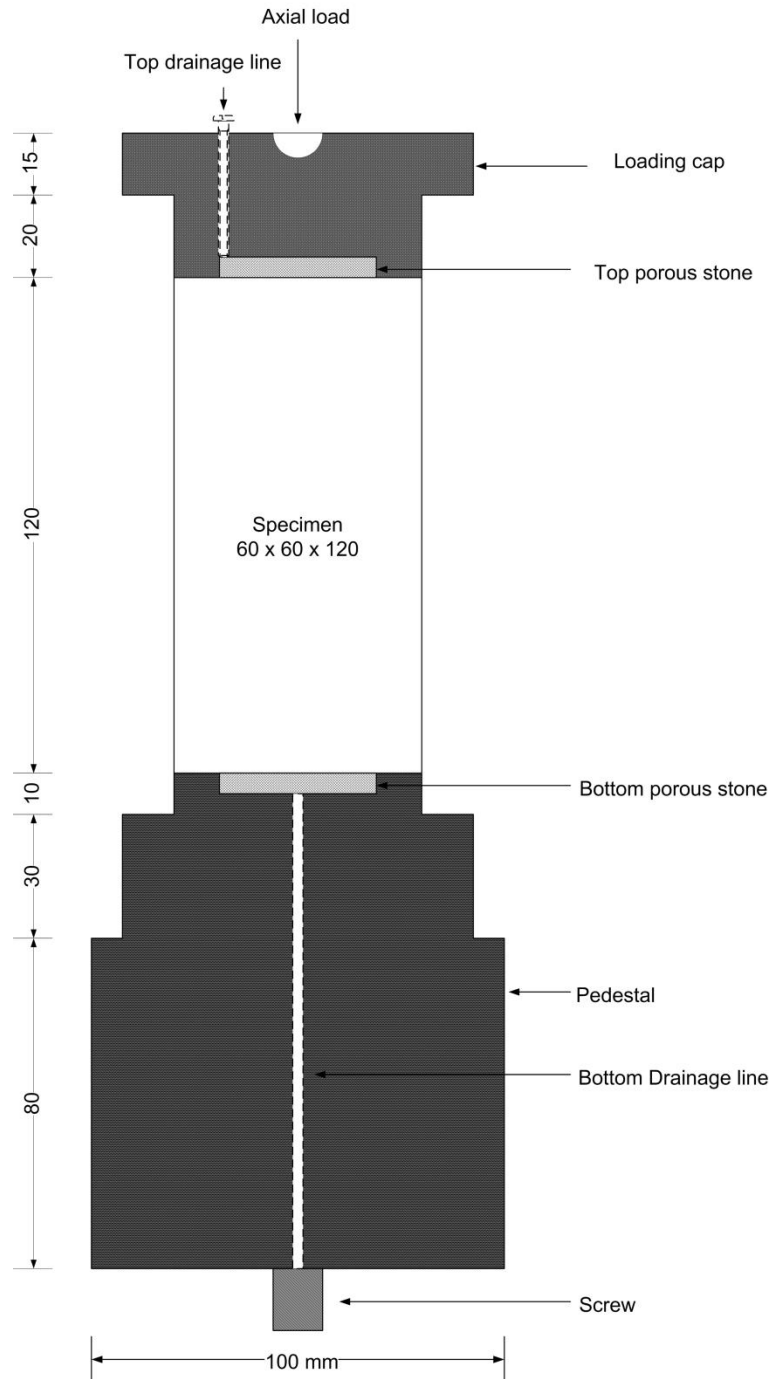
Figure 4.4 Schematic of the plane strain testing apparatus (vertical cross section through the centre) [All dimensions are in mm].
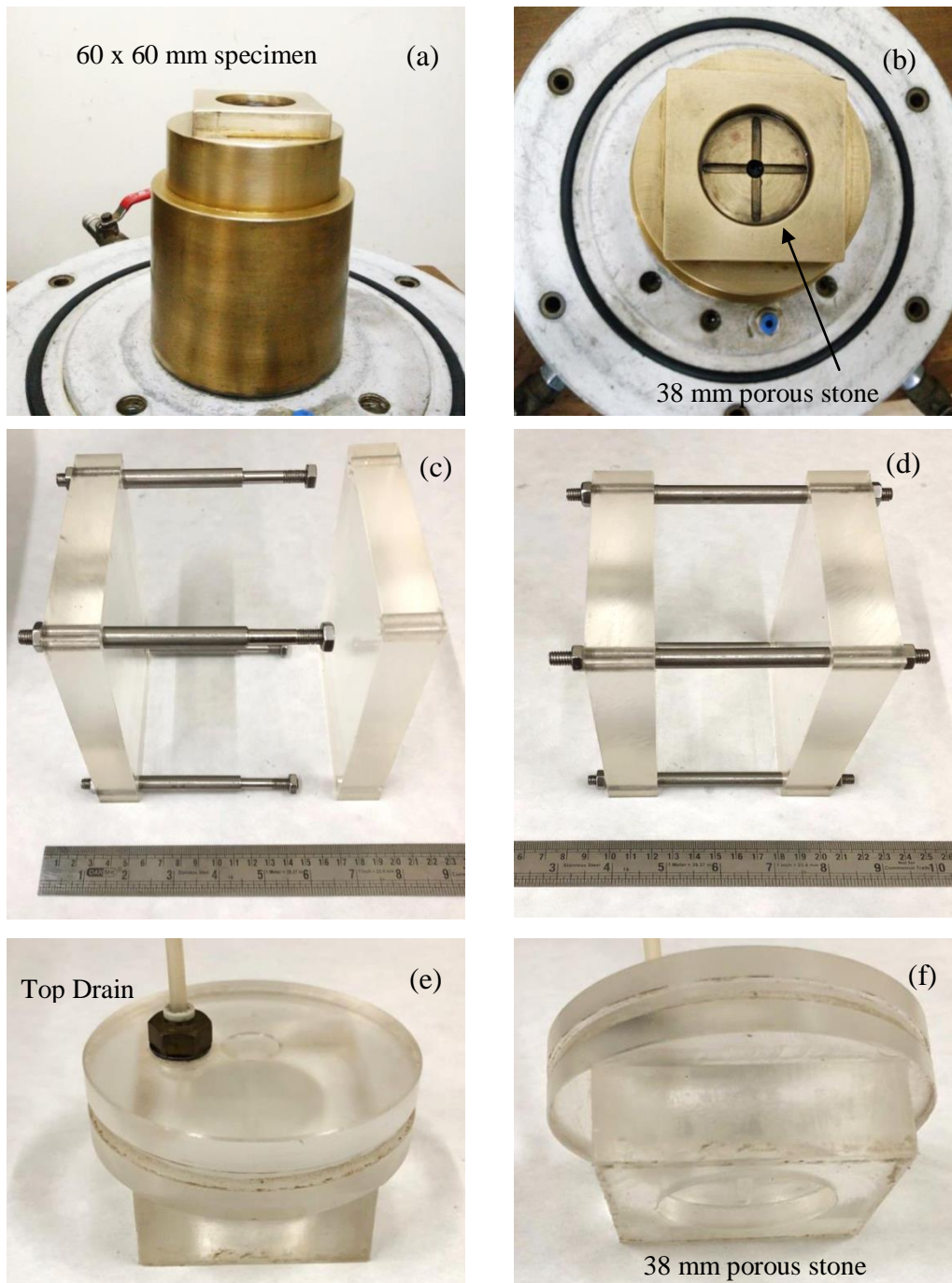
Figure 4.5 Components of plane strain apparatus (a), (b) Pedestal (c), (d) Platens and (e), (f) Loading cap.

Two acrylic platens of 137 x 100 x 25 mm size were used to impose plane strain condition, as shown in Figures 4.5 (c, d). Platens were made sufficiently thick (25 mm) so as to make it capable to withstand high stresses. Acrylic platens of similar thickness were used by several researchers (Alshibli et al., 2000, 2004; Alshibli and Akbas, 2007) in the plane strain apparatus, so as to restrain lateral deformations. Stainless steel screws were used to tighten the platens. The platens were lubricated with silicon grease so as to reduce friction between the specimen and platens.

The loading cap had one square end and the other portion circular for the rubber membrane to rest on, as shown in Figures 4.5 (e, f). Top drain arrangement was provided on top of the loading cap, to flush the entrapped air out of the specimen and water was circulated through the bottom drainage line for faster saturation. Drainage at both ends of the specimen was provided by two 38 mm porous stones kept at the centres of loading cap and pedestal, as shown in Figure 4.5 (b).

4.5 PLANE STRAIN TESTING PROGRAM

Consolidated undrained plane strain tests were performed using a digital triaxial loading frame of 50 kN capacity and capable of applying a deformation rate to a precision of 0.0001 mm/min. Loads were measured using an external load cell of 15 kN capacity. An external pore pressure transducer of 1000 kPa capacity was used to measure excess pore water pressures. The plane strain set-up ready for testing is shown in Figure 4.6. VJ Tech hydraulic pressure-volume controllers of 3500 kPa capacity were used for the applications of cell pressure and back pressure. Both the pressure lines were de-aired before placing the specimen on the pedestal.

Specimens prepared at cement contents of 10%, 15% and 20%, were tested under confining pressures of 50, 100, 200 and 400 kPa. Plane strain condition was imposed using the platens. Platens were kept tight enough to maintain the plane strain condition throughout the test. Sufficient lubrication was ensured to reduce the friction between the platen and the cement treated soil. Good number of O-rings were used on the pedestal and loading cap to ensure absolute confinement of specimen within the membrane. The tube used for top drain was de-aired before the start of testing. Figure 4.6 (a) shows the plane strain specimen assembled in the test set-up. Figure 4.6 (b) shows the entire test set-up while the test is in progress.

Testing was carried out in the same way as triaxial testing described above. Saturation process was performed in pressure increments of 50 kPa, maintaining an effective pressure of 10 kPa. As discussed above, loading cap with top drain arrangement was used here as well. This method greatly helped in accelerating the saturation process and the entire saturation stage could be completed within a day. A back pressure of 290 kPa was found to be sufficient to attain a B-value of 0.95. Once the specimen is saturated, consolidation was performed at the required effective confining pressure. Consolidation process was quick and got over within 15 to 20 minutes. The volume change measured by the back pressure controller during consolidation was used to calculate the dimension of the specimen at the start of shearing.

A slow deformation rate of 0.025 mm/min as adopted in triaxial tests was provided during shearing. Shearing was performed under undrained conditions, by keeping the back pressure valve closed during the entire stage.
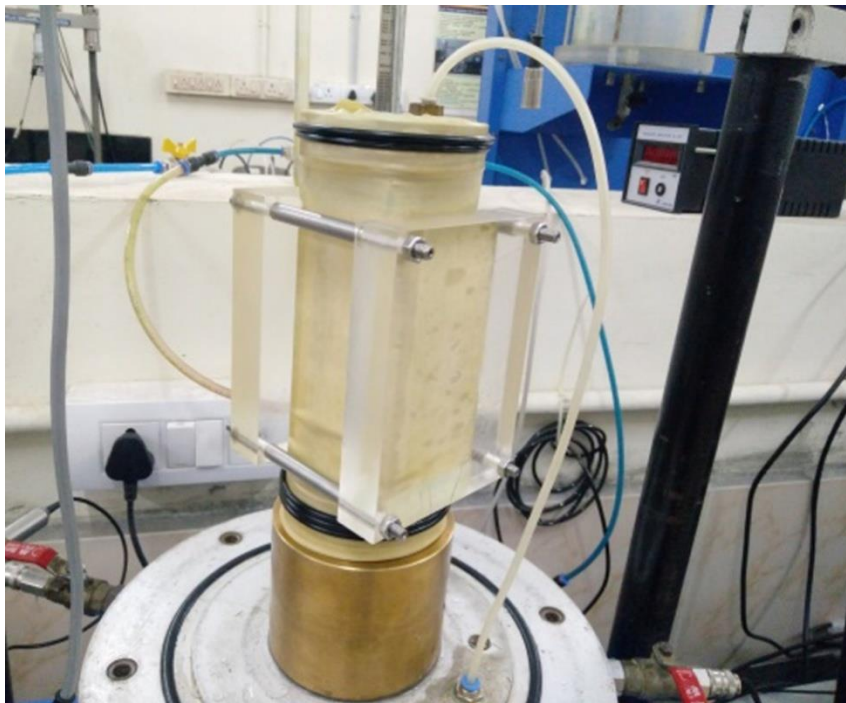
(a)
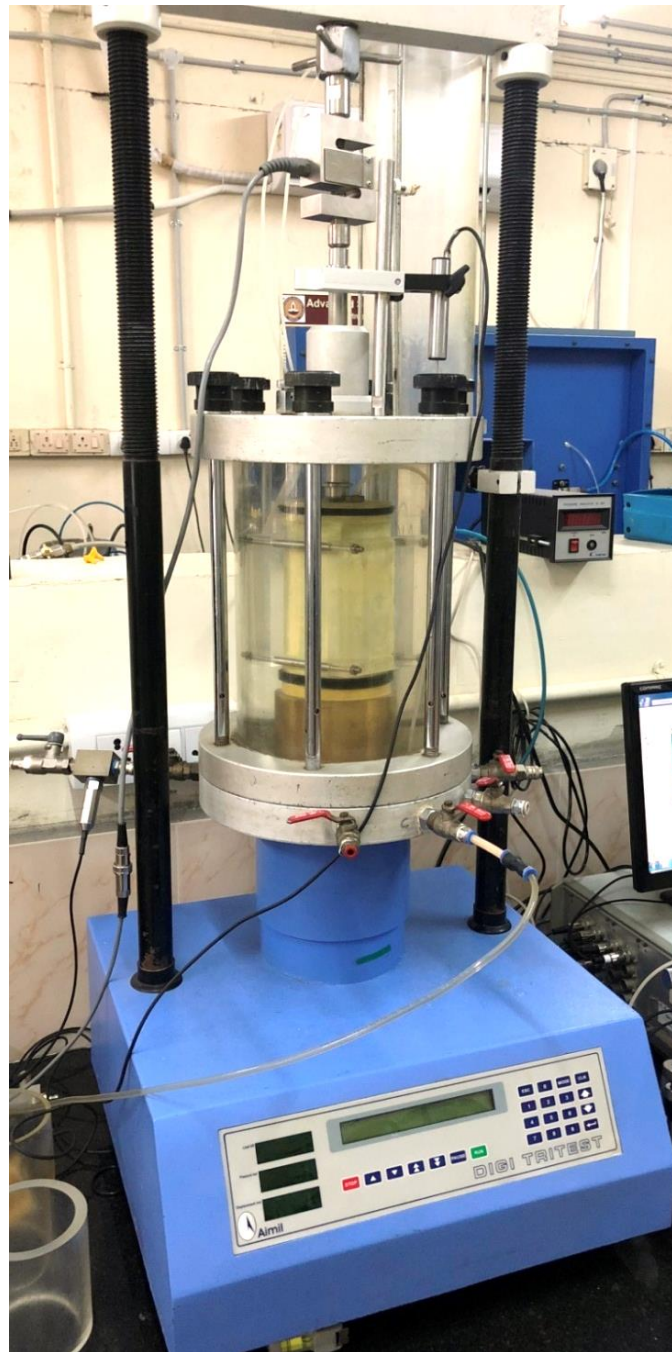
(b)

Figure 4.6 (a) Plane strain specimen assembled in the setup and (b) Plane strain specimen under testing.

The load and excess pore water pressures were measured throughout this stage. Shearing was continued till a residual value was obtained after the peak strength, to capture the post peak regime. Plots of deviator stress versus axial strain, excess pore water pressure versus axial strain and q-p' (where q is the deviator stress and p' is the mean effective stress) stress path were made.

Following two issues needs consideration in any plane strain setup.
1. The friction between the platens and soil and
2. Lateral deflection of the platens during testing.

In order to address the above issues, a test setup was arranged as shown in Figure 4.7. After assembling the plane strain test setup, two dial gauges of 1 micron accuracy were attached, as shown in the figure. The dial gauges measure the displacement at the middle of the platen. The rods used to fix the dial gauges were mounted on the base of the cell. This ensures that relative movement does not occur between the dial gauge and the platen.

The maximum lateral deformation of the platen was recorded as 0.056 mm. The corresponding lateral strain is 0.09%. Marachi et al. (1981) carried out a detailed study on the effect of lateral strain on plane strain test results. They reported that the variations in results will be insignificant, if the lateral strain is within 40% of the axial strain at failure. In the present study, the lateral strain is only 5.14% of the axial strain at failure. Hence, plane strain condition was ensured throughout testing. A pair of load cells was placed beneath the platens to measure any frictional force transferred to the platen. The maximum frictional force recorded by the load cell was found to be 37 N. The corresponding frictional stress is 5.13 kPa (contact area is 60mm x 120 mm), which is less than 1% of the deviator stress at failure (The deviator stress obtained in the present study ranges between 733.8 to 1118.7 kPa). Therefore, the plane strain condition is achieved with negligible specimen-platen friction and negligible lateral strain.
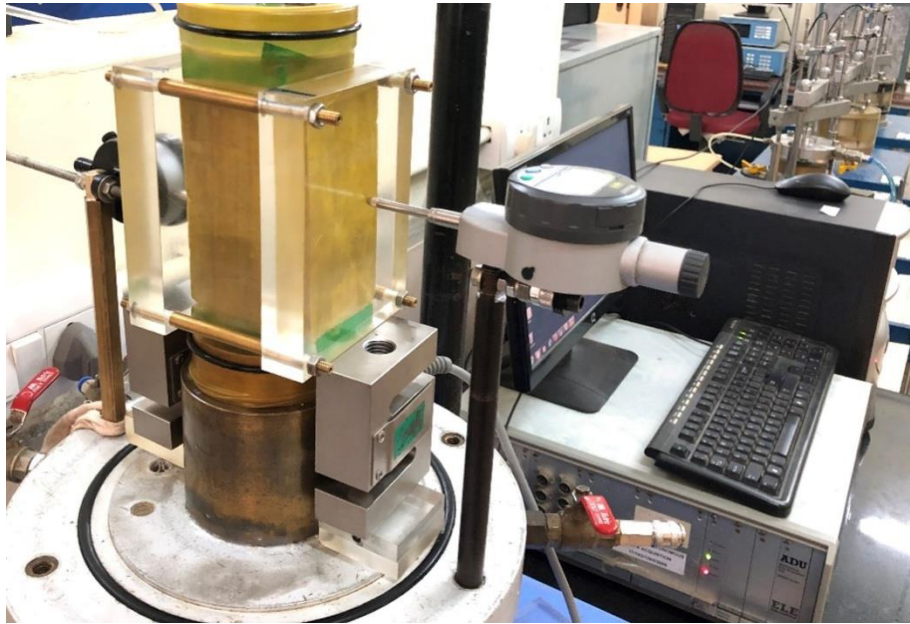
Figure 4.7 Setup to measure the deformation of the acrylic plate and frictional resistance between membrane and the plates.

4.6 FORMULATIONS USED

Formulations to be used in plane strain testing are different from triaxial tests, as the intermediate principal stress (σ_2') is not equal to the effective confining pressure (σ_3'). The differences in formulation for the intermediate principal stress, deviator stress (q) and mean effective stress (p') are shown in Table 4.1.

Unlike triaxial tests, plane strain tests require the value of Poisson's ratio for the determination of intermediate principal stress and hence, deviator stress. Literatures suggest that Poisson's ratio of in-situ cement treated soil can be taken as 0.25 to 0.45, irrespective of the unconfined compressive strength (Kitazume and Terashi 2013; Bruce et al., 2013). It is to be noted that within the above range of Poisson's ratio, a maximum variation of peak deviator stress was found to be only about 4%. Furthermore, the values assumed in the literatures were mostly drained Poisson's ratio values. Since the plane strain tests in this study were performed under

undrained conditions, a Poisson's ratio value close to 0.5 would be ideal, considering the fact that no volume change happens during the testing process. Hence, a value of 0.49 was assumed in the present study.

Table 4.1 Formulations used in plane strain and triaxial tests

Test	Plane Strain Test	Triaxial Test
Intermediate Principal Stress	$\sigma_2' = \upsilon(\sigma_1' + \sigma_3')$	$\sigma_2' = \sigma_3'$
Deviator Stress	$q = \sqrt{\dfrac{(\sigma_1 - \sigma_2)^2 + (\sigma_2 - \sigma_3)^2 + (\sigma_1 - \sigma_3)^2}{2}}$	$q = \sigma_1' - \sigma_3' = \sigma_a'$
Mean Effective Stress	$p' = \dfrac{\sigma_1' + \sigma_2' + \sigma_3'}{3}$	$p' = \dfrac{\sigma_1' + 2\sigma_3'}{3}$

Note: υ is the Poisson's ratio

4.7 TRIAXIAL RESPONSE

4.7.1 Effect of confining pressure

Variations of deviator stress versus axial strain, excess pore pressure versus axial strain and q-p' stress paths for 10%, 15% and 20% cement contents are shown in Figures 4.8, 4.9 and 4.10, respectively. The effect of confining pressure on the specimen was studied by the application of confining pressures ranging from 50 kPa to 400 kPa. The increase in peak deviator stress with an 8 fold increase confining pressure was found to be 23% for 10% and 15% cement contents, and 40% for 20% cement content. This can be observed in Figures 4.8 (a), 4.9 (a) and 4.10 (a) respectively. Hence, the role of confining pressure in strength gain in case of cement treated soil is not very significant in case of lower cement contents. This is in line with the previous findings by Sariosseiri and Muhunthan (2009). Furthermore, strain softening behaviour was observed for all the confining pressures. This phenomenon has been reported in the literatures in case of cement treated clay (Kamaruzzaman et al., 2009; Subramaniam et al., 2015).

Figures 4.8 (b), 4.9 (b) and 4.10 (b) show the variations of excess pore water pressure with axial strain, at various confining pressures, for cement contents of 10%, 15% and 20%, respectively. Clearly, the excess pore water pressure largely depends on the applied confining pressure. Increase in confining pressure led to increase in excess pore pressure and the peak values of excess pore pressure fell close to the corresponding confining pressure applied. Negative pore pressures were recorded post attaining peak stress, only for lower confining pressures.

Figures 4.8 (c), 4.9 (c) and 4.10 (c) show the variation of stress path at various confining pressures, for cement contents of 10%, 15% and 20%, respectively. Evidently, cement treated clay shows over-consolidated behaviour. However, a slight transition from over-consolidated (OC) to normally consolidated (NC) behaviour was seen at higher confining pressures.

4.7.2 Effect of cement content

Figure 4.11 (a) shows the typical variation of deviator stress with axial strain, for triaxial specimens prepared at different cement contents and tested at a confining pressure of 100 kPa. In the figure, CTC refers to conventional triaxial compression test results. Interestingly, 15% and 20% cement contents recorded relatively same strength at a certain confining pressure. To verify this trend at other confining pressures, the variation of peak deviator stress with cement content was plotted for various confining pressures, as shown in Figure 4.12. This data strengthens the previous assumption that cement content above 15% does not result in significant strength gain. Moreover, a slight reduction was also observed at some confining pressures.

To get a better insight into the above trend, unconfined compressive strength tests (UCS) were performed for specimens prepared at various cement contents. The variation of UCS values with cement content was intriguing (Figure 4.13). Only negligible increase in strength (2.3%) compared to 15% cement content was observed, for specimens prepared at 20% cement content.

Figure 4.8 Triaxial test results for 10% cement content at various confining pressures (a) Deviator stress vs. axial strain (b) Excess pore pressure vs. axial stress and (c) Stress paths.
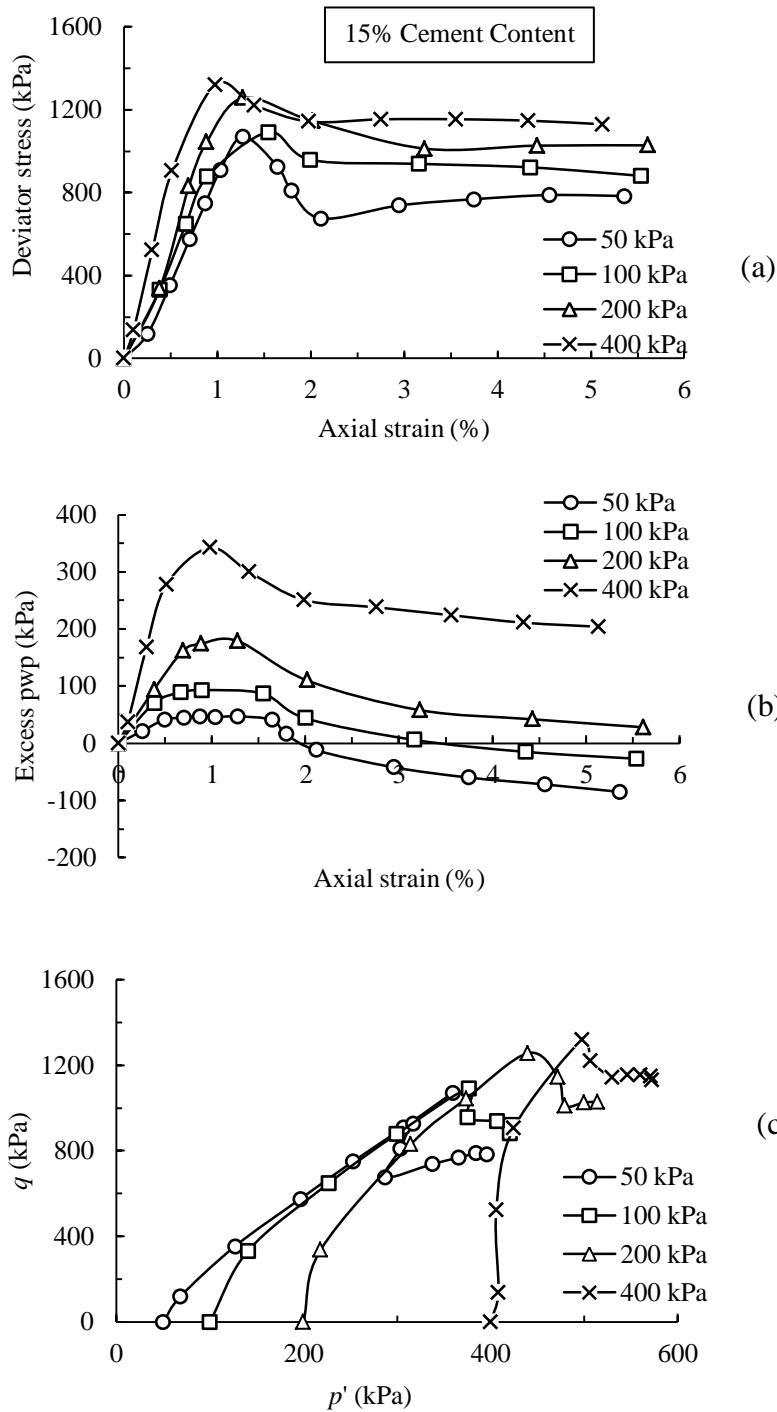
Figure 4.9 Triaxial test results for 15% cement content at various confining pressures (a) Deviator stress vs. axial strain (b) Excess pore pressure vs. axial stress and (c) Stress paths.
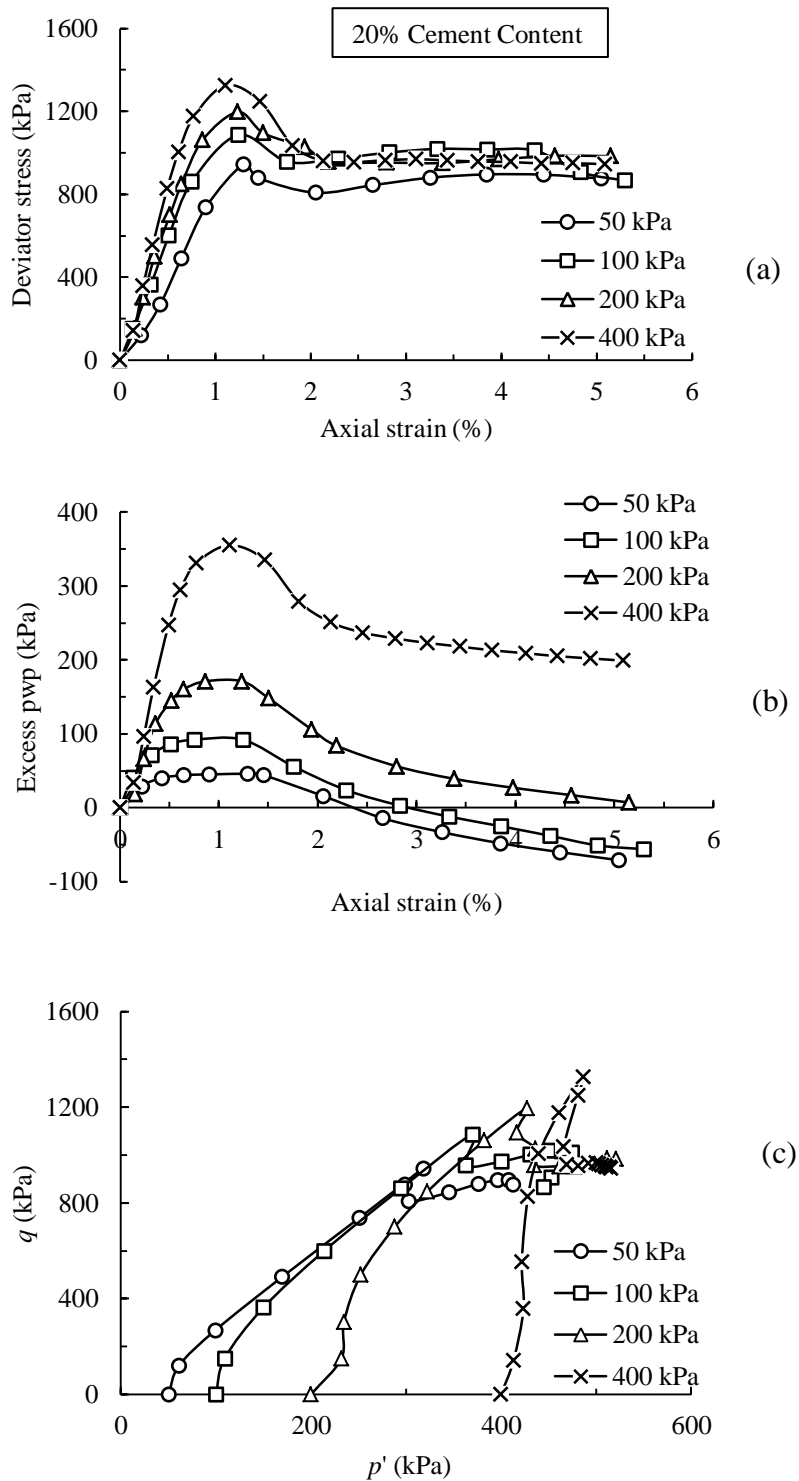
Figure 4.10 Triaxial test results for 20% cement content at various confining pressures (a) Deviator stress vs. axial strain (b) Excess pore pressure vs. axial stress and (c) Stress paths.

Evidently, the increase in strength for higher cement contents (25% and 30%) was also not significant. This means, the addition of cement beyond this 15% cement content would be highly uneconomical with no remarkable increase in strength. Hence 15% cement content can be treated as the optimum cement content for improvement, for the soil used in the study. Jan and Mir (2018) recently reported such a trend in case of cement treated dredged clay, wherein 16% cement content gave lesser strength than 12% cement content. The reason behind such a trend from micro-structural considerations is discussed in Horpibulsuk et al. (2010). This was discussed in detail in Chapter 2. It was reported that strength development upon increase in cement content can be classified into three zones – active zone, inert zone and deterioration zone (Figure 2.3). The maximum strength development happens during active zone wherein strength keeps on increasing with increase in cement content. Strength increase upon increase in cement content is negligible during inert zone. Addition of cement beyond this zone leads to decrease in strength, which reflects the deterioration zone. The above literature confirms the existence of optimum cement content for a soil. In this study, the optimum cement content was found to be 15%.

Figure 4.11 (b) shows the variation of excess pore pressure with axial strain, for specimens prepared at various cement contents and tested at a confining pressure of 100 kPa. Interestingly, all the cement contents recorded approximately equal values of peak excess pore water pressure, at the same confining pressure. Hence, the development of excess pore pressure is a direct function of confining pressure and the cement content has negligible influence on the same.

Figure 4.11 (c) shows the stress path for various cement contents, at a confining pressure of 100 kPa. All the cement contents followed the same path up to the peak deviator stress, at a particular confining pressure. Just like the excess pore pressure variation, path taken by cement treated soil was found to be largely dependent on the confining pressure. However, the peak deviator stress was a function of cement content.
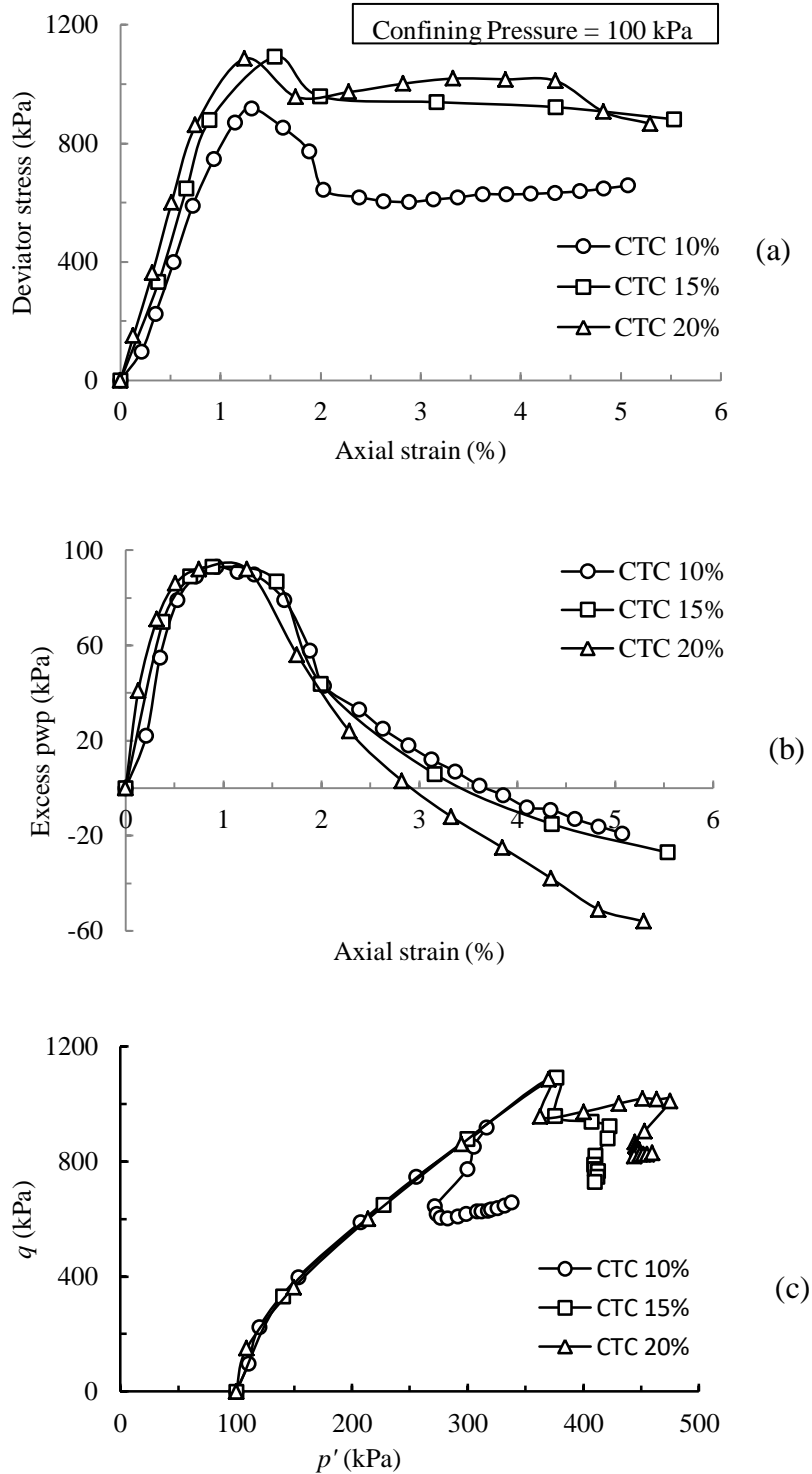
Figure 4.11 Triaxial test results for various cement contents at a confining pressure of 100 kPa (a) Deviator stress vs. axial strain (b) Excess pore pressure vs. axial strain and (c) Stress paths.
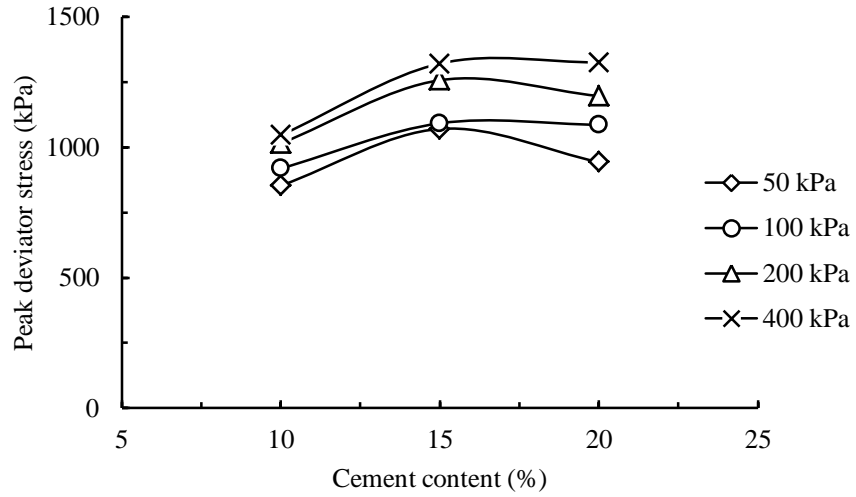
Figure 4.12 Variation of peak deviator stress with cement content for various confining pressures in triaxial tests.
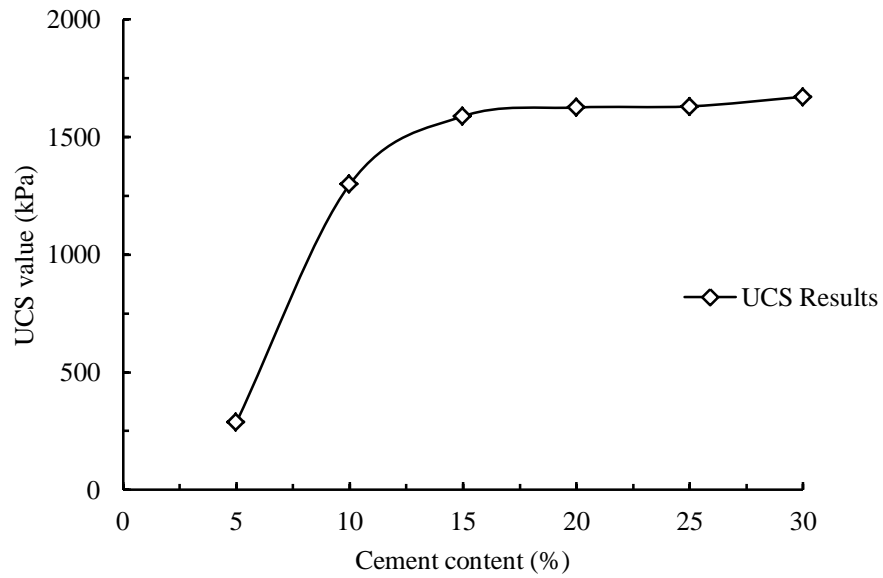
Figure 4.13 Unconfined compressive strength (UCS) values of specimens prepared at different cement contents.

Table 4.2 shows the shear strength parameters obtained for different cement contents, after performing triaxial tests. Talking in terms of shear strength parameters (c' and ϕ'), effective friction angle (ϕ') was found to be nearly constant for all the cement contents. However, the effective cohesion (c') value recorded significant changes, with variation in cement content. 15% cement content recorded the maximum strength with the highest cohesion value of 209 kPa. 20% cement content recorded a lower strength with reduction in cohesion value, but a small increase in friction angle was observed.

To conclude, confining pressure was seen to be a predominant factor which governs the development of pore pressure and path taken by soil in triaxial tests. However, peak strength was found to be largely dependent upon the cement content. The strength increased with increase in cement content up to 15% and then more or less remained constant.

Table 4.2 Shear strength parameters obtained for different cement contents under triaxial testing

Cement content (%)	Confining pressure (kPa)	Shear strength parameters
10	50 100 200 400	$\phi' = 46^0$ $c' = 172$ kPa
15	50 100 200 400	$\phi' = 47^0$ $c' = 209$ kPa
20	50 100 200 400	$\phi' = 54^0$ $c' = 152$ kPa

4.8 PLANE STRAIN RESPONSE

4.8.1 Effect of confining pressure

The results obtained at various confining pressures for plane strain specimens prepared at cement contents of 10%, 15% and 20% are shown in Figures 4.14, 4.15 and 4.16 respectively. Figures 4.14 (a), 4.15 (a) and 4.16 (a) show the variation of deviator stress with axial strain at various confining pressures. The change in applied confining pressure led to change in strength, but the change was not linear. An 8-fold increase in confining pressure resulted in a mere 9% increase in peak deviator strength for 10% cement content, and 16% each for 15% and 20% cement contents respectively. This shows that confining pressure has a meagre influence on strength gain under plane strain testing. Values of peak deviator stress for all cement contents and confining stresses and their corresponding excess pore water pressures are tabulated in Table 4.3.

Moreover, plane strain specimens were seen to suffer severe softening after reaching peak stress, at all confining pressures. The amount of softening observed in plane strain samples was different when subjected to different confining pressures.

Figures 4.14 (b), 4.15 (b) and 4.16 (b) show the variation of excess pore water pressure with axial strain, at various confining pressures. The development of excess pore pressure was found to be hugely dependent upon the applied confining pressures, for all cement contents. Higher pore pressures were developed at higher confining pressures and negative pore pressures were obtained at lower confining pressures.

Figures 4.14 (c), 4.15 (c) and 4.16 (c) shows the stress path variations at various confining pressures. Clearly, over-consolidated behaviour was observed for all cement contents. However, slight transition was observed from OC to NC behaviour at higher confining pressures very similar to triaxial results.
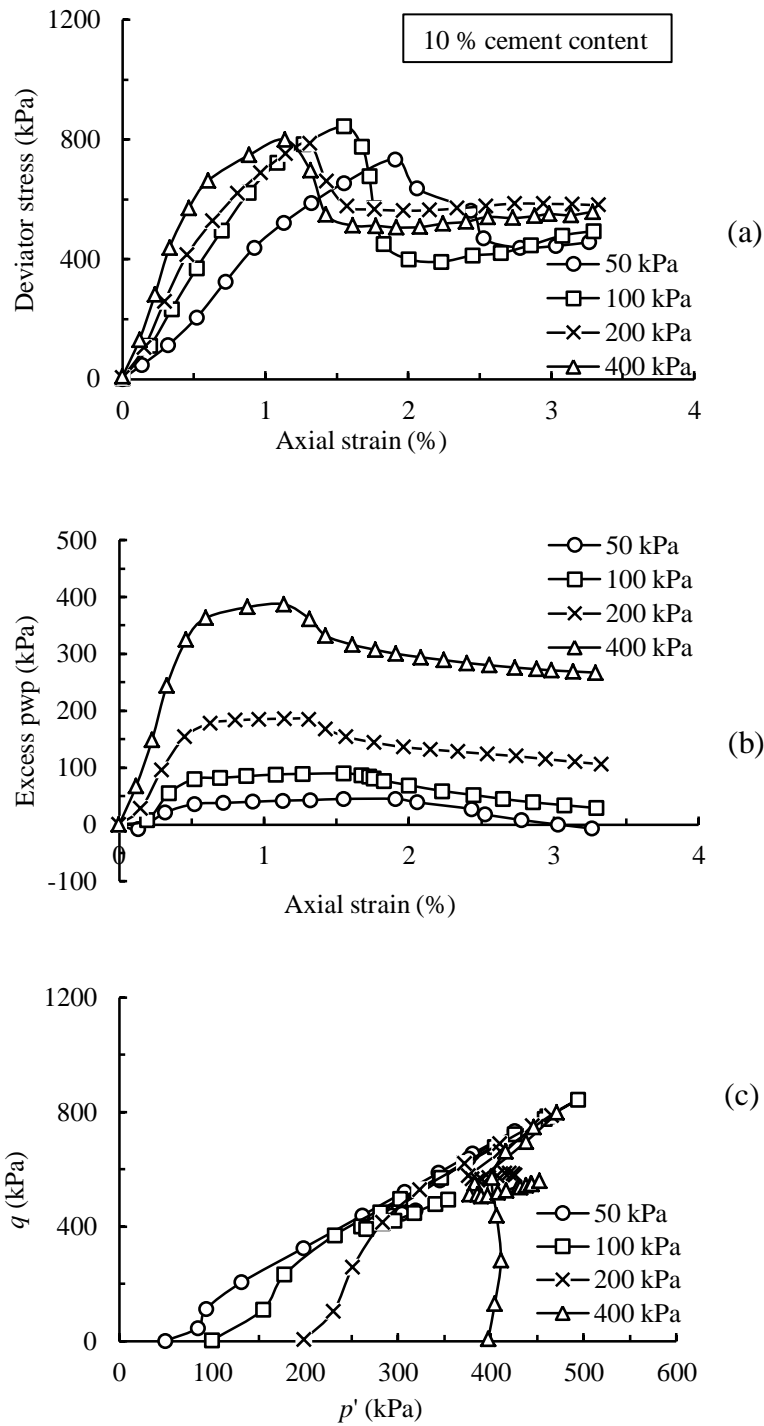
Figure 4.14 Plane strain tests for 10% cement content at various confining pressures (a) Deviator stress vs. axial strain (b) Excess pore pressure vs. axial strain and (c) Stress paths.
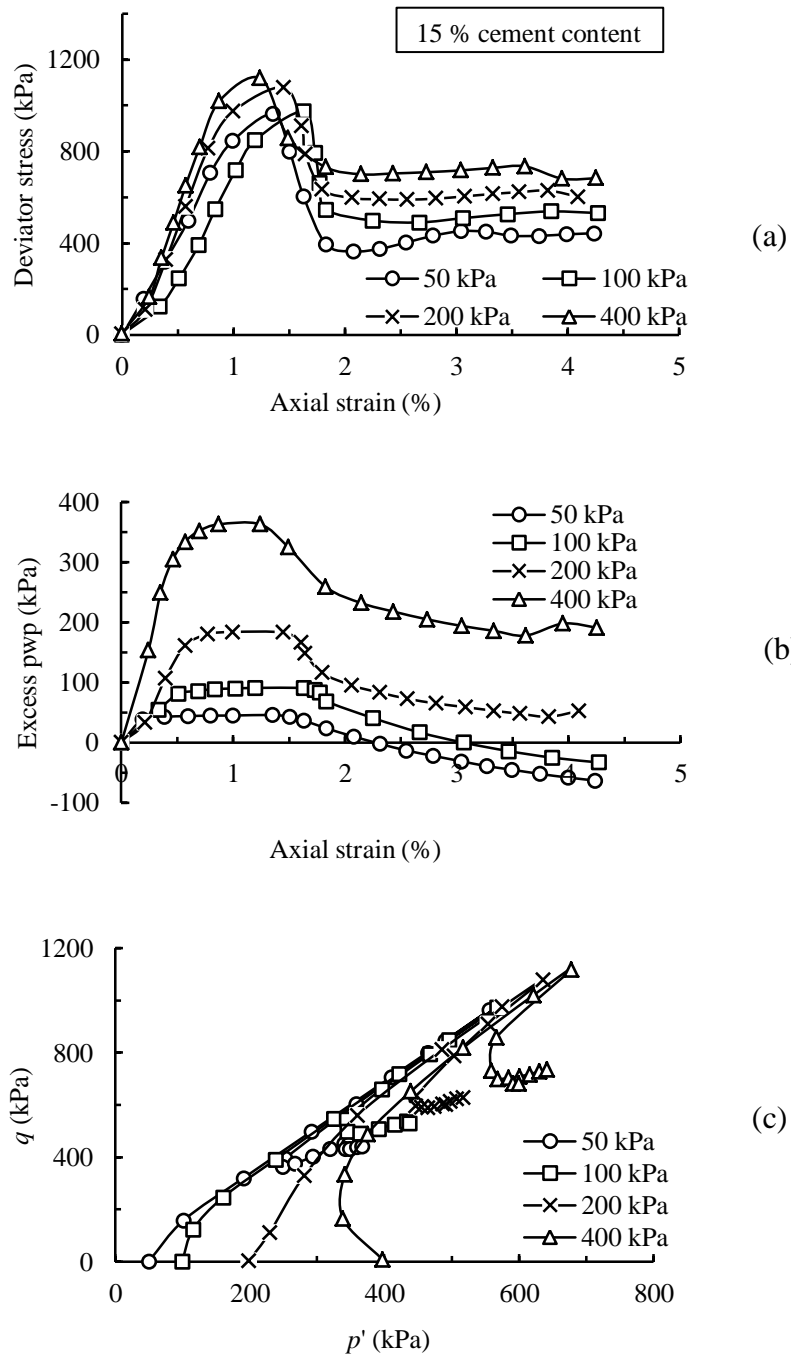
Figure 4.15 Plane strain tests for 15% cement content at various confining pressures (a) Deviator stress vs. axial strain (b) Excess pore pressure vs. axial strain and (c) Stress paths.
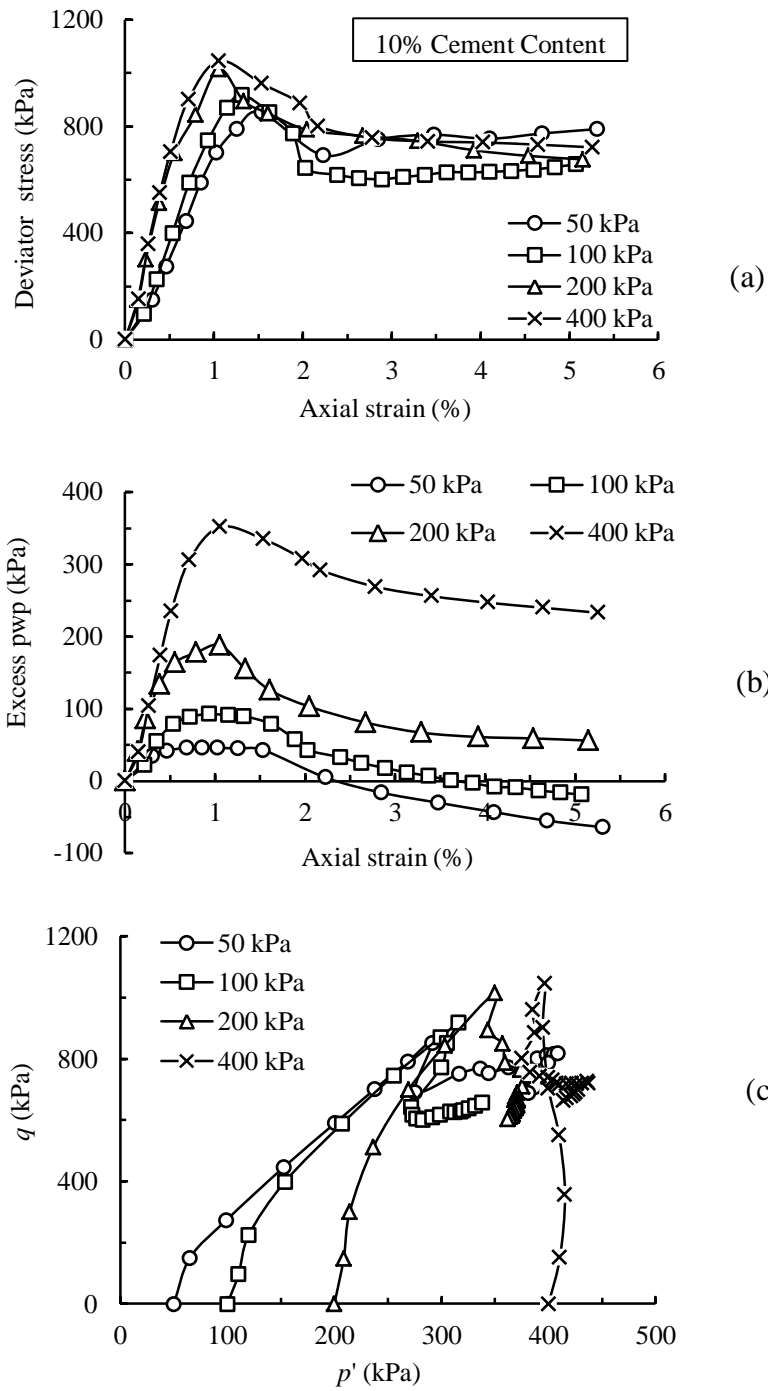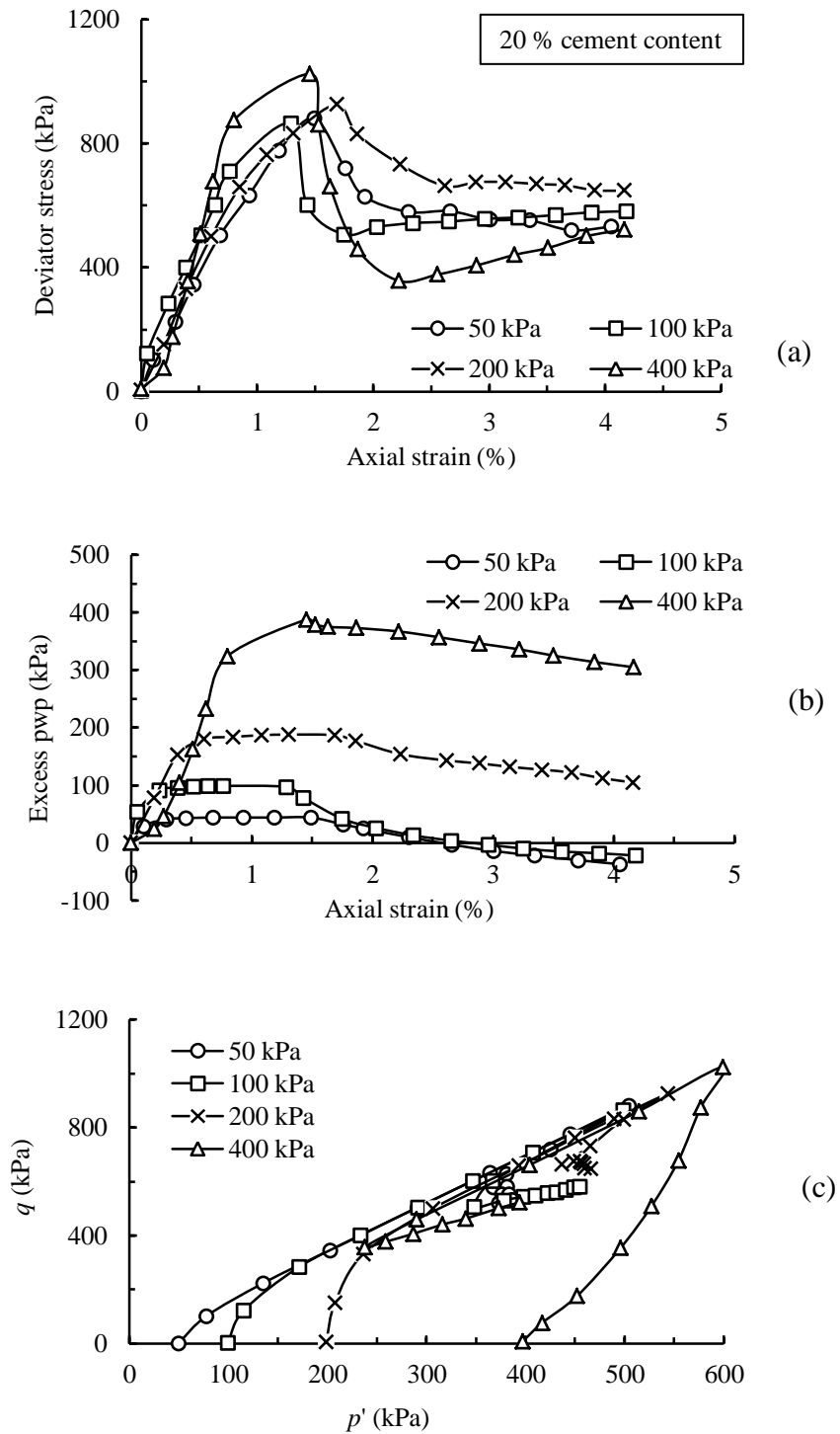
Figure 4.16 Plane strain tests for 20% cement content at various confining pressures (a) Deviator stress vs. axial strain (b) Excess pore pressure vs. axial strain and (c) Stress paths.

## 4.8.2 Effect of cement content

Figure 4.17 (a) shows the variation of deviator stress with axial strain for various cement contents, tested at a confining pressure of 100 kPa. Clearly, there is an increase in strength when cement content is increased from 10% to 15%. However, a reduction in strength is observed when cement content is increased to 20%.

Figure 4.17 (b) shows the variation of excess pore water pressure with axial strain for various cement contents. All the cement contents recorded relatively equal peak pore pressure values, at a particular confining pressure. This shows that pore pressure developed majorly depends on the applied confining pressure and not on cement content.

Figure 4.17 (c) shows the stress path variation for various cement contents. Same path was followed by all cement contents, at a particular confining pressure. However, the peak deviator stress was dependent on the cement content.

Figure 4.18 shows the variation of peak deviator stress values with cement content. The drop in strength for 20% in plane strain tests is slightly more significant compared to triaxial tests. This consolidates the hypothesis that this trend is characteristic of cement treated soil.

Table 4.3 shows the shear strength parameters obtained for different cement contents under plane strain testing. The shear strength parameters in case of plane strain tests were found out in the same manner as in triaxial test conditions. Shear strength parameters are still governed by major and minor principal stress values. Intermediate principal stress has no effect on the shear strength parameters in case of plane strain tests (Parry, 2014). In case of 10% and 20% cement contents, the angle of internal friction (ϕ') contributes significantly to shear strength along with considerable cohesion (c'). On the other hand, cohesion was found to be a major strength parameter in case of 15% cement content. The friction angle was found to be the same as that in triaxial test.
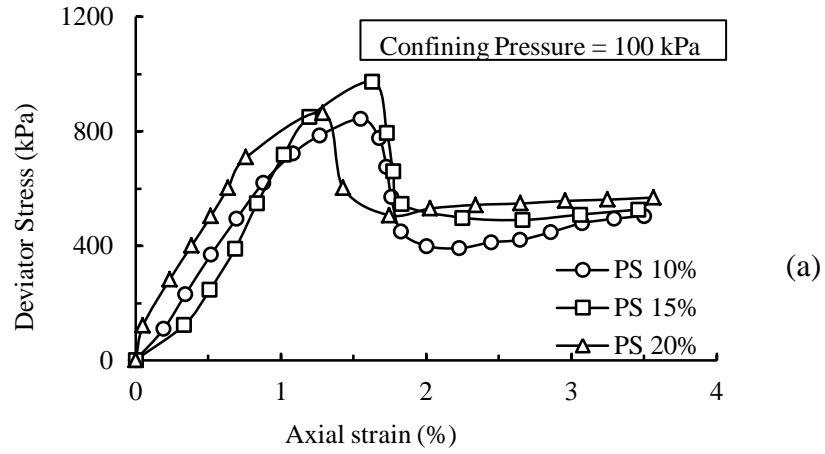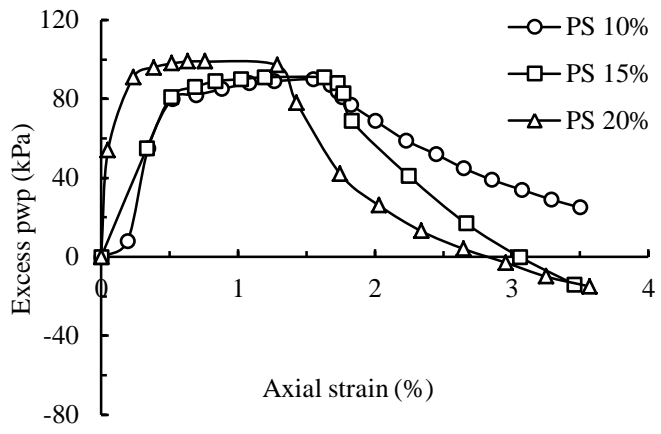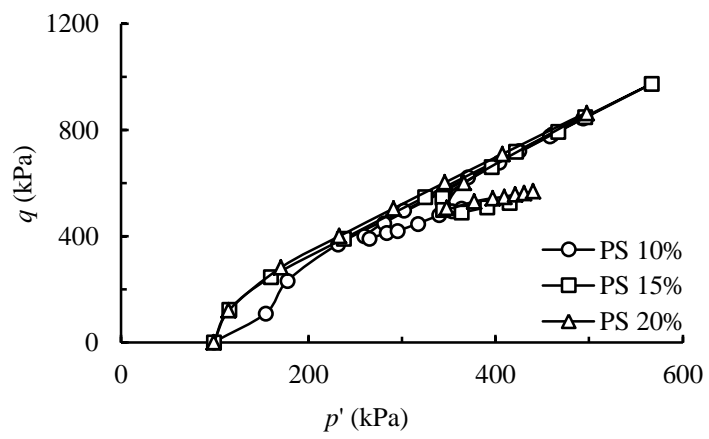
Figure 4.17 Plane strain results for various cement contents obtained at a confining pressure of 100 kPa (a) Deviator stress vs. axial strain (b) Excess pore pressure vs. axial strain and (c) Stress paths.
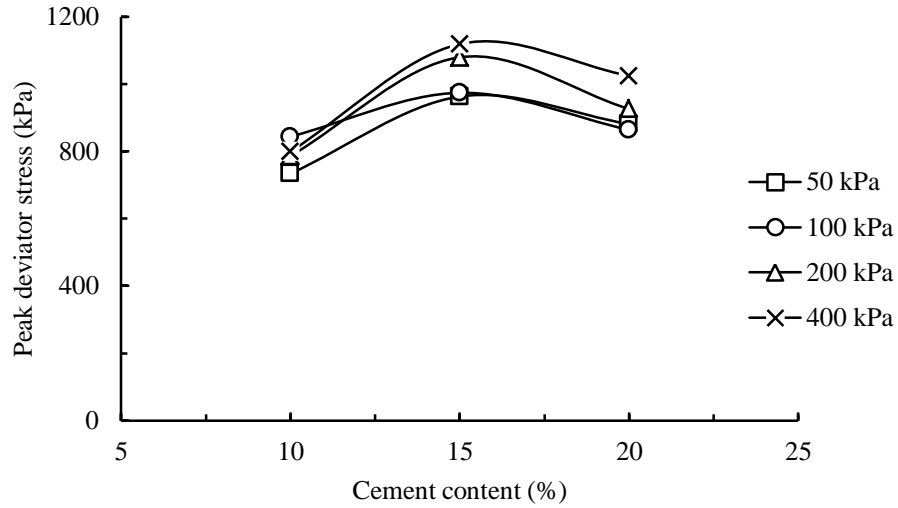
Figure 4.18 Variation of peak deviator stress with cement content for all confining pressures in plane strain tests.

Table 4.3 Shear strength parameters obtained for different cement contents under plane strain testing

Cement content (%)	Confining pressure (kPa)	Shear strength parameters
	50	$\phi' = 63^0$
	100	
10	200	$c' = 72$ kPa
	400	
	50	$\phi' = 47^0$
	100	
15	200	$c' = 184$ kPa
	400	
	50	$\phi' = 64^0$
	100	
20	200	$c' = 87$ kPa
	400	

85

To conclude, the trends shown by plane strain tests were seen to be approximately the same as in case of triaxial tests. However, comparison of results obtained from both the tests is essential to arrive at a rational conclusion.

4.9 COMPARISON OF BEHAVIOUR UNDER PLANE STRAIN AND TRIAXIAL CONDITIONS

The main objective of this study is to compare the behaviour of cement treated clays tested under triaxial and plane strain conditions. A comparison was made between the plots of deviator stress – axial strain, excess pore water pressure – axial strain and stress paths in case of triaxial and plane strain tests. Figures 4.19, 4.20 and 4.21 show the comparison of the results obtained from the two testing methods at cement contents of 10%, 15% and 20%, respectively and tested at a confining pressure of 100 kPa.

Clearly, Figures 4.19 (a), 4.20 (a) and 4.21 (a) reveal that samples tested under triaxial testing conditions exhibit higher strength compared to the specimens tested under plane strain conditions. This trend was observed at all cement contents, showing that this is an inherent property of cement treated clay. Chang et al. (1999) reported the same trend in case of over consolidated clays. Hence this trend is justified because cement treated clays behave just like over consolidated clays within the pre-yield stress zone. Reverse trend has been reported in the literatures (Chang et al., 1999; Alshibli and Akbas, 2007) in case of normally consolidated clays.

Strength under triaxial condition was found to be 1.1 to 1.3 times the strength under plane strain condition. Therefore, the use of shear strength parameters obtained from triaxial tests may lead to overestimation of strength. Furthermore, severe softening was observed in case of plane strain samples post peak stress, whereas it was minimal in case of triaxial samples. This phenomenon is to be taken into account, as far as field conditions are concerned. Furthermore, the failure strains were found to be comparable in both modes of testing. This is against the findings by Lee (1970) in sands, where plane strain specimens failed at smaller axial strains than triaxial specimens.
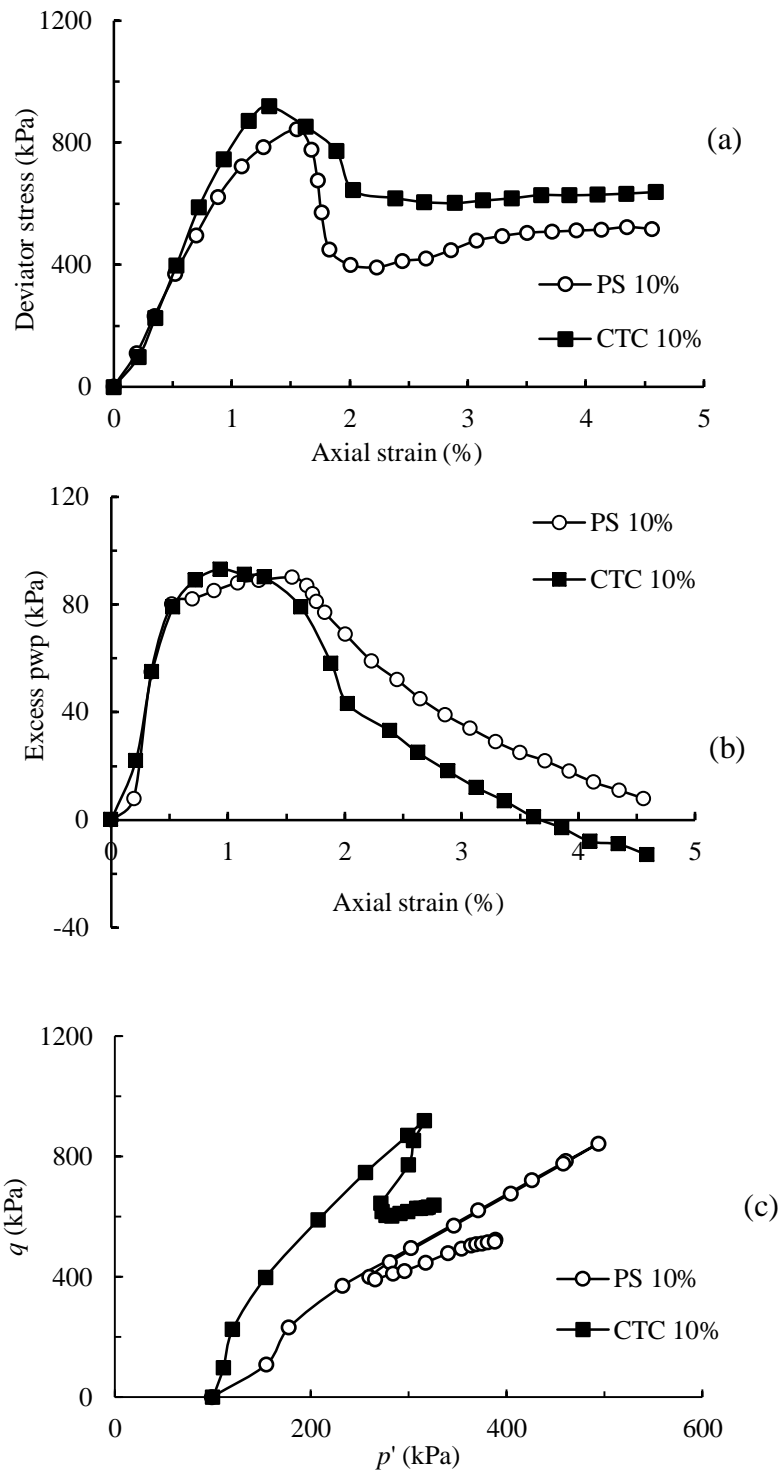
Figure 4.19 Plane strain vs. triaxial test results for 10 % cement content (a) Deviator stress vs. axial strain (b) Excess pore pressure vs. axial strain and (c) stress paths.
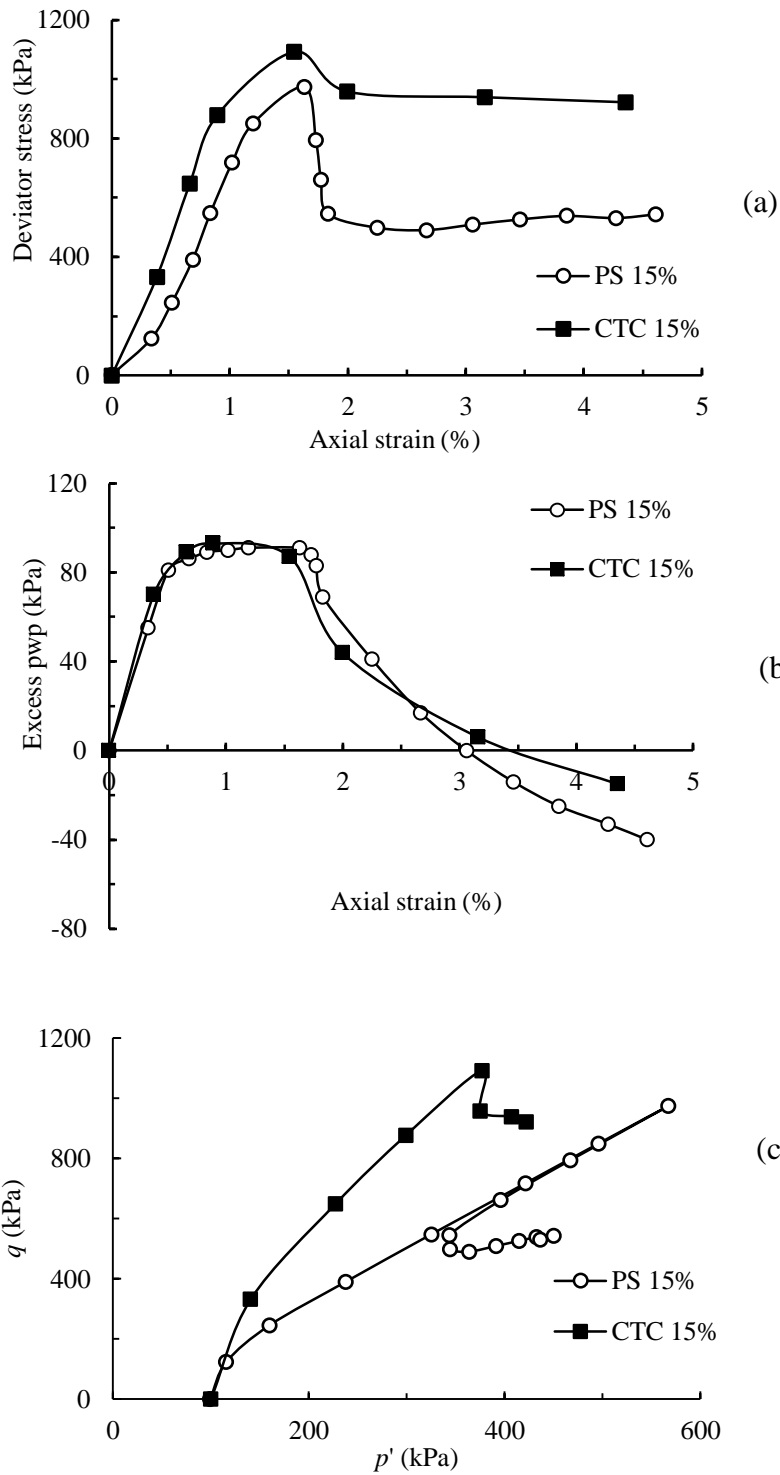
Figure 4.20 Plane strain vs. triaxial test results for 15 % cement content (a) Deviator stress versus axial strain (b) Excess pore water pressure versus axial strain and (c) stress path.

Figure 4.21 Plane strain vs. triaxial test results for 20 % cement content (a) Deviator stress versus axial strain (b) Excess pore water pressure versus axial strain and (c) stress path.

From Figures 4.19 (b), 4.20 (b) and 4.21 (b), the excess pore water pressures developed were found to be approximately the same in both triaxial and plane strain tests, tested at a particular confining pressure (100 kPa). This shows that the development of excess pore pressure solely depends on the confining pressure and is independent of cement content or mode of testing.

Figures 4.19 (c), 4.20 (c) and 4.21 (c) show the stress paths for various cement contents under plane strain and triaxial loading conditions. It is evident that the samples follow different stress paths to failure, under different testing conditions. This is obviously because, the mean effective stress (p') values are different in case of triaxial and plane strain conditions.

As far as the failure patterns after testing are concerned, Figures 4.22 (a) and (b) show that different patterns of failure are observed under the two modes of testing. While clear shear band was observed for plane strain specimens, complicated failure pattern was observed for triaxial specimen. This is in line with the findings in the literature (Mokni and Desrues, 1999; Alshibli et al., 2000, 2003; Alshibli and Akbas, 2007). However, bulging failure pattern was not observed in triaxial specimens, as observed in previous studies. This is obviously because of the brittle nature of cement treated clay.
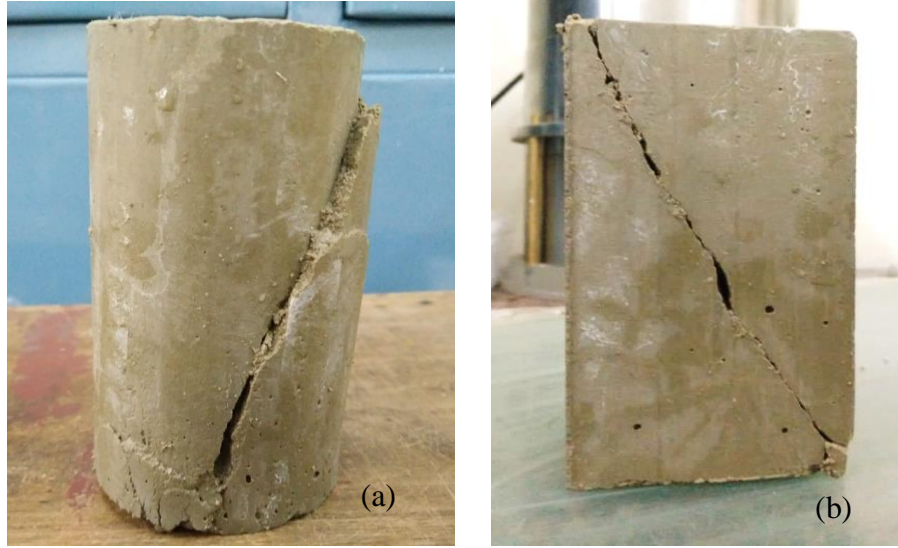
Figure 4.22 Failure patterns for (a) Triaxial and (b) Plane strain tests.

4.10 SUMMARY

Based on the comparative study between plane strain and triaxial testing on cement treated marine clay, the following conclusions are drawn.

1. The variation of deviator stress with axial strain, excess pore pressure with axial strain and stress path show that cement treated soil behaves like over consolidated clays. This was observed for both modes of testing i.e. under triaxial and plane strain conditions.

2. Excess pore pressure developed was found to be entirely dependent on the confining pressure applied but not on the cement content or the mode of testing. Both triaxial and plane strain tests at a particular confining pressure resulted in approximately the same excess pore water pressure for all cement contents. Specimens prepared at different cement contents and tested at a particular confining pressure also gave excess pore pressure values in a close range.

3. Strength under plane strain condition was found to be lower than that under triaxial condition. This is similar to the behaviour of over consolidated clays reported previously

in the literature. This trend is justified since cement treated soil also shows an over consolidated behaviour. In this study, strength under triaxial condition was found to be 1.1 to 1.3 times that under plane strain condition.

4. Plane strain test samples undergo severe softening post peak stress, whereas minimum softening is only visible in case of triaxial test. This means that specimens undergo rapid reduction in strength after attaining peak strength. This phenomenon is not significant in case of triaxial test.

CHAPTER 5

FAILURE ENVELOPE OF CEMENT TREATED CLAY UNDER DRAINED AND UNDRAINED CONDITIONS

5.1 INTRODUCTION

The mechanical behaviour of cement treated clay has been well established in the literature. However, most of them are based on consolidated undrained (CU) triaxial tests or unconfined compressive strength (UCS) tests, as these tests are relatively faster. Effective shear strength parameters are often derived from undrained (CU) tests. In practice, drained triaxial tests are rarely performed for both stabilized and non-stabilized clays as the tests are often time consuming. While the consolidated drained (CD) and consolidated undrained (CU) tests yield comparable results in terms of effective stress for natural soils, literature suggests that this holds true only for normally consolidated soils and not for over-consolidated soils (Holtz et al., 2015). It is well established that cement treated clays apparently behave like over consolidated soils. In view of this, the present study focuses on studying the behaviour of cement treated marine clay under both drained and undrained conditions.

Owing to the over consolidated nature of cement treated soils, the failure envelope may be expected to be curved or non-linear. This non-linearity of failure envelope in cemented sands has been discussed by many researchers (Consoli et al., 2012; Sharma et al., 2011; Asghari et al., 2003). This aspect has also been discussed in the case of cement treated marine clays (Panda and Rao, 1997; Sankar and Paul, 1997). On the contrary, linear Mohr-Coulomb failure envelope has also been reported by some researchers for cemented soils (Amini and Hamidi, 2014; Chiu et al., 2008). However, all these studies were carried out for low levels of cement treatment. Studies are scarce in case of heavily cemented marine clays which are used in deep soil mixing. Attempt has been made in this study to assess the failure envelopes of heavily cemented marine clays (with cement contents greater than 10%), under both drained and undrained testing conditions.

Results pertaining to undrained testing have already been discussed in Chapter 4. The behaviour of cement treated clay under drained conditions along with the results of undrained tests will be discussed in this chapter. Results corresponding to both triaxial and plane strain conditions will be discussed.

5.2 CONSOLIDATED DRAINED TRIAXIAL TESTS

5.2.1 Testing Procedure

Consolidated drained triaxial tests were performed on cement treated clay specimens of 50 mm diameter and 100 long, after a curing period of 28 days. Tests were performed using a fully automated VJ Tech triaxial apparatus capable of applying deformation to a precision of 0.0001 mm/min. Specimens were prepared at cement contents of 10%, 15% and 20%, and were tested at confining pressures of 50 kPa, 100 kPa, 200 kPa and 400 kPa. VJ Tech hydraulic pressure-volume controllers of 3000 kPa capacity were used for the applications of cell pressure and back pressure. The volume change measured by the back pressure controller and used during consolidation and shearing stages, were used for analysing the test results. The pressure lines of triaxial apparatus were de-aired before placing the specimen. An external load cell and a pore pressure transducer with capacities of 10 kN and 1000 kPa were used for measuring the axial force and pore pressure, respectively. The test setup is the same as that used for undrained triaxial tests.

The saturation and consolidation of drained triaxial tests were performed just as discussed in case of undrained triaxial tests. This was discussed in great length in Chapter 4 and will not be repeated in this chapter. To make sure that excess pore water pressure is not generated at any time during shearing stage, a very slow deformation rate of 0.0125 mm/min was adopted for drained shearing. Since, shearing stage is to be conducted under drained condition, back pressure valve was kept open during the shearing stage. The load values recorded by the load cell and the corresponding volume change recorded by the back pressure controller were noted during this stage. Shearing was continued till a residual value was obtained after the peak strength, to capture the post peak regime. Plots of deviator stress versus axial strain, volumetric strain

pressure versus axial strain and q versus p' (where q is the deviator stress and p' is the mean effective stress) stress path were made.

5.2.2 Results

Drained triaxial results obtained for cement contents of 10%, 15% and 20% are shown in Figures 5.1, 5.2 and 5.3 respectively. In these figures, CTC represents conventional triaxial compression test results. The sub-sections (a), (b) and (c) in these figures show the plots of deviator stress versus axial strain, volumetric strain versus axial strain and q versus p' stress paths respectively.

Figures 5.1 (a), 5.2 (a) and 5.3 (a) show a strong softening behaviour after the attainment of peak deviator stress. This indicates an over-consolidated behaviour, which is typically observed in cement treated soils (Subramaniam et al., 2015). However, the softening behaviour was found to have reduced at a higher confining pressure of 400 kPa, indicating a transition towards normally consolidated behaviour.

Figures 5.1 (b), 5.2 (b) and 5.3 (b) show the volumetric strain behaviour for different cement contents. Dilative behaviour was visible across all cement contents and confining pressures. However, contractive behaviour was observed for confining pressure of 400 kPa. As mentioned in the deviator stress response, this indicates a transition from over-consolidated to normally consolidated behaviour.

Figures 5.1 (c), 5.2 (c) and 5.3 (c) show the drained stress paths for different cement contents. As expected, a stress path of slope equal to 3 in 1 was observed across all cement contents and confining pressures.
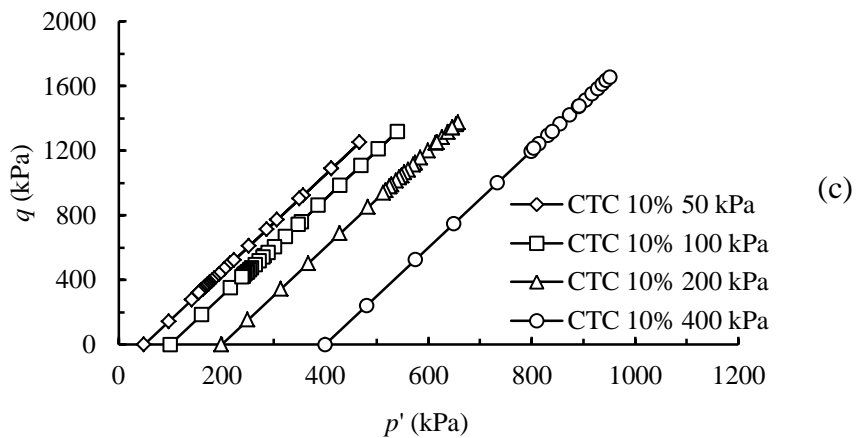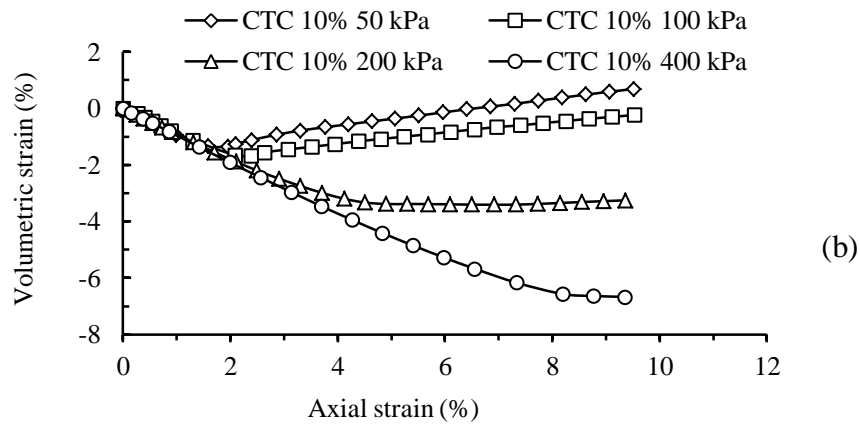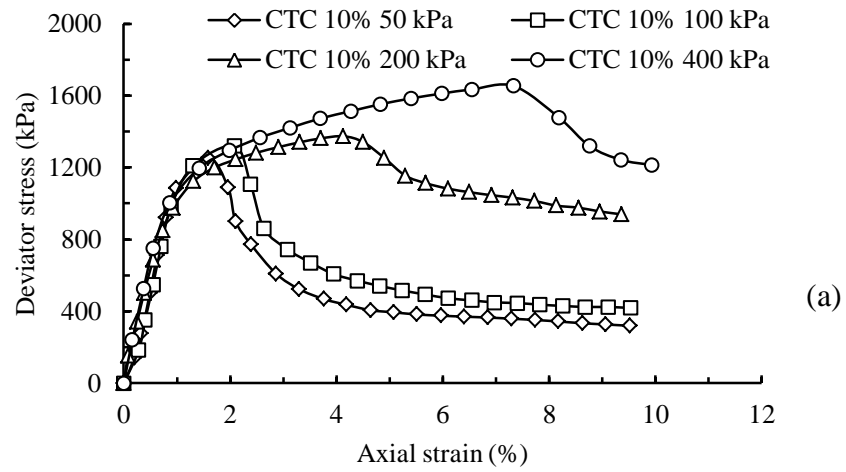
Figure 5.1 Drained triaxial test results for 10% cement content: (a) Deviator stress versus axial strain (b) Volume change versus axial strain and (c) Drained stress paths.
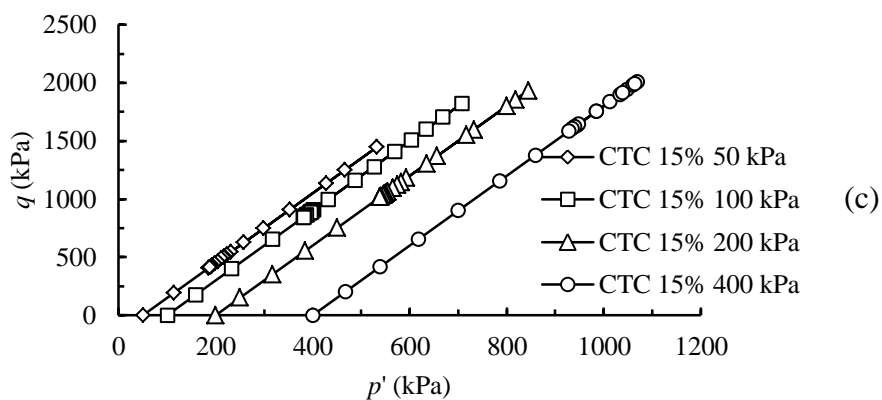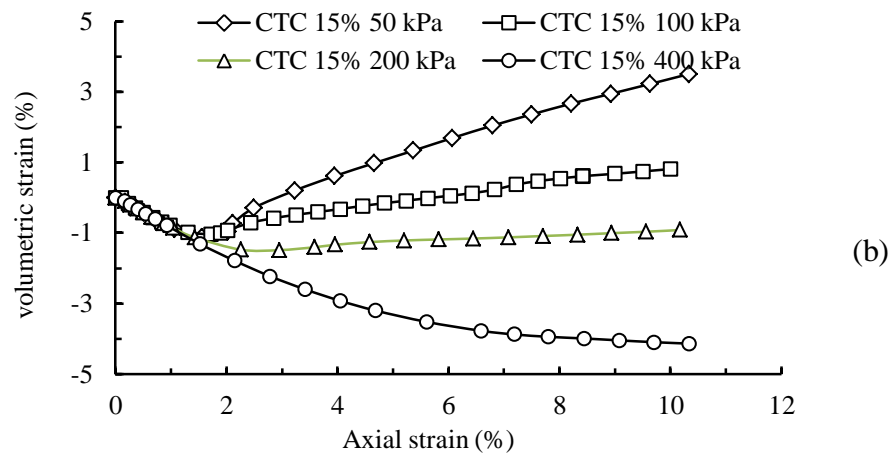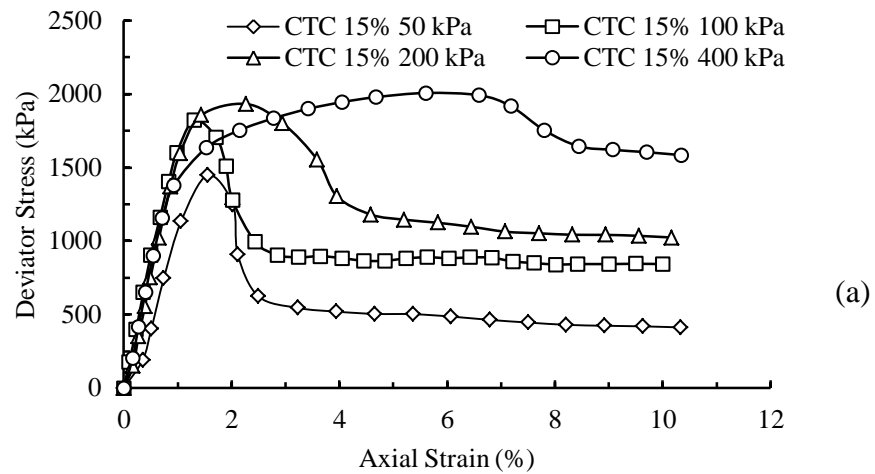
Figure 5.2 Drained triaxial test results for 15% cement content: (a) Deviator stress versus axial strain (b) Volume change versus axial strain and (c) Drained stress paths.
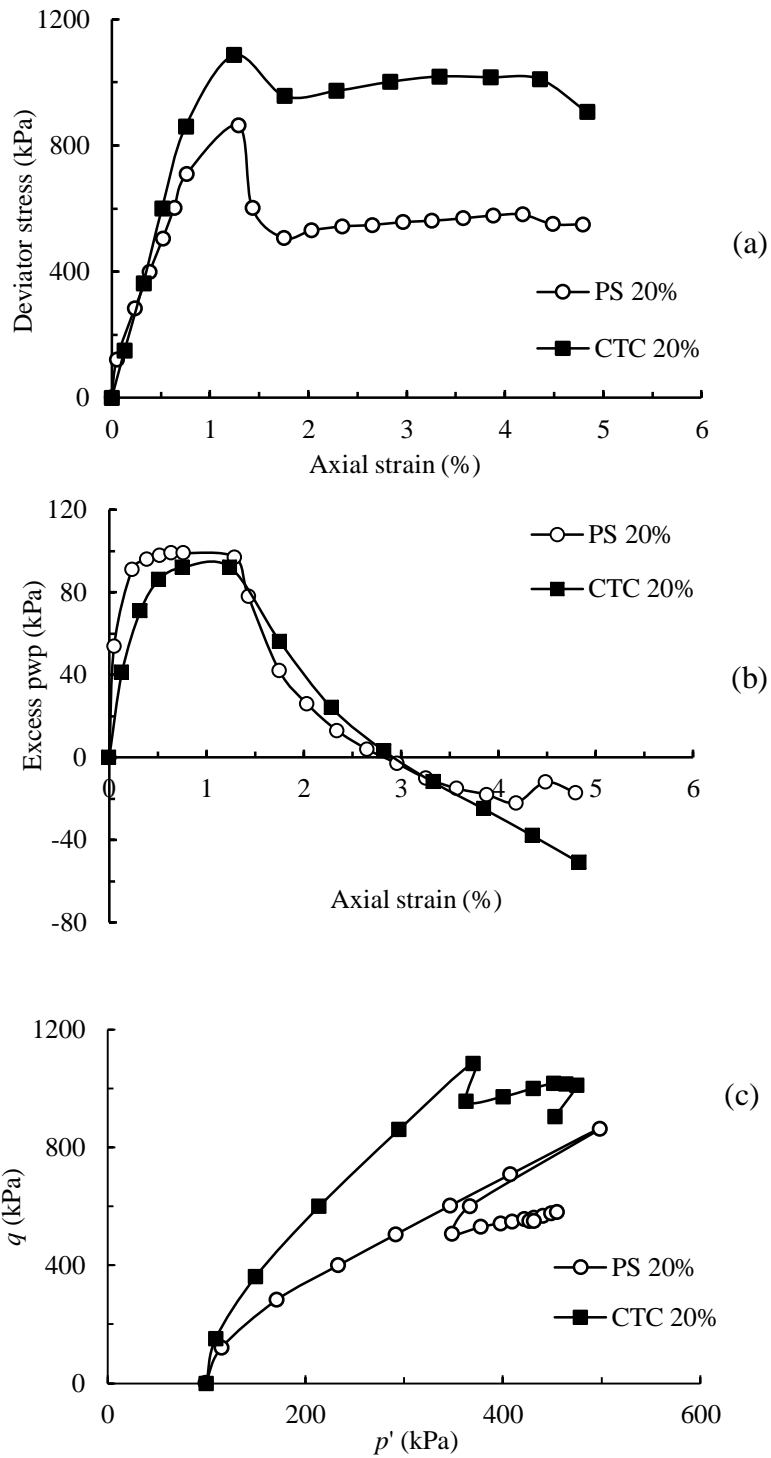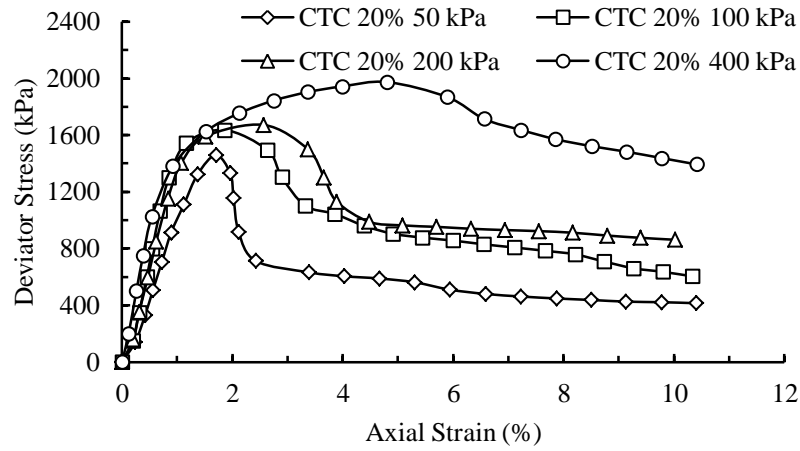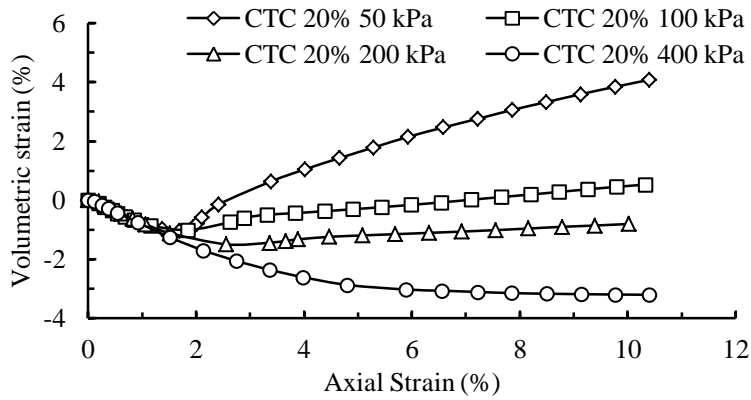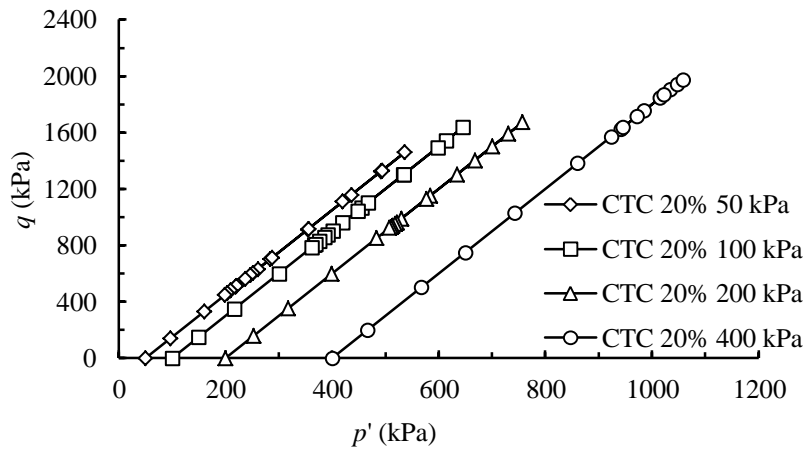
Figure 5.3 Drained triaxial test results for 20% cement content: (a) Deviator stress versus axial strain (b) Volume change versus axial strain and (c) Drained stress paths.

5.2.3 Shear Strength Parameters

Effective shear strength parameters (c' and ϕ') are often determined using modified Mohr-Coulomb envelope, plotted between $(\sigma_1' - \sigma_3')/2$ and $(\sigma_1' + \sigma_3')/2$. The peak deviator stress values are used to plot this envelope. The shear strength parameters under undrained conditions were already discussed in Chapter 4. The shear strength parameters under both drained and undrained conditions will be compared in this chapter.

Table 5.1 provides an idea about the differences in shear strength parameters of cement treated clay, under drained and undrained conditions. Stark contrast can be observed in the shear strength parameters. Peak deviator stress values were found to be substantially higher for drained tests compared to the corresponding undrained tests, as shown in Table 5.2. This is the reason for such a contrast in shear strength parameters.

It was already pointed out that over-consolidated soils yield different results under drained and undrained conditions. The trend observed in this study is hence justified as the cement stabilized soils behave like over consolidated soils. An increased cohesion intercept and decreased friction angle were observed under drained conditions. This points towards an increased over-consolidated nature of cement treated clay, under drained condition. The deviator stress versus axial strain plots for all the cement contents are in agreement with this argument. Furthermore, the highest cohesion value and peak deviator stress were obtained for a cement content of 15%. This aspect was already discussed in detail in Chapter 4. The observance of same trend under drained and undrained conditions strengthens the existence of optimum cement content.

5.3 COMBINATION OF UNDRAINED AND DRAINED TRIAXIAL TEST RESULTS

As shown in Table 5.1, the effective shear strength parameters of cement treated clay under drained and undrained conditions were not the same. In order to find out the reasons for why this occurs, the modified failure envelope from drained and undrained conditions were compared in the same plot, as shown in Figure 5.4. Interestingly, the results were found to lie on a single curved envelope. However, the plots were non-linear for all the cement contents. This shows that

the higher cohesion intercept and lower angle of internal friction obtained in drained test is due to the non-linear failure envelope and that drained and undrained tests individually do not follow two separate failure envelopes. Considering two individual failure envelopes for drained and undrained tests separately for a narrow range of confining pressures, can lead to highly contrasting shear strength parameters. The mean effective stress $(\sigma_1' + \sigma_3')/2$ is lower in case of undrained tests due to the presence of excess pore water pressure. Hence, the lower value of $(\sigma_1' - \sigma_3')/2$ in case of undrained tests is due to the existence of a single curved failure envelope passing through both drained and undrained test results. This also means that doing a drained test at very low confining pressure should result in a strength value close to undrained test results.

Table 5.1 Shear strength parameters for drained and undrained triaxial tests

Cement content (%)	Confining pressure (kPa)	Shear Strength Parameters	
		Drained	Undrained
10	50	$\phi' = 21^0$ $c' = 406$ kPa	$\phi' = 46^0$ $c' = 172$ kPa
	100		
	200		
	400		
15	50	$\phi' = 26^0$ $c' = 471$ kPa	$\phi' = 47^0$ $c' = 209$ kPa
	100		
	200		
	400		
20	50	$\phi' = 24^0$ $c' = 459$ kPa	$\phi' = 54^0$ $c' = 152$ kPa
	100		
	200		
	400		

Table 5.2 Peak deviator stress values for drained and undrained triaxial tests

Cement content (%)	Confining pressure (kPa)	Peak Deviator Stress (kPa)	
		Drained	Undrained
10	50	1252	853
	100	1319	919
	200	1374	1015
	400	1653	1046
15	50	1447	1070
	100	1822	1092
	200	1932	1257
	400	2007	1321
20	50	1450	943
	100	1636	1087
	200	1672	1196
	400	1975	1325

As can be clearly seen in Figure 5.4, use of a linear approximation of the entire envelope may result in significant errors, especially at higher confining pressures. Hence, the use of Mohr-Coulomb theory may not be appropriate for the case of cement treated clays. Use of non-linear failure envelope similar to the case of rocks (Singh et al., 2011; Shen et al., 2018) may be more appropriate. However, a suitable constitutive model needs to be selected to represent this failure envelope. If successful, this can form a simple constitutive framework to predict the behaviour of cement treated clays.
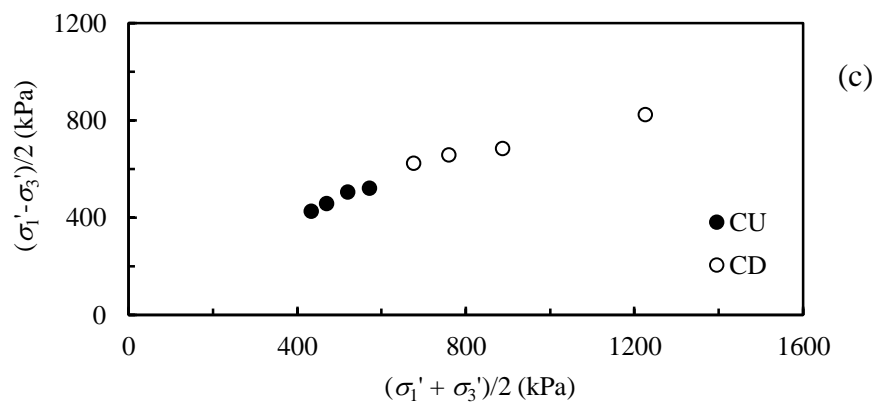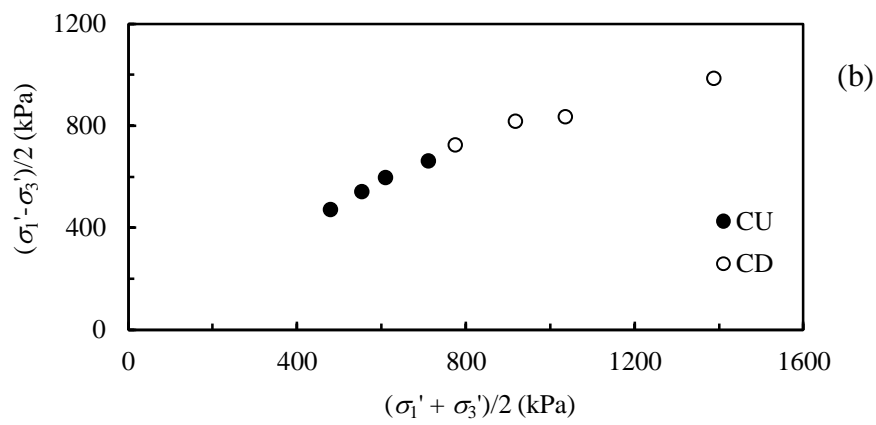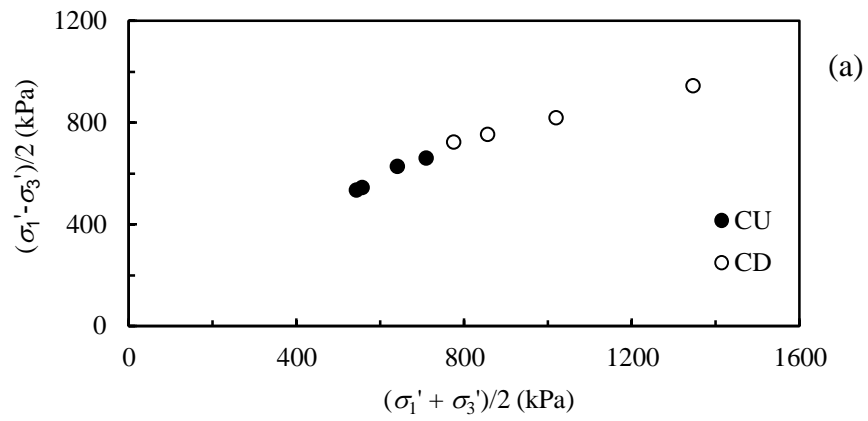
Figure 5.4 Drained and undrained triaxial results put together (a) 10% cement content (b) 15% cement content and (c) 20% cement content.

5.3.1 Use of a Non-linear Failure Envelope

Different non-linear relations have been used by researchers to describe the shear strength of soil. Simple non-linear power law functions have been used in many studies (de Melo, 1977; Charles and Watts, 1980; Charles and Soares, 1984; Collins et al., 1988; Maksimovic, 1989; Perry, 1994). Later, generalized non-linear Mohr envelopes were used by Baker (2004) and Sharma et al. (2011). The above theories have successfully predicted the shear strength of soils employing the results from either drained or undrained tests. However, in this study, non-linearity was observed for a failure envelope encompassing the results from both drained and undrained tests.

An attempt was made in this study to use Hoek-Brown model (Hoek and Brown, 1980) for the representation of non-linear failure envelope of cement treated clays. This model is widely used for rocks and has seldom been used for soils. The ability of the model to simulate non-linear and brittle behavior of geomaterial, makes it a viable option to be used for cement treated clay. The fact that cement treated soil behaves like a very soft rock, the applicability of the model may be valid.

This model was initially proposed for intact rocks. Later, generalized Hoek-Brown criterion was introduced by Hoek and Brown (1997) for the representation of rock mass strength and can be expressed as,

$$\sigma'_1 = \sigma'_3 + \sigma_c (m_b \frac{\sigma'_3}{\sigma_c} + s)^a \tag{1}$$

where σ'_1 and σ'_3 are major and minor effective principal stresses

σ_c is the uniaxial compressive strength of rock

m_b, s and a are empirical material constants

This version of the model is capable of addressing the discontinuities and joints in rock mass and was used in this study. The variation in parameter "a" enables the adjustment of shape of

principal stress plot (Hoek and Brown, 2018). In the initial version (Hoek and Brown, 1980), the material constants were assumed as: $s = 1$, $a = 0.5$ and $m_b = m_i$.

For this study, σ_c was assumed to be the unconfined compressive strength of cement treated clay, as assumed in the latest version of Hoek-Brown model (Hoek and Brown, 2018). The material constants (m, s and a) were found out through non-linear regression analysis. The non-linear failure envelope was established using the following procedure.

1. The drained and undrained results were plotted together on a plot of effective major principal stress versus effective minor principal stress.
2. σ_c was assigned as the UCS value for a particular cement content and hence, remains constant throughout the curve. The same values of σ_3', as obtained from the experimental results, were chosen to fit the curve. The material constants (m_b, s and a) are chosen as fitting variables, to obtain the best fit curve.
3. Non-linear regression analysis was then performed using a least square fitting tool called *Solver* in *Microsoft Excel*. The values of material constants for a best fit curve were deduced.
4. The procedure was repeated for all cement contents and Hoek-Brown failure envelopes were established for all the cases.

The Hoek-Brown material parameters thus obtained for all the cement contents are given in Table 5.3. The UCS values are also provided for reference. Figure 5.5 shows the Hoek-Brown failure envelopes hence, established.

As can be seen in Figure 5.5, the failure envelopes were found to be in reasonable agreement with the experimental data. Moreover, the envelopes were also found to encompass the results of both drained and undrained triaxial test data.
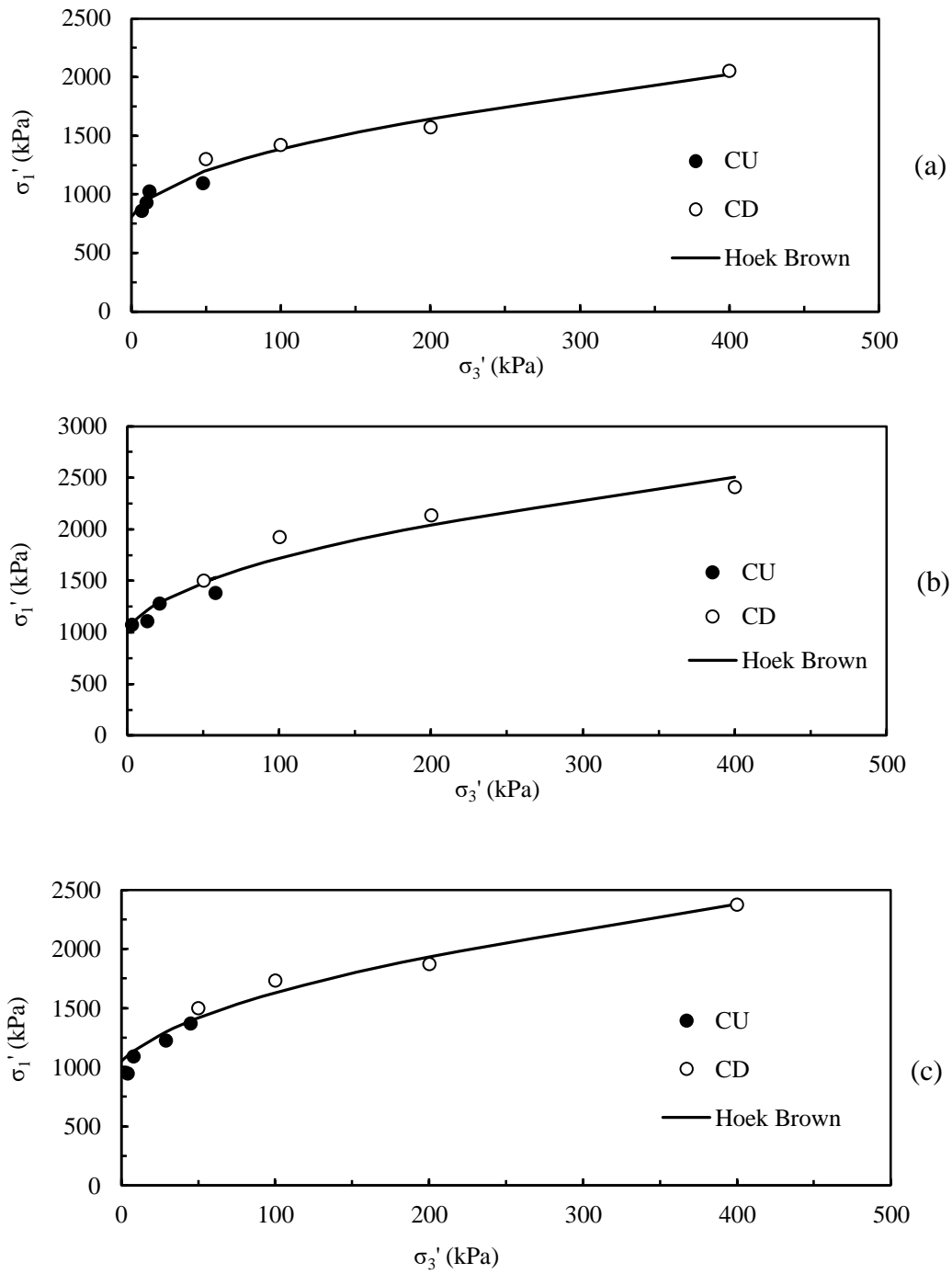
Figure 5.5 Hoek Brown failure envelopes for triaxial tests (a) 10% cement content (b) 15% cement content and (c) 20% cement content.

Table 5.3 Hoek Brown material parameters for triaxial tests

Cement Content (%)	UCS values (kPa)	s	m_b	a
10	1298	0.066	11.416	0.175
15	1588	0.126	15.434	0.203
20	1635	0.012	9.874	0.206

To verify this argument, tests were conducted at zero effective confining pressure. The conventional unconfined compressive strength (UCS) test does not guarantee zero effective confining pressure, as pore water pressure generation cannot be prevented. Hence, drained test should be conducted at zero confining pressure. This test will be referred to as 'drained UCS' and will be discussed in the subsequent section.

5.3.2 Drained UCS Test

Conventional UCS test is conducted at a faster deformation rate. Typically, ASTM D2166 recommends using an axial strain rate of 0.5 to 2% per minute, which accounts to deformation rates of 0.5 to 2 mm/min. A deformation rate of 0.625 mm/min was adopted for conventional UCS tests in this study. Moreover, the test should be completed within 15 minutes. This leads to development of pore water pressure during shearing. Therefore, the test is expected to be under undrained conditions. In a drained test, pore water pressure should be allowed to dissipate. Moreover, specimens should be saturated before shearing, to allow for comparison with other results.

To facilitate saturation, the specimens used for these tests were submerged in water for 10 days before curing period was due. Care was taken to maintain the overall curing period as 28 days. Tests were conducted in a triaxial cell, with water filled only up to three-quarters of the cell such that specimen is surrounded by water, as shown in Figure 5.6 (a). This method ensures that cell pressure does not increase upon shearing all through the testing. Water around the specimen also

facilitates dissipation of negative pore water pressures developed during shearing. Moreover, the specimen is free to take in or release water during shearing. If the sample dilates, water can enter the specimen to counter the negative pore pressure developed. If the specimen contracts, water can leave the specimen to dissipate the positive pore pressure developed. In other words, testing under drained condition is facilitated by this method. However, volume change was not measured, due to obvious difficulties involved to do the same. Since the test is to be conducted at zero confining pressure, consolidation was not performed. As the specimen is cemented, the failure is expected to be brittle in nature. Therefore, the failure occurs at very small strain levels of about 1 to 1.5%. Hence, the area change during shearing is negligible. The test was conducted at a very slow deformation rate (0.0125 mm/min), same as that used for drained triaxial tests, to avoid development of pore water pressure. This testing procedure was expected to produce results corresponding to zero effective confining pressure.

Figure 5.6 (b) shows the stress versus axial strain plots of drained UCS tests, for different cement contents. The specimens failed at strain levels of around 1 to 1.1%. Therefore, the error due to area change correction is negligible. Interestingly, the peak stress values in drained UCS tests fall close to the peak deviator stress values of undrained triaxial tests performed at 50 kPa confining pressure, as can be seen in Table 5.4. This is because, in those undrained tests, the effective confining pressures were close to zero, by virtue of very high pore water pressures. This confirms our assumption that performing a drained test at zero confining pressure would yield results close to that of undrained tests performed at low confining pressure. This also confirms that a single non-linear failure envelope exists for all effective confining pressures for both drained and undrained tests.

The drained UCS results were now plugged into the already established Hoek-Brown envelopes, to check how they fit into the curves. Figure 5.7 shows the Hoek-Brown failure envelopes including the results from drained UCS tests. The drained UCS test results were found to fit in well with the established Hoek-Brown envelopes for all cement contents.

(a)
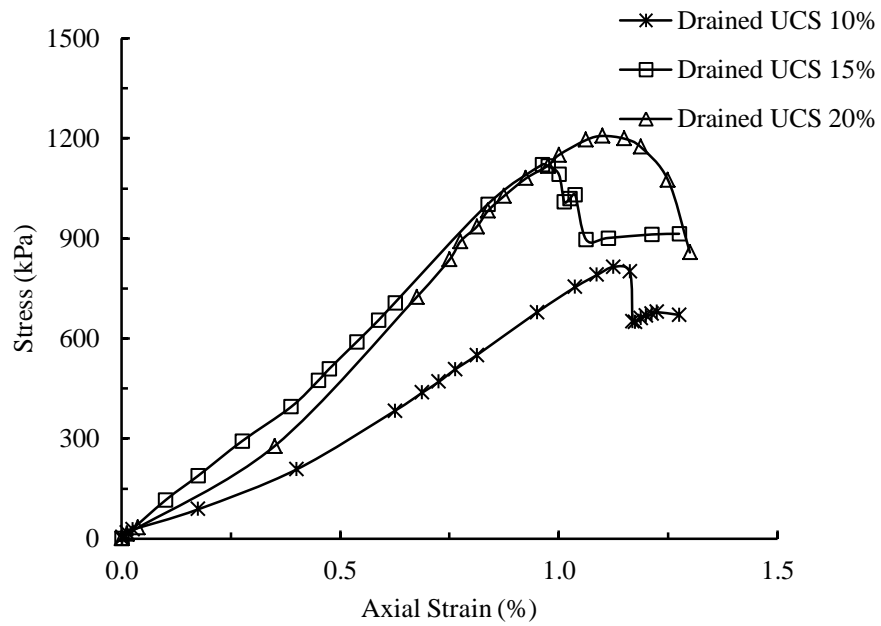
(b)

Figure 5.6 Drained UCS test (a) Set-up and (b) Stress - strain results.
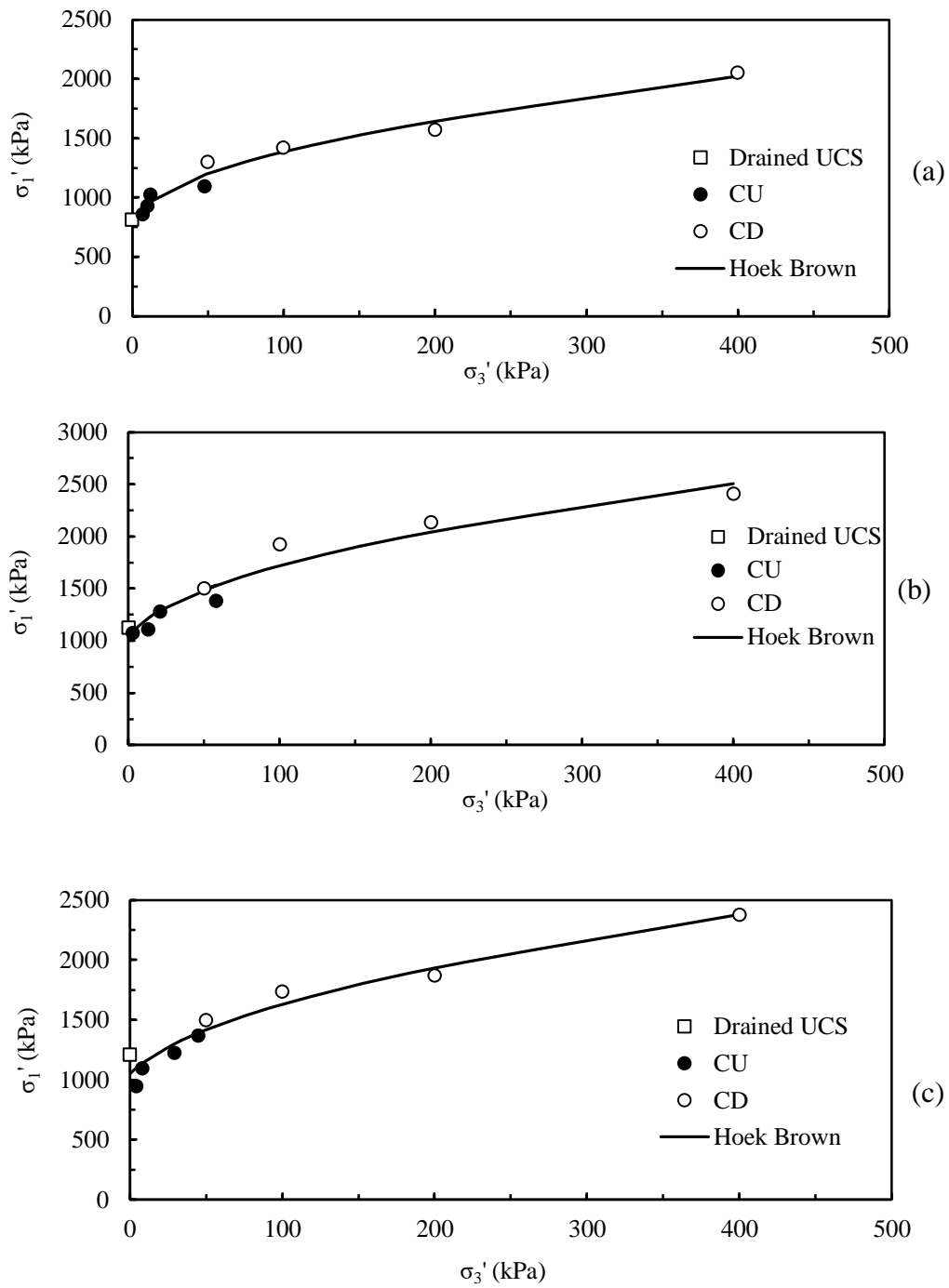
Figure 5.7 Hoek Brown failure envelopes for triaxial tests (a) 10% cement content (b) 15% cement content and (c) 20% cement content.

Table 5.4 Comparison of drained UCS test results and undrained triaxial tests at 50 kPa confining pressure

Cement content (%)	Peak deviator stress (kPa)	
	Drained UCS	Undrained triaxial tests at 50 kPa confining pressure
10	815	860
15	1122	1073
20	1207	947

5.3.3 Incorporation of Tensile Strength to Hoek-Brown Failure Envelope

The conventional Hoek-Brown envelope usually includes the tensile strength of geomaterial. If the obtained failure envelope is extended to its tensile strength, it could act as a good tool to predict the behaviour of cement treated clay even under tensile stresses.

The determination of tensile strength was already discussed in Chapter 3. In the generalized Hoek Brown criterion, tensile strength (σ_t) is actually calculated by substituting $\sigma_1 = \sigma_3 = \sigma_t$, in equation 1 (Hoek et al., 2018). However, this corresponds to tensile strength obtained from biaxial tension tests. In case of rocks, tension tests under biaxial and uniaxial test conditions are assumed to yield comparable results (Hoek et al., 2018). However, this aspect has not been verified in case of cement treated clay. Hence, the above assumption was not made in this study. The direct tension test results discussed in Chapter 3, were directly incorporated into the already established failure envelopes. In this way, the Hoek Brown material parameters do not change with the inclusion of tensile strength. This method also gives a leverage to replace the tension test results with results obtained from other tensile testing methods, if found more appropriate. The complete Hoek Brown failure envelopes for all cement contents, including the tensile strengths, are shown in Figure 5.8.
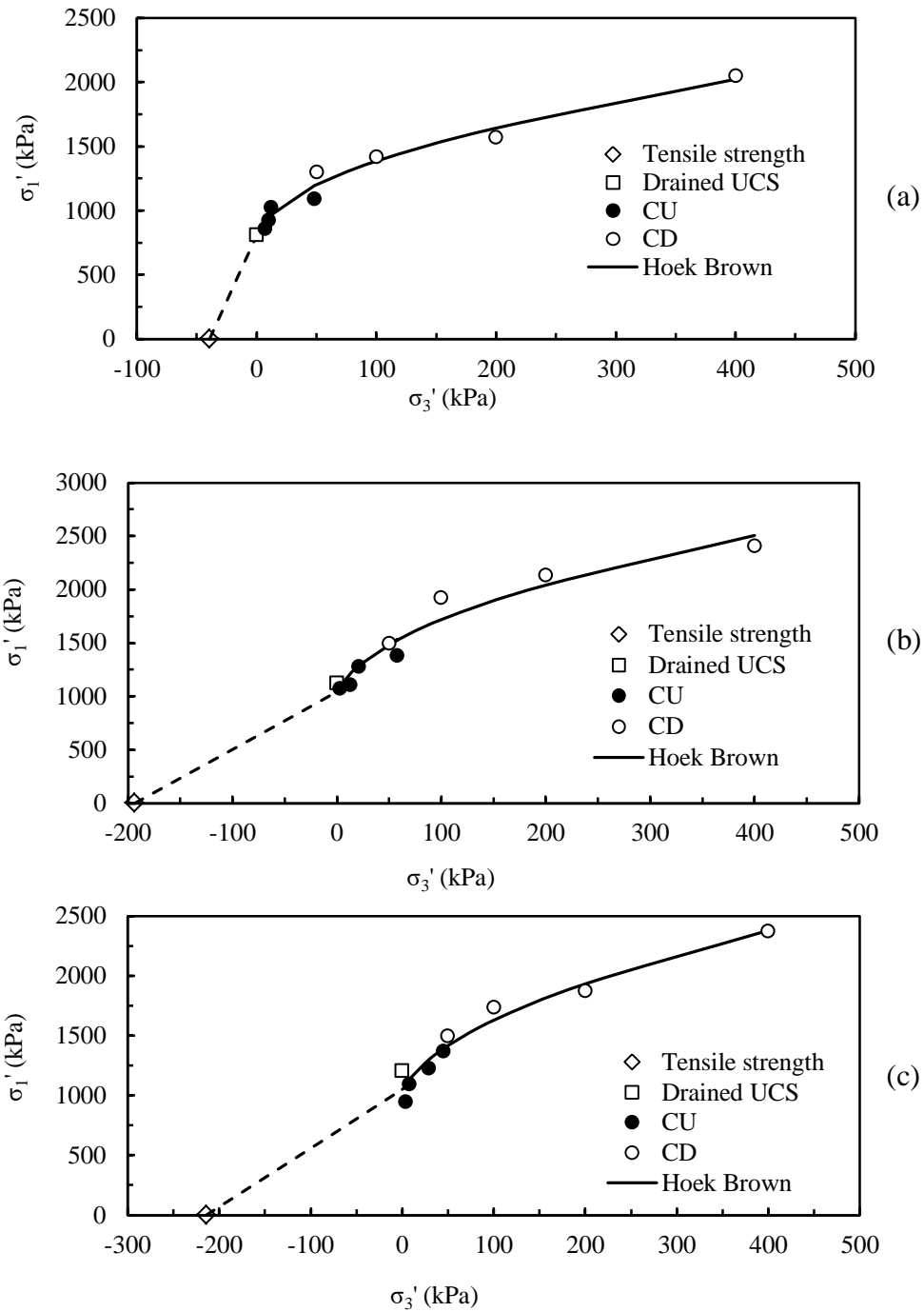
Figure 5.8 Hoek Brown envelope including tensile strength (a) 10% cement content (b) 15% cement content and (c) 20% cement content.

This can act as a good tool in predicting the behaviour of cement treated clay for any given stress range, including the tensile regime.

5.4 HOEK-BROWN FAILURE ENVELOPE FOR PLANE STRAIN TESTS

Having established the failure envelopes in case of triaxial tests, the applicability of such an envelope was verified in case of plane strain testing too. The undrained plane strain test results were already discussed in Chapter 4. The drained plane strain test results will be discussed in this section.

5.4.1 Plane Strain Tests under Drained Condition

The drained plane strain tests were conducted using the same plane strain apparatus described in Chapter 4. Tests were performed on prismatic specimens of 60 mm by 60 mm cross-section and 120 mm long, after a curing period of 28 days. Specimens were prepared at cement contents of 10%, 15% and 20% and were tested at confining pressures of 50 kPa, 100 kPa, 200 kPa and 400 kPa. VJ Tech hydraulic pressure-volume controllers were used for back pressure and cell pressure applications. Back pressure-volume controller was used to measure the volume change during consolidation and shearing stages. An external load cell of 15 kN was used to measure the applied load and hence, calculate deviator stress. A pore pressure transducer of 1000 kPa capacity was used to measure excess pore water pressure.

Saturation of specimen was performed at an effective pressure of 10 kPa. Air was flushed out of the specimen during the initial saturation stage which helped in accelerating the saturation process, as explained in case of triaxial tests. The back pressure was increased till a B value of 0.95 or above was achieved. Back pressure of 290 kPa was found to be sufficient to achieve this B value. Consolidation was carried out at four different confining pressures, as mentioned above, for each cement content. A very slow deformation rate of 0.0125 mm/min was employed for drained tests, same as that used in drained triaxial tests. Axial load, axial deformation and volume change during shear were measured for all the tests.

5.4.2 Drained Plane Strain Test Results

The drained plane strain test results obtained for cement contents of 10%, 15% and 20% are shown in Figures 5.9, 5.10 and 5.11, respectively. Figures 5.9 (a), 5.10 (a) and 5.11 (a) show the variation of deviator stress with axial strain for different cement contents. Over-consolidated behaviour characterized by strong softening behaviour after peak deviator stress was observed for all the confining pressures, just as in drained triaxial tests. However, the softening behaviour was found to have reduced at a higher confining pressure of 400 kPa, indicating a transition towards normally consolidated behaviour.

The variations of volumetric strain with axial strain for different cement contents are shown in Figures 5.9 (b), 5.10 (b) and 5.11 (b). Just as in drained triaxial tests, dilative behaviour was visible at lower confining pressures and contractive behaviour was observed for a confining pressure of 400 kPa. This again shows a transition towards normally consolidated behaviour.

Figures 5.9 (c), 5.10 (c) and 5.11 (c) show the drained stress paths in plane strain tests. A slope of 3 in 1, as expected in drained triaxial stress paths, was not followed. This is because of higher intermediate principal stress in plane strain tests. A slope of roughly around 2 in 1 was found to be followed.

Table 5.5 provides the differences in effective shear strength parameters (c' and ϕ') under drained and undrained plane strain tests. As observed in triaxial tests, different results were observed for drained and undrained testing conditions. Higher cohesion and lower friction angle were observed under drained conditions, just as in triaxial tests. Moreover, highest cohesion was recorded for a cement content of 15%. All the four testing conditions, viz. undrained triaxial, undrained plane strain, drained triaxial and drained plane strain, followed the same trend. Hence, the assumption of optimum cement content was found to be verified in this study. Furthermore, higher peak deviator stress was observed under drained condition, as observed in triaxial conditions. This is shown in Table 5.6.
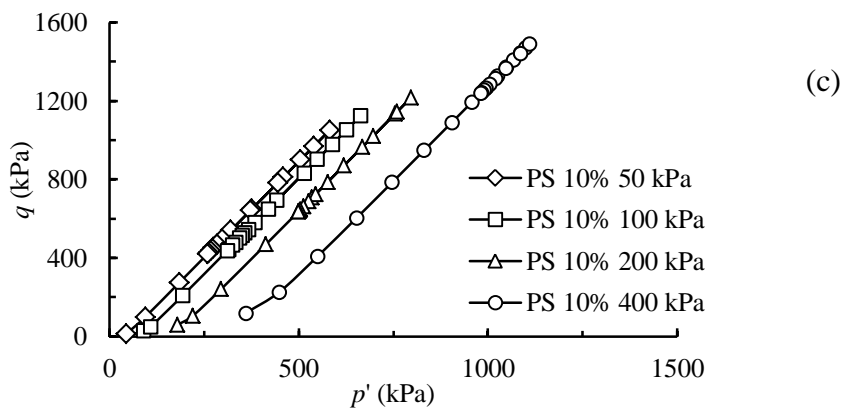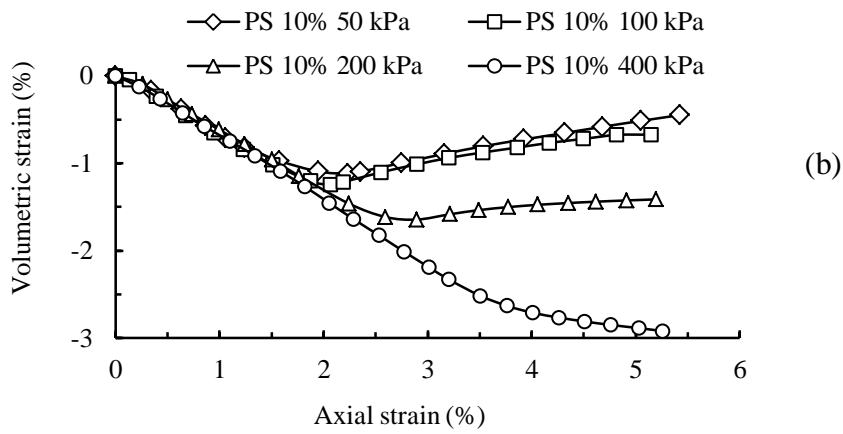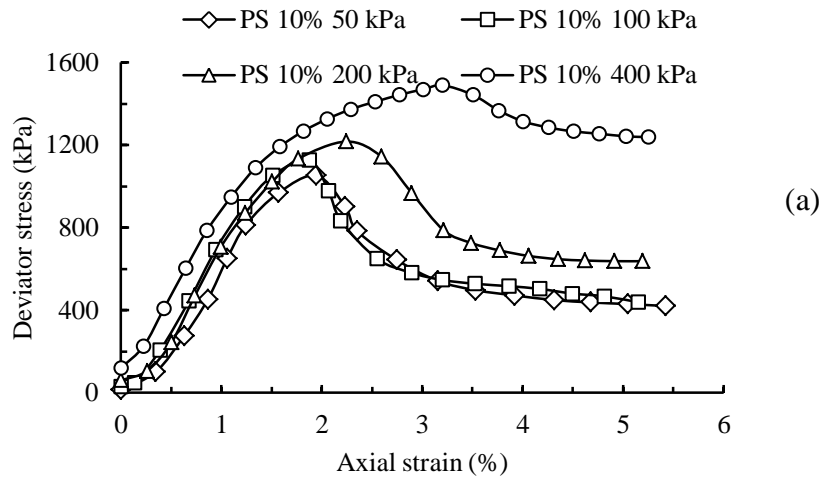
Figure 5.9 Drained plane strain tests for 10% cement content (a) Deviator stress versus axial strain (b) Volumetric strain versus axial strain and (c) Drained stress paths.
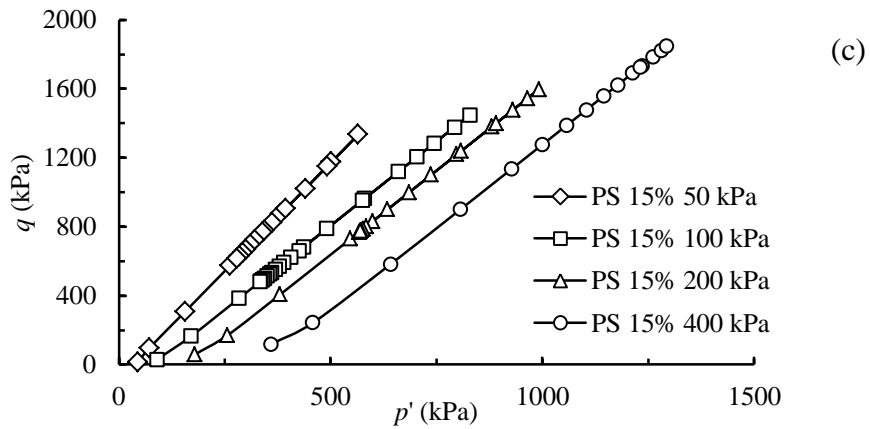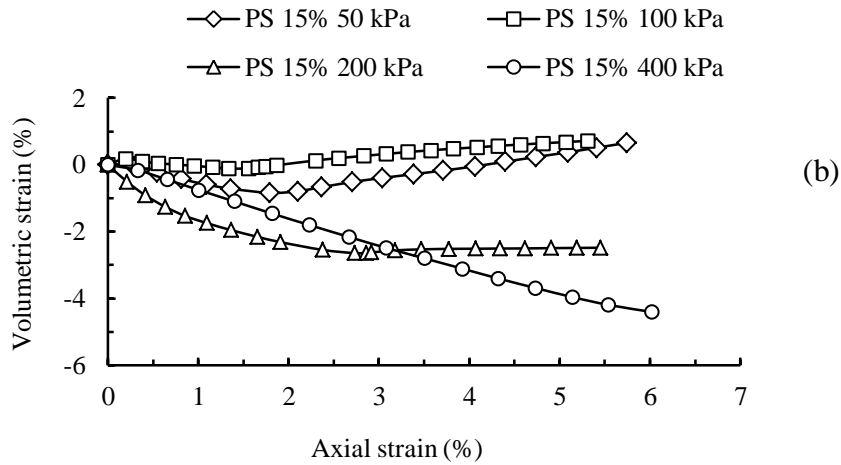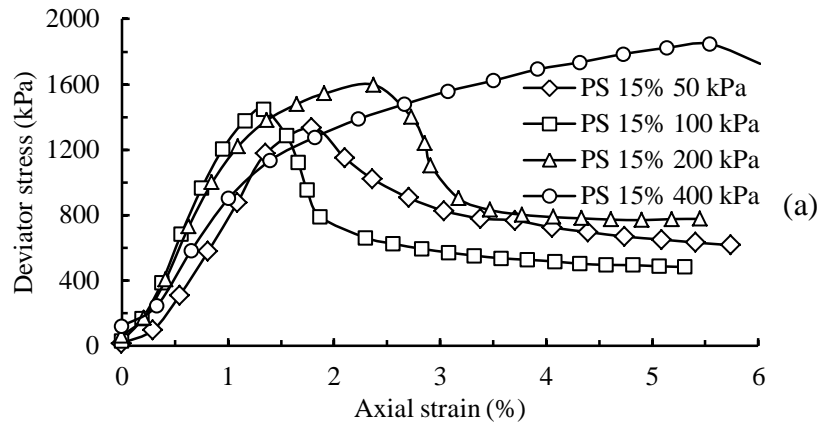
Figure 5.10 Drained plane strain tests for 15% cement content (a) Deviator stress versus axial strain (b) Volumetric strain versus axial strain and (c) Drained stress paths.
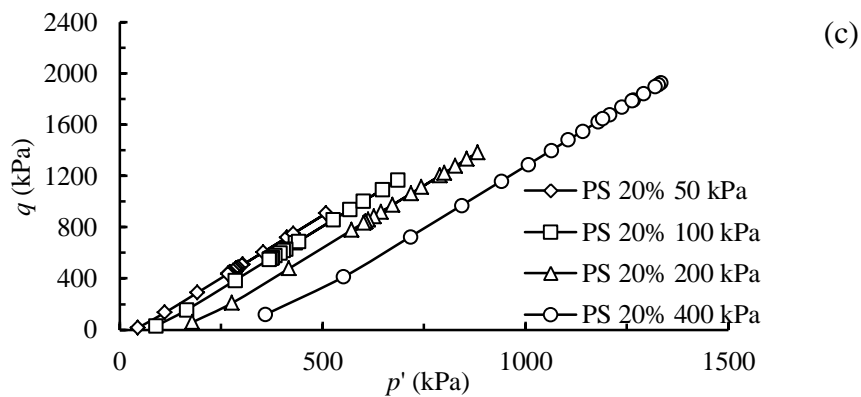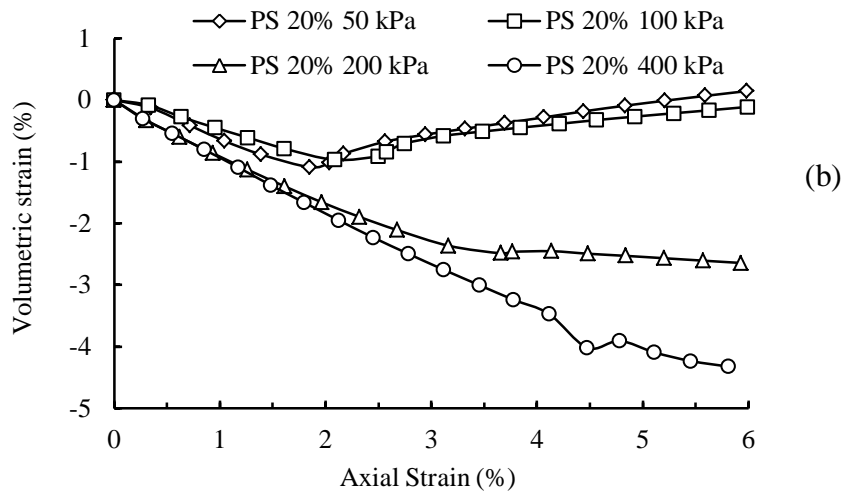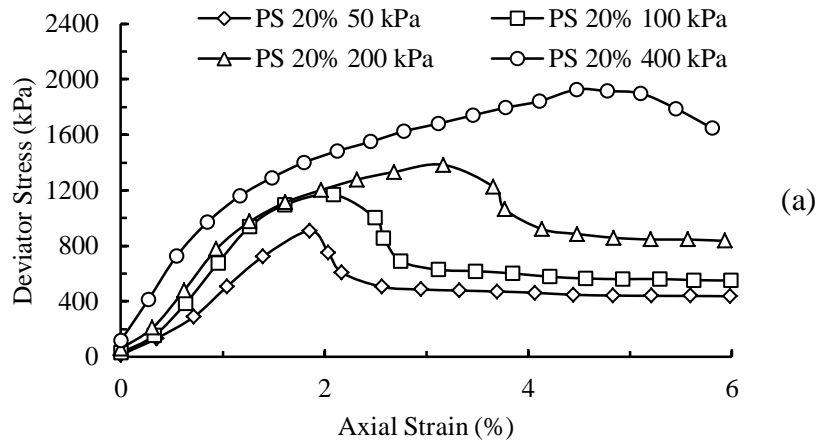
Figure 5.11 Drained plane strain tests for 20% cement content (a) Deviator stress versus axial strain (b) Volumetric strain versus axial strain and (c) Drained stress paths.

Table 5.5 Shear strength parameters for drained and undrained plane strain tests

Cement content (%)	Confining pressure (kPa)	Shear Strength Parameters	
		Drained	Undrained
10	50	$\phi' = 22^0$ $c' = 331$ kPa	$\phi' = 63^0$ $c' = 72$ kPa
	100		
	200		
	400		
15	50	$\phi' = 25^0$ $c' = 414$ kPa	$\phi' = 47^0$ $c' = 184$ kPa
	100		
	200		
	400		
20	50	$\phi' = 36^0$ $c' = 211$ kPa	$\phi' = 64^0$ $c' = 87$ kPa
	100		
	200		
	400		

Table 5.6 Peak deviator stress values for drained and undrained plane strain tests

Cement content (%)	Confining pressure (kPa)	Peak Deviator Stress (kPa)	
		Drained	Undrained
10	50	1052	734
	100	1126	844
	200	1217	786
	400	1489	799

	50	1336	963
15	100	1449	974
	200	1598	1079
	400	1848	1119
20	50	908	881
	100	1169	864
	200	1384	926
	400	1927	1025

5.4.3 Combination of Drained and Undrained Test Results

Drained and undrained test results were then put together on a plot of $(\sigma_1' - \sigma_3')/2$ versus $(\sigma_1' + \sigma_3')/2$, to check if a single non-linear failure envelope exists. The plots for different cement contents are shown in Figure 5.12. The figure clearly shows the existence of a single non-linear envelope in case of plane strain tests as well. Since, cement treated clay shows this trend under two different modes of testing, this can be considered to be the inherent property of cement treated clay.

5.4.4 Hoek-Brown Envelope for Plane Strain Tests

The Hoek-Brown envelope is plotted between major and minor principal stresses. The intermediate principal stress is not included. In case of plane strain tests, the intermediate principal stress is used in the calculation of deviator stress and mean effective stress. One may wonder whether neglecting the intermediate principal stress has any effect on the appropriateness of the failure envelope. However, literature shows that the effect of intermediate principal stress in the determination of Hoek-Brown envelope is negligible (Brace, 1964). Hence, the same method used for triaxial tests, was used for developing the Hoek-Brown failure envelope in plane strain tests. The material parameters were deduced, as shown in Table 5.7.
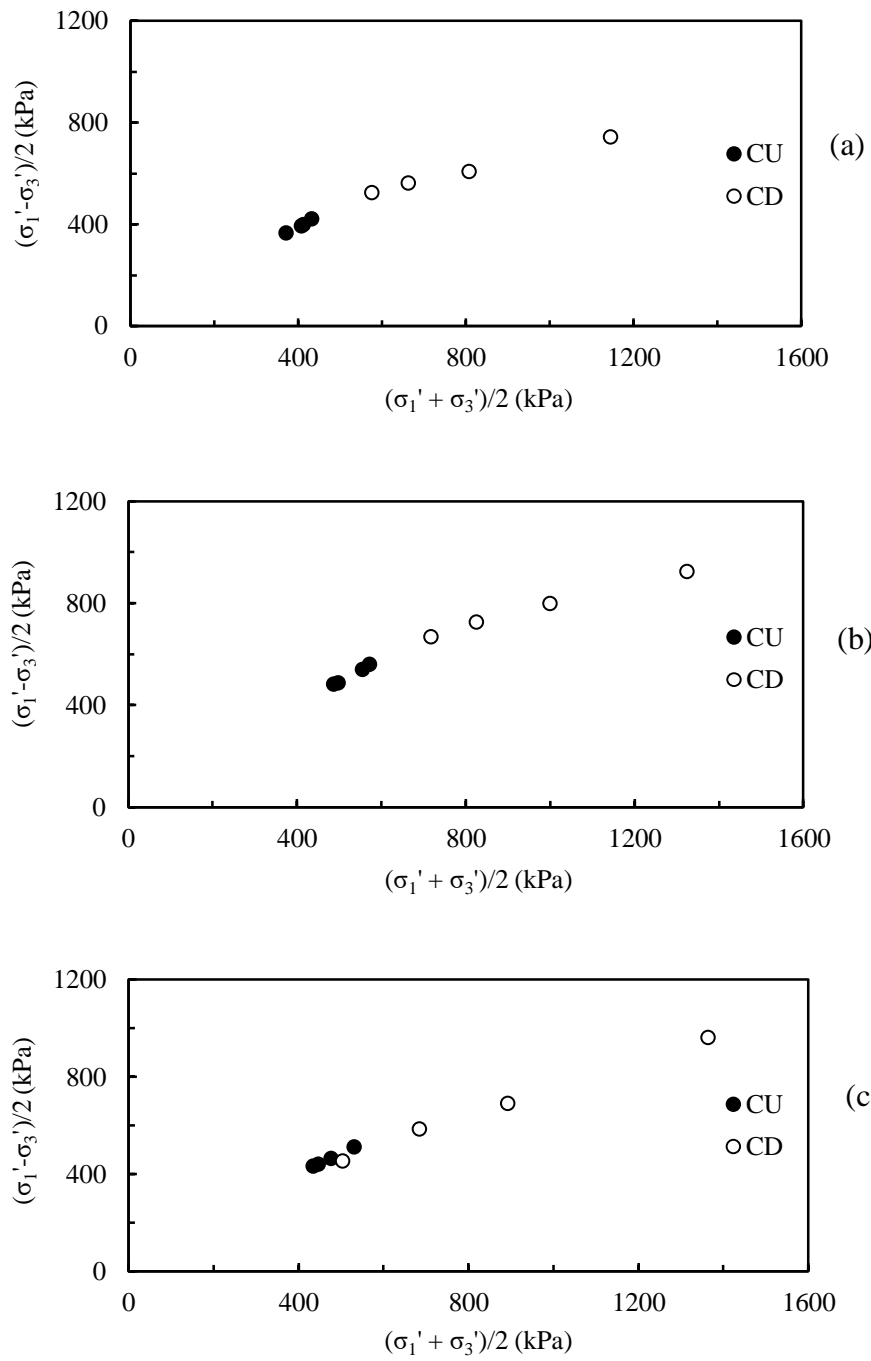
Figure 5.12 Drained and undrained plane strain results put together (a) 10% cement content
(b) 15% cement content (c) 20% cement content.

Table 5.7 Hoek Brown material parameters for plane strain tests

Cement Content (%)	UCS values (kPa)	s	m_b	a
10	1298	0.034	5.8	0.194
15	1588	0.050	8.344	0.198
20	1635	0.605	2.201	1.226

The Hoek Brown failure envelopes for different cement contents are shown in Figure 5.13. The envelope was found to be in sync with the experimental results and hence, Hoek Brown theory was found to be valid in case of plane strain tests as well. While non-linear envelopes were found to exist for 10% and 15% cement contents, the envelope was closely linear for 20% cement content. Since, drained UCS and tension tests were performed for axisymmetric specimens, these results were not included in the plane strain failure envelopes. Special arrangements need to be made for performing such tests on plane strain specimens, and hence, they are left as future scope of this work.
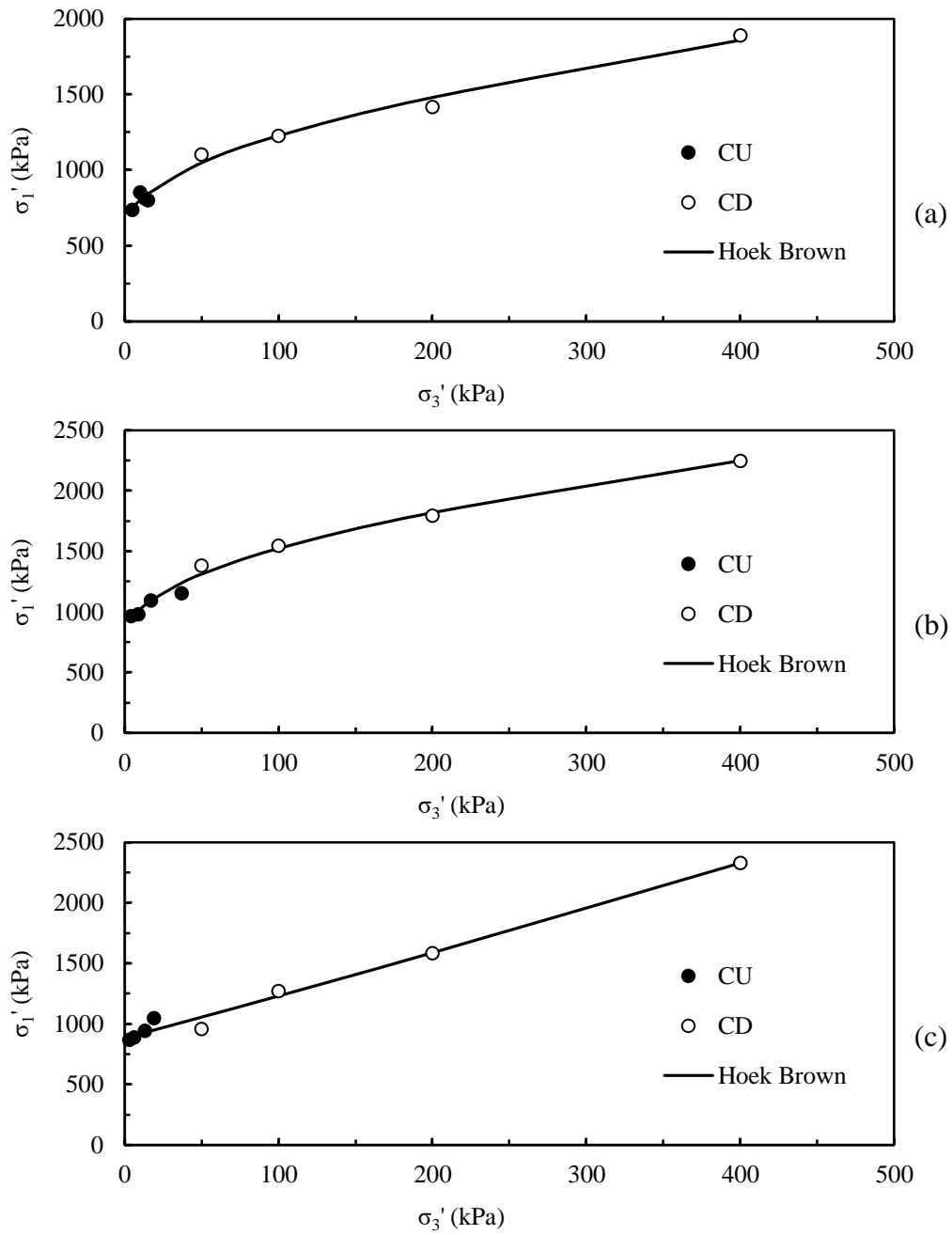
Figure 5.13 Hoek Brown failure envelopes for plane strain tests (a) 10% cement content (b) 15% cement content and (c) 20% cement content.

5.5 SUMMARY

For the conventional drained and undrained triaxial tests carried out on cement treated marine clay, prepared at various cement contents, significant differences were observed in the peak deviator stress and shear strength parameters. The assumption of a linear failure envelope for a narrow range of effective confining stress was found to be the reason for such a discrepancy. However, drained and undrained test results put together in a modified Mohr-Coulomb plot were found to lie on a single non-linear failure envelope. Generalized Hoek-Brown theory was used to predict this non-linear failure envelope, encompassing both drained and undrained test results. The same trend was visible for plane strain test results as well. This shows that the concept of a single non-linear failure envelope is an inherent feature of cement treated marine clay. Hence, establishment of this failure envelope could play key role in predicting the behavior of cement treated clays under different stress conditions.

CHAPTER 6

NUMERICAL SIMULATION OF TRIAXIAL AND PLANE STRAIN TESTS USING THE DEVELOPED FAILURE ENVELOPE

6.1 INTRODUCTION

Failure envelopes for cement treated clays for different cement contents, under triaxial and plane strain testing conditions, were established using the generalized Hoek-Brown criterion (Hoek, 1994). In this chapter, an attempt was made to simulate the laboratory experiments by implementing the corresponding failure envelopes into a numerical platform. This exercise serves to verify the efficiency of the established failure envelopes in predicting the behaviour of cement treated clays.

Hoek-Brown constitutive model comes in-built in many commercial numerical platforms. However, most of them follow original Hoek-Brown criterion (Hoek and Brown, 1980) which is meant only for intact rocks. This version of Hoek-Brown model employs a constant value of 0.5 for the material parameter 'a'. The failure envelopes in this study were established using generalized Hoek-Brown criterion (Hoek, 1994). This version allows variation in parameter 'a', which enables adjustment in the shape of principal stress plot.

This chapter discusses the methodology adopted to perform numerical simulations and compares the simulated results with the experimental results. The advantages and limitations of using this approach will be also discussed.

6.2 FINITE DIFFERENCE FORMULATION

Two dimensional finite difference continuum modelling of element tests, presented in chapters 4 and 5, were carried out using a commercial package, *FLAC* (version 7.0). The Hoek-Brown constitutive model incorporated in *FLAC* follows the generalized Hoek-Brown criterion with following input parameters,

1. Density
2. Bulk modulus

3.   Shear modulus

4.   Hoek-Brown material parameters

5.   Poisson's ratio

6.   Confining pressure

7.   Deformation rate of shearing

Density was obtained by simply dividing the mass of specimen before testing by its volume. Bulk modulus (K) and shear modulus (G) are calculated from modulus of elasticity (E), which is obtained from the stress-strain plots. Since, linear variation was observed up to the peak deviator stress for all the plots of deviator stress versus axial strain, the slope of this plot directly gives modulus of elasticity. Bulk and shear moduli were then calculated using equations connecting modulus of elasticity and Poisson's ratio (v), as shown in equation 6.1.

$$\left.\begin{array}{l} G = \dfrac{E}{2(1+v)} \\[4mm] K = \dfrac{E}{3(1-2v)} \end{array}\right\} \quad (6.1)$$

Values of Poisson's ratio were selected as 0.49 and 0.35 for undrained and drained conditions, respectively, as discussed in Chapters 4 and 5. Hoek-Brown material parameters were provided based on the failure envelope under consideration. Simulations were run for four confining pressures for all the cement contents. The rates of deformation were provided as 0.025 mm/min and 0.0125 mm/min for undrained and drained tests, respectively, as discussed in Chapters 4 and 5.

For generating grids for numerical simulations, *FLAC* requires the user to specify the configuration of the grid. By default, all the analyses in *FLAC* are carried out under plane strain condition. Hence, for simulation of plane strain tests, no special mention of the configuration is required. However, since specimen is under axisymmetric condition in triaxial tests, axisymmetric configuration needs to be specified. Though the generated grid looks the same in both cases, the difference in analysis depends on specifying this configuration.

6.3 NUMERICAL SIMULATION OF TRIAXIAL TESTS

6.3.1 Methodology Adopted

Triaxial tests were performed on axisymmetric specimens. Attempts were made in this study to simulate both drained and undrained triaxial tests, using the established failure envelopes. Since, the failure envelopes were developed encompassing both drained and undrained test results, a single set of Hoek-Brown material parameters is sufficient to represent both. However, the moduli values need to be selected based on the stress-strain plots.

An axisymmetric mesh representing one half of the actual triaxial specimen of diameter 50 mm and length 100 mm, was developed to perform numerical simulations. Owing to the symmetry of the axisymmetric specimen, this mesh is considered to be sufficient to represent the entire triaxial specimen. This mesh was then divided into 5 zones in horizontal direction and 10 zones in vertical direction, for increased sensitivity. 2:1 length to diameter ratio was maintained in grid generation. The boundary conditions used for the numerical model are shown in Figure 6.1. In the figure, X, Y and B refer to fixities in horizontal, vertical and both directions, respectively. Vertical fixity on top represents the loading cap and that the load is acted upon uniformly on the specimen. Vertical fixity at the bottom signifies the rigid pedestal on which the specimen is placed. The left boundary is provided with horizontal fixity to represent that only half the specimen has been considered. Fixity in both directions happen at the corners due to the overlap of both fixities. The confining pressure was applied on the right hand side of the specimen, as shown in Figure 6.1.

As observed in the experimental results (Chapters 4 and 5), cement treated clays show strain softening behaviour post peak deviator stress. This behaviour can be simulated by specifying that the Hoek Brown material properties, σ_{ci}, m_b, s and a, change with respect to plastic strain. Softening behaviour was incorporated by assigning tables that relates each of these material properties with plastic strain. Material properties corresponding to the peak and post peak regime were assigned for the respective plastic strain values in the table. It is assumed that the properties vary linearly between two consecutive entries. Plastic strain is chosen based on physical grounds.
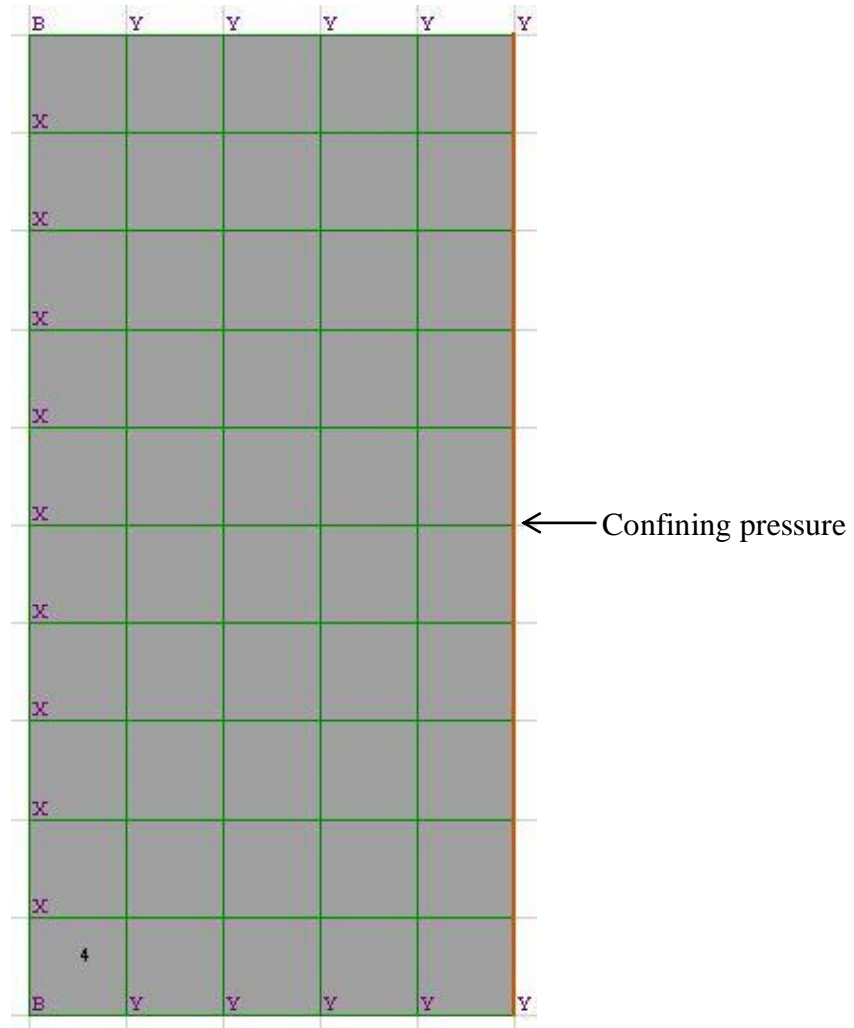
Figure 6.1 Grid generated for simulation of triaxial tests.

In this study, the plastic strain was chosen as axial strain itself, as demonstrated in Yapage and Liyanapathirana (2017). The material constants corresponding to the post yield residual portion were determined using the method demonstrated by Tan et al. (2015) and Cundall et al. (2003). These studies suggested the use of a reduction factor, r_d, which is defined as the ratio of difference in peak and residual deviator stress to the peak deviator stress, as shown in equation 6.2. This reduction factor was then used to find out the residual Hoek Brown parameters, as shown in equation 6.3. This procedure is employed at all confining pressures and cement contents to achieve realistic softening behaviour.

$$r_d = \frac{\Delta\sigma}{\sigma} \qquad (6.2)$$

128

where $\Delta\sigma$ is the difference between peak and residual deviator stress, σ is the peak deviator stress (as defined by Tan et al., 2015).

$$\left.\begin{array}{l} \sigma_{ci}{}^d = \sigma_{ci}(1 - r_d) \\ m_b{}^d = m_b(1 - r_d) \\ s^d = s \\ a^d = a \end{array}\right\} \tag{6.3}$$

where superscript 'd' represents the residual Hoek Brown parameters.

The properties implemented to simulate softening behaviour for undrained and drained triaxial tests are shown in Tables 6.1 and 6.2, respectively. As can be observed in these tables, the peak plastic strain and residual strain were not related to each other. This is in line with the findings of Yapage and Liyanapathirana (2017).

Table 6.1 Properties to represent softening in undrained triaxial tests

Cement content (%)	σ_3 (kPa)	Peak deviator stress (kPa)	Peak plastic strain (%)	Residual deviator stress (kPa)	Residual plastic strain (%)	r_d	$m_b{}^d$	$\sigma_{ci}{}^d$ (kPa)
10	50	852.9	1.53	690.1	2.2	0.191	9.237	1050.346
	100	918.5	1.32	657.6	2.6	0.284	8.174	929.467
	200	1014.8	1.05	603.2	3.9	0.406	6.785	771.560
	400	1046.0	1.06	719.2	2.17	0.312	7.850	892.584
15	50	1070.2	1.27	710.2	2	0.336	10.242	1053.541
	100	1091.8	1.54	728.8	2	0.332	10.303	1059.744
	200	1256.9	1.27	942.7	3.2	0.250	11.576	1190.717
	400	1320.6	0.98	1063.2	1.98	0.195	12.425	1278.105
20	50	943.1	1.29	689.2	2	0.269	7.216	1194.857
	100	1086.5	1.24	835.3	2	0.231	7.591	1257.017
	200	1196.3	1.23	854.1	2	0.286	7.050	1167.339
	400	1325.3	1.11	937.3	2.13	0.293	6.983	1156.294

Table 6.2 Properties to represent softening in drained triaxial tests

Cement content (%)	σ_3 (kPa)	Peak deviator stress (kPa)	Peak plastic strain (%)	Residual deviator stress (kPa)	Residual plastic strain (%)	r_d	$m_b{}^d$	$\sigma_{ci}{}^d$ (kPa)
10	50	1252.2	1.59	304.5	6	0.757	2.776	315.694
	100	1319.1	2.09	415.8	7	0.685	3.599	409.216
	200	1373.7	4.13	939.2	8	0.316	7.805	887.509
	400	1653.1	7.34	1157.6	9.36	0.300	7.994	909.029
15	50	1447.4	1.55	392.6	7.5	0.729	4.186	430.623
	100	1821.6	1.30	843.2	7	0.537	7.145	734.909
	200	1932.3	2.27	1010.6	7	0.477	8.072	830.306
	400	2007.1	5.61	1489.7	8.44	0.258	11.455	1178.302
20	50	1449.5	1.70	389.5	8	0.731	2.653	439.357
	100	1636.4	1.85	577.4	8	0.647	3.484	576.920
	200	1672.2	2.57	855.9	8	0.488	5.054	836.880
	400	1974.5	4.80	1321.0	9.77	0.331	6.606	1093.899

The simulations were run at the same deformation rate and confining pressure, as those used for laboratory testing. In *FLAC*, the desired output from a numerical simulation is obtained by assigning *FISH* functions. The values recorded by these functions during each time step are stored as *history* variables, to facilitate preparing the desired plots. In this study, only the plots for deviator stress versus axial strain were prepared for different cement contents and confining pressures. The number of time steps were decided based on the magnitude of axial strain required to be simulated. This again depends on deformation rate applied and type of testing. The residual stress is achieved at relatively higher strain levels in case of drained tests and higher time steps are required.

Regarding the stress calculations, major principal stress (σ_1) was calculated as the ratio of force to the cross-sectional area. σ_1 minus the applied confining pressure (σ_3) was calculated deviator stress, at each timestep. Similarly, axial strain was calculated as the ratio of axial deformation to the length of the specimen. These two parameters were calculated by defining them in the form of *FISH* functions. These functions were then stored as history variables to

record their output at each timestep. This facilitates making the plots of deviator stress versus axial strain.

6.3.2 Results and Discussions

(i) Undrained Triaxial Results

The numerical simulation plots of deviator stress versus axial strain obtained for undrained triaxial tests are discussed here. The plots obtained for cement contents of 10%, 15% and 20% are shown in Figures 6.2, 6.3 and 6.4, respectively. Sub-sections (a), (b), (c) and (d) in these figures correspond to the responses obtained for confining pressures of 50 kPa, 100 kPa, 200 kPa and 400 kPa, respectively. The experimental results are also shown in the same plots for comparison purposes.

In all the responses, reasonable agreement was observed between the experimental and numerical results, up to the peak deviator stress. The initial portion of stress-strain behaviour is well captured using the derived and assumed parameters in Hoek Brown model. The values of peak deviator stress obtained by numerical simulations are reasonably close to the experimental results. However, in case of 400 kPa confining pressure, simulated peak deviator stress is slightly on the higher side compared to experimental results. It is worth mentioning that the Hoek-Brown failure envelope had slight mismatch at places with the experimental results, as seen in Chapter 5. This is because an average curve was attempted, which can encompass as much data points as possible. Hence, this mismatch at certain data points is directly reflected on the simulation results. Had many trials, under different confining pressures, been performed individually under undrained conditions, this error could have been even more minimised.

Furthermore, small discrepancies are also observed in the post peak regime, in few cases. However, it is worth mentioning that cement treated clays undergo breakage after attaining peak deviator stress, owing to their brittle nature. The stress system that exists after breakage in the experimental specimen is complicated and therefore difficult to simulate. As far as field problems are concerned, the peak deviator stress is more relevant (Pan et al., 2018). The post peak strength of cement treated clay cannot be relied upon, in case of real problems on the field. Hence, this discrepancy may be overlooked.
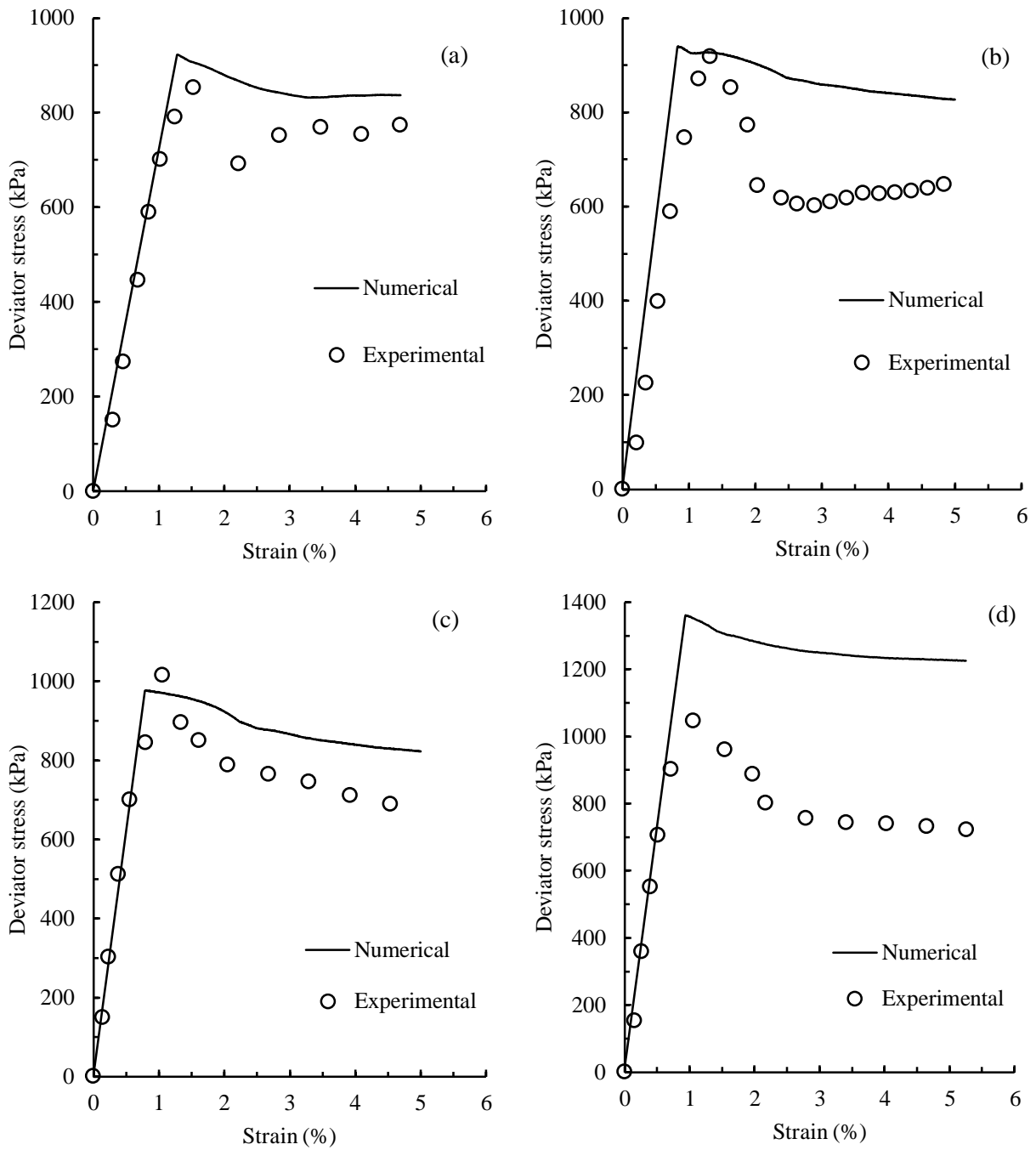
Figure 6.2 Undrained triaxial tests: Numerical versus experimental results for 10% cement content at confining pressures of (a) 50 kPa (b) 100 kPa (c) 200 kPa (d) 400 kPa.

Figure 6.3 Undrained triaxial tests: Numerical versus experimental results for 15% cement content at confining pressures of (a) 50 kPa (b) 100 kPa (c) 200 kPa (d) 400 kPa

133

Figure 6.4 Undrained triaxial tests: Numerical versus experimental results for 20% cement content at confining pressures of (a) 50 kPa (b) 100 kPa (c) 200 kPa (d) 400 kPa

(ii) Drained Triaxial Results

The numerical simulation plots of deviator stress versus axial strain obtained for drained triaxial tests are discussed here. The plots obtained for cement contents of 10%, 15% and 20% are shown in Figures 6.5, 6.6 and 6.7, respectively. The sub-sections (a), (b), (c) and (d) corresponds to confining pressures of 50 kPa, 100 kPa, 200 kPa and 400 kPa respectively. The experimental results are also shown in the same plots for comparison purposes.

Reasonable agreement was obtained between the numerical simulation results and experimental results, subject to slight discrepancies observed in peak deviator stress at certain places. The reason cited in undrained tests holds in this case as well. Some mismatch in the post peak regime was also observed in some cases. However, this aspect can be possibly overlooked because peak deviator stress plays the most important role in field problems involving cement treated clay.

6.3.3 Summary of Simulation of Triaxial Tests

The established Hoek-Brown failure envelope can predict the behaviour of cement treated clay subjected to triaxial testing, to reasonable accuracy. The pre-peak regime and peak deviator stress was captured well, in all the cases. However, post-peak regime showed discrepancies in some cases and hence, this model is not capable of predicting the behaviour of cement treated clay, post peak deviator stress.

6.4 NUMERICAL SIMULATION OF PLANE STRAIN TESTS

6.4.1 Methodology Adopted

It's common knowledge that specimens under plane strain condition can be analysed as two-dimensional problems. Hence, attempts were made in this study to simulate both drained and undrained plane strain tests, using the established failure envelopes. The same procedure, as followed in the case of triaxial tests was followed here too. However, the most important difference between the two tests is the adopted configuration. By default, *FLAC* carries out all the analyses under plane strain condition, until specified otherwise.

Figure 6.5 Drained triaxial tests: Numerical versus experimental results for 10% cement content at confining pressures of (a) 50 kPa (b) 100 kPa (c) 200 kPa (d) 400 kPa
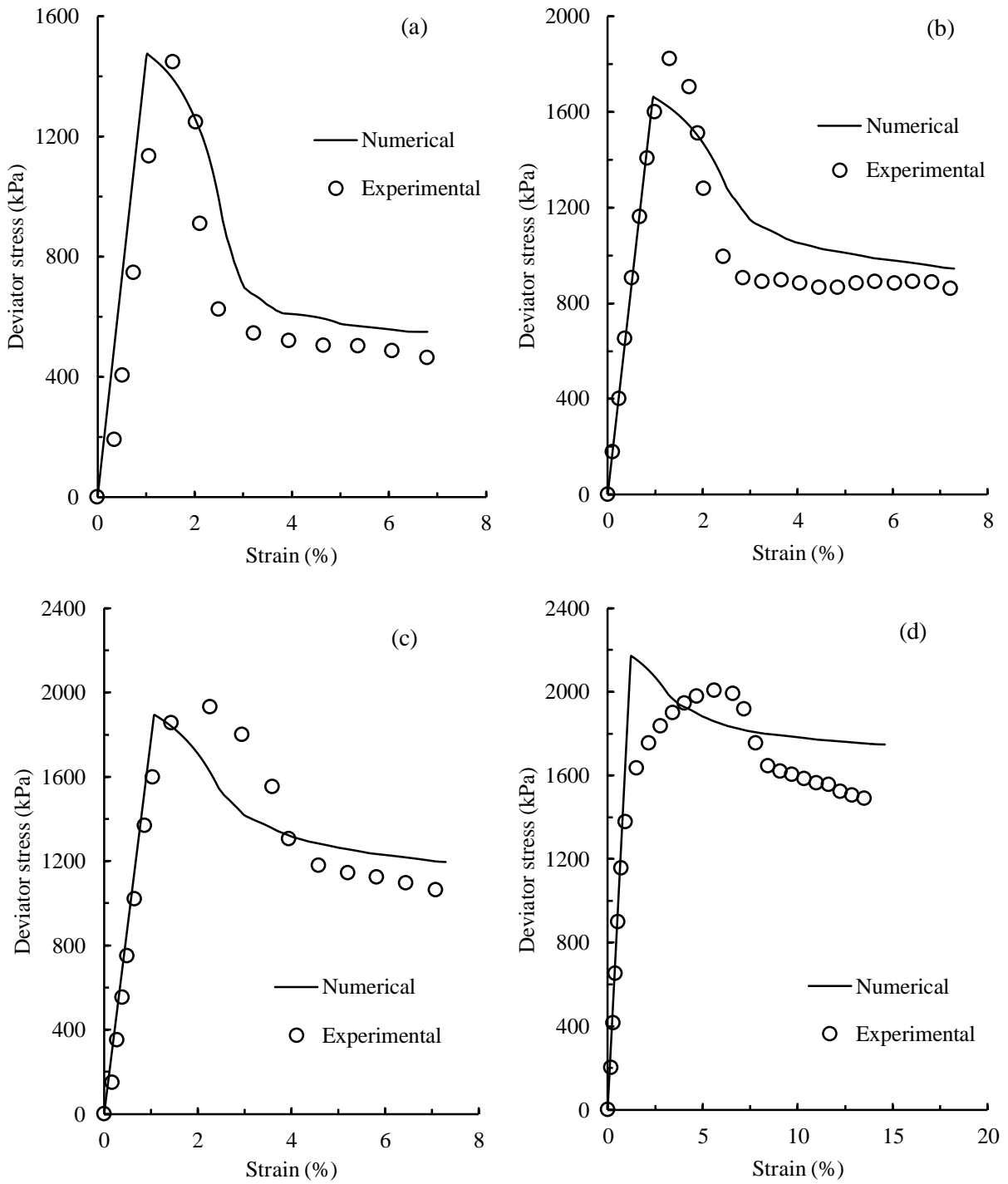
Figure 6.6 Drained triaxial tests: Numerical versus experimental results for 15% cement content at confining pressures of (a) 50 kPa (b) 100 kPa (c) 200 kPa (d) 400 kPa
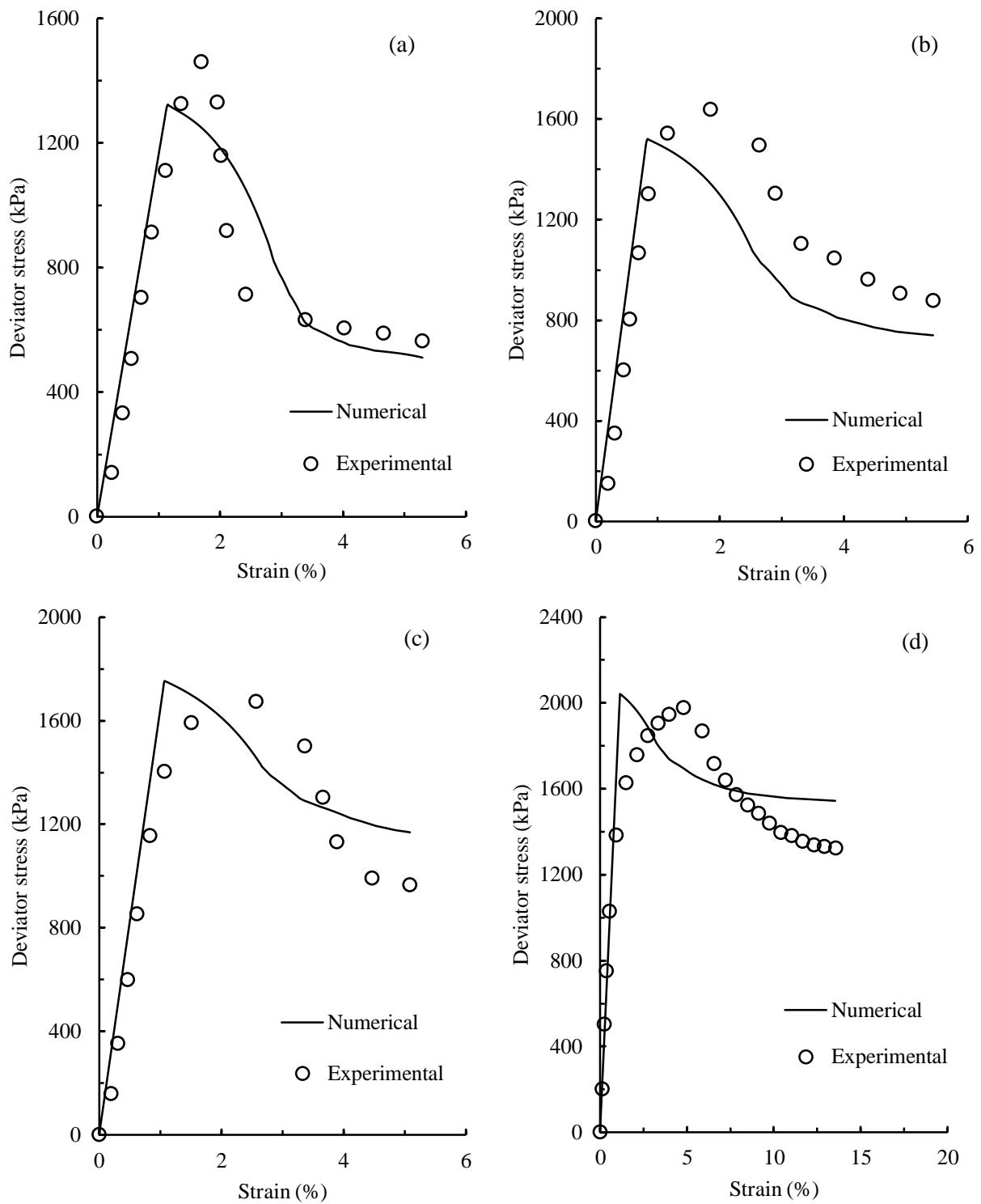
Figure 6.7 Drained triaxial tests: Numerical versus experimental results for 20% cement content at confining pressures of (a) 50 kPa (b) 100 kPa (c) 200 kPa (d) 400 kPa
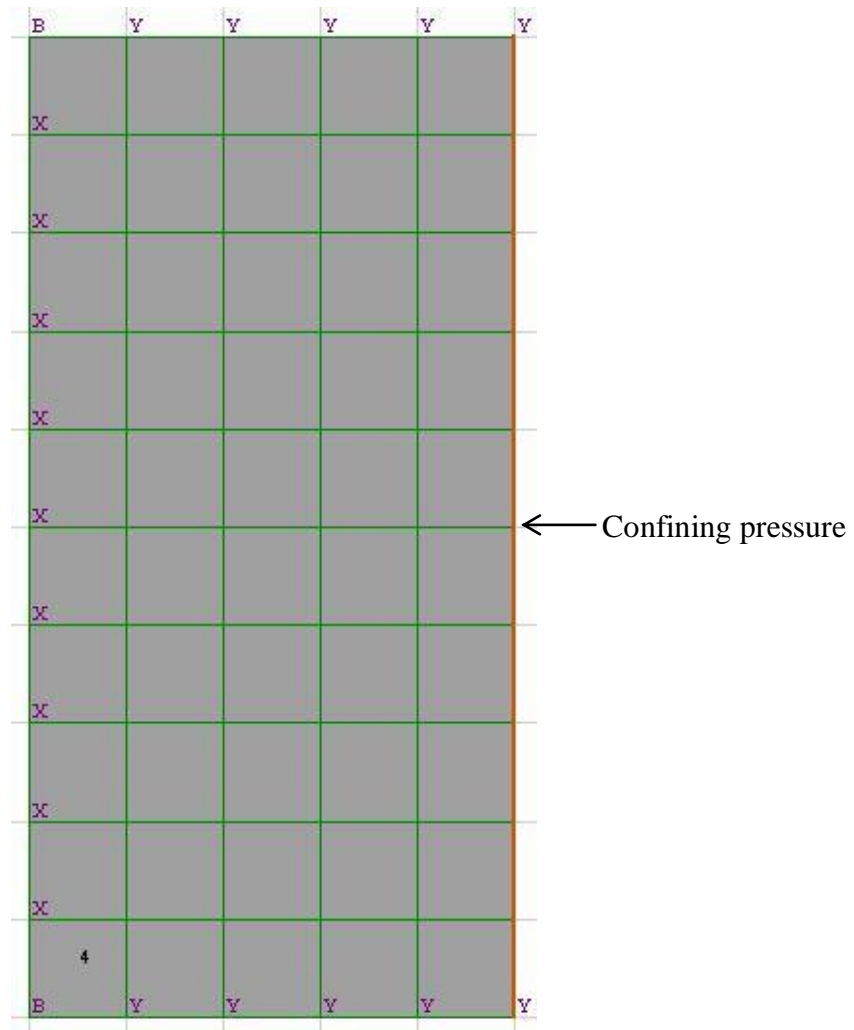
Figure 6.8 Grid generated for simulation of plane strain tests.

A mesh representing one half of the plane strain specimen was developed to perform numerical simulations, as shown in Figure 6.8. The actual size of plane strain specimen considered in the experimental programme was 60 x 60 x 120 mm. The plane strain condition was imposed on one of the faces of size, 60 x 120 mm. Hence, the two-dimensional geometry to be analysed is again 60 x 120 mm. The advantage of symmetry of this element was made use of while developing the grid. This mesh was then divided into 5 zones in horizontal direction and 10 zones in vertical direction, for increased sensitivity. 2:1 length to width ratio was maintained in grid generation. The boundary conditions used for the numerical model are shown in Figure 6.8. In the figure, X, Y and B refer to fixities in horizontal, vertical and both directions respectively. Vertical fixity on top represents the loading cap and that the load is

acted upon uniformly on the specimen. Vertical fixity at the bottom signifies the rigid pedestal on which the specimen is placed. The left boundary is provided with horizontal fixity to represent that only half the specimen has been considered. The confining pressure was applied on the right hand side of the specimen, as shown in Figure 6.8. Though the meshes considered for triaxial and plane strain specimens look alike, the analyses were carried out under axisymmetric and plane strain conditions, respectively.

The strain softening phenomenon observed in the plane strain specimens post peak deviator stress was implemented using the same procedure adopted for triaxial tests. Detailed explanation had already been provided in section 6.3.1 and will not be repeated herein. The properties used to represent softening in undrained and drained plane strain tests are given in Tables 6.3 and 6.4, respectively.

Another important aspect to be considered in plane strain analysis is the calculation of stresses. Stresses were calculated in the same way as the experimental programme. The formulations used were explained in Chapter 4. *FISH* functions were defined for the calculation of axial strain, major principal stress, intermediate principal stresses and deviator stress. These functions were then stored as history variables to record their output at each timestep. The plots of deviator stress versus axial strain were then prepared.

Table 6.3 Properties to represent softening in undrained plane strain tests

Cement content (%)	σ_3 (kPa)	Peak deviator stress (kPa)	Peak plastic strain (%)	Residual deviator stress (kPa)	Residual plastic strain (%)	r_d	$m_b{}^d$	$\sigma_{ci}{}^d$ (kPa)
10	50	733.8	2.01	379.5	2.87	0.483	3.000	671.427
	100	843.8	1.55	502.5	2.22	0.404	3.455	773.078
	200	786.2	1.21	603.5	1.57	0.232	4.453	996.421
	400	799.4	1.14	565.9	2.17	0.292	4.107	918.966
15	50	962.8	1.36	470.8	2.08	0.511	4.081	776.410
	100	973.8	1.63	503.3	2.67	0.483	4.312	820.473
	200	1079.4	1.34	614.5	2.24	0.431	4.750	903.796
	400	1118.7	1.53	743.6	1.98	0.335	5.546	1055.245

Cement content (%)								
20	50	881.1	1.49	564.8	3.7	0.359	1.411	1048.128
	100	863.8	1.29	576.4	2.03	0.333	1.469	1091.021
	200	925.8	1.69	666.1	3.01	0.281	1.583	1176.370
	400	1024.5	1.07	648.1	2.22	0.367	1.392	1034.371

Table 6.4 Properties to represent softening in drained plane strain tests

| Cement content (%)	σ_3 (kPa)	Peak deviator stress (kPa)	Peak plastic strain (%)	Residual deviator stress (kPa)	Residual plastic strain (%)	r_d	m_b^d	σ_{ci}^d (kPa)
10	50	1052.1	1.95	350.7	5.04	0.667	1.934	432.704
	100	1126.4	1.87	429.1	5.46	0.619	2.210	494.493
	200	1216.9	2.24	628.5	4.62	0.484	2.996	670.453
	400	1489.2	3.20	1239.1	5.25	0.168	4.826	1080.063
15	50	1335.6	1.79	572.5	6.09	0.571	3.577	680.508
	100	1449.3	1.33	482.0	3.82	0.667	2.775	528.016
	200	1597.8	2.37	776.5	4.07	0.514	4.055	771.525
	400	1847.8	5.54	1361.1	9.05	0.263	6.146	1169.425
20	50	908.0	1.85	418.7	3.7	0.539	1.015	753.919
	100	1168.8	2.09	527.0	4.57	0.549	0.992	737.160
	200	1383.9	3.17	847.5	5.2	0.388	1.348	1001.267
	400	1927.1	4.47	1515.4	7.15	0.214	1.731	1285.685
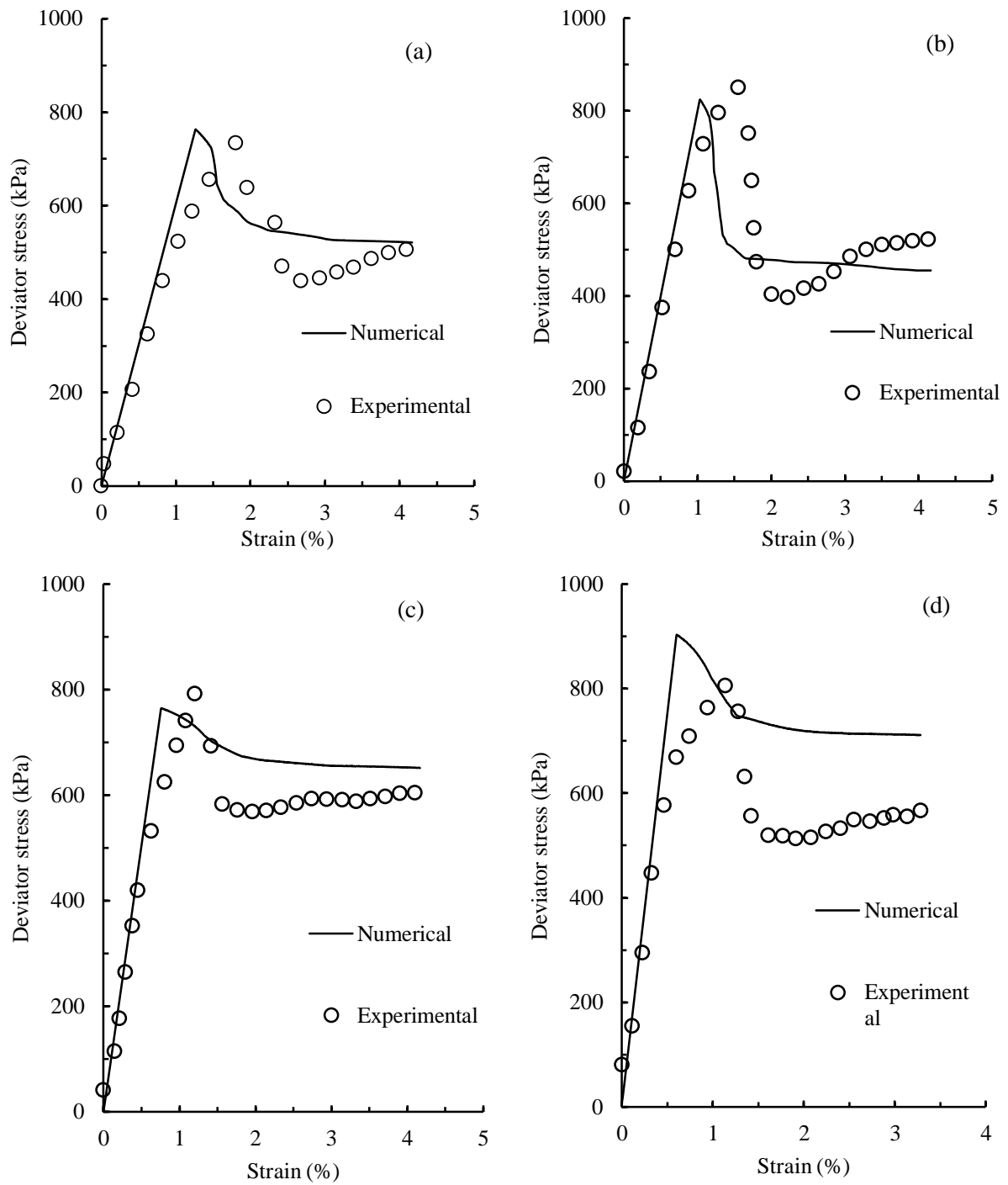
Figure 6.9 Undrained plane strain tests: Numerical versus experimental results for 10% cement content at confining pressures of (a) 50 kPa (b) 100 kPa (c) 200 kPa (d) 400 kPa.
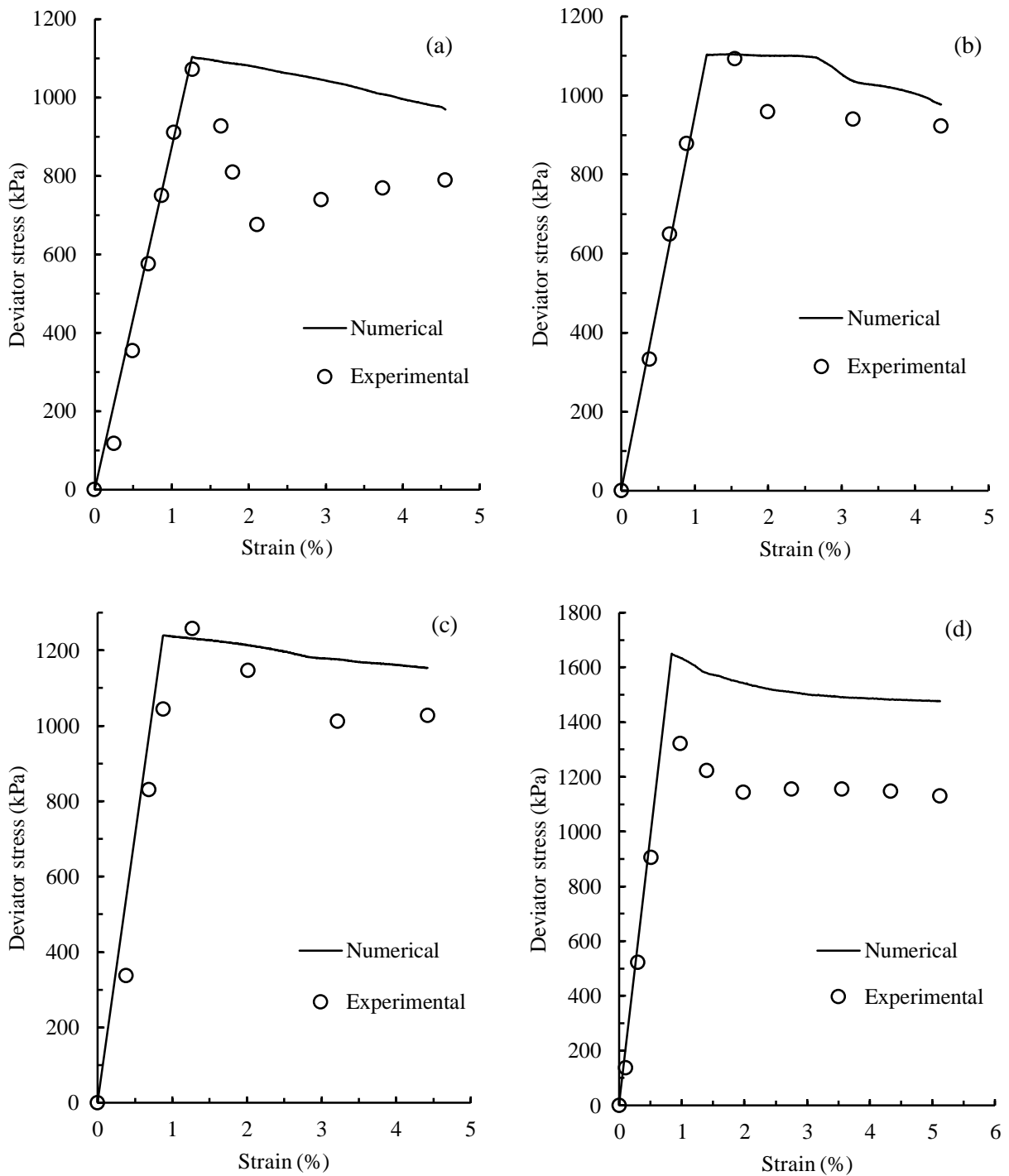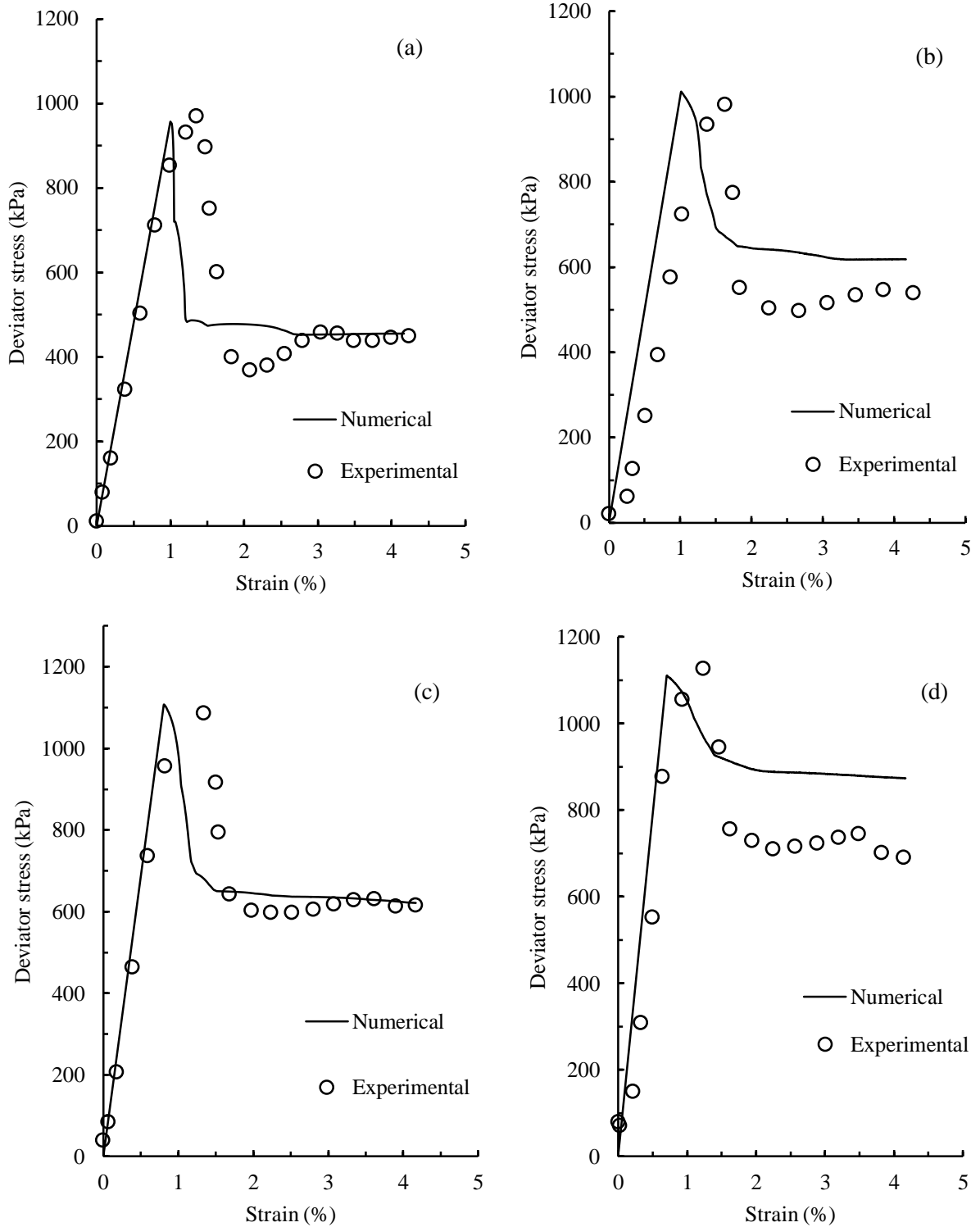
Figure 6.10 Undrained plane strain tests: Numerical versus experimental results for 15% cement content at confining pressures of (a) 50 kPa (b) 100 kPa (c) 200 kPa (d) 400 kPa
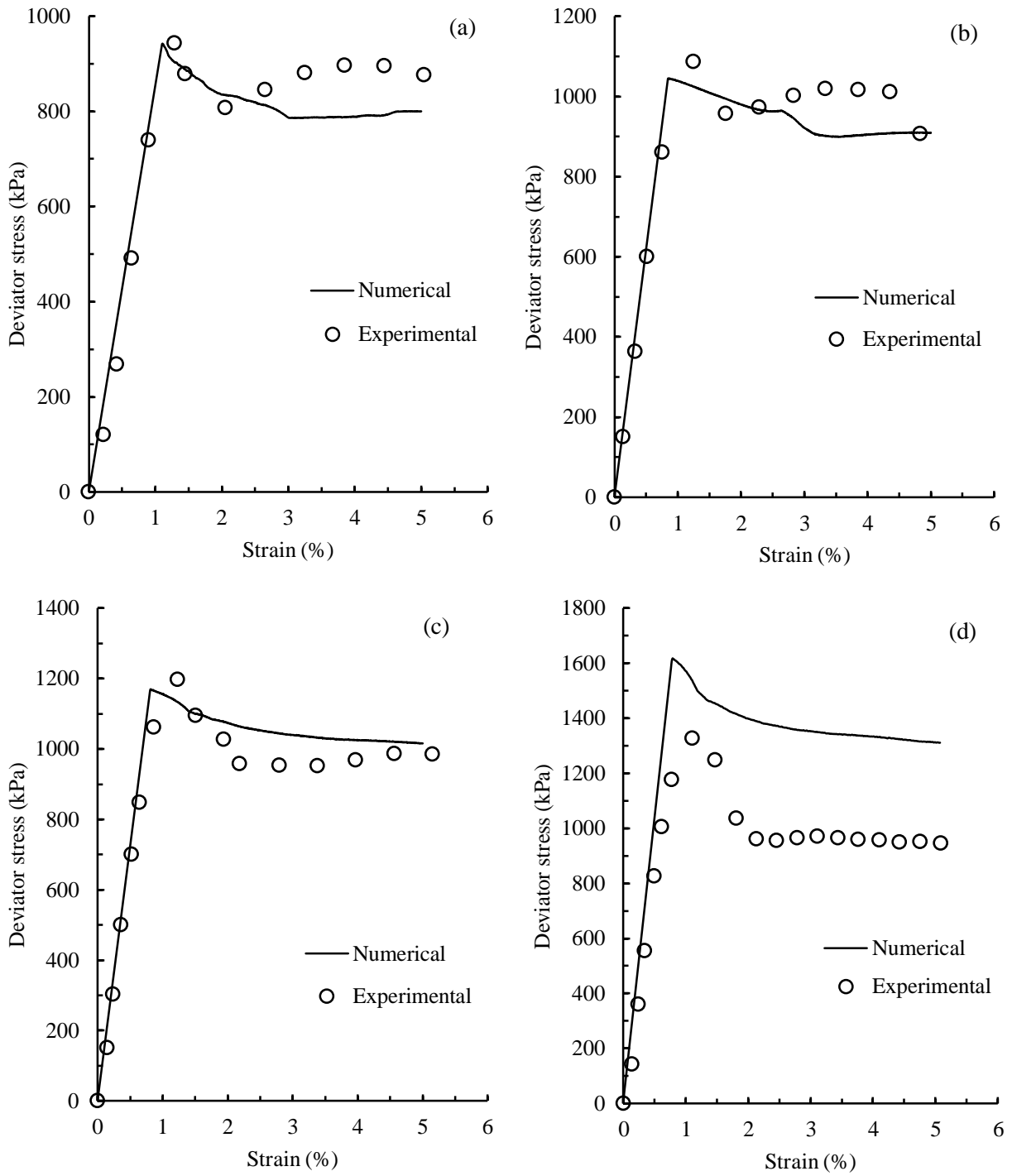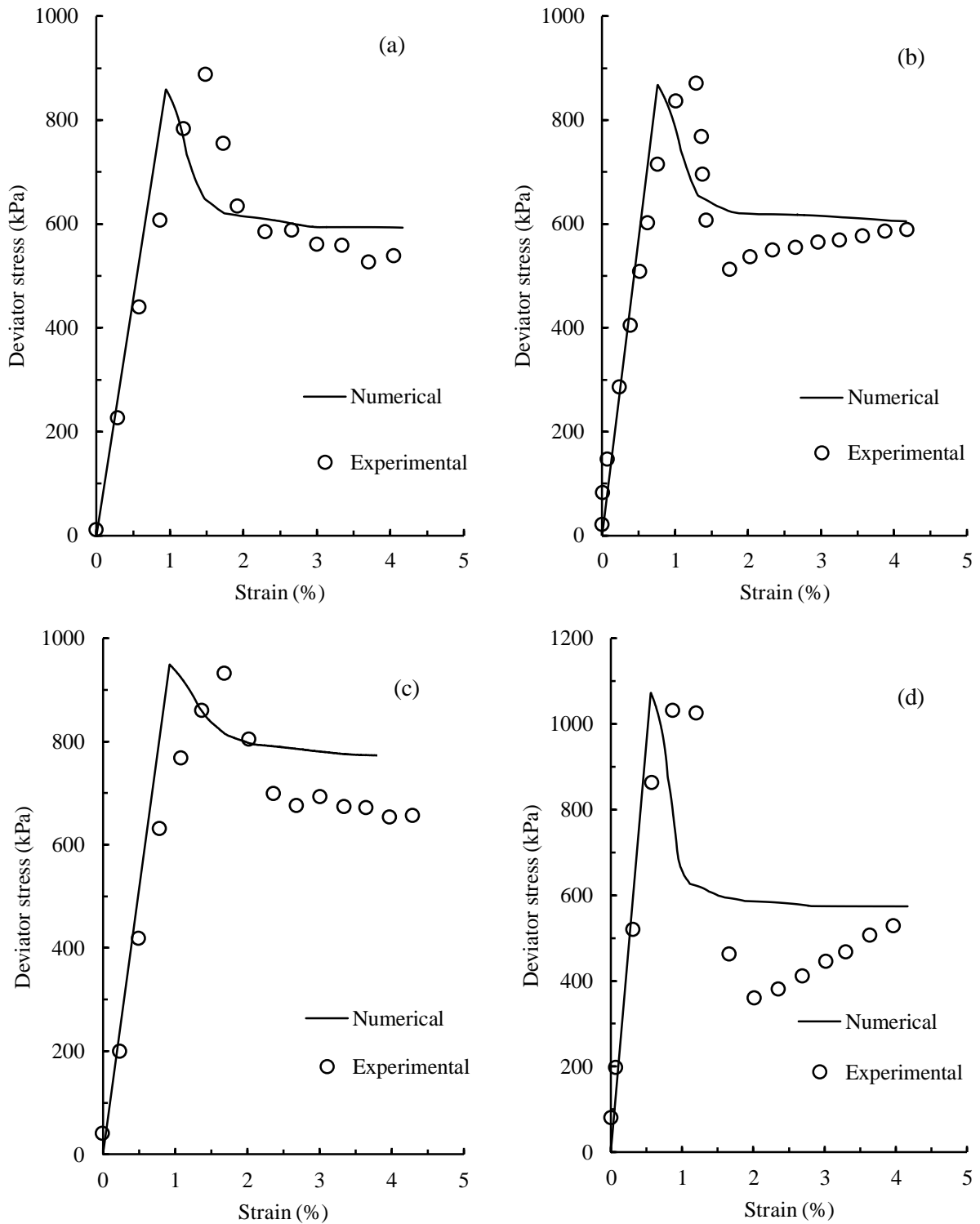
Figure 6.11 Undrained plane strain tests: Numerical versus experimental results for 20% cement content at confining pressures of (a) 50 kPa (b) 100 kPa (c) 200 kPa (d) 400 kPa
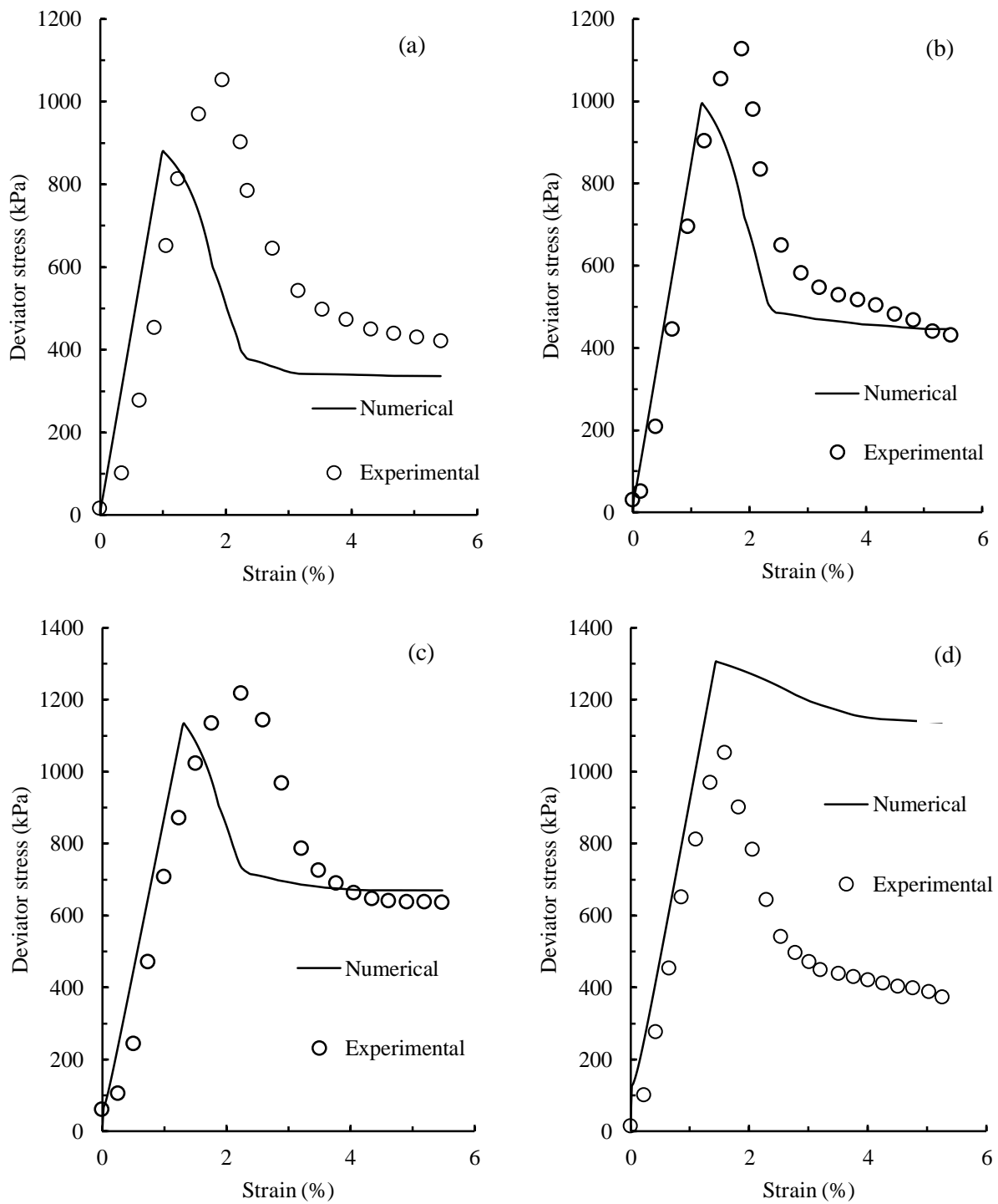
Figure 6.12 Drained plane strain tests: Numerical versus experimental results for 10% cement content at confining pressures of (a) 50 kPa (b) 100 kPa (c) 200 kPa (d) 400 kPa.
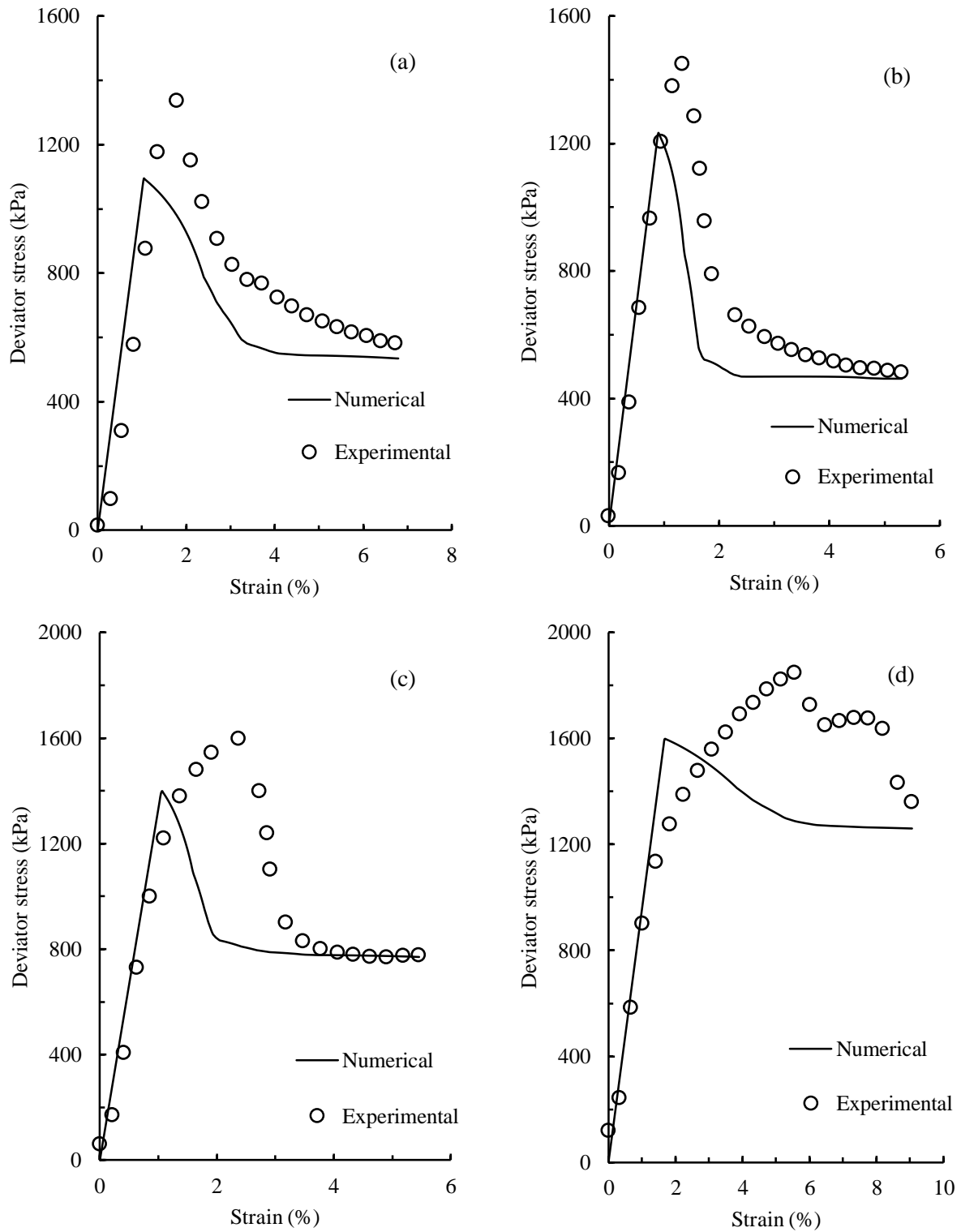
Figure 6.13 Drained plane strain tests: Numerical versus experimental results for 15% cement content at confining pressures of (a) 50 kPa (b) 100 kPa (c) 200 kPa (d) 400 kPa.
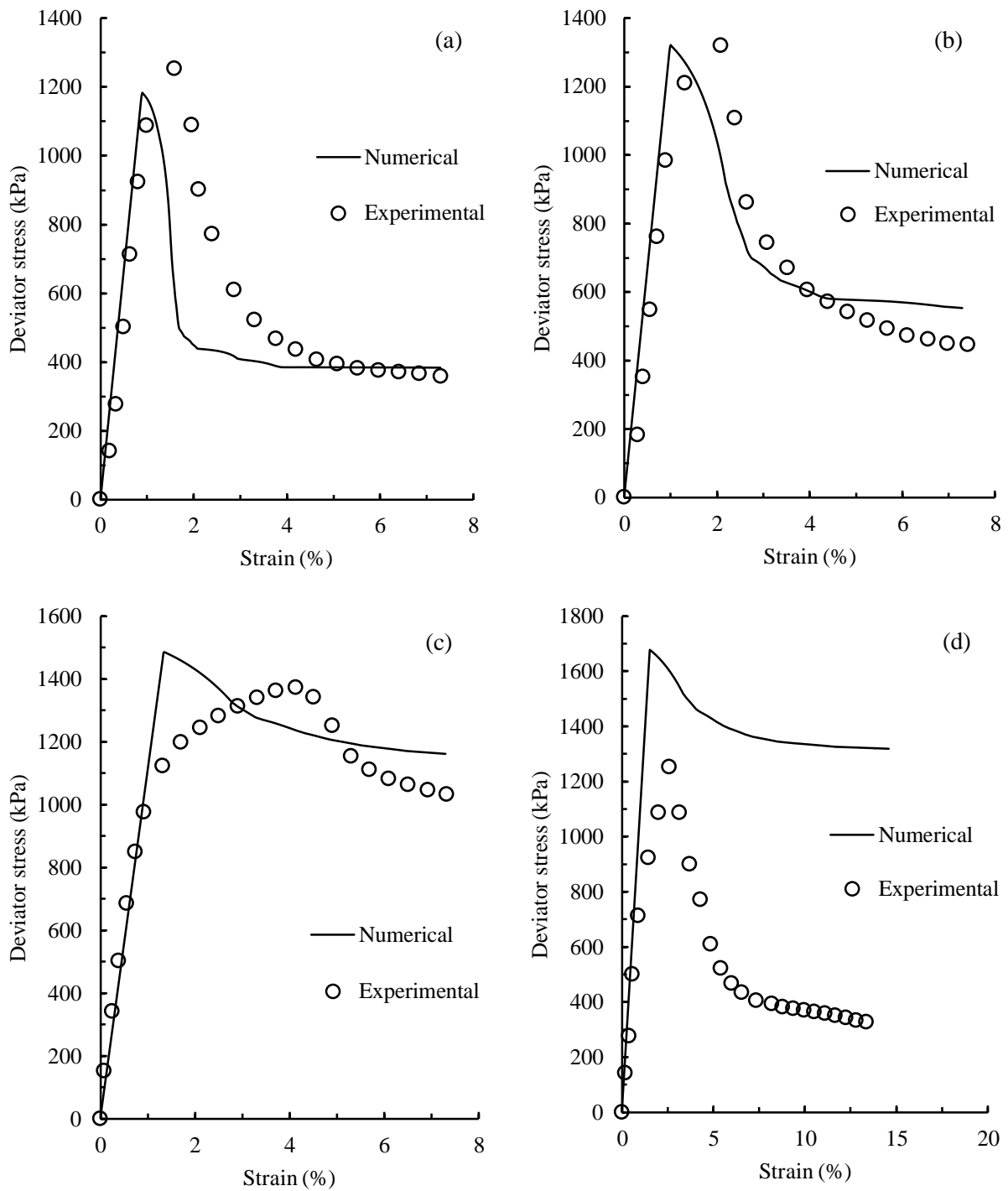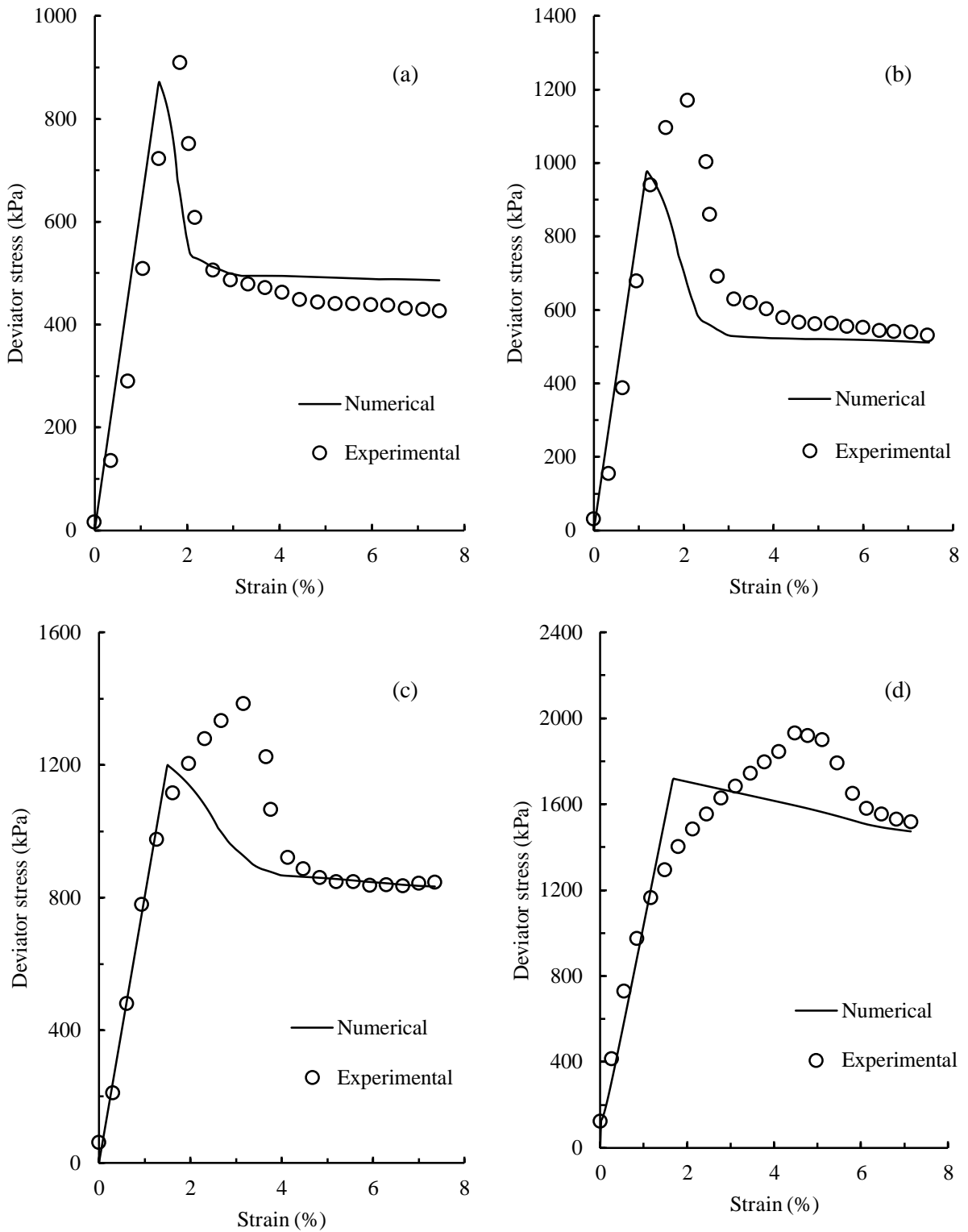
Figure 6.14 Drained plane strain tests: Numerical versus experimental results for 20% cement content at confining pressures of (a) 50 kPa (b) 100 kPa (c) 200 kPa (d) 400 kPa.

### 6.4.2 Results and Discussions

(i) Undrained Plane Strain Results

The numerical simulation plots of deviator stress versus axial strain obtained for undrained plane strain tests are discussed here. The plots obtained for cement contents of 10%, 15% and 20% are shown in Figures 6.9, 6.10 and 6.11, respectively. Sub-sections (a), (b), (c) and (d) in these figures correspond to the responses obtained for confining pressures of 50 kPa, 100 kPa, 200 kPa and 400 kPa, respectively. The experimental results are also shown in the same plots for comparison purposes.

Just like in triaxial tests, reasonable agreement was observed between the experimental and numerical results, up to the peak deviator stress. The initial portion of stress-strain behaviour was well captured using the assumed parameters in Hoek-Brown model. Except 400 kPa confining pressure, the peak deviator stress obtained by numerical simulations were close to the experimental results. As mentioned in case of triaxial tests, slight mismatch at certain data points in the Hoek-Brown failure envelope with regard to experimental results is the reason for such a discrepancy.

Furthermore, small discrepancies were also observed in the post peak regime, in few cases. However, as mentioned before, field problems involving cement treated clays mainly rely on the peak deviator stress. Hence, this discrepancy can be overlooked.

(ii)   Drained Plane Strain Results

The numerical simulation plots of deviator stress versus axial strain obtained for drained plane strain tests are discussed here. The plots obtained for cement contents of 10%, 15% and 20% are shown in Figures 6.12, 6.13 and 6.14, respectively. The sub-sections (a), (b), (c) and (d) corresponds to confining pressures of 50 kPa, 100 kPa, 200 kPa and 400 kPa, respectively. The experimental results are also shown in the same plots for comparison purposes.

As observed in the drained triaxial tests, slight discrepancies were observed in the simulated peak deviator stress in few cases, compared to experimental results. However, the differences in the results are not excessive. As in every other case, post peak regime were not captured well by the model.

6.4.3 Summary of Simulation of Plane Strain Tests

Just as in triaxial tests, the behaviour of cement treated clay under plane strain tests were also captured reasonably well by the established Hoek-Brown failure envelope. However, slight discrepancies could not be avoided for certain cases. The reason for such discrepancies is the mismatch at certain points in the Hoek-Brown failure envelope. This problem may be rectified by considering the results obtained at many confining pressures. In this way, the best fit curve will have more closer match with each of the data points. Furthermore, post peak regime could not be captured well in few cases. However, this part of the curve is irrelevant for field problems.

6.5 LIMITATIONS OF THE MODEL

The Hoek-Brown failure envelope, with the parameters derived from the experimental data, is capable of simulating both triaxial and plane strain behaviour of cement treated clay subjected to drained and undrained testing conditions. However, the model suffers from the following limitations.

- The accuracy of results is by and large dependent on the Hoek-Brown material parameters. Hence, a failure envelope which is the closest possible with each and every experimental output will give the most accurate result. The solution to this is to include test data from many confining pressures, in all the testing conditions.
- The model fails to deliver consistent results in the post-peak regime of deviator stress versus axial strain plot. This means, this model can be used only for those problems where peak strength is the main focus. This model cannot be used where the user is interested in simulating the post peak regime.

6.6 SUMMARY

This chapter serves as a validation of the established Hoek-Brown failure envelopes in predicting the stress-strain curves. After performing numerical simulations for triaxial and plane strain tests, good comparison could be made with the experimental results. Both the results from plane strain tests and triaxial tests pointed to the same set of conclusions, which are summarised below.

1. Hoek Brown constitutive model, with its material parameters obtained from the developed failure envelopes could reasonably predict the behaviour of cement treated clay, up to the peak deviator stress.

2. The accuracy of results can be improved by deducing a failure envelope out of a much larger pool of experimental results.

3. The model, however, shows some discrepancy in the post peak response. This could be attributed to the fact that cement treated clay is extremely brittle and undergoes breakage after achieving the peak stress. This leads to a change in the stress system in the experimental specimen and therefore, the response is questionable. Moreover, in case of brittle materials, the main focus is on peak strength and the residual strength is often neglected for field problems. Hence, this discrepancy may be overlooked.

CHAPTER 7

USE OF PLANE STRAIN INPUT PROPERTIES FOR STABILIZED EXCAVATION PROBLEMS

7.1 INTRODUCTION

For deep excavation projects where soft clay exists well below the final excavation level, cement-stabilization of soil below the final excavation level is one of the common practices adopted to enhance the lateral support to retaining wall (Nakagawa et al., 1996; Lee et al., 1998; McGinn, 2003; Arroyo et al., 2012). Typically, jet grouting or deep soil mixing techniques are used for soil stabilization and are carried out before the commencement of excavation (Tanaka, 1993). Excavations where such stabilization practices are carried out will be hereafter referred to as stabilized excavations. Since, excavations are usually treated as plane strain problems, Cement-Stabilized Soil Layers (CSSL) covering the entire plan area of excavation (called embedded improved soil strut) can be also analysed as plane strain problems. As mentioned in Chapter 2, the behaviour of embedded improved soil strut has been studied in detail by many researchers (Kongsomboon 2002; Lim 2003; Tan et al., 2003; Yang et al., 2011; Pan et al., 2018; Wang et al., 2019). Conventionally most of the studies have used the unconfined compressive strength (UCS) or triaxial test data as input parameters to characterize the cement treated clay layer. In other words, parameters obtained under axisymmetric idealisation are used for input properties of the cement treated clay layer, which is in fact under plane strain condition. For any excavation problem, lateral deflection of retaining wall is the most crucial aspect to be monitored (Hsieh et al., 2003). Since, cement treated clay exhibits lower strength under plane strain loading condition (as discussed in Chapter 4), this practice could under-estimate the lateral deflection of retaining wall.

This chapter compares the lateral wall deflection obtained by using parameters obtained under plane strain and triaxial conditions, in a stabilized excavation problem. For this, two case studies

of excavation problems were selected from the literature. First a shallow excavation problem, studied using centrifuge model tests carried out at National University of Singapore, Singapore was selected (Kongsomboon, 2002). The second problem is a deep excavation work carried out as a part of MR Residential Basement (MRRB) project in Taiwan (Hsieh et al., 2003). The details of these case studies and the modifications made to these problems to suit the interest of this study will be discussed in the subsequent sections.

7.2 CASE STUDY-1: CENTRIFUGE STUDY OF A STABILISED EXCAVATION

Kongsomboon (2002) carried out series of centrifuge studies to find out the behaviour of an excavation stabilised by embedded improved soil. This study was explained in detail in Chapter 2 and hence, only the details relevant to this chapter will be briefly repeated herein.

Three models of excavations; TW/O, TST and TB-L100, were considered for the centrifuge study (Figure 2.3). These configurations refer to no improvement, provision of embedded improved soil strut and provision of embedded improved soil berm, respectively. Only embedded improved soil strut is relevant to this study.

The centrifuge containers were designed to represent plane strain excavations and the tests were carried out at a scale of 1:100. The model retaining wall considered in the analysis was made of aluminium alloy with a thickness of 4 mm and embedded 160 mm into the ground, which would represent a depth of 16m in the prototype scale. Figure 7.1 gives the schematic of excavation problem considered in this study. The dimensions in the model scale and the corresponding field scale are also shown. As seen in this figure, the retaining wall was extended above ground level by 30 mm, which would represent 3 m above ground level in the field scale. This is owing to difficulties involved in instrumentation below ground level. The lateral displacements of the retaining wall were noted at the topmost point of retaining wall, i.e. 3 m above ground level. As seen in Figure 7.1, three layers of soils are present. It is to be noted that, a single layer of kaolin clay was used for the study. However, placing and consolidation of clay in the centrifuge container resulted in the formation of thin over-consolidated layers at the top. It is also to be noted that no mention of water table was made in this study and hence, a dry excavation analysis is only performed.
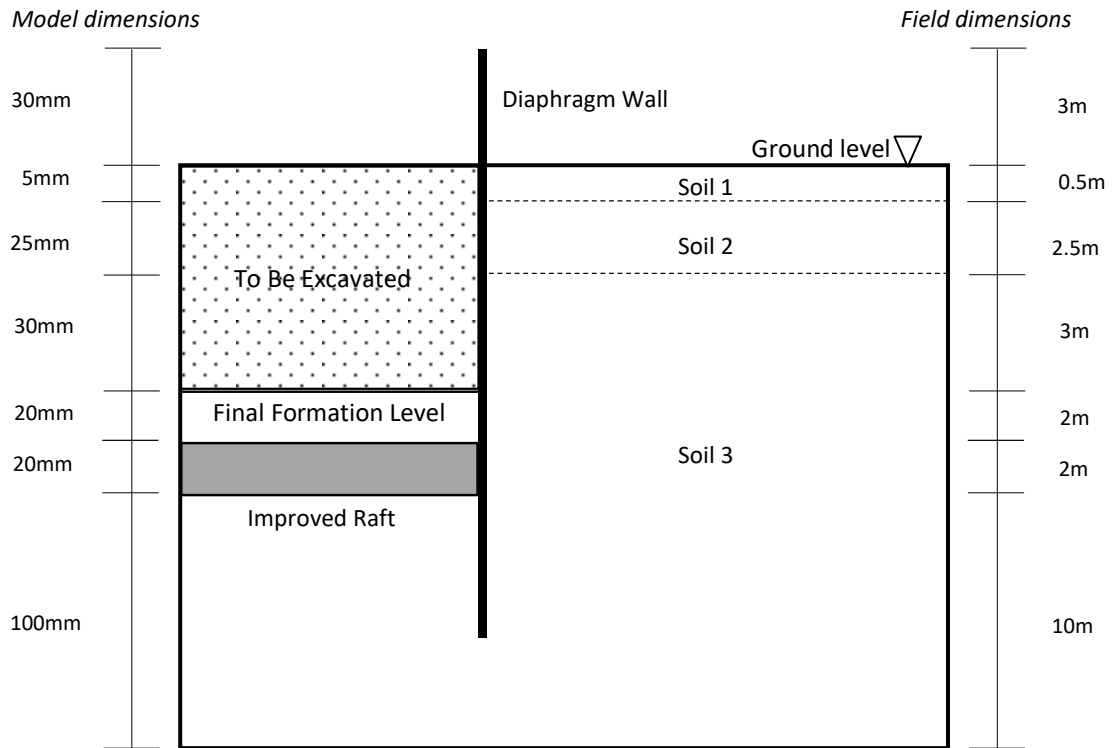
Figure 7.1 Schematic of excavation provided with embedded improved soil strut, as used in Kongsomboon (2002)

The properties used for the soil layers, improved soil layer, constitutive model and diaphragm wall are provided in Table 7.1, as used in Kongsomboon (2002) for the numerical simulation of the centrifuge study. Modified Cam-Clay model and conventional Mohr-Coulomb model were used for the analysis of clay layers and cement treated soil layer, respectively.

As shown in Figure 7.1, an excavation of 6 m (in field scale) was considered in the study. Excavations were carried out in increments of 0.5 m depth and hence, 12 stages of excavation were involved. The improved layer was provided 2 m below the final excavation level. The rationale behind leaving a 2 m layer of untreated soil between the final formation level and the improved layer has not been commented upon in the study. The lateral deflection of retaining wall was noted at every excavation stage till the final formation level and deflection profile was

154

plotted against excavation depth. The deflection profile was already shown in Chapter 2 (Figure 2.4).

Table 7.1 Properties and constitutive model used for various components of excavation problem, as reported by Kongsomboon (2002)

Material	Properties*	Constitutive model
Soil Layer 1	$K_0 = 1.505$, $\lambda = 0.4$, $\kappa = 0.05$, $M = 1.0$, $\mu = 0.3$, $N = 3.643$, $\gamma = 17$ kN/m^3	Modified Cam Clay
Soil Layer 2	$K_0 = 0.7920$, $\lambda = 0.4$, $\kappa = 0.05$, $M = 1.0$, $\mu = 0.3$, $N = 3.643$, $\gamma = 17$ kN/m^3	Modified Cam Clay
Soil Layer 3	$K_0 = 0.6012$, $\lambda = 0.4$, $\kappa = 0.05$, $M = 1.0$, $\mu = 0.3$, $N = 3.643$, $\gamma = 17$ kN/m^3	Modified Cam Clay
Improved layer	$E = 190$ MPa, $\mu = 0.3$, $c = 495$ kPa, $\phi = 0$, $\gamma = 17$ kN/m^3	Mohr-Coulomb
Diaphragm wall	$E = 72$ GPa, $\mu = 0.2$, $\gamma = 22$ kN/m^3	Linear Elastic

*Note: K_0 is the earth pressure coefficient at rest; λ, κ, M and N are critical state parameters; γ is the unit weight; μ is the Poisson's ratio; c and ϕ are the shear strength parameters of the soil; E is the Young's modulus. The same notations followed by Kongsomboon (2002) have been used here.

7.2.1 Numerical Simulation of Case Study-1

Attempts were made to validate the centrifuge study carried out by Kongsomboon (2002). Numerical simulations were carried out using a finite difference software package, *FLAC* (version 7, 2011). The following construction sequences are adopted in the present study:

1. Generation of model grid, assignment of material properties and boundary conditions to represent the problem under consideration.
2. Establish the initial in-situ stress state of the ground, in case of problems involving water table.
3. Establish the initial in-situ stress state of the ground, after installing the diaphragm wall.
4. Carry out stage-wise excavation up to the desired depth.

Each of the above steps signifies individual stages of simulation. This method facilitates noting the responses corresponding to each stage of the problem.

Following the above sequence, model grid for the problem was developed to be in the same way as the centrifuge model and is shown in Figure 7.2. While horizontal fixity was assigned at left and right ends of the numerical model, full fixity was provided in both horizontal and vertical directions at the bottom. Only half the excavation was considered in the centrifuge study, taking advantage of the symmetry of geometry. The same geometry was assigned to the numerical model. Hence, the numerical model grid shown in Figure 7.2 represents the right half of excavation. Since, excavations of 0.5 m depth were to be carried out in each of the stages, size of each individual grid was selected as 0.5×0.5 m^2.

Mesh sensitivity analysis was performed by varying the mesh size from 0.5×0.5 m^2 to 0.1×0.1 m^2. The differences in lateral wall deflections were found to be within 5%. Hence, 0.5×0.5 m^2 was selected as the mesh size to save computational time and effort.

Materials and constitutive models for all the components were selected based on the details provided in Table 7.1. Each colour in the grid represents different sets of properties assigned for

the respective soil layer. All the required constitutive models mentioned in the table, come in-built in *FLAC* materials library.
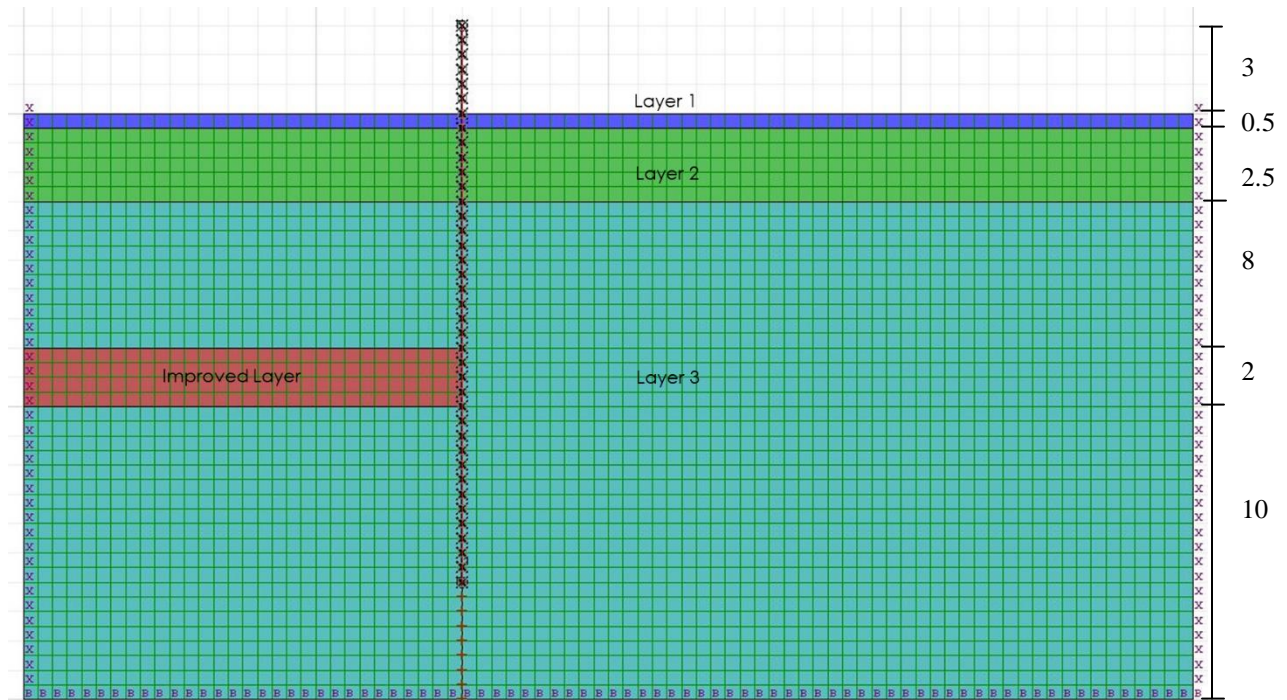
Figure 7.2 Grid generated to simulate the centrifuge problem (All dimensions are in m).

Diaphragm wall was provided using a structural beam element and all the properties, except density were assigned. Density is not assigned at this stage, to allow the equilibrium stress state in the soil to be established. It is to be noted that diaphragm wall is actually a plane stress problem. For plane strain analysis, the Young's modulus of the wall should be divided by $(1 - \mu^2)$ to convert the plane-stress formulation to the plane-strain condition. Hence, this converted value of Young's modulus was input to the numerical simulations. The soil-wall interface properties need to be also specified at this stage, in terms of normal and shear stiffness. The interface stiffness should be comparable with the stiffness of adjoining zone (Cundall and Hart, 1992). However, an interface stiffness of at least ten times the equivalent stiffness of the stiffest neighbouring zone is essential to ensure that the deformability at the interface will have minimal

influence on the compliance of the model. This guideline has been specified in the *FLAC* user manual (2011). Stiffness values higher than this can also be provided, to be on the safer side, by compromising on the computational time. The equivalent stiffness is defined as, max $[(K+4G/3)/\Delta z_{min}]$, where K and G are bulk and shear moduli, and Δz_{min} is the smallest width of an adjoining zone in the normal direction. A soil-wall interface stiffness of 100 times the value of equivalent stiffness was provided to make sure that the deflection of retaining wall is not influenced by the interface.

The next stage is to install diaphragm wall. This was simulated by assigning the density of diaphragm wall at this point. Stresses in the soil were then allowed to equilibrate.

The first increment of excavation of 0.5 m depth was carried out in the next stage. Excavation was simulated by assigning null model to the required zones in the grid. After establishing the equilibrium state, the lateral deflection of retaining wall was noted at topmost tip of the wall, i.e. at 3 m above the ground level. The remaining increments of excavations were carried out in the subsequent stages, till a depth of excavation of 6 m was achieved. The grid corresponding to 1 m depth of excavation and final 6 m depth of excavation are shown in Figure 6.3. The lateral wall deflection was noted at all the stages and was plotted against the depths of excavation. The variation of lateral wall deflection with the depth of excavation, obtained in centrifuge studies have been published in Tan et al. (2003). These results were digitised and were compared with the numerical simulations carried out in this study.

Figure 7.4 shows the variation of the lateral deflection of retaining wall with excavation depth, as reported by Tan et al. (2003) along with present numerical analyses results.
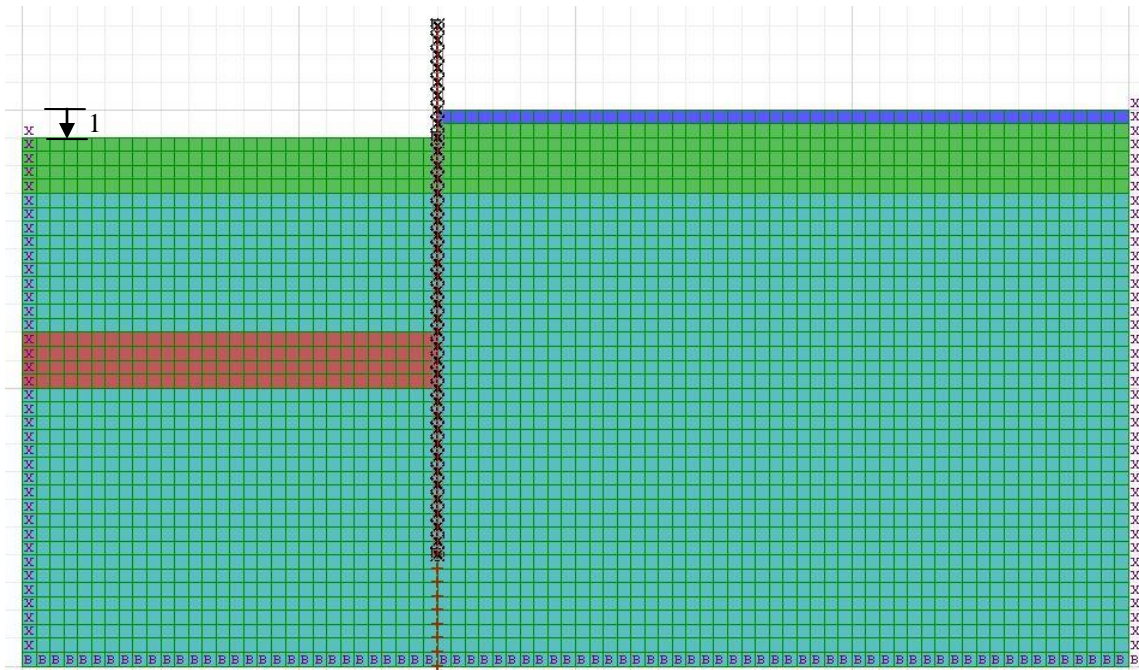
(a)
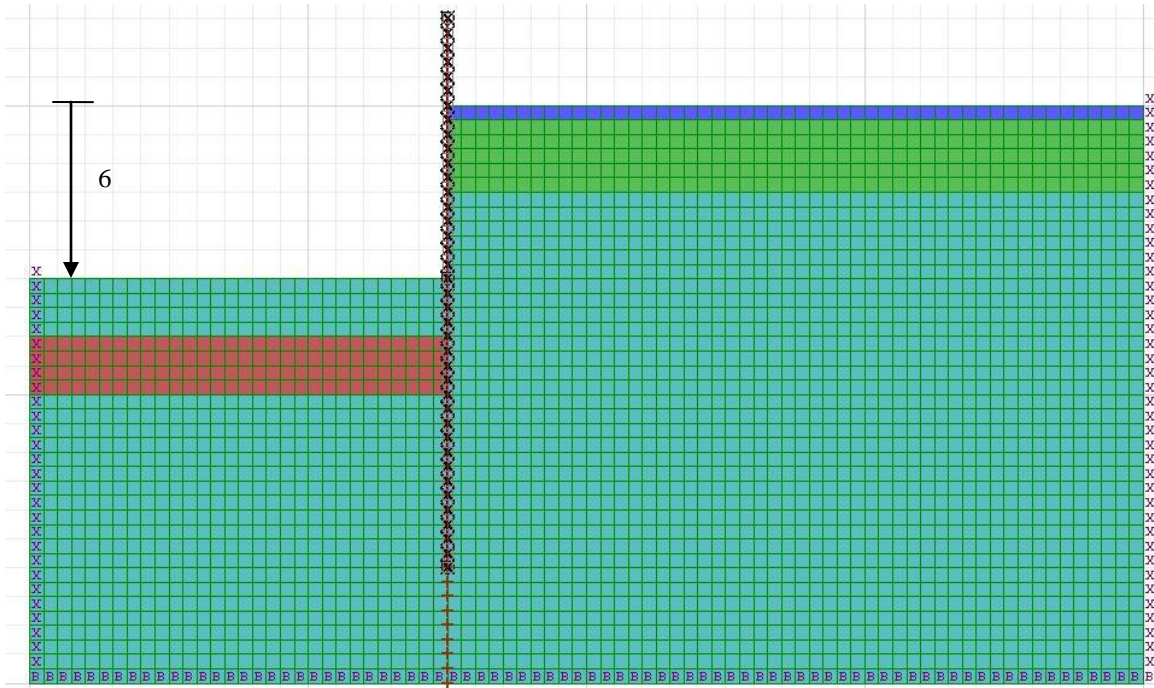
(b)

Figure 7.3 Grids at excavations of depth (a) 1 m and (b) 6 m (All dimensions are in m).

The negative signs of deflection and depth indicate that these values were in negative x and y directions, respectively. The wall was found to deflect towards the excavation side. This is expected for an un-strutted excavation, where the backfill soil pushes the wall, as the excavation proceeds. As can be seen, though the numerical analysis over-predicts the centrifuge test results up to an excavation depth of 2.5m, the deflections at the final excavation level were reasonably predicted by the simulation. This shows that the numerical model adopted in the study was appropriate for the simulation of centrifuge problem considered in this study.
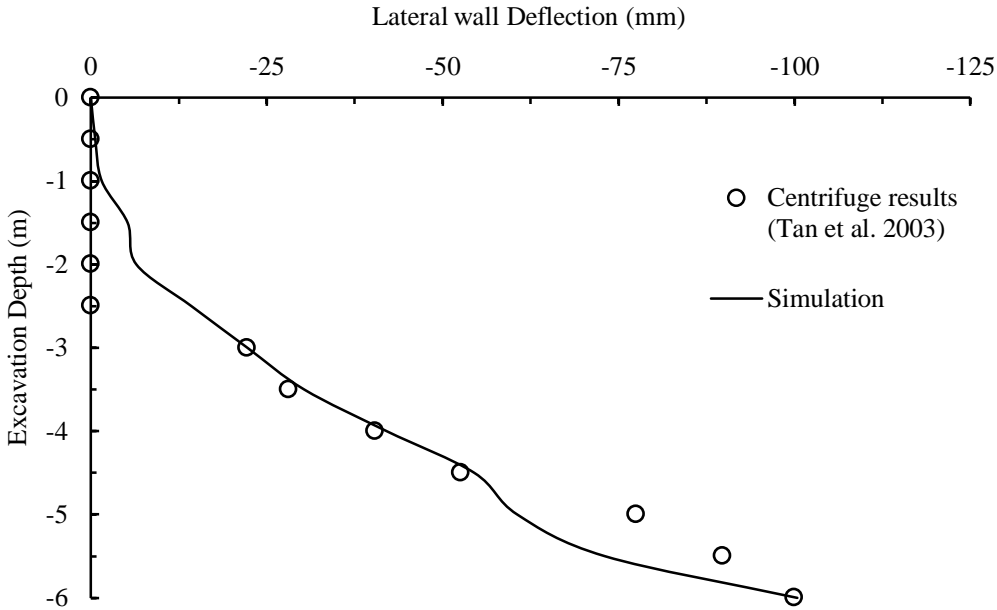
Figure 7.4 Validation results for the centrifuge excavation study.

7.2.2 Parametric Studies on Case Study-1

The main objective of this study is to demonstrate the importance of using plane strain properties for cement treated clay in excavation problems stabilized with cement treatment. For this, the properties of the improved layer used in Kongsomboon (2002) were replaced with the plane

strain properties obtained for different cement contents, as discussed in Chapters 4 and 5. The Hoek-Brown model and the associated material parameters for different cement contents (as discussed in Chapter 5) were implemented in *FLAC* (as discussed in Chapter 6) to represent the improved layer in the problem.

Figure 7.5 shows the lateral wall deflection against the excavation depth, for different cement contents. Clearly, 15% cement content recorded the least deflection, followed by 20% and 10% cement contents, respectively. However, the deflections recorded by 10% and 20% cement contents were quite similar. It is noteworthy that the same trend was followed in the strength too under both drained and undrained conditions, as discussed in Chapters 4 and 5. Hence, the lateral wall deflection experienced by the wall is a direct function of the strength of improved layer provided below the final formation level.

Since, the cement treated layer is under plane strain condition, it is believed that the input of plane strain properties would give a realistic response. To highlight this point, the improved layer properties were now replaced with properties obtained from triaxial testing using the Hoek-Brown failure envelope (as discussed in Chapters 5 and 6). To facilitate a better understanding of the importance of input properties for such field problems, the lateral wall deflection response obtained for triaxial input properties of each of the cement contents were compared with the corresponding response for plane strain (PS) input properties, as shown in Figure 7.6.

Figure 7.6 clearly shows that triaxial input properties under-predicts the lateral deflection of retaining wall, especially at the final formation level. This was evident for all the cement contents. In the strength point of view, it was already reported that plane strain testing of cement treated clay resulted in lower strength compared to triaxial testing. The lateral wall deflection was found to be higher when plane strain properties were input to the improved layer and this was observed across all the cement contents. Another important observation is that the deflection values for plane strain and triaxial properties were almost the same, up to an excavation depth of about 5 m. The difference in deflection was immediately observed after this depth. This could be an indication that the difference in lateral wall deflection might be higher for deeper excavations. However, such a conclusion requires verification.

To analyse the differences in lateral deflection of retaining wall for greater depths of excavation, the excavation was continued further for an extra 2 m with the input of both plane strain and triaxial properties. It may be recalled that there was a 2 m thickness of soil which was left untreated between the final formation level and the top of improved layer in the centrifuge study. This area to be excavated is shown in Figure 7.7. Hence, the new excavation depth will now be increased from 6 m to 8m.
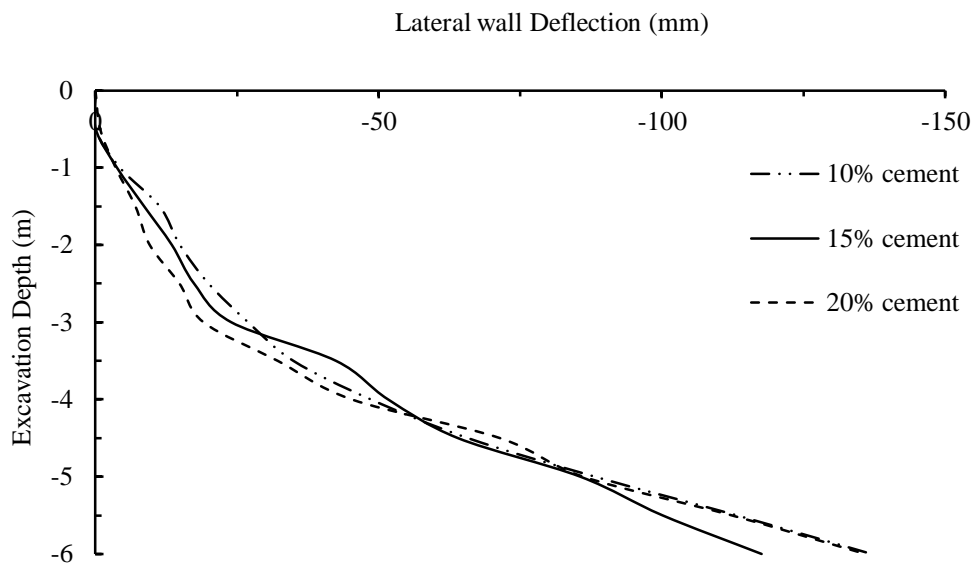
Figure 7.5 The variation of lateral wall deflection for different cement contents using plane strain input properties

Lateral wall Deflection (cm)
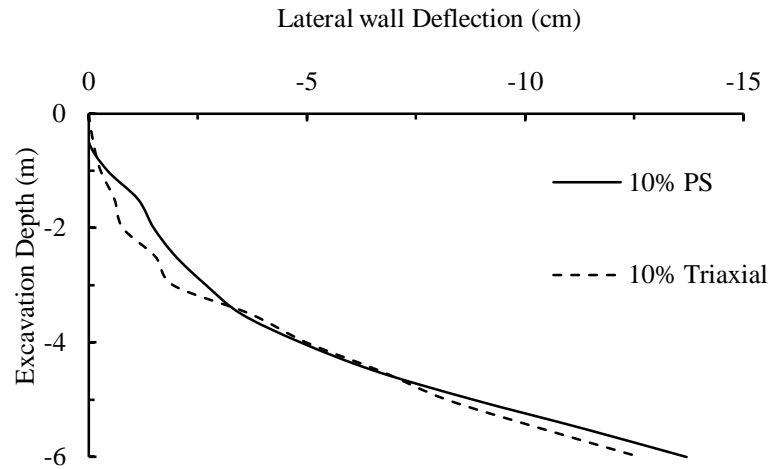
(a)
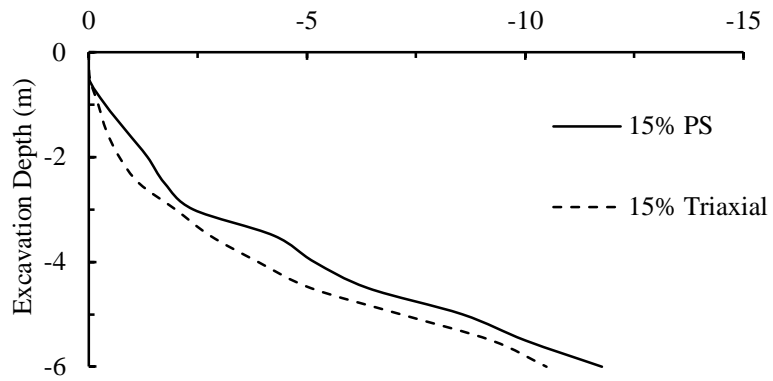
(b)
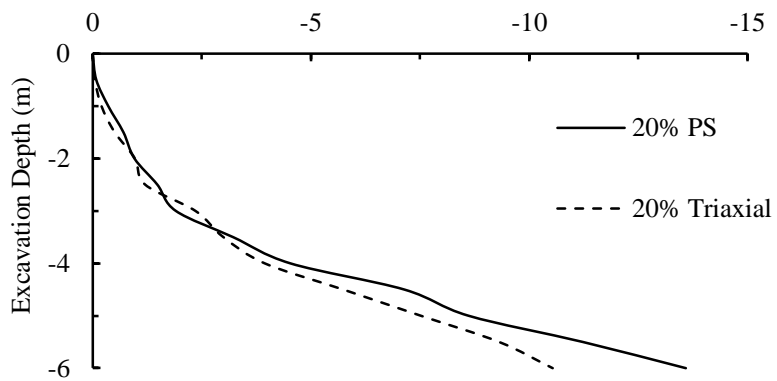
(c)

Figure 7.6 The differences in lateral wall deflection upon the input of plane strain and triaxial properties for cement contents of (a) 10% (b) 15% and (c) 20%.


```
30mm ─┤   │  Diaphragm Wall              │  ├─ 3m
       │   │                             │
 5mm ──┤ ┌─┼─── Soil 1 ──────────────────┤  ├─ 0.5m
       │ │ │                             │
25mm ──┤ │ │    Soil 2                   │  ├─ 2.5m
       │ │ ┼── - - - - - - - - - - - - --┤
30mm ──┤ │ │                             │  ├─ 3m
       │ │ │  Final Formation Level      │
20mm ──┤ │ █ To Be Excavated             │  ├─ 2m
       │ │ │              Soil 3          │
20mm ──┤ │ ▓ Improved Raft               │  ├─ 2m
       │ │ │                             │
       │ │ │                             │
100mm ─┤ │ │                             │  ├─ 10m
       │ └─────────────────────────────┘
```
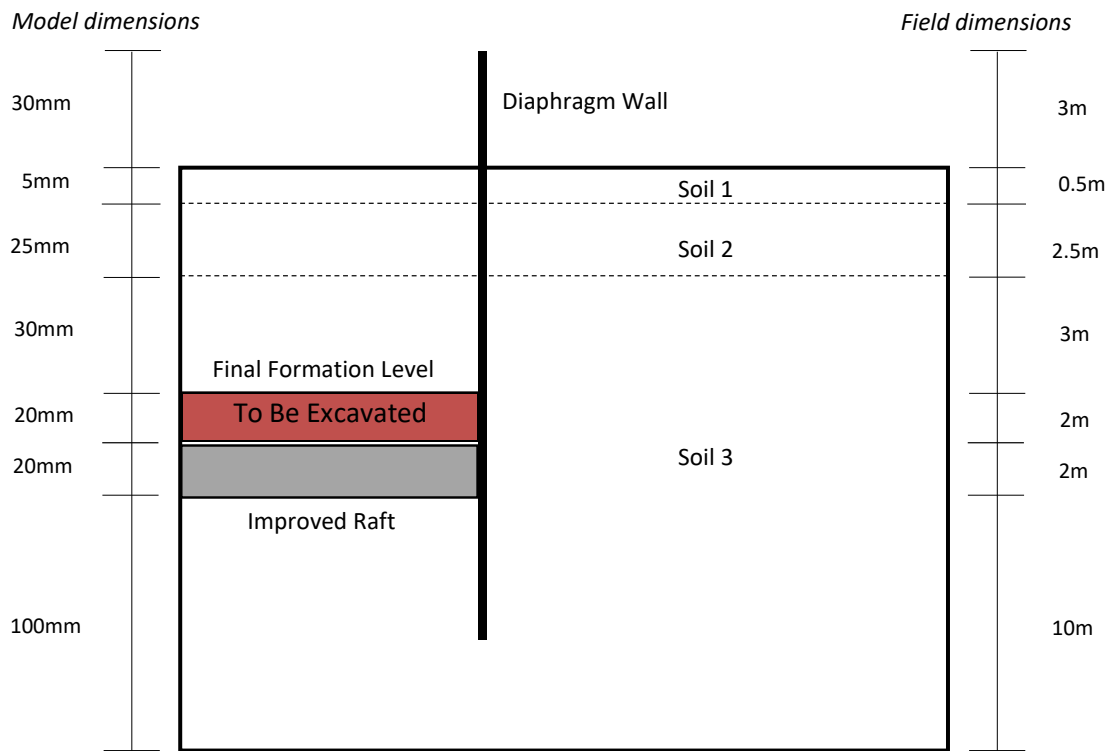
Figure 7.7 Extra excavation to be made to analyse the response for deeper excavations.

Wall Response

In any excavation problem, two major aspects of the wall which are of interest to the field engineer are, lateral deflection of retaining wall and bending moment. The typical profiles for lateral deflection of retaining wall and bending moment are shown in Figure 7.8. The lateral wall deflection responses for an excavation depth of 8 m, with the input of plane strain and triaxial input properties, are compared in Figure 7.9. As can be seen in the figure, the differences in lateral wall deflections were found to be much more pronounced at greater excavation depths. The final wall deflections at the formation level for cement contents of 10%, 15% and 20% were found to be under-predicted by 8%, 15% and 36%, respectively with the use of triaxial input

properties. In other words, owing to the higher strength recorded under triaxial testing conditions, the lateral deflection of retaining wall was under-estimated.

The variations of maximum bending moment values with excavation depth for different cement contents are shown in Figure 7.10. The negative signs of bending moment and depth indicate that these values were in negative x and y directions, respectively. The maximum bending moment was recorded towards the excavation side. This is expected for an un-strutted excavation, where the backfill soil pushes the wall, as the excavation proceeds. The differences in bending moment with the input of triaxial and plane strain properties were not significant for 10% and 15% cement contents. Slight differences were visible in case of 20% cement content. The maximum bending moment values experienced by the retaining wall at the final excavation stage, are given in Table 7.2. Though not significantly different, lower bending moments were recorded in case of plane strain input properties. This could be because of higher movement experienced by the wall in this case. The maximum difference observed was 12%, in case of 20% cement content. In other words, the wall bending moment was slightly over-predicted by triaxial input properties, in case of a shallow excavation problem.

Ground response

The ground response is of great interest for excavation problems on the field, as excessive ground movements could disturb the adjacent buildings. The ground movements include both surface settlement and horizontal movement of backfill soil. The ground movements were recorded at 5 m behind the retaining wall, as was recorded in the centrifuge study (Kongsomboon, 2002) and are shown in Figure 7.11. The negative sign indicates that the displacements and depth were measured in the negative x and y directions, respectively. As expected, both the movements were found to be higher with the use of plane strain input properties. Table 7.3 gives a clear indication of the differences in ground movements with the use of triaxial and plane strain input properties, when the final excavation level was reached.

165
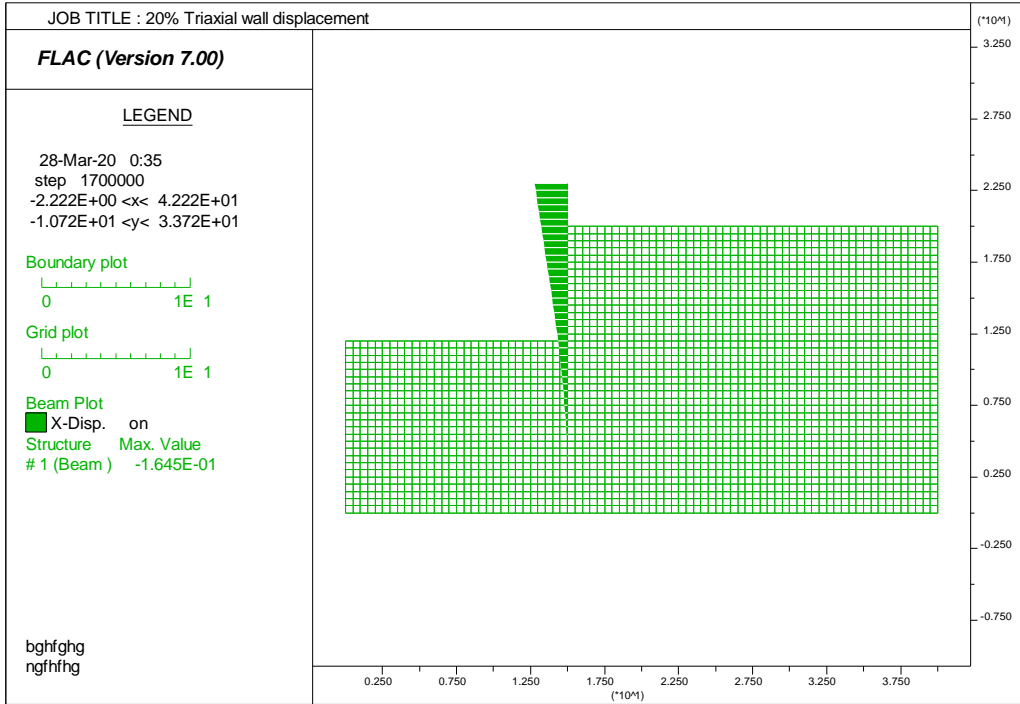
(a)
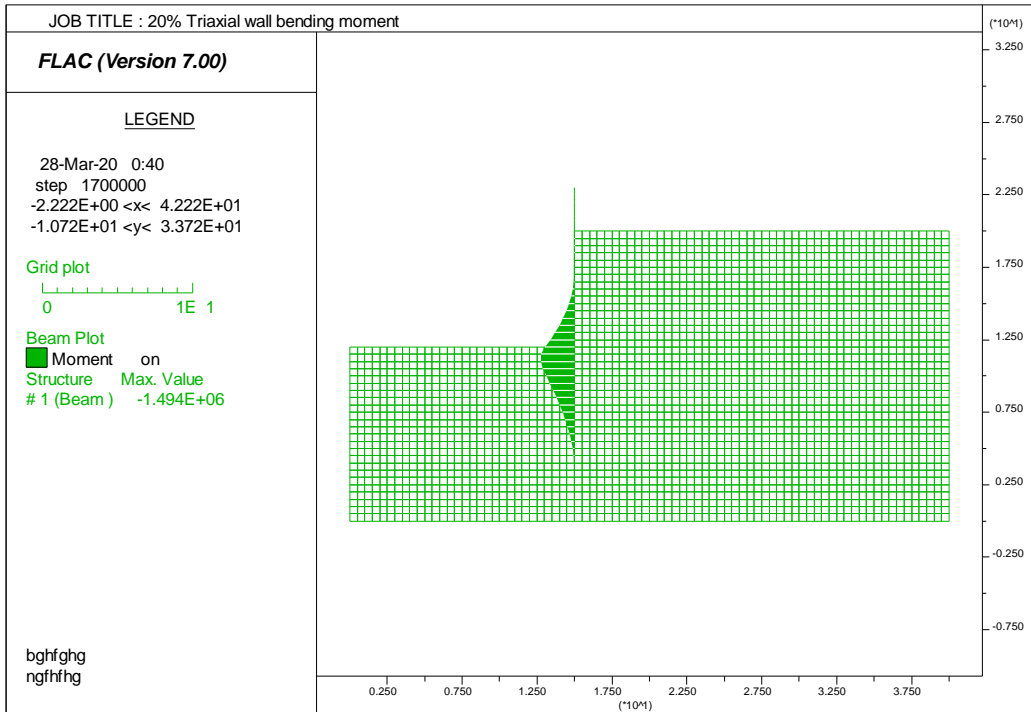
(b)

Figure 7.8 Typical wall profiles for (a) Lateral deflection (b) Bending moment

166

Lateral wall Deflection (cm)
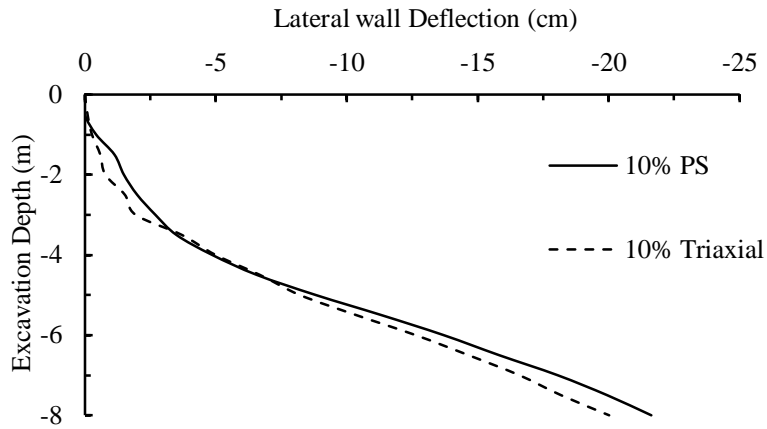
(a)
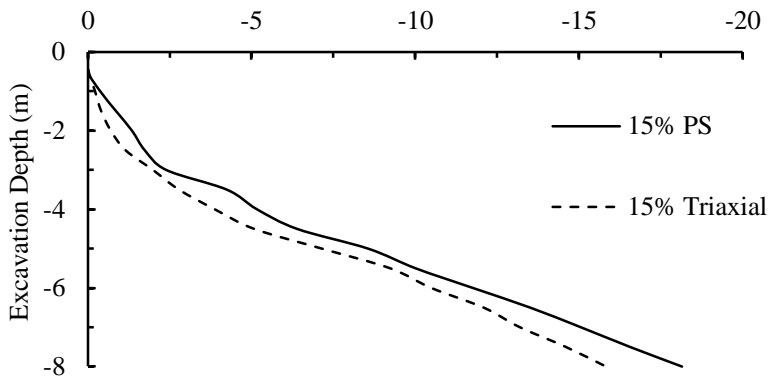
(b)
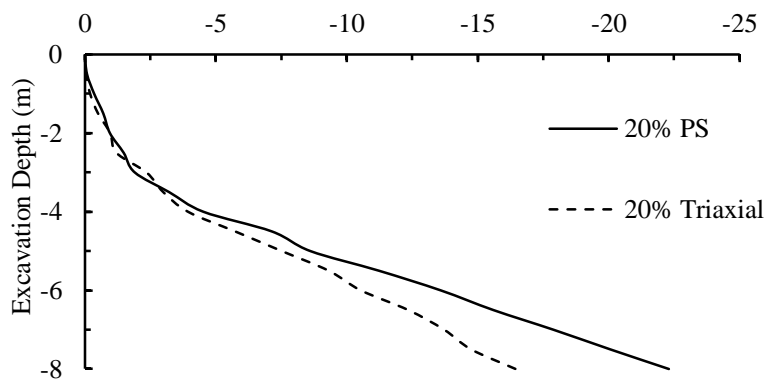
(c)

Figure 7.9 The lateral wall deflections for an excavation depth of 8 m using plane strain and triaxial input properties for cement contents of (a) 10% (b) 15% and (c) 20%.

Bending Moment $*10^5$ (N-m)
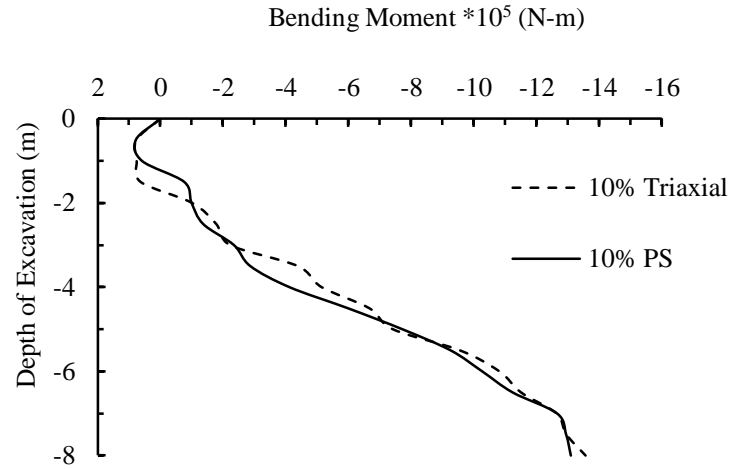
(a)
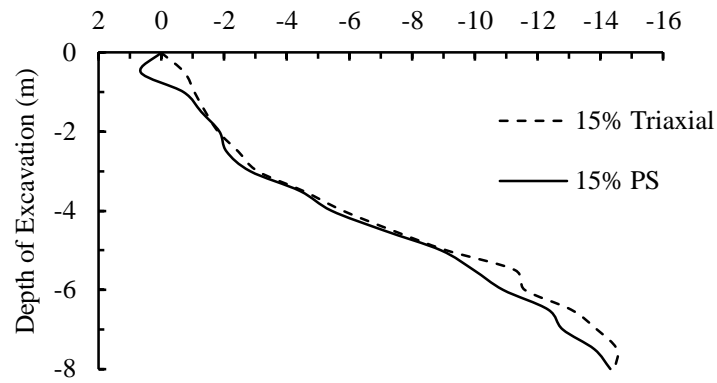
(b)
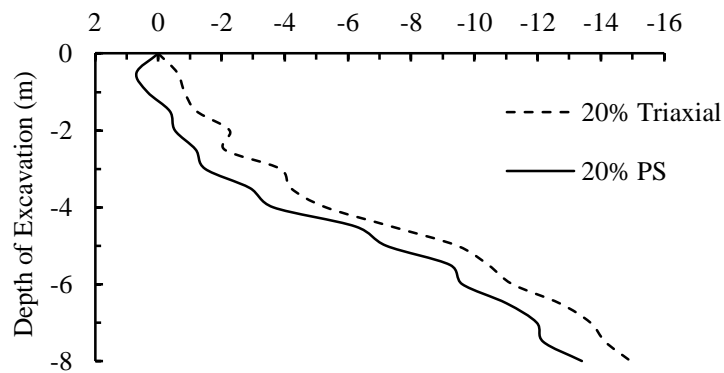
(c)

Figure 7.10 Bending moment profiles of retaining wall for cement contents of (a) 10% (b) 15% and (c) 20%.

Table 7.2 Maximum bending moment values for different input properties of improved layer

Cement Content (%)	Maximum Bending Moment $* 10^5$ (N-m)		
	Triaxial Input Properties	Plane Strain Input Properties	% Difference in Bending Moment (%)
10	-13.6	-13.1	4
15	-14.5	-14.3	1
20	-14.9	-13.4	12

The % increase in displacements with the use of plane strain input parameters compared to triaxial input parameters, are also shown in the Table 7.3. The maximum differences in displacements were observed in case of 20% cement content. Horizontal and vertical ground displacements recorded under plane strain input properties were higher than those obtained under triaxial properties by about 40% and 52%, respectively. However, the differences were minimal for 10% cement content. In other words, the use of triaxial input properties may greatly under-predict the ground movements, especially at higher cement contents.

Typical shapes of deformed meshes at the final excavation stage, for triaxial and plane strain input properties, are shown in Figure 7.12. Clearly, the one obtained with the input of plane strain input properties looks more deformed compared to that obtained using triaxial properties.
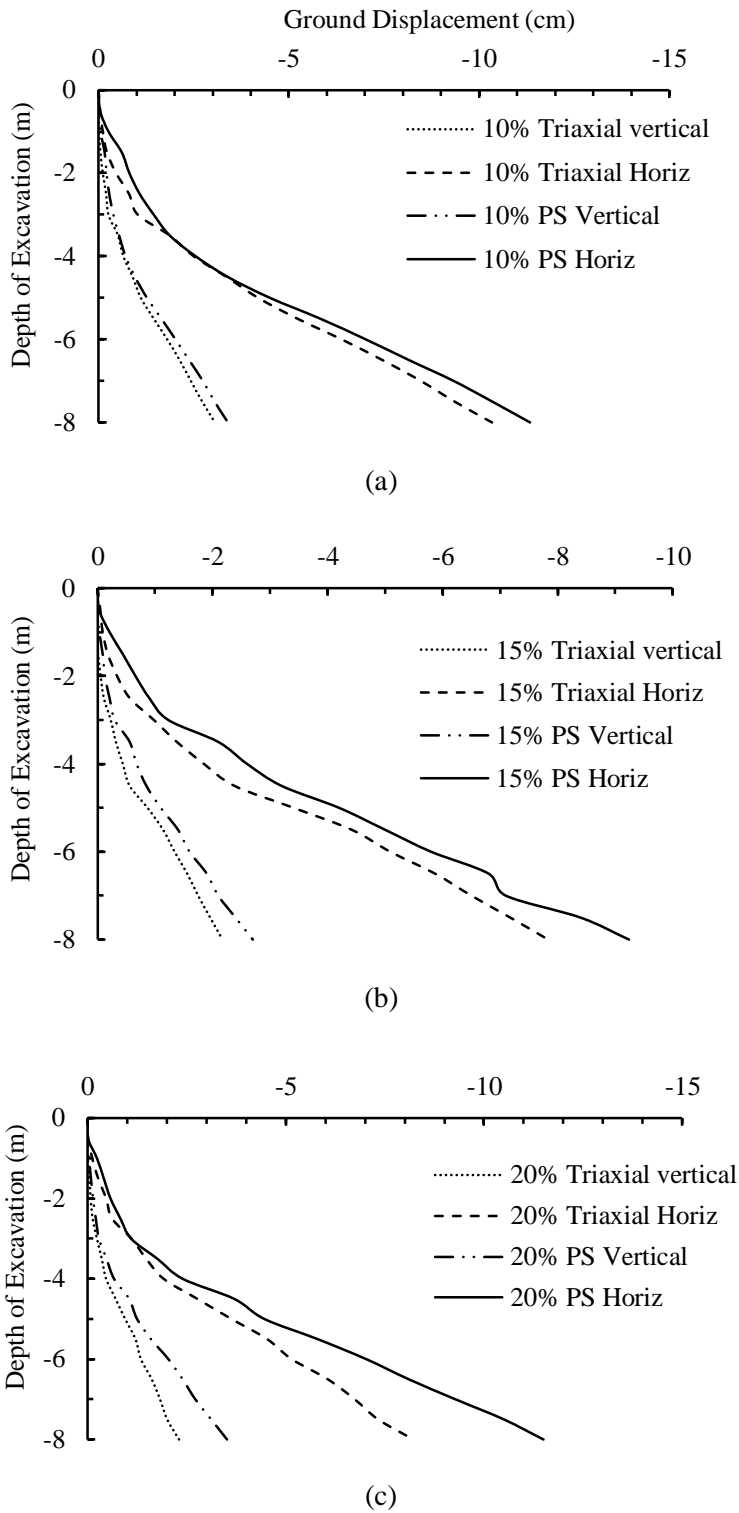
Figure 7.11 Wall displacements for plane strain and triaxial input properties of cement contents (a) 10% (b) 15% and (c) 20%.

Table 7.3 Ground movements for different input properties of improved layer

Cement Content (%)	Horizontal Movements (cm)			Vertical Settlement (cm)		
	Triaxial	PS	Difference (%)	Triaxial	PS	Difference (%)
10	-10.3	-11.3	10	-3.1	-3.4	11
15	-7.8	-9.2	18	-2.2	-2.7	24
20	-8.2	-11.5	40	-2.3	-3.5	52

7.2.3 Discussion

The above exercise helped in understanding the importance of providing the right input properties for the improved layer in a stabilized excavation problem. For a plane strain excavation problem, it is more realistic to input plane strain properties for the cement treated layer. Since, cement treated clays recorded higher strength under triaxial testing compared to plane strain testing, the lateral wall deflection was greatly under-predicted, with the input of triaxial properties. It is also worth mentioning that lateral wall deflections contributed heavily to other ground movements. In other words, use of plane strain input properties resulted in higher ground movements in the backfill side. Hence, careful use of input properties is essential to predict the actual performance of the system and to avoid catastrophes.
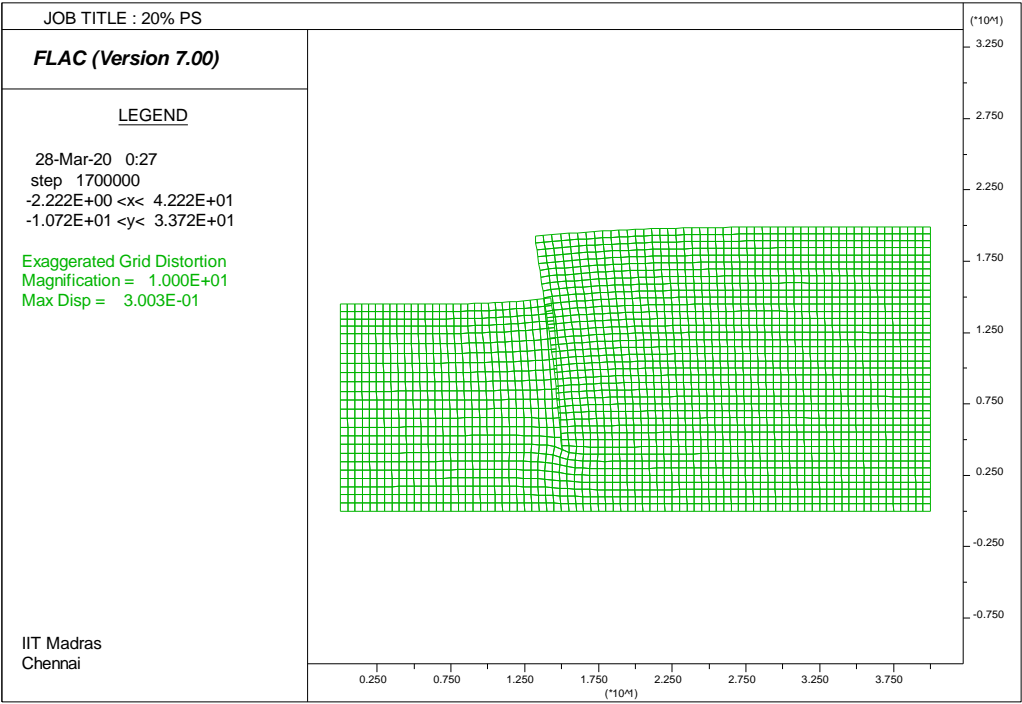
(a)
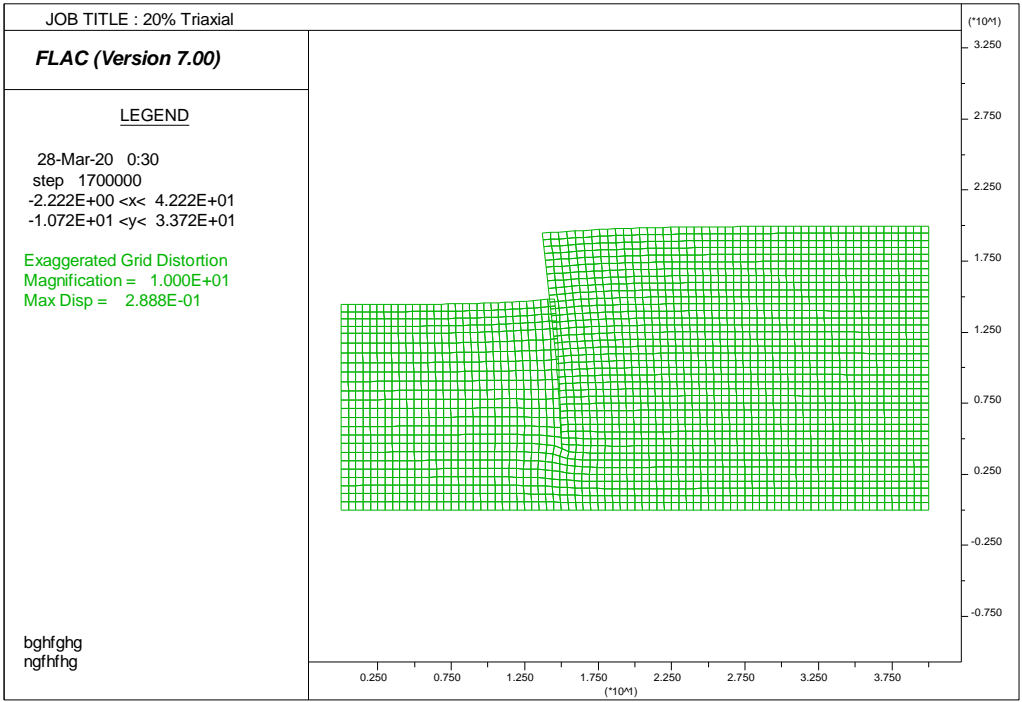
(b)

Figure 7.12 Deformed mesh at the end of final excavation stage for (a) Plane strain and (b) Triaxial properties.

7.3 CASE STUDY – 2: MRRB EXCAVATION PROJECT, TAIWAN

The first case study illustrated the differences in wall and ground responses for a shallow excavation problem with the input of plane strain and triaxial properties. This case study attempts to bring out the differences in response in case of a deep excavation. For this, a real field excavation problem, MR Residential Building (MRRB) project in Taiwan, was selected. Details regarding this excavation problem are available in Hsieh et al. (2003) and are briefly described below.

MR Residential Building (MRRB) is a 35 storey building with six levels of basement. It is located in a densely populated city in Taiwan. The project site was at a distance ranging from 0.2 to 12 m from the existing buildings. Piezometer readings indicated that groundwater table was available at a depth of 3.1 to 3.3 m below the ground level. The depth of excavation required for the basement was 22.3 m. A concrete diaphragm wall of 1 m thickness, extending down to a depth of 36 m was used as the retaining wall for excavation. In addition, 7 levels of temporary internal bracings in the form of horizontal struts were used to strengthen the retaining system. The struts were H steel sections and were pre-stressed after each stage of excavation. The horizontal spacing between the rows of struts was 6.5 m. The plan layout of the project and the proposed bracing systems is shown in Figure 7.13. The profile of horizontal struts is shown in Figure 7.14.

The excavation was carried out in the following sequence:

1. Excavation up to GL – 3.05 m; installation and preloading of 1st level of strut
2. Excavation up to GL - 7.30 m; installation and preloading of 2nd level of strut
3. Excavation up to GL – 11.10 m; installation and preloading of 3rd level of strut
4. Excavation up to GL – 13.20 m; installation and preloading of 4th level of strut
5. Excavation up to GL – 15.20 m; installation and preloading of 5th level of strut
6. Excavation up to GL – 17.90 m; installation and preloading of 6th level of strut
7. Excavation up to GL – 20.50 m; installation and preloading of 7th level of strut
8. Final excavation up to GL – 22.30 m.
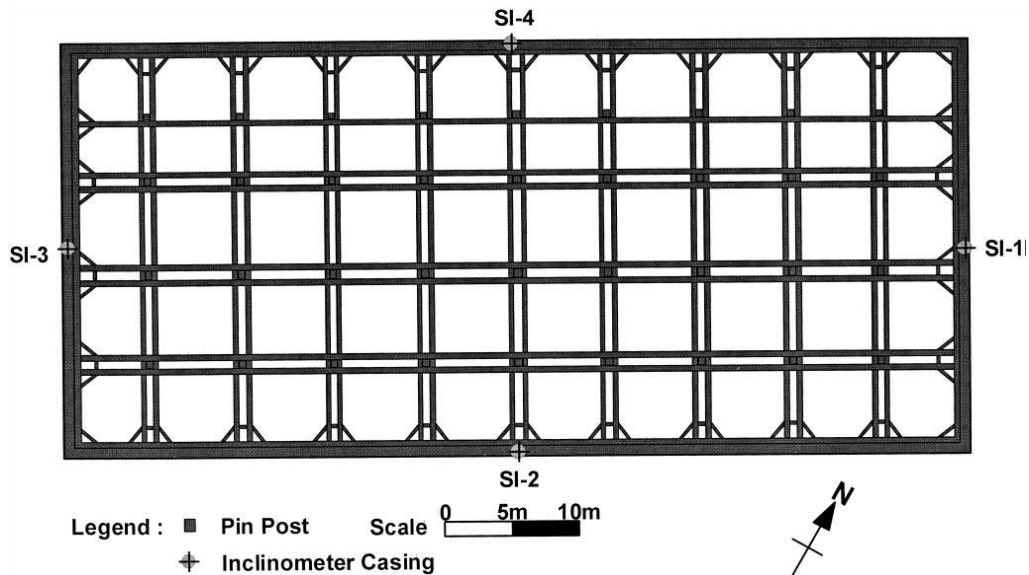
Figure 7.13 Plan layout of MRRB Project (Hsieh et al., 2003)

For carrying out the basement excavation, the project owner, consulting engineers and contractors came to an agreement that protective measures should be taken to prevent damage to adjacent buildings. As mentioned earlier, the lateral displacement of retaining wall is the most crucial parameter to be put under check, to limit the excavation induced ground movements. After considering various possibilities, it was agreed that soil beneath the final formation level of excavation was proposed to be improved by jet grouted columns, as shown in Figure 7.15 (a). As seen in the figure, 6 m of soil (GL – 21.0 to – 27.0) was improved using jet grouted columns. Each jet grout column was 0.6 m in diameter and was spaced at 2 m intervals (centre to centre). The improved layer now has jet grouted columns surrounded by untreated layer. This can be considered as a composite layer, with different properties for individual materials.

Strut (Level 1)
← Preload = 1470kN , GL. -2.20m   Stage 1
GL. -3.05m

Strut (Level 2)
← Preload = 1960kN , GL. -6.45m   Stage 2
GL. -7.30m

Strut (Level 3)
← Preload = 2350kN , GL. -10.25m   Stage 3
GL. -11.10m
Strut (Level 4)
← Preload = 2350kN , GL. -12.35m   Stage 4
GL. -13.20m
Strut (Level 5)
← Preload = 2350kN , GL. -14.35m   Stage 5
GL. -15.20m

Strut (Level 6)
← Preload = 2350kN , GL. -17.05m   Stage 6
GL. -17.90m
Strut (Level 7)
← Preload = 2350kN , GL. -19.65m   Stage 7
GL. -20.50m
Stage 8
GL. -22.30m

Figure 7.14 Profile of horizontal struts (Hsieh et al., 2003)

In order to simplify the analysis procedure, equivalent shear strength parameters were determined for the composite layer using equation (7.1), as proposed by Hsieh et al. (1995). In other words, this composite layer was converted into an equivalent improved layer, as shown in Figure 7.15 (b), and this layer will have a single set of equivalent shear strength properties.

$$c_{\text{eqv}} = c_{\text{org}} (1\text{-}I_r) + \alpha_c \, c_{JGP} \, I_r \qquad (7.1)$$

where, c_{eqv} = equivalent cohesion of improved soil mass; c_{org} = cohesion of untreated soil; I_r = improvement ratio, defined as the ratio of treated area to the total area; α_c = an empirical factor often taken as 0.5 (Hsieh et al., 1991); c_{JGP} = one half the unconfined compressive strength of jet grouted pile.

In this case, the improvement ratio was only 7% and was found to be sufficient for this problem. Similar approach was adopted by Ou et al. (1996) to analyse a composite layer with deep cement mixed columns in soft clay. It was also reported that the equivalent layer can then be analysed under plane strain condition, with reasonable accuracy. This was discussed in detail in Chapter 2. The details pertaining to soil profile and strut properties are given in Tables 7.4 and 7.5, respectively.

In Table 7.4, two sets of properties, separated by '/', are given for the depth 21 to 27 m. The properties pertaining to the improved layer are represented by superscript 'a' and are to be used in the excavation zone. The other set of properties should be used in the backfill zone. The lateral displacement of diaphragm wall was the main concern for this excavation problem. It was measured using inclinometers placed at various locations on the diaphragm wall, as shown in Figure 7.13. Inclinometers, SI-1 and SI-3 are placed on the shorter side of the excavation and would be of interest for a plane strain numerical analysis. SI-2 and SI-4 recorded the lateral displacements of diaphragm wall along the longer side of excavation.
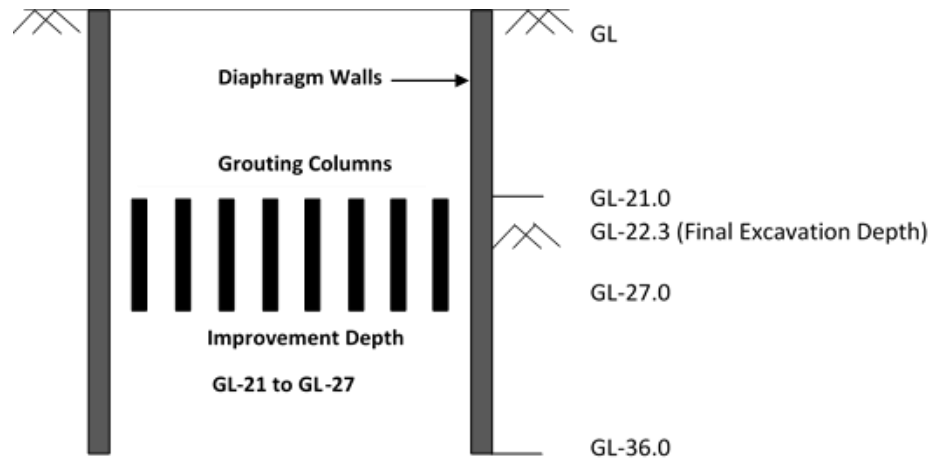
(a)
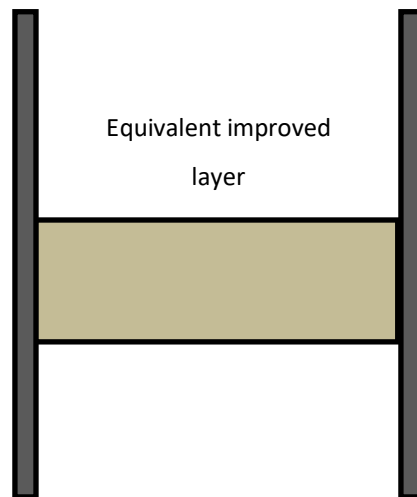
(b)

Figure 7.15 Schematic of (a) Proposed soil improvement scheme (b) Equivalent improved

layer for numerical analysis (Hsieh et al., 2003)

Table 7.4 Soil profile and soil properties for numerical analysis (Hsieh et al., 2003)

Soil layer (m)	Soil Type	γ (kN/m^3)	E (kPa)	μ	S_u (kPa)	ϕ (degree)
0 - 11.1	SM	19.2	5,270	0.3	0	29
11.1 – 12.4	CL	18.7	24,200	0.48	40	0
12.4 – 21.0	SM	18.9	12,000	0.3	0	28
21.0 – 27.0	CL	19.2	48,700/78,000[a]	0.48	82/130[a]	0
27.0 – 30.5	CL	19.2	59,400	0.48	100	0
30.5 – 44.7	CL	18.8	96,000	0.48	160	0
44.7 – 57.0	CL	19.0	130,000	0.48	215	0

[a] Parameters of improved soil

Table 7.5 Details of horizontal struts (Hsieh et al., 2003)

Strut level	Dimensions (mm)	Area (cm^2)	Installation depth (m)	Preload (kN)
1	2H350x350x12x19	347.8	GL – 2.20	1470
2	2H400x400x13x21	437.4	GL – 6.45	1960
3	2H400x400x13x21	437.4	GL – 10.25	2350
4	2H400x400x13x21	437.4	GL – 12.35	2350
5	2H400x400x13x21	437.4	GL – 14.35	2350
6	2H400x400x13x21	437.4	GL – 17.05	2350
7	2H400x400x13x21	437.4	GL – 19.65	2350

7.3.1 Numerical Simulation of Case Study-2

The excavation problem discussed in Hsieh et al. (2003) was simulated using a finite difference software, *FLAC* (version 7, 2011). The methodology and sequence of modelling discussed in section 7.2.1 was followed in this problem. It is to be noted that groundwater table and horizontal struts were not present in the previous case study. However, this problem considers them both. The numerical model grid for any excavation problem should be decided based on the anticipated influence of the surrounding area. A settlement trough which extends outwards by 3 to 4 times the excavation depth, should be anticipated (Woo and Moh, 1990). In other words, the excavation procedure might affect the buildings situated within a radius of around 70 to 90 m from the excavation site. Hence, the grid was developed such that it extends to 90 m beyond the diaphragm wall, in the backfill side. The developed grid for this problem is shown in Figure 7.17.

Only half of the excavation was considered, taking advantage of symmetry in geometry. As seen in the figure, the size of each individual grid was selected as 1 m^2. Hence, 1 x 1 m^2 was selected as the mesh size to save computational time and effort. The decimals in the soil profile and excavation depths were rounded off to the nearest integer for simplicity. Mesh sensitivity analysis was performed by varying the mesh size from 1 x 1 m^2 to 0.1 x 0.1 m^2. The differences in lateral wall deflections were found to be within 4 to 5%. The total model grid was 99 m wide and 57 m deep. The soil profile was available for a depth of 57 m and hence, this depth was selected. The width of excavation was calculated from Figure 7.15 (a). The typical boundary conditions used for an excavation problem were provided for this problem. The left and right boundaries were fixed for horizontal movement, the bottom boundary was fixed for both vertical and horizontal movements and the top was completely free to move. The soil properties for each depth were assigned as per Table 7.4. Different colours represent individual soil properties in the soil profile. Groundwater table was assigned at 3 m below the ground level. The diaphragm wall was also assigned during grid generation and the properties were assigned. Diaphragm wall was input as a beam element with a flexural stiffness of 1,151,000 kN-m^2. However, density of diaphragm wall was assigned only in the next stage. This facilitates equilibration of stresses upon the installation of diaphragm wall.

Once the diaphragm wall was installed, the next step was to lower the groundwater table. For simplicity, the groundwater table was instantly lowered from 3 m below ground level to 2 m below the proposed final excavation level (i.e. 29 m below GL). This method was adopted because no data pertaining to lowering of water table was available in Hsieh et al. (2003). Moreover, the settlements induced by lowering of water table were not substantial on the field and hence, was neglected for calculation of excavation induced wall displacements.
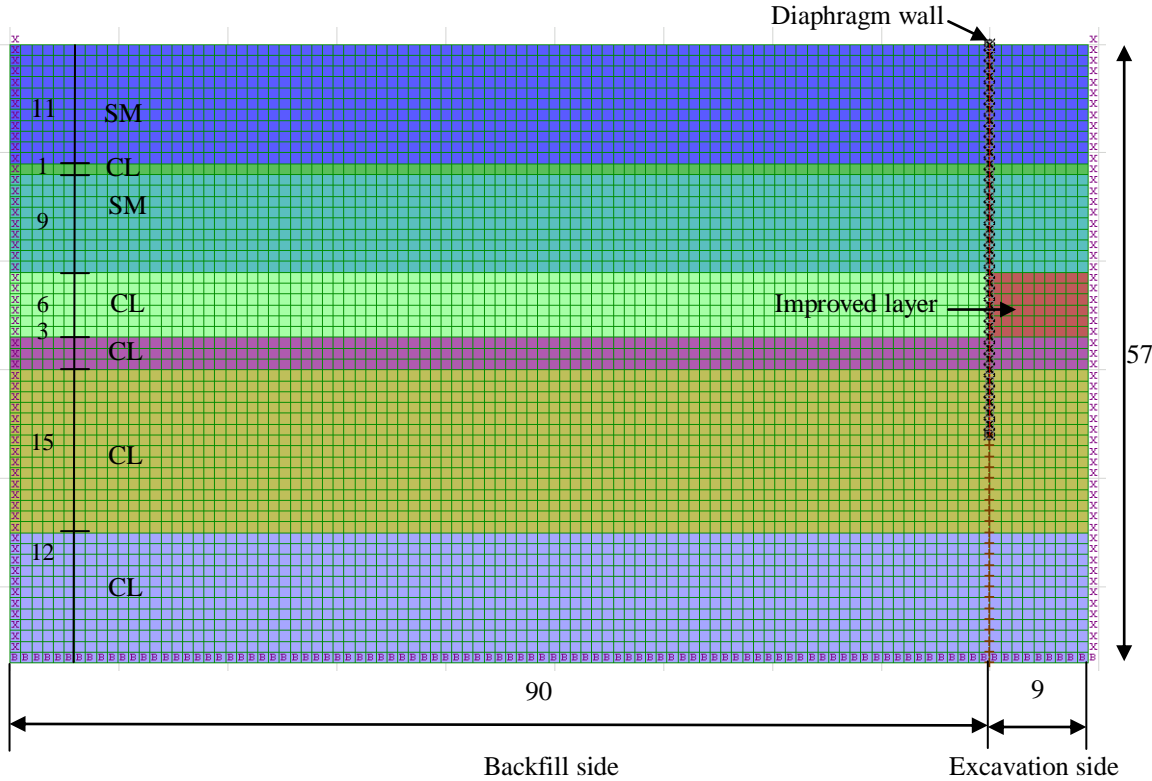
Figure 7.16 Numerical model grid for simulation of case study-2 (All dimensions are in m).

The first stage of excavation was then carried out and equilibrium was established. Excavation was simulated by assigning null model to the required zone. In the next stage, first horizontal strut was installed, and preloading was applied. The strut properties and magnitude of preload

was provided as per Table 7.5. The sequence of excavation mentioned in the previous section was followed for further excavations. This was continued till the final formation level was reached. At every excavation stage, the lateral displacement of retaining wall was measured at each node of the diaphragm wall. The diaphragm wall was assigned with a node at each 1 m depth of the wall. Hence, the wall had 36 nodes along its depth. The field data is available only for the last three stages of excavation. The simulation results were compared with these field results to check for the efficiency of this model. As mentioned previously, inclinometers SI-1 and SI-3 are of interest for plane strain problems. These readings were digitised from the field results and were compared with the results obtained through simulation, as shown in Figure 7.17.

A very good match was obtained between the field results and simulated results for the last three stages of excavation. Stage 8 refers to the final excavation level. The positive values of wall displacement show that the wall moves into the excavation side, as the case should be. Hence, this numerical model was efficient and could effectively simulate the excavation problem described in Hsieh et al. (2003).

7.3.2 Parametric Studies on Case Study-2

As discussed in section 7.2.2, the properties of the improved layer used in Hsieh et al. (2003) were replaced with the plane strain properties obtained for different cement contents and the wall displacements were evaluated. Hoek-Brown model was used for this layer, as demonstrated in Chapter 6. To illustrate the importance of using plane strain properties for the improved layer, the wall displacements were also evaluated with the input of triaxial properties for the improved layer and both the responses were compared. Apart from the input properties of the improved layer, every other parameter and the adopted numerical procedure remained unchanged.

181
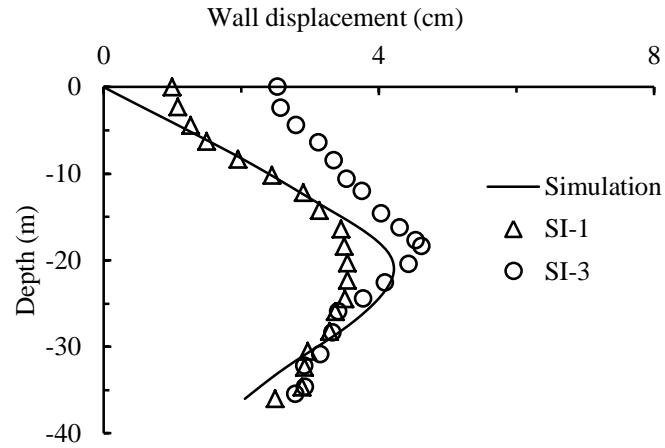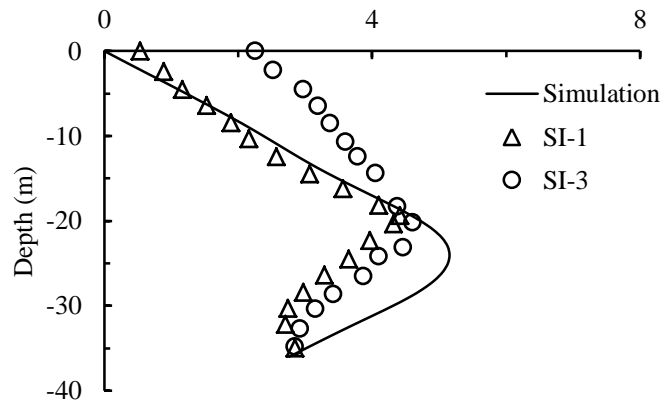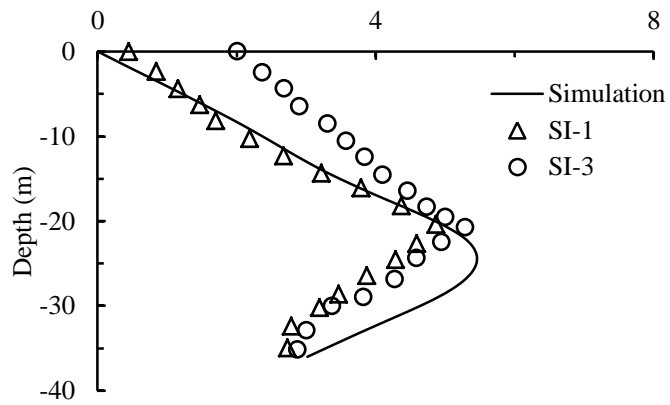
Figure 7.17 Comparison of simulation results with field results for (a) Stage 6 (b) Stage 7 and
(c) Stage 8.

Wall Response

A comparison of the lateral deflections of retaining wall at the final stage of excavation, with the input of plane strain and triaxial properties for the improved layer, is shown in Figure 7.18. Positive values of wall deflections indicate that the wall deflects towards the excavation side. This can be understood from Figure 7.16. As seen in Figure 7.18, prominent differences were obtained in the lateral deflections of diaphragm wall, for the inputs of plane strain and triaxial properties. Compared to the wall deflections obtained with plane strain input properties, triaxial input properties were found to under-predict the lateral wall deflections by 16%, 23% and 61% for cement contents of 10%, 15% and 20%, respectively. This is obviously because of higher strength recorded by cement treated clay under triaxial condition. Moreover, the responses obtained in Figure 7.18 are in line with the responses obtained for the shallow excavation problem, discussed as case study-1 (Figure 7.9). However, the differences in lateral wall deflections under the two input properties were 15%, 13% and 29%, for a shallow excavation of 8 m. Hence, the differences have significantly increased in case of a deep excavation problem. Furthermore, the differences are higher for higher cement contents, the highest for 20% cement content. This may be attributed to the fact that the difference in strength under plane strain and triaxial conditions was the highest in case of 20% cement content.

The variations of maximum bending moment values with excavation depth for different cement contents, with the input of plane strain and triaxial properties, are shown in Figure 7.19. The negative signs of bending moment and depth indicates values in the negative x and y directions, respectively. It may be noted that the unusual variation in bending moment could be due to the presence of horizontal struts at different levels of excavation depth. On the other hand, the variation was more or less linear for the un-strutted excavation considered in case study-1 (Figure 7.10). While, maximum bending moment was observed to be towards the excavation side in case study-1 (Figure 7.8), the same was observed towards the backfill side in this study. This could be also due to the horizontal force imposed on the diaphragm wall by the horizontal struts.

183
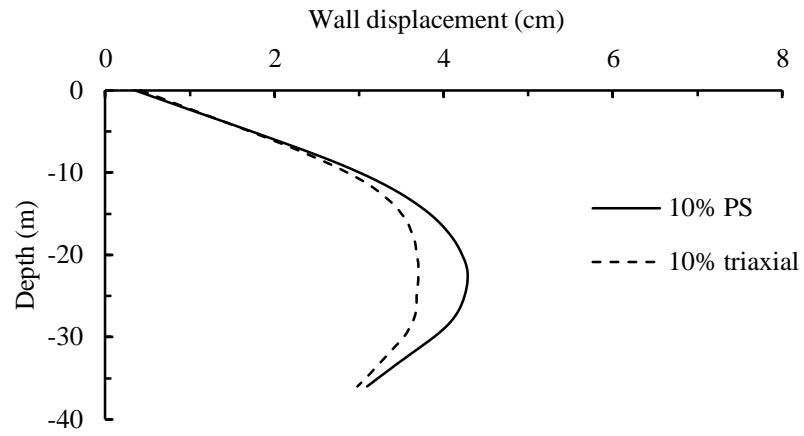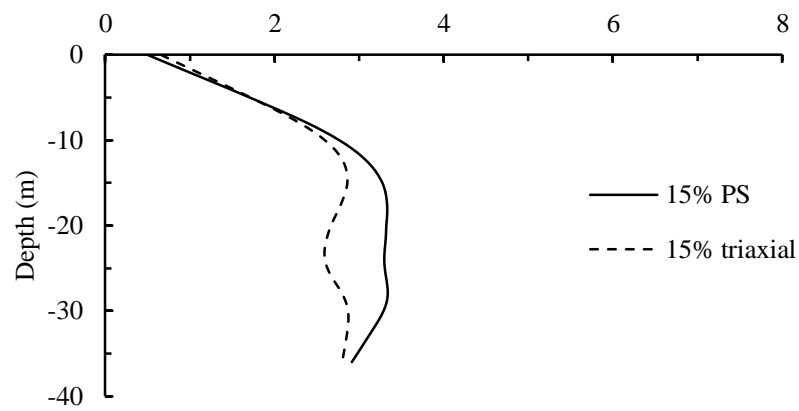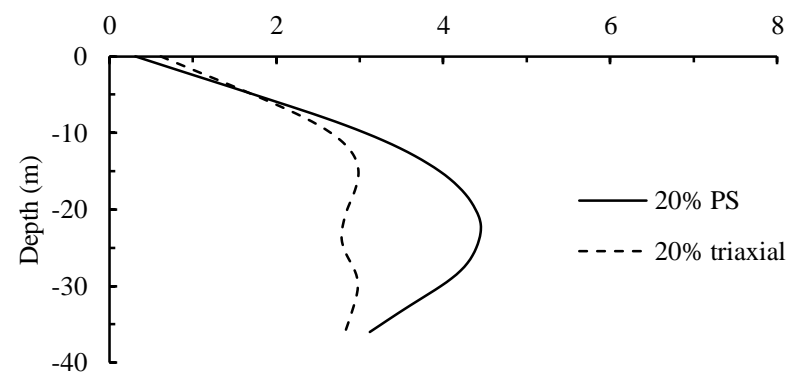
Figure 7.18 Comparison of lateral wall deflections with the input of plane strain and triaxial properties for the improved layer of cement contents (a) 10% (b) 15% and (c) 20%.

The differences in maximum bending moments were found to be negligible under the two conditions for cement contents of 10% and 15%. However, lower bending moments were recorded under plane strain condition. The maximum bending moment values at the end of final excavation stage are given in Table 7.6. The difference in bending moments, in case of 20% cement content, was as high as 21%. In other words, use of triaxial input properties in case of deep excavations could lead to over-design of retaining wall.

Table 7.6 Maximum bending moment values for different input properties of improved layer

Cement Content (%)	Maximum Bending Moment $\times 10^5$ (N-m)		
	Triaxial Input Properties	Plane Strain Input Properties	% Difference in Bending Moment (%)
10	-4.5	-4.25	6
15	-5.24	-4.76	10
20	-5.15	-4.26	21

Ground Response

Ground movements observed were found to be negligible, for both triaxial and plane strain input properties. The maximum ground settlement observed did not exceed 1 cm in any of the cases, when the final excavation was reached. This could be due to the provision of strong horizontal struts after every excavation level.

Bending Moment *10^5 (N-m)
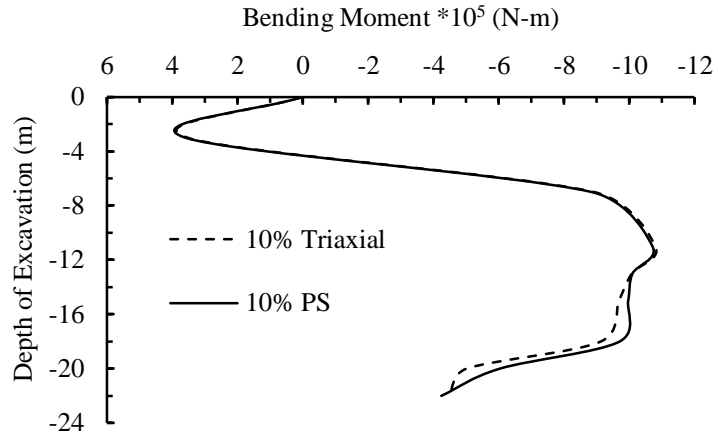
(a)
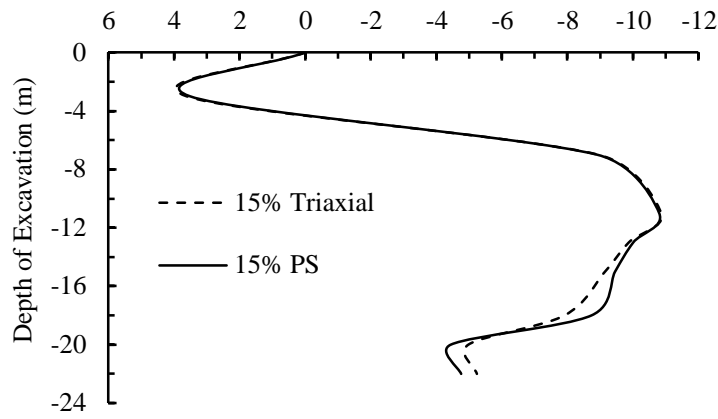
(b)
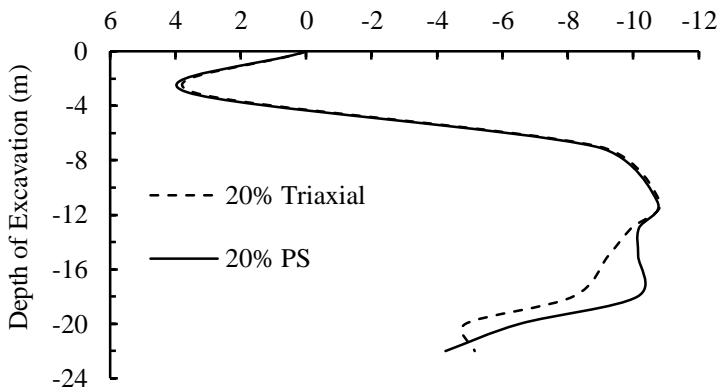
(c)

Figure 7.19 Bending Moment profiles of retaining wall for cement contents of (a) 10% (b) 15% and (c) 20%.

Moreover, the displacements recorded for both the input properties were similar. Hence, for strutted excavations, the ground movements are taken care of by the struts and are not influenced by the input parameters

7.3.3 Discussion

From the analysis of a deep excavation problem, it could be concluded that the lateral wall deflection is significantly under-predicted with the use of triaxial input properties. The difference in wall deflection for 20% cement content was as high as 61%. The bending moments were also higher with the use of triaxial input properties. The differences in maximum bending moments for triaxial and plane strain input parameters were negligible for 10% and 15% cement contents. However, the difference was around 21% for 20% cement content. In other words, since the difference in strength under plane strain and triaxial conditions were the highest for 20% cement content, the highest difference in lateral wall deflection and wall bending moment were recorded in this case. Therefore, input properties should be selected based on the field condition. However, the provision of struts took care of ground movements in vertical and horizontal directions. Only a maximum displacement of 1 cm was recorded for all the cases and the results were very close with the use of both triaxial and plane strain input properties.

7.4 SUMMARY

From the analysis of two case studies described above, the following findings were established.

1. Since, the cement treated layer in an excavation problem is under plane strain condition, the input properties obtained from plane strain testing would best represent the field condition.

2. The use of input properties obtained from triaxial (axisymmetric) testing resulted in under-prediction of lateral wall deflection. The highest difference under the two input properties was obtained for the highest cement content (20%). This is because of the highest strength difference observed between the triaxial and plane strain testing conditions, at this cement content

3. The differences in lateral wall deflection under the two input parameters were significantly increased with increase in depth of excavation. While, the maximum difference in lateral wall deflection was 36% for shallow excavation problem, the same was found to be around 61% for the deep excavation problem.

4. Ground movements in vertical and horizontal directions in the backfill side were higher with the input of plane strain properties. In other words, the use of triaxial input properties under-predicted the ground movements. Difference in ground settlements of around 52% was observed at a cement content of 20%. However, it is to be noted that the provision of bracings in the form of horizontal struts reduced the ground movements. No significant differences were observed with the two input properties in this case.

5. The maximum bending moment experienced by the retaining wall was found to be lower, with the input of plane strain properties. This could be due to higher deflections recorded under plane strain input properties. However, the difference was not significant (a maximum of 12%) for the shallow excavation problem. On the other hand, the difference in bending moment was found to around 21% for 20% cement content, in case of deep excavation problem. Hence, over-design of retaining wall is possible with the use of triaxial input properties.

CHAPTER 8

SUMMARY AND CONCLUSIONS

8.1 SUMMARY

Soft clays possess characteristics like low bearing capacity, high compressibility and low shear strength. When excavations are carried out in such soils, the retaining walls undergo large lateral deflections and associated ground movements. In some cases, soft clay exists up to large depths and retaining walls cannot be taken down to the hard stratum. In such situations, the retaining wall floats in soft clay and undergoes maximum deflection beneath the final formation level. The horizontal bracings in the form of struts can be provided only above the final formation level. Improving the soft clay beneath the final formation level by cement treatment, using techniques like deep mixing or jet grouting, have been proven to be efficient in controlling the lateral wall deflection below the final excavation level. Cement stabilization below the proposed final excavation level is usually carried out prior to the commencement of excavation procedures. Hence, the stabilized layer acts as a horizontal strut from the beginning of excavation. Stabilization is generally performed from wall to wall, covering the entire plan area of excavation, resulting in the formation of a soil-cement slab beneath the final excavation level. Such an improved layer is called embedded improved soil strut.

In practice, most of the excavation problems are analysed as plane strain problems, since one of the dimensions is usually very large compared to the other dimensions. Hence, the embedded improved soil strut, which exists along the entire plan area of excavation, can also be analysed using two-dimensional plane strain analysis. For such an analysis, it is desirable to obtain the input properties under the same testing conditions. In other words, the properties of cement treated clay under plane strain testing conditions should ideally be used for numerical analysis, to obtain realistic results. The common practice is to use the properties obtained by performing unconfined compression strength tests or triaxial tests in the laboratory. However, these tests are performed using axisymmetric specimens. The behaviour of cement treated clay under plane

strain condition has not been explored in the literature. However, there are ample studies to show that natural soil behaves differently under plane strain and triaxial conditions. Hence, one can expect a different behaviour in case of cement treated clays too.

Hence, one of the main objectives of this study was to compare the shear behaviour of cement treated clay under triaxial and plane strain testing conditions. A plane strain apparatus was developed as a part of this study. Tests were performed on specimens prepared at cement contents of 10%, 15% and 20%. The cement treated clay specimens were prepared after determining the optimum value of remoulding water content, which was found to be 1.20 times the liquid limit of base clay. Cement was added in slurry form at a water-cement ratio of 0.6, as used in the literature. The plane strain and triaxial responses of cement treated clay were studied at confining pressures of 50 kPa, 100 kPa, 200 kPa and 400 kPa. For both drained and undrained tests, plane strain specimens recorded lower peak deviator stress values compared to triaxial specimens, when tested under identical testing conditions. This trend was followed for all cement contents and confining pressures. In other words, cement treated clay exhibits lower strength under plane strain condition. Hence, for the numerical analysis of the excavation problem described above, the input properties from plane strain testing of cement treated clay would be ideal. Moreover, 15% cement content was found to be the optimum cement content, as it recorded a higher strength than 20% cement content under both triaxial and plane strain testing conditions.

For efficient numerical analysis of the above excavation problem, the right constitutive model needs to be selected for the cement treated soil layer. A simple constitutive model which could represent the behaviour of cement treated clay is still missing in the literature. The advanced effective stress models available in the literature are quite complicated to comprehend and implement. Moreover, cement treated clay exhibits non-linear behaviour. Hence, a simple non-linear constitutive model is to be identified. For this, non-linear failure envelopes were established for cement treated clay of different cement contents, using the drained and undrained experimental data. Interestingly, both drained and undrained test results obtained at different confining pressures, were found to lie on a single non-linear failure envelope, for all cement contents on a t' versus s' stress path system [$(\sigma_1' - \sigma_3')/2$ versus $(\sigma_1' + \sigma_3')/2$). Failure envelopes

were established both for triaxial and plane strain test data (as discussed in Chapter 5). Non-linear Hoek-Brown model could then be successfully employed to represent these failure envelopes. Hoek-Brown material parameters were deduced for each cement content and mode of testing, using non-linear regression analysis. This Hoek-Brown model along with the associated material parameters can be directly implemented into a numerical platform, to serve as a constitutive framework for cement treated clay. The validity of these failure envelopes were verified by back analysis of the corresponding experimental data.

Another objective of this study was to demonstrate the effect of input properties of the improved layer on the performance of an excavation stabilized by cement treatment. In other words, it was attempted to bring out the differences in the performance of excavation, upon the input of triaxial or plane strain properties for cement treated layer. For this, two excavation problems were selected from the literature, where cement treatment below the final excavation level was employed. One was a shallow un-strutted excavation of 6 m depth, which was considered as part of a centrifuge study carried out at National University of Singapore (NUS), Singapore. The other was a six level basement excavation which was carried out as part of MR Residential project in Taiwan. In both these problems, the effect of soil stabilization below the final excavation level on the lateral deflection of retaining wall was focussed. These excavation problems were first validated using a finite difference program, *FLAC*. Close match was observed between the simulated and reported results. The properties of improved layer were now replaced with triaxial and plane strain properties obtained for cement treated clay, in this study. These properties were input using the Hoek-Brown constitutive model and the corresponding material parameters. Comparing the response of wall deflections under triaxial and plane strain input properties, it was found that triaxial input properties under-predicted the lateral deflections of retaining wall. Lesser ground movements were also recorded with the use of triaxial input properties, for the un-strutted excavation. However, the use of struts in the deep excavation resulted in comparable ground movements in both the cases. Moreover, the ground movements were found to be minimal with the use of struts. Furthermore, the use of triaxial input properties was found to over-predict the bending moment response of diaphragm wall. Hence, the input properties of cement treated clay beneath the final excavation level of an excavation should be carefully selected based on the field condition.

8.2 CONCLUSIONS

Some important conclusions drawn from the current study are listed below:

- The water present in clay just before the addition of cement, called remoulding water content, plays a major role in strength development of cement treated clay. For the clay considered in this study, the maximum strength upon cementation was achieved at an optimum remoulding water content of 1.20 times the liquid limit of base clay.

- Cement treated clay was found to behave differently under plane strain and triaxial testing conditions. It exhibited lower peak deviator stress under plane strain testing condition. The undrained strength under triaxial condition was found to be 1.1 to 1.3 times the strength under plane strain condition. This is due to the inherent over-consolidated nature of cement treated clay. Literature suggests that over-consolidated clays exhibit a similar trend.

- The highest difference in strength under plane strain and triaxial testing condition was exhibited by specimens prepared at 20% cement content. For testing conducted at confining pressures ranging from 50 kPa to 400 kPa, the difference in peak deviator stress ranged from 7% to 29%, respectively, under undrained testing. However, under drained condition, it ranged from 60% to 3%, respectively. In other words, the difference in undrained strengths increases with increase in confining pressure and the difference in drained strengths diminishes with increase in confining pressure.

- However, the strains at which the peak deviator stress was achieved was found to be comparable under both plane strain and triaxial testing conditions. Furthermore, similar values of excess pore water pressures and volumetric strains were recorded under the two testing conditions at a certain confining pressure. Therefore, these are inherent properties of cement treated clay which depend on confining pressure and not on testing condition.

- Among the three cement contents considered in this study, viz., 10%, 15% and 20%, cement content of 15% was found to be the optimum cement content. Slightly higher strength was observed for this cement content compared to 20% cement content, at all confining pressures and drainage conditions, under both triaxial and plane strain testing

conditions. Unconfined compressive strength (UCS) testing recorded comparable UCS values for 15% and 20% cement contents. Literature suggests that strength increment in clay upon adding cement can be classified into three zones, viz. active, inert and deterioration zone. While strength keeps on increasing with increase in cement in active zone, strength increase is negligible in inert zone and strength decreases in deterioration zone. Hence, addition of cement beyond 15% cement content could be pushing the clay into inert or deterioration zone.

- When drained and undrained test results were presented together on a single t' versus s' stress path system, a single non-linear failure envelope was found to exist encompassing both drained and undrained test results. The use of generalised Hoek-Brown theory was successful in representing these failure envelopes under both triaxial and plane strain testing conditions. Hoek-Brown material parameters were established through non-linear regression analysis. The Hoek-Brown constitutive model along with the associated material parameters, served as a good constitutive framework, to represent the cement treated clay prepared at different cement contents. Failure envelopes were established for both triaxial and plane strain conditions.

- Using the Hoek-Brown framework, the experimental results could be back-analysed to reasonable accuracy. However, the model failed to predict the post-peak response of cement treated clay in many cases. It may be noted that, the peak deviator stress forms the main focus in most of the field problems and hence, this limitation may be overlooked.

- For the numerical analyses of excavations stabilized by cement treatment at the base, the improved layers could be successfully represented using the Hoek-Brown framework.

- Upon performing parametric studies on a shallow un-strutted excavation of depth 8 m and a deep strutted excavation of depth 22 m, the use of triaxial input properties was found to under-predict the lateral deflection of retaining wall. While the maximum difference in lateral wall deflection under the two input properties was about 36% for the shallow excavation problem, the difference was found to be about 61% for the deep excavation problem. It may be recalled that higher strength was observed under triaxial condition compared to plane strain condition, and hence, this trend is justified.

194

- The highest differences in wall response and ground movements, with triaxial and plane strain input properties, were exhibited at a cement content of 20% for both the excavation problems. This is due to the fact that the highest difference in strength under plane strain and triaxial testing conditions was exhibited at this cement content.

- For the un-strutted excavation problem, the ground movements due to excavation procedures were found to be lesser, when triaxial input properties were used. This is clearly because of lesser deflections undergone by the wall with the use of triaxial input properties. The use of triaxial input properties were found to under-predict the ground settlement by about 52%, for a cement content of 20%. However, for deep strutted excavations, there was no difference in the ground movements under both the input properties. The use of struts also significantly reduced the overall ground movements.

- The use of triaxial input properties slightly over-predicted the bending moment response of the wall for both shallow and deep excavation problems. While the difference in maximum bending moment was only 12% under the different input properties, the difference increased to about 21% for the deep excavation. In other words, the use of triaxial properties may result in over-design of retaining wall.

To conclude, this study mainly intended to demonstrate the importance of using plane strain input properties for cement treated clay layer beneath the final formation level of excavations. The present study shows that the current practice of using input parameters from triaxial test leads to erroneous predictions of wall and ground responses. Hence, the input properties from plane strain testing would best represent the improved layer in excavation problems stabilized by cement treatment.

8.3 SCOPE FOR FUTURE STUDIES

Though extensive experimental and numerical studies were carried out in the present study, the following aspects may be investigated in future to strengthen this work.

- Detailed micro-structural studies may be conducted to throw more light on the rationale behind the optimum cement content and optimum remoulding water content.

- Slight discrepancies observed in the established failure envelopes could be avoided, if more tests were conducted at other confining pressures. Data points at closer intervals of confining pressures may result in a better fit of failure envelope.

- The current study focussed only on the plane strain properties of improved layer. Ideally, the properties assigned for the soil layers should also be under plane strain condition. Hence, a more realistic response may be obtained by assigning plane strain properties for both soil profile and the improved layer.

REFERENCES

1. **Ahnberg, H.** (2004). Effects of back pressure and strain rate used in triaxial testing of stabilized organic soils and clays. *Geotechnical testing journal*, 27(3): 250-259.

2. **Åhnberg, H. and Johansson, S.E.** (2005). Increase in strength with time in soils stabilised with different types of binder in relation to the type and amount of reaction products. *Deep Mixing*, 5, pp.195-202.

3. **Alshibli, K.A. and Akbas, I.S.** (2007) Strain localization in clay: plane strain versus triaxial loading conditions. *Geotech Geol Eng.,* 25:45–55.

4. **Alshibli, K.A. and Sture, S.** (2000). Shear band formation in plane strain experiments of sand. *J. Geotech. Geoenviron. Eng.,* 126 (6): 495-503.

5. **Alshibli, K.A., Batiste, S.N. and Sture, S.** (2003). Strain localization in sand: plane strain versus triaxial compression. *J. Geotech. Geoenviron. Eng.,* 129(6): 483-494

6. **Alshibli, K.A., Godbold, D.L. and Hoffman, K.** (2004). The Louisiana plane strain apparatus for soil testing. *Geotechnical Testing Journal*, 27(4), pp.337-346.

7. **Amini, Y. and Hamidi, A.** (2014). Triaxial shear behavior of a cement-treated sand–gravel mixture. *Journal of Rock Mechanics and Geotechnical Engineering*, 6(5), pp.455-465.

8. **Arroyo, M., Ciantia, M., Castellanza, R., Gens, A., and Nova, R.** (2012). Simulation of cement-improved clay structures with a bonded elasto-plastic model: A practical approach. *Computers and Geotechnics*, Vol. 45, pp. 140–150, DOI: https://doi.org/10.1016/j.compgeo.2012.05.008.

9. **Asghari, E., Toll, D.G. and Haeri, S.M.** (2003). Triaxial behaviour of a cemented gravely sand, Tehran alluvium. *Geotechnical & Geological Engineering*, 21(1), 1-28. 10.1061/9780784413388.008

10. **ASTM C496.** (2011). Standard test method for splitting tensile strength of cylindrical concrete specimens. ASTM International, West Conshohocken, PA, USA.

11. **ASTM D2487.** (2017). Standard Practice for Classification of Soils for Engineering Purposes (Unified Soil Classification System). ASTM International, West Conshohocken, PA, USA.

12. **ASTM D2584.** (2002). Standard test method for ignition loss of cured reinforced resins. Vol. 100, ASTM International, West Conshohocken, PA, USA.

13. **Baker, R.** (2004). Nonlinear Mohr envelopes based on triaxial data. *Journal of Geotechnical and Geoenvironmental Engineering*, 130(5), 498-506. 10.1061/(ASCE)1090-0241(2004)130:5(498)

14. **Baudet, B., and S. Stallebrass.** (2004). A Constitutive Model for Structured Clays. *Géotechnique*, 54 (4): 269–278.

15. **Bergado, D. T. and Lorenzo G. A.** (2005). Economical mixing method for cement deep mixing. *Proc. Innovations in Grouting and Soil Improvement,* pp 1-10, Geo-Frontiers Congress, Texas

16. **Bishop, A.W. and Henkel, D.J.** (1962). *The measurement of soil properties in the triaxial test*. Second Edition, Edward Arnold Publishers Limited, London, United Kingdom.

17. **Bruce, D.A.** (2000). An Introduction to Deep Soil Mixing Methods as used in Geotechnical Applications. (2000). *US Department of Transportation, Federal Highway Administration*, Vol. 1, FHWA-RD-99-138.

18. **Bruce, M. E. C., Berg, R. R., Collin, J. G., Filz, G. M., Terashi, M. and Yang, D. S.** (2013). *Federal Highway Administration design manual: deep mixing for embankment and foundation support* (No. FHWA-HRT-13-046).

19. **Bushra, I. and Robinson, R.G.** (2009). Consolidation behaviour of cement stabilised marine soil. *Indian Geotechnical Conference, 2009,* Guntur, India, pp.431 – 434

20. **Bushra, I., and Robinson, R. G.** (2012). Shear strength behavior of cement treated marine clay. *International Journal of Geotechnical Engineering*, Taylor & Francis, 6(4): 455-465.

21. **Campanella, R. G., and Vaid, Y. P.** (1974). Triaxial and plane strain creep rupture of an undisturbed clay. *Canadian Geotechnical Journal,* 11(1), 1-10.

22. **Chang, M. F., Teh, C. I., and Cao, L.** (1999). Critical state strength parameters of saturated clays from the modified Cam clay model. *Canadian Geotechnical Journal*, *36*(5), 876-890.

23. **Charles, J. A., and Soares, M. M.** (1984). Stability of compacted rockfill slopes. *Geotechnique*, 34(1), 61–70. 10.1680/geot.1984.34.1.61

24. **Charles, J. and Watts, K.** (1980). The influence of confining pressure on the shear strength of compacted rockfill. *Géotechnique*, 30(4), 353-367. 10.1680/geot.1980.30.4.353

25. **Chen, E.J., Liu, Y. and Lee, F.H.** (2016). A statistical model for the unconfined compressive strength of deep-mixed columns. *Géotechnique*, *66*(5), pp.351-365.

26. **Chew, S. H., Lee, F. H., Lee, Y. and Yogarajah, I.** (1997). Jet grouting in Singapore marine clay. *Proceedings of the 3rd young geotechnical engineers conference*, Singapore, pp. 231–238.

27. **Chew, S.H., Kamruzzaman, A.H.M. and Lee, F.H.** (2004). Physicochemical and engineering behaviour of cement treated clays. *Journal of geotechnical and geoenvironmental engineering*, 130(7), pp.696-706.

28. **Chiu, C.F., Zhu, W. and Zhang, C.L.** (2009). Yielding and shear behaviour of cement-treated dredged materials. *Engineering Geology*, 103(1-2), 1-12. 10.1016/j.enggeo.2008.07.007

29. **Clough, G. W., Sitar, N., Bachus, R. C., and Rad, N. S.** (1981). Cemented sands under static loading. *J. Geotech. Eng*., 1076, 799–817.

30. **Coastal Development Institute of Technology (CDIT).** (2002). The Deep Mixing Method: Principle, Design, and Construction. Balkema, Lisse, Netherlands.

31. **Collins, I. F., Gunn, C. I. M., Pender, M. J., and Wang, Y.** (1988). Slope stability analyses for materials with a nonlinear failure envelope. *Int. J. Numer. Analyt. Meth. Geomech.*, 12(5), 533–550. 10.1016/0148-9062(89)90302-1

32. **Consoli, N.C., Heineck, K.S., Casagrande, M.D.T. and Coop, M.R.** (2007). Shear strength behavior of fiber-reinforced sand considering triaxial tests under distinct stress paths. *Journal of geotechnical and geoenvironmental engineering*, ASCE, *133*(11), pp.1466-1469.

33. **Consoli, N.C., Cruz, R.C., Consoli, B.S. and Maghous, S.** (2012). Failure envelope of artificially cemented sand. *Géotechnique*, 62(6), 543-547. 10.1680/geot.11.p.037

34. **Cornforth, D. H.** (1964). Some experiments on the influence of strain conditions on the strength of sand. *Geotechnique,* 14(2), 143-167.

35. **Cundall, P.A. and Hart, R.D.** (1992). Numerical modeling of discontinua. *In Analysis and design methods*, pp. 231-243. Pergamon.

36. **Andrieux, P., Brummer, R., Detournay, C. and Hart, R.** (2003). A new constitutive model based on the Hoek-Brown criterion. In *FLAC and Numerical Modeling in Geomechanics 2003,* pp. 22-30, CRC Press.

37. **Das, B. M., Yen, S. C., and Dass, R. N.** (1995). Brazilian tensile strength test of lightly cemented sand. *Can. Geotech. J*., 32, 166–171.

38. **De Mello, V.B.F.** (1977). Reflections on design decisions of practical significance to embankment dams. *Geotechnique*, 27(3), 281-355. 10.1016/0148-9062(78)90872-0

39. **Desrues, J., Lanier, J., & Stutz, P.** (1985). Localization of the deformation in tests on sand sample. *Engineering fracture mechanics,* 21(4), 909-921.

40. **Dong, Y.P., Burd, H.J. and Houlsby, G.T.** (2016). Finite-element analysis of a deep excavation case history. *Géotechnique*, 66(1), pp.1-15.

41. **Drescher, A., Vardoulakis, I., and Han, C.** (1990). A Biaxial Apparatus for Testing Soils. *Geotechnical Testing Journal,* Vol. 13, No. 3, pp. 226-234

42. *Fast lagrangian analysis of continua (FLAC), version 7.0, user's manual.* (2011). Ithasca Consulting Group, Minneapolis.

43. **Fauziah, M. and Nikraz, H. R.** (2008). The behaviour of unsaturated compacted clay under plane strain condition. *In Geo-Environment and Landscape Evolution III, Proc., 3rd International Conference on Evolution, Monitoring, Simulation, Management and Remediation of the Geological Environment and Landscape*, vol. 100, 11177, WIT Press.

44. **Finno, R. J., Lawrence, S. A., Allawh, N. F. and Harahap, I. S.** (1991). Analysis of performance of pile groups adjacent to deep excavation. *Journal of Geotechnical Engineering,* 117(6), 934-955.

45. **Finno, R. J., Blackburn, J. T. and Roboski, J. F.** (2007). Three-dimensional effects for supported excavations in clay. *Journal of Geotechnical and Geoenvironmental Engineering,* 133(1), 30-36.

46. **Gaba, A. R.** (1990), Jet grout at Newton Station, Singapore, *10th Southeast Asian Geotechnical Conference,* Taipei.

47. **Gens, A., and R. Nova.** (1993). Conceptual Bases for a Constitutive Model for Bonded Soils and Weak Rocks. *Proceedings of the International Symposium on Hard Soils-Soft Rocks,* Vol. 1, edited by A.Anagnostopoulos, 485–494, Athens.

48. **Ghee, C.K.** (2006). *Constitutive behaviour of cement treated marine clay.* Doctoral dissertation, Department of Civil Engineering, National University of Singapore.

49. **Haibo, Y.** (2009). *Mobilised mass properties of embedded improved soil raft in an excavation*. Diss. PhD Thesis, Department of Civil Engineering, National University of Singapore.

50. **Hambly, E. C.** (1972). Plane strain behaviour of remoulded normally consolidated kaolin. *Geotechnique*, 22(2), 301-317.

51. **Han, C. and Drescher, A.** (1993). Shear bands in biaxial tests on dry coarse sand. *Soils and Foundations*, 33(1), pp.118-132.

52. **Han, J.** (2015). *Principles and practice of ground improvement*. John Wiley & Sons.

53. **Hashash, Y. M., and Whittle, A. J.** (1996). Ground movement prediction for deep excavations in soft clay. *Journal of Geotechnical Engineering,* 122(6), 474-486.

54. **Hashash, Y. M., Levasseur, S., Osouli, A., Finno, R. and Malecot, Y.** (2010). Comparison of two inverse analysis techniques for learning deep excavation response. *Computers and geotechnics,* 37(3), 323-333.

55. **Head, K.H.** (1986). *Manual of Soil Laboratory Testing*, Vol. 3, Pentech Press, London, UK.

56. **Ho, M. and Chan, C.** (2011). Some Mechanical Properties of Cement Stabilized Malaysian Soft Clay. *World Academy of Science, Engineering and Technology, International Journal of Civil, Environmental, Structural, Construction and Architectural Engineering,* Vol.5, No.2

57. **Hoek, E. and Brown, E.T.** (1997). Practical estimates of rock mass strength. *International journal of rock mechanics and mining sciences*, 34(8), pp. 1165-1186. https://doi.org/10.1016/S1365-1609(97)80069-X.

58. **Hoek, E. and Brown, E.** (2018). The Hoek–Brown failure criterion and GSI – 2018 edition. *Journal of Rock Mechanics and Geotechnical Engineering*, 11(3), 445-463. 10.1016/j.jrmge.2018.08.001.

59. **Hoek, E., and Brown, E. T.** (1980). Empirical strength criterion for rock masses. *Journal of Geotechnical and Geoenvironmental Engineering*, ASCE., 10.1016/0148-9062(81)90766-x/ 106: 15715.

60. **Holtz, R. D., Kovacs, W. D., and Sheahan, T. C.** (2015). *An Introduction to Geotechnical Engineering*. Second edition, Pearson India Education, Bengaluru, India.

61. **Horpibulsuk, S., Miura, N. and Nagaraj, T.S.** (2003). Assessment of strength development in cement-admixed high water content clays with Abrams' law as a basis. *Geotechnique*, 53(4), pp.439-444.

62. **Horpibulsuk, S., Miura, N. and Bergado, D. T.** (2004) Undrained shear behaviour of cement admixed clay at high water content. *J. Geotech. Geoenviron. Eng.,* 130(10), 1096-1105.

63. **Horpibulsuk, S., Miura, N. and Nagaraj, T.S.** (2005). Clay–water⁄cement ratio identity for cement admixed soft clays. *Journal of geotechnical and geoenvironmental engineering*, 131(2), pp.187-192.

64. **Horpibulsuk, S., Rachan, R., Chinkulkijniwat, A., Raksachon, Y. and Suddeepong, A.** (2010). Analysis of strength development in cement-stabilized silty clay from microstructural considerations. *Construction and Building Materials*, 24(10), 2011-2021.

65. **Horpibulsk, S., Rachan, R., Suddeepong, A. and Chinkulkijniwat, A.** (2011). Strength development in cement admixed Bangkok clay: laboratory and field investigations. *Soils and Foundations*, 51(2), pp.239-251.

66. **Hsi, J.P and Yu, J.B.Y.** (2005) Jet grout application for excavation in soft marine clay. *Proceedings of the 16th International Conference on Soil Mechanics and Geotechnical Engineering,* Osaka. Millpress, Rotterdam, the Netherlands, vol. 3, pp. 1485–1488.

67. **Hsieh, H. S., Chien, M. C., and Chen, C. T.** (1991). Design, construction and performance of a deep excavation in soft clay. *Proc., First Young Asian Geotechnical Engineers Conf., Asian Institute of Technology, Bangkok,* Thailand, 41–50.

68. **Hsieh, H. S., Lu, F. C., Wu, L. H., and Lin, Y. K.** (1995). Application of JG and DMP to reduce excavation induced diaphragm wall deflection. *Proc., 10th Asian Regional Conf. on Soil Mechanics and Foundation Engineering, International Academic Publisher,* Beijing, 403–406.

69. **Hsieh, H.S., C.C. Wang, and C.Y. Ou.** (2003). Use of Jet Grouting to Limit Diaphragm Wall Displacement of a Deep Excavation. *Journal of Geotechnical and Geoenvironmental Engineering,* 129:146–157.

70. **Hsiung, B.C.B., Lin, H.D. and Lin, W.B.** (2006). Influences of Use of Pile–type Cross-walls on Deep Excavations. *In Proceedings of the 5th International Con ference of TC28 of the ISSMGE: Geotechnical Aspects of Underground Construction in Soft Ground, ed. K.J. Bakker, A. Bezuijen, W. Broere, and E.A. Kwast,* 803–808. Amsterdam, The Netherlands, 15-17 June 2005.

71. **Ignat, R., Baker, S., Larsson, S. and Liedberg, S.** (2015). Two-and three-dimensional analyses of excavation support with rows of dry deep mixing columns. *Computers and Geotechnics,* 66, 16-30.

72. **Indraratna, B., Muttuvel, T. and Khabbaz, H.** (2009). Modelling the erosion rate of chemically stabilized soil incorporating tensile force–deformation characteristics. *Canadian Geotechnical Journal*, 46(1), pp.57-68.

73. **IS: 1498.** (1970). Classification and Identification of Soils for General Engineering Purposes. Bureau of Indian Standards, New Delhi.

74. **IS: 2720-Part 3.** (1980). Methods of Test for Soils: Determination of Specific Gravity, Section 1: Fine Grained Soils. Bureau of Indian Standards, New Delhi.

75. **IS: 2720–Part 4.** (1985). Methods of Test for Soils: Grain Size Analysis. Bureau of Indian Standards, New Delhi.

76. **IS: 2720 –Part 5.** (1985). Methods of Test for Soils: Determination of Liquid and Plastic Limit. Bureau of Indian Standards, New Delhi.

77. **IS: 2720-Part 6.** (1972). Indian Standard Methods of Test for Soils: Determination of Shrinkage Factors. Bureau of Indian Standards, New Delhi.

78. **IS: 2720-Part 10.** (1991). Method of test for soils: Determination of unconfined compressive strength. Bureau of Indian Standards, New Delhi.

79. **IS: 2720-Part 22.** (1972). Method of test for soils: Determination of organic matter. Bureau of Indian Standards, New Delhi.

80. **IS: 2720-Part 26.** (1987). Method of test for soils: Determination of pH Value. Bureau of Indian Standards, New Delhi.

81. **Jan, O. Q., and Mir, B. A.** (2018). Mechanical Behavior of Cement Stabilized Dredged Soil. *Global Journal of Research in Engineering*, 17(4): version 1.

82. **Kamruzzaman, A.H., Chew, S.H. and Lee, F.H.** (2009). Structuration and destructuration behaviour of cement-treated Singapore marine clay. *Journal of geotechnical and geoenvironmental engineering*, 135(4), pp.573-589.

83. **Kasama, K., H. Ochiai, and N. Yasufuku.** (2000) On the Stress–Strain Behaviour of Lightly Cemented Clay Based on an Extended Critical State Concept. *Soils and Foundations* 40 (5): 37–47.

84. **Kasama, K., H. Ochiai, and N. Yasufuku.** (2000) On the Stress–Strain Behaviour of Lightly Cemented Clay Based on an Extended Critical State Concept. *Soils and Foundations* 40 (5): 37–47.

85. **Kavvadas, M., and A. Amorosi.** (2000). A Constitutive Model for Structured Soils. Géotechnique 50 (3): 263–273.

86. **Kitazume, M. and Terashi, M.** (2013). *The Deep Mixing Method.* CRC press.

87. **Kongsomboon, T.** (2002). *Behaviour of an embedded improved soil berm in an excavation.* Diss. PhD Thesis, Department of Civil Engineering, National University of Singapore.

88. **Koseki, J., Salas-Monge, R. and Sato, T** (2005). Plane strain compression tests on cement-treated sands. *Geomechanics: Testing, Modelling and Simulation,* 429-443.

89. **Koutsoftas, D. C. and Ladd, C. C.** (1985). Design strengths for an offshore clay. *Journal of Geotechnical Engineering,* 111(3), 337-355.

90. **Kusakabe, O.** (1996). Braced excavation and shafts, *Geotechnical Aspects of Underground Construction in Soft Ground,* Balkema, Rotterdam.

91. **Lade, P. V. and Wang, Q.** (2001). Analysis of shear banding in true triaxial tests on sand. *Journal of Engineering Mechanics,* Vol. 127, No. 8, pp.762-768.

92. **Liu, Y., Lee, F.H., Quek, S.T., Chen, E.J. and Yi, J.T.** (2015). Effect of spatial variation of strength and modulus on the lateral compression response of cement-admixed clay slab. *Géotechnique*, 65(10), pp.851-865.

93. **Lee, F. H., Yong, K. Y. and Quan, K. C.** (1998). Effect of corners in strutted excavations: field monitoring and case histories. *J. Geotech. Geoenviron. Engng,* ASCE, 124, No. 4, 339–349.

94. **Lee, F.H., Lee, Y., Chew, S.H. and Yong, K.Y.** (2005). Strength and modulus of marine clay-cement mixes. *Journal of geotechnical and geoenvironmental engineering*, ASCE, 131(2), pp.178-186.

95. **Lee, F.H., Hong, S.H., Gu, Q. and Zhao, P.** (2011). Application of large three-dimensional finite-element analyses to practical problems. *International Journal of Geomechanics*, 11(6), pp.529-539.

96. **Lee, K. L.** (1970). Comparison of plane strain and triaxial tests on sand. *Journal of the Soil Mechanics and Foundations Division,* 96(3), 901-923.

97. **Lee, K., D. Chan, and K. Lam.** (2004). Constitutive Model for Cement Treated Clay in a Critical State Framework. *Soils and Foundations*, 44(3), 69–77.

98. **Li, G. J., Wong, K. S., and Ng, P. B.** (2011). Back analysis of a braced excavation with DCM ground improvement. *Proc. Underground Singapore 2011*, Singapore.

99. **Liao, H. J. and Tsai, T. L.** (1993), Passive Resistance of Partially Improved Soft Clayey Soil, *Proc 11th SEAGC, Singapore*, pp.751-756.

100. **Lim, G.T.** (2003). *Stabilisation of an excavation by an embedded improved soil layer*. PhD Thesis, National University of Singapore.

101. **Liu, M and Carter, J.** (2002). A structured Cam Clay model. *Canadian Geotechnical Journal*. 10.1139/T02-069.

102. **Liu, M. D., Carter, J. P., Horpibulsuk, S. and Liyanapathirana, D. S.** (2006). Modelling the behaviour of cemented clay. *In Ground Modification and Seismic Mitigation,* GeoShanghai International Conference, 65-72.

103. **Liu, Y., Lee, F.H., Quek, S.T., Chen, E.J. and Yi, J.T.** (2015). Effect of spatial variation of strength and modulus on the lateral compression response of cement-admixed clay slab. *Géotechnique*, *65*(10), 851-865.

104. **Lo, K.W., Mita, K.A. and Thangayah, T.** (2000). Plane strain testing of overconsolidated clay. *ISRM International Symposium, International Society for Rock Mechanics*, 19-24 November, Melbourne, Australia.

105. **Lorenzo, G.A. and Bergado, D.T.** (2004). Fundamental parameters of cement-admixed clay—New approach. *Journal of geotechnical and geoenvironmental engineering,* 130(10), 1042-1050.

106. **Lorenzo, G.A. and Bergado, D.T.** (2006). Fundamental Characteristics of Cement-Admixed Clay in Deep Mixing. *Journal of Materials in Civil Engineering,* 18, No. 2, 161-174.

107. **Maksimovic, M.** (1989). Nonlinear failure envelope for soils. *J. Geotech. Eng.*, 115(4), 581–586. 10.1061/(asce)0733-9410(1989)115:4(581)

108. **Marachi, N., Duncan, J., Chan, C. and Seed, H.** (1981), Plane-Strain Testing of Sand. *In Laboratory Shear Strength of Soil,* ASTM International, West Conshohocken, PA, 294-302.

109. **McGinn, A. J**. (2003). *Performance of deep excavations in Boston marine clay stabilized by deep mixing methods*. PhD thesis, Cornell University, Ithaca, NY, USA.

110. **Mitachi, T. and Kitago, S.** (1980). Undrained triaxial and plane strain behaviour of saturated remolded clay. *Soils and Foundations*, 20(1), pp.13-28.

111. **Mita, K. A.** (2002). *Constitutive testing of soil on the dry side of critical state*. Doctoral dissertation, National University of Singapore.

112. **Mita, K. A., Dasari, G. R. and Lo, K. W.** (2004). Performance of a three-dimensional Hvorslev–Modified Cam Clay model for overconsolidated clay. *International Journal of Geomechanics,* 4(4), 296-309.

113. **Mitachi, T., and Kitago, S.** (1980). Undrained triaxial and plane strain behaviour of saturated remoulded clay. *Soils and Foundations,* 20(1), 13-28.

114. **Mitchell, J. K.** (1981). Soil improvement state of the art report. *Proc., 10th Int. Conf. on Soil Mechanics and Foundation Engineering*, 4, 509–565.

115. **Miura, N., Horpibulsuk, S., and Nagaraj, T. S.** (2001). Engineering behavior of cement stabilized clay at high water content. *Soils and Foundations*, 41(5), 33-45.

116. **Modoni, G., Flora, A., Lirer, S., Ochmański, M. and Croce, P.** (2016). Design of jet grouted excavation bottom plugs. *Journal of Geotechnical and Geoenvironmental Engineering*, 142(7), p.04016018.

117. **Mokni, M., and Desrues, J.** (1999). Strain localization measurements in undrained plane-strain biaxial tests on Hostun RF sand. *Mechanics of Cohesive frictional Materials,* 4(4), 419-441

118. **Nagaraj, T. S., Srinivasa Murthy, B. R., and Vatsala, A.** (1990). Discussion on 'Change in pore size distribution due to consolidation of clays. *Geotechnique*, 40(2), 303–305.

119. **Nakagawa, S., Kamegaya, I., Kureha, K. and Yoshida, T.** (1996). Case history and behavioural analyses of braced large scale open excavation in very soft reclaimed land in coastal area. *In Geotechnical aspects of underground construction in soft ground*, 179-184.

120. **Namikawa, T. and Koseki, J.** (2007). Evaluation of Tensile Strength of Cement-Treated Sand Based On Several Types of Laboratory Tests. *Soils and Foundations*, 47(4), pp.657–674. DOI: 10.3208/sandf.47.657.

121. **Namikawa, T. and Koseki, J.** (2013). Effects of spatial correlation on compression behavior of cement-treated column. *J. Geotech. Geoenviron. Engng*, ASCE 139, No. 8, 1346–1359.

122. **Namikawa, T., Hiyama, S., Ando, Y. and Shibata, T.** (2017). Failure behavior of cement-treated soil under triaxial tension conditions. *Soils and Foundations*, 57(5), pp.815–827. DOI: 10.1016/j.sandf.2017.08.011.

123. **Neville, A. M.** (1995). Properties of Concrete, *Pearson Education Limited,* 4th Edition.

124. **Newcomb, D. E. and Birgisson, B.** (1999). Measuring in situ mechanical properties of pavement subgrade soils. *Transportation Research Board,* Vol. 278, 19-20.

125. **Ng, C. W. and Lings, M. L.** (1995). Effects of modelling soil nonlinearity and wall installation on back-analysis of deep excavation in stiff clay. *Journal of Geotechnical Engineering,* ASCE, 121(10), 687-695.

126. **Nguyen, B., Takeyama, T. and Kitazume, M.** (2016). Internal failure of deep mixing columns reinforced by a shallow stabilized soil beneath an embankment. *Int. J. of Geosynth. and Ground Eng.* **2,** 30. https://doi.org/10.1007/s40891-016-0072-4

127. **O'Rourke, T.D. and McGinn, A.J.** (2006). Lessons learned for ground movements and soil stabilization from the Boston Central Artery. *Journal of Geotechnical and Geoenvironmental Engineering,* ASCE, 132(8): 966–989.

128. **Omine, K., H. Ochiai, and N. Yoshida.** (1998). Estimation of In-situ Strength of Cement-treated Soils Based on a Two-phase Mixture Model. *Soils and Foundations 38:17–29.*

129. **O'Rourke, T.D. and O'Donnell, C.J.** (1997). Field behaviour of excavation stabilized by deep soil mixing. *J. Geotech. Geoenviron. Eng.,* 123(6): 516-524

130. **Ou, C.Y., Wu, T-S. and Hsieh, H-S** (1996). Analysis of deep excavation with column type of ground improvement in soft clay. *J. Geotech. Eng.,* 1996, 122(9), 709-716.

131. **Pan, Y., Shi, G., Liu, Y. and Lee, F.H.** (2018). Effect of spatial variability on performance of cement-treated soil slab during deep excavation. *Construction and Building Materials*, 188, pp.505-519.

132. **Pan, Y., Liu, Y., Lee, F.H. and Phoon, K.K.** (2019). Analysis of cement-treated soil slab for deep excavation support–a rational approach. *Géotechnique*, 69(10), pp.888-905.

133. **Panda, A. and Rao, S. (1998).** Undrained strength characteristics of an artificially cemented marine clay. *Marine Georesources and Geotechnology*, 16(4), 335-353. 10.1080/10641199809379976

134. **Parry, R.H.** (2014) *Mohr circles, stress paths and geotechnics.* CRC Press.

135. **Peric, D., Runesson, K., and Sture, S.** (1992). Evaluation of plastic bifurcation for plane strain versus axisymmetry. *Journal of engineering mechanics,* 118(3), 512-524.

136. **Perry, J.** (1994). A technique for defining non-linear shear strength envelopes and their incorporation in a slope stability method of analysis. *J. Eng. Geol.*, 27(3), 231–241. 10.1144/gsl.qjegh.1994.027.p3.04

137. **Petchgate, K., Sukmongkol, W. and Voottipruex, P.** (2001). Effect of height and diameter ratio on the strength of cement stabilized soft Bangkok clay. *Geotech. Eng.,* 31, 227-239.

138. **Peters, J.F., Lade, P.V. and Bro, A.** (1988) Shear band formation in triaxial and plane strain tests. *Advanced triaxial testing of soil and rock.* ASTM International, pp. 604-627.

139. **Prashant, A., and Penumadu, D.** (2004). Effect of intermediate principal stress on overconsolidated kaolin clay. *Journal of geotechnical and geoenvironmental engineering,* 130(3), 284-292.

140. **Rouainia, M., and D. Muir Wood.** (2000). A Kinematic Hardening Constitutive Model for Natural Clays with Loss of Structure. *Géotechnique*, 50 (2): 153–164.

141. **Rutherford, C.J.** (2004). *Design manual for excavation support using deep mixing technology*. Doctoral dissertation, Texas A&M University.

142. **Sankar, N., and Paul, V.K.** (1997). Behaviour of a coastal deposit under cyclic loading. *Second Indian National Conference on Harbour and Ocean Engineering (Inchoe-97)*, Thiruvananthapuram, India, 1-10 December, 1:334-343.

143. **Sariosseiri, F. and Muhunthan, B.** (2009) Effect of cement treatment on geotechnical properties of some Washington state soils. *Engineering geology,* 104(1-2): 119-125.

144. **Sharma, R.M.S., Baxter, C.D.P, Hoffmann, W., Moran, K. and Vaziri, H.** (2011). Characterization of weakly cemented sands using nonlinear failure envelopes. *International journal of rock mechanics and mining sciences*, 48(1), 146-151. 10.1016/j.ijrmms.2010.06.008

145. **Shen, B., Shi, J., and Barton, N.** (2018). An approximate nonlinear modified Mohr-Coulomb shear strength criterion with critical state for intact rocks. *Journal of Rock Mechanics and Geotechnical Engineering*, 10(4), 645-652.

146. **Shirlaw, J.N., Tan, T.S. and Wong, K.S.** (2005). Deep excavations in Singapore marine clay. In *Geotechnical Aspects of Underground Construction in Soft Ground: Proc. of the 5-th Int. Symposium,* Amsterdam, 13-28.

147. **Singh, M., Raj, A., and Singh, B.** (2011). Modified Mohr–Coulomb criterion for non-linear triaxial and polyaxial strength of intact rocks. *International Journal of Rock Mechanics and Mining Sciences*, 48(4), 546-555.

148. **Subramaniam, P., Sreenadh, M. M., and Banerjee, S.** (2015). Critical State Parameters of Dredged Chennai Marine Clay Treated with Low Cement Content. *Marine Georesources and Geotechnology*, 34(7), 603-616.

149. **Suebsuk, J., S. Horpibulsuk, and M. D. Liu.** (2010). Modified Structured Cam Clay: A Generalised Critical State Model for Destructured, Naturally Structured and Artificially Structured Clays. *Computers and Geotechnics*, 37 (7–8): 956–968.

150. **Sugawara, S., Shigenawa, S., Gotoh, H. and Hosoi, T.** (1996), Large-scale jet grouting for pre-strutting in soft clay, *Proc. of IS-Tokyo '96 / 2nd Int. Conf. on Ground Improvement Geosystems,* Tokyo, 1, 353-356.

151. **Taiebat, M., Y. Dafalias, and P. Peek.** (2010). A Destructuration Theory and Its Application to SANICLAY Model. *International Journal for Numerical and Analytical Methods in Geomechanics*, 34 (10): 1009–1040.

152. **Tan, T. S., Yong, K. Y., Goh, T. L. and Kongsomboon, T.** (2003). Behaviour of an embedded improved soil layer in an excavation. *Proceedings of Underground Singapore,* 95-102.

153. **Tan, T.S., Goh, T.L. and Yong, K.Y.** (2002) Properties of Singapore marine clays improved by cement mixing. *Geotech. Test. J.,* Vol. 25(4), 422-433.

154. **Tan, X., Konietzky, H. and Frühwirt, T.** (2015). Numerical simulation of triaxial compression test for brittle rock sample using a modified constitutive law considering degradation and dilation behavior. *Journal of Central South University*, 22(8), pp.3097-3107.

155. **Tanaka, H.** (1993). Behaviour of braced excavation stabilized by deep mixing method. *Soils and Foundations,* 33, No. 2, 105-115.

156. **Tanaka, H.** (1994). Behaviour of a Braced Excavation in Soft Clay and the undrained shear strength for passive earth pressure. *Soils and Foundations,* 34(1), pp.53-64

157. **Tatsuoka, F., Sakamoto, M., Kawamura, T., & Fukushima, S.** (1986). Strength and deformation characteristics of sand in plane strain compression at extremely low pressures. *Soils and Foundations,* 26(1), 65-84.

158. **Thakur, V., Nordal, S., Viggiani, G. and Charrier, P.** (2017). Shear bands in undrained plane strain compression of Norwegian quick clays. *Canadian Geotechnical Journal,* 55(1), pp.45-56.

159. **Topolnicki, M., Gudehus, G., & Mazurkiewicz, B. K.** (1990). Observed stress–strain behaviour of remoulded saturated clay under plane strain conditions. *Geotechnique,* 40(2), 155-187.

160. **Tyagi, A., Zulkefli, M. F. B., Pan, Y., Goh, S. H. and Lee, F. H.** (2017). Failure modes of tunnels with improved soil surround. *J. Geotech. Geoenviron. Engng*, 143, No. 11, 04017088.

161. **Uddin, K., Balasubramaniam A.S. and Bergado D.T.** (1997). Engineering behaviour of cement-treated Bangkok soft clay. *Geotech. Eng.*, 28(1), 89-121.

162. **Vaid, Y. P.** (1968). *A plane strain apparatus for soils*. Doctoral dissertation, University of British Columbia.

163. **Vatsala, A., R. Nova, and B. R. Sirinivasa Murthy.** (2001). Elastoplastic Model for Cemented Soils. *Journal of Geotechnical and Geoenvironmental Engineering*, 127 (8): 678–687.

164. **Viggiani, G., Finno, R. J., and Harris, W. W.** (1994). Experimental observations of strain localisation in plane strain compression of a stiff clay. *Localization and bifurcation theory for soils and rocks*, 189-198.

165. **Wanatowski, D. and Chu, J.** (2005). Stress-strain behaviour of a granular fill measured by a new plane-strain apparatus. *Geotechnical Testing Journal*, 29(2), pp.149-157.

166. **Wanatowski, D. and Chu, J.** (2007). Drained behaviour of Changi sand in triaxial and plane-strain compression. *Geomechanics and Geoengineering*, 2(1), pp.29-39.

167. **Wang, J.G., C.F. Leung, and Y. Ichikawa** (2002). A Simplified Homogenisation Method for Composite Soils. *Computers and Geotechnics*, 29, 477–500.

168. **Wang, Q., Du, X. and Gong, Q.** (2014). Undrained shear strength of k_0 consolidated soft clays under triaxial and plane strain conditions. *International Journal of Applied Mechanics,* 6(03), 1450032.

169. **Wang, L., Liu, Y., Pan, Y., Danovan, W., Kumarasamy, J. and Lee, F.H.** (2019). Measure for Reducing the Tensile Stress in Cement-Treated Soil Layer in Deep Excavation in Soft Clay. *KSCE Journal of Civil Engineering*, 23(9), pp.3924-3934.

170. **Wheeler, S., A. Näätänen, M. Karstunen, and M. Lojander.** (2003). An anisotropic elastoplastic model for soft clays. *Canadian Geotechnical Journal*, 40 (2): 403–418.

171. **Wong, L.W. and Patron, B.C.** (1993), Settlement induced by deep excavations in Taipei, *11th Southeast Asian Geotechnical Conference,* 4-8 May, Singapore.

172. **Wong, K.S., Goh, A.T.C., Jaritngam, S. and Chang, L.J.D.** (1998). Optimisation of jet grout configuration for braced excavation in soft clay. *Proc. 2nd Int. Conf. on Ground Improvement Techniques*, Singapore.

173. **Wong, I.H. and Poh, T.Y.** (2000). Effects of jet grouting on adjacent ground and structures. *Journal of Geotechnical and Geoenvironmental Engineering,* 126(3), 247–256.

174. **Woo, S. M., and Moh, Z. C.** (1990). Geotechnical characteristics of soils in the Taipei basin. *Proc., 10th Southeast Asian Geotech. Conf., Southeast Asian Geotechnical Society,* Taipei, Taiwan, 2, 51–65.

175. **Wroth, C. P., and G. T. Houlsby.** (1985). Soil Mechanics – Property Characterization and Analysis Procedures. *Proceedings of the 11th International Conference on Soil Mechanics and Foundation Engineering*, Vol. 1, San Francisco, CA, Balkema, August 12–16, 1985, 1–65.

176. **Xiao, H., Lee, F.H. and Chin, K.G.** (2014). Yielding of cement-treated marine clay. *Soils and Foundations*, *54*(3), pp.488-501.

177. **Yang, H., Tan, T.S. and Leung, C.F.** (2011). Mass behaviour of embedded improved soil raft in an excavation. *Proceedings of the Institution of Civil Engineers-Geotechnical Engineering*, 164(1), pp.11-25.

178. **Yaodong, Z.** (2004). An embedded improved soil berm in an excavation-mechanisms and capacity. Diss. Ph. D Thesis, National University of Singapore.

179. **Yaodong, Z., Tan, T.S. and Leung, C.F.** (2008). Undrained end bearing capacity of an improved soil berm in an excavation. *Soils and Foundations,* 48, 433–446.

180. **Yapage, N. N. S. and Liyanapathirana, D. S.** (2017) A review of constitutive models for cement-treated clay, *International Journal of Geotechnical Engineering*, DOI: 10.1080/19386362.2017.1370878

181. **Yasin, S. J. M., Umetsu, K., Tatsuoka, F., Arthur, J. R. F., and Dunstan, T.** (1999). Plane strain strength and deformation of sands affected by batch variations and different apparatus types. *Geotechnical Testing Journal, GTJODJ,* Vol. 22, pp. 80–100.

182. **Yoo, C. and Lee, D.** (2008). Deep excavation-induced ground surface movement characteristics–A numerical investigation. *Computers and Geotechnics,* 35(2), 231-252.

LIST OF PAPERS SUBMITTED ON THE BASIS OF THIS THESIS

1. **REFEREED JOURNALS**

    1. **Azneb, A.S., Banerjee, S. and Robinson, R.G.** (2019). Shear strength of cement-treated marine clay under triaxial and plane strain conditions. *Proceedings of the Institution of Civil Engineers-Ground Improvement*, pp.1-14*.,* DOI: 10.1680/jgrim.18.00090

    2. **Azneb, A.S., Banerjee, S. and Robinson, R.G.** (2020). Failure envelope of cement treated clay under drained and undrained conditions. *International Journal of Geomechanics, ASCE* (under review)

2. **PRESENTATIONS IN CONFERENCES**

    1. **Azneb, A.S., Banerjee, S. and Robinson, R.G.** (2021). Tensile strength of cement treated clay. *Baltic Sea Geotechnical Conference,* 18-21 January 2021, Helsinki, Finland, May 25-27, 2020 (Accepted)

CURRICULUM VITAE

1. **Name**   :   Azneb Abdul Salam

2. **Date of Birth**   :   21st June 1990

3. **Educational Qualifications**

    2012   *Bachelor of Technology (B.Tech)*

Institution	:	University of Calicut
Specialization	:	Civil Engineering

    2015   *Master of Technology (M.Tech)*

Institution	:	National Institute of Technology Karnataka, Surathkal, Karnataka, India
Specialization	:	Geotechnical Engineering

    2020   *Doctor of Philosophy (Ph.D.)*

Institution	:	Indian Institute of Technology Madras, Chennai, Tamil Nadu, India
Specialization	:	Geotechnical Engineering
Registration Date	:	14-07-2015